IAEA-TECDOC-223

NUCLEAR DATA FOR FUSION REACTOR TECHNOLOGY

PROCEEDINGS OF THE ADVISORY GROUP MEETING
ON NUCLEAR DATA FOR FUSION REACTOR TECHNOLOGY
ORGANIZED BY THE
INTERNATIONAL ATOMIC ENERGY AGENCY
AND HELD IN
VIENNA, 11–15 DECEMBER 1978

A TECHNICAL DOCUMENT ISSUED BY THE
INTERNATIONAL ATOMIC ENERGY AGENCY, VIENNA, 1979

NUCLEAR DATA FOR FUSION REACTOR TECHNOLOGY
IAEA, VIENNA, 1979

Printed by the IAEA in Austria
December 1979

PLEASE BE AWARE THAT
ALL OF THE MISSING PAGES IN THIS DOCUMENT
WERE ORIGINALLY BLANK

The IAEA does not maintain stocks of reports in this series. However, microfiche copies of these reports can be obtained from

INIS Microfiche Clearinghouse
International Atomic Energy Agency
Wagramerstrasse 5
P.O. Box 100
A-1400 Vienna, Austria

on prepayment of US $1.00 or against one IAEA microfiche service coupon.

FOREWORD

The Advisory Group Meeting on Nuclear Data for Fusion Reactor Technology was convened by the IAEA Nuclear Data Section at IAEA Headquarters in Vienna, Austria, from 11-15 December 1978. The meeting was attended by 34 scientists from 15 Member States and 3 international organizations.

The main objectives of this meeting were to determine specific nuclear data requirements for fusion reactor technology, to assess the adequacy of available data in relation to these requirements, and to formulate recommendations for future activities needed to remedy the identified data deficiencies.

This report contains the text of a set of review papers, prepared specifically for this meeting, which address both the requirements and the status of nuclear data for fusion applications. The recommendations for future activities, formulated at the meeting, are contained in a companion report INDC(NDS)-101/LF.

A. Lorenz and D.W. Muir
Editors

Table of Contents

Editors' note: According to the reviewer of topic B5, most of the important developments discussed in his presentation are contained in two reports: "Status of ENDF/B-V Neutron Emission Spectra Induced by 14-MeV Neutrons," by D.M. Hetrick, D.C. Larson and C.Y. Fu, ORNL/TM-6637 (1979); and "A Consistent Nuclear Model for Compound and Pre-compound Reactions with Conservation of Angular Momentum," by C.Y. Fu, ORNL/TM-7042 (to be published).

INTRODUCTORY PAPER

Nuclear Data Requirements of the Magnetic Fusion Power Program of the United States of America

by

Charles R. Head
Reactor Systems and Applications Branch
Division of Development and Technology
Office of Fusion Energy
Department of Energy, U.S.A.

Abstract

The purpose of this paper is twofold, first to give a brief introductory overview of the future course of magnetic confinement fusion device construction as this task is currently perceived by the U.S. Department of Energy, and second to present for your consideration the most current version of the statement of nuclear data needs of the U.S. magnetic confinement fusion power program.

Overview of Construction Plans

To set the stage for the discussion of fusion device construction, it is appropriate to briefly review the current status of the experimental program. This will hopefully aid the reader in assessing the degree of certainty in the discussion of power producing devices which is to follow. The Princeton Large Torus (PLT) has recently achieved ion temperatures in excess of 60 million degrees, thus pushing tokamak plasma temperatures deep into the collisionless regime for the first time. Succeeding devices, namely PDX, Doublet III, Alcator C and ISX-B, are either in preoperational shakedown or are entering the final stages of construction as I write this paper. These devices should push the plasma parameters well into reactor like regimes and achieve plasma conditions equivalent to energy gains near unity. They should also provide initial tests of plasma shape scaling, impurity control measures, alternate plasma heating techniques and other basic plasma data needed to lay a firm basis for design of a first generation fusion power producing device. However, these devices will only contain hydrogen or deuterium plasmas.

Close behind these devices is the Tokamak Fusion Test Reactor (TFTR) at the Princeton Plasma Physics Lab. This device is expected to begin operation in 1981, and will be the first to use a deuterium-tritium plasma. TFTR should demonstrate plasma energy breakeven in 1983. It is expected to start operation in a two component mode with approximately 20 MW of neutral beam heating in 0.5 second pulses. Planning has started on a TFTR improvements project (TIP) which would double the neutral beam power level and extend the pulse length to 1.5 seconds, thus pushing TFTR into the bulk burning mode which is expected to be used in fusion power reactors.

This takes us up through the currently operating experiments and those currently under construction. It should be emphasized that all of these devices are experiments, intended primarily to study plasma physics. Although some radiation is produced, the fluence levels even in TFTR are still low ($\sim 5 \times 10^{16} \frac{\text{neutrons}}{\text{M}^2}$).

The next step is fundamentally different. In the United States it is called the Engineering Test Facility (ETF) and it is envisioned as a device capable of producing net electrical power. The ETF will be used primarily to develop fusion reactor technology in preparation for the succeeding fusion power reactor projects. It is presently conceived of as a $600 million device capable of producing a near ignition plasma for extended burns of up to 30 seconds. It is currently intended to be a device which will evolve through a preplanned series of upgrades from a long pulse plasma experiment, through a first generation fusion

power production experiment, to finally become a national facility for technology development and experiments which require an intense source of 14 MeV neutrons. It is intended to have an operating life of approximately ten years, and while the ETF will probably be a tokamak it could be a mirror or alternate concept device. In any case, the ETF is intended to demonstrate plasma physics and technologies required for other confinement concepts.

The ETF will undergo preliminary conceptual design at an ETF Design Center to be composed of personnel from all three TNS design teams and from elsewhere in the fusion power development community. Oak Ridge National Laboratory has been chosen to host the ETF Design Center and Don Steiner has been chosen as the ETF Design Center manager. The Design Center will begin staffing as soon as possible and initiate operation in parallel with the staffing. One of the first tasks of the Design Center will be to organize an ETF Mission Workshop to develop for submittal to the Office of Fusion Energy a more detailed Mission Statement for the ETF. We hope the design work done by the Design Center will be sufficiently convincing to allow initiation of an ETF Project in 1984 with initial operation scheduled for 1992.

Following the ETF, the current Department of Energy planning calls for a decision to choose one concept, either a magnetic confinement device or an inertial confinement device for development as an Engineering Prototype Reactor. This device is defined as an integrated system producing net usable energy in a manner indicative of an economically competitive design. All technological and engineering requirements will be met with a solution which is transferrable to commercial designs. This device is expected to cost approximately $1 billion with project initiation in 1997 and initial operation in 2004.

Beyond the EPR, the final step before commercial deployment of fusion power is planned to be the Commercial Demonstration Reactor or Demo. This device would be designed and built in a manner such that each requirement is met with an economically competitive solution; solutions which would convince industry to take the next step on their own. The Demo project is intended to start in about 2005 with initial operation in 2015, however, these dates have been developed more to indicate general programmatic intent than as strict planning dates. No cost estimate has been proposed for the fusion Demo.

The reader will note that no mention of hybrids of other alternate applications has been made. This is not intended to imply that we have no intention of developing these technologies, but rather that progress in these areas is not advanced enough to justify incorporating them into the long range program projections. In any case, the ETF will probably be designed such that experimental hybrid or synfuel modules can be inserted for test, and who knows? The EPR might be a hybrid.

Enough of fusion power program plans, now we move on to nuclear data needs. For convenience and to minimize errors in transcription, I present the nuclear data requirements here in the same form in which they are used by the Office of Fusion Energy. This statement of nuclear data needs is a periodically updated document which was initially developed, primarily for the TNS project, at a workshop attended by representatives from throughout the U.S. fusion power development community in April 1976. It was updated in 1977, March 1978, and again two weeks ago to incorporate the latest information from our most recent reactor design studies, and to include requirements from all appropriate portions of the U.S. magnetic confinement fusion power program. Thus it is not a static document, but we do exercise restraint and minimize changes in an attempt to avoid creating chaos in the nuclear data community. I would expect the next major revision to occur (if it occurs at all) when the ETF design begins to firm up. Other than that, the changes will probably be refinement, addition of detail, and differentiation of required data which is currently being worked on from that on which work needs to be initiated.

At this point, I refer you to the documented statement of U.S. Magnetic Fusion Power Program Nuclear Data Needs which is reproduced below. I trust that it is complete, accurate and self-explanatory. If it is not, I will welcome your comments and corrections.

A. Priority I

1. Data for the Fusion Materials Development Program

a. Shielding Data for FMIT (Fusion Materials Irradiation Test Facility):

Information is needed by October 1979 to May 1980 to support shielding design. The required information is total cross section, angular dependent elastic scattering cross section, and total nonelastic cross section data for selected energies from 20 MeV to 50 MeV. The need for data is most acute for Fe and O, with less critical interest in Si, Ca and C. The accuracy required is ± 10-15%.

Due to the short time available for obtaining this data, most of the needs must be met within the FMIT Project. Experiments have already been performed at UC-Davis on total cross sections for Fe and Ca at 35, 40 and 50 MeV and on "removal" cross sections for Fe, O, Ca and C at 40 and 50 MeV. More measurements are planned by the FMIT Project, but complimentary efforts will be welcomed. These activities should be coordinated directly with the FMIT Project.

Somewhat longer term needs (i.e., by mid 1979 through 1983) are also anticipated to allow retrofitting of shielding or changing shield compositions to make the shielding more effective. High accuracy measurements (±5%) are needed on a few of the materials specified above, such as the total cross section measurements made by the U.S. National Bureau of Standards, to validate and calibrate theoretical cross sections and to corroborate near term measurements being made at UC-Davis.

b. Dosimetry Data

Dosimetry reaction data is needed at selected energies in the 1 MeV to 50 MeV range to support material irradiations now being conducted at UC-Davis as well as testing planned to be done in the FMIT. The data is needed as soon as possible to improve the accuracy of flux-spectral measurements and material damage rate calculations being performed now and by 1983 to support FMIT initial operation.

In formulating the dosimetry needs, the following criteria should be used to guide the selection of materials and reactions:

1) The half life of the reaction product should be reasonably long; > 30 days for FMIT; > 2 days for UC-Davis.

2) The material should have several usable reaction products, if possible, to facilitate handling (especially cutting) and counting of samples.

3) Mono-isotopic elements are preferred since otherwise total cross-sections are needed and are harder to measure or calculate.

4) Reaction products should have easily detected activities (gamma preferred), except for He analysis materials.

5) Materials should be readily available, reasonably cheap and easily handled.

These criteria are not absolute, except for the first one, and do not have to be simultaneously satisfied by all materials. Although the dosimetry materials used for initial characterization studies may not meet these criteria, the materials used in routine dosimetry should be more carefully chosen to produce the maximum amount of information with the least effort.

A brief summary of the most important materials and reactions is as follows:

1) Cobalt -- This material appears to satisfy all five criteria for five distinct reactions spanning the entire range of energies of interest to materials damage studies. The (n, p) reaction needs further characterization above 14 MeV. Some calculations and data are available for the (n, 2n) and (n, 3n) reactions to 28 MeV, and nothing is known about the (n, 4n) reaction. High priority should be given to developing these reactions in the 28 MeV to 50 MeV range.

2) Gold -- Only the (n, 2n) and (n, 3n) reactions have sufficiently long half-lives. Data is needed above 28 MeV.

3) Iron -- The $^{54}Fe(n, p)\ ^{54}Mn$ reaction has a long half-life, but is subject to signficant interference from ^{56}Fe. Hence, total production data from iron is required above 14 MeV. Data is needed at all energies for the $^{54}Fe\ (n, \alpha)\ ^{51}Cr$ reaction.

4) Nickel -- The (n, p) reactions on ^{58}Ni and ^{60}Ni both need development above 14 MeV. The $^{58}Ni\ (n, 3n)\ ^{56}Ni$ reaction also needs development.

Many other materials and reactions could be mentioned including Zr, Y, Tm, Er, Ir, Ag, Nb, Al and Na, although most do not meet the five criteria. Rare earths are difficult to handle since organic binders may perturb the spectrum and metal foils are expensive and somewhat unstable. Nevertheless, some redundance is required to reduce the errors involved in spectral unfolding, especially during the initial characterization of FMIT. Thus we urge that as many reactions as possible be developed. Also, since total He generation data can be used for fluence-spectrum unfolding, He generation data is required for all dosimetry materials.

It should be emphasized that the reaction cross sections should be developed in an orderly, planned fashion. A few well-planned measurements coupled with calculations should suffice to produce the required accuracies of 10-20% below 20 MeV and 20-40% at higher energies. At present, some information is known about enough reactions to produce the desired accuracy in the 2 MeV to 30 MeV range for UC-Davis irradiations, as confirmed by integral testing. However, more reactions with longer half-lives are needed for FMIT and there is virtually no data above 28 MeV. As before, we encourage individuals working in this area to coordinate their activities directly with the FMIT Project.

c. FMIT Material Damage Calculations

Data defining the He and H generation rate, differential angular cross section for elastic and nonelastic scattering and the energy distribution of emitted particles is needed for selected incident neutron energies from 15 MeV to 35 MeV for Fe, Ni, Cr, V, Ti, Nb, Cu and Sn. This data will be used for FMIT material damage calculations. Accuracy requirements for these reactions will range from 10 to 50%

and will be established by sensitivity studies yet to be performed.

2. Data for the Next Generation of D-T Reactor Designs:

   a. Neutron emission spectra data is needed as a function of secondary angle and energy for selected incident neutron energies in the 9 MeV to 14 MeV range for the materials listed below. This data is needed for shielding, activation, and neutron transport calculations. The accuracy required is ± 10%.

Material	Use
^{7}Li	^{3}H Breeding Material and Potential Coolant
C	Blanket Structure
Ni	Structure
Si	Structure
Cu	Electrical Conductor
^{11}B	Shield
Fe	Structure
Cr	Structure
Pb	Low Activation Shield

   b. He and H production data is needed as a function of selected incident neutron energies in the 9 MeV to 14 MeV range for the materials listed below. This data is needed for radiation damage calculations. The specific material uses are as specified in A.2.a above. For accuracy required, see A.1.c above.

^{7}Li	C	Ni	Si	Cu
^{11}B	Fe	Cr	Pb	

3. Nuclear Physics Data -- The following data is all needed by the early 1980's to support operation of experimental devices initiating operation at that time or for design studies of later experiments:

   a. Cross-Sections for Near-Term Fuels

      1) D-T -- The accuracy of this cross section needs to be improved for energies below 10 KeV. The desired accuracy is specified in Table II. (Note: The existing National Bureau of Standards (NBS) program using the inverse reaction to measure the D-T cross-section has significantly improved the accuracy of the low energy values.)

      2) T-T -- Cross-section measurements are needed to assist in identifying contributions to the continuum of background neutrons, and to estimate tritium ion temperature. The desired accuracy is specified in Table II. (Note: The Division of Basic Energy Science will begin a program to do this measurement at LASL in FY 79. This program is expected to be completed in the required time.)

      3) Elastic Cross-Sections -- Measurements are needed to characterize the interaction between superthermal alphas and D-T fuel up to a few MeV. This data is required to calculate the heating of plasma fuel by the fusion product alphas. The desired accuracy is specified in Table II. (Note: No specific program is currently focused on this need. Effort to get this data will have to be initiated in the next 2-3 years if the requirement is to be met.)

3. b. Cross Sections for Advanced Fuels -- An advanced fuel is generally defined as everything other than 50-50 D-T. The operating temperatures for these fuels vary widely, i.e., from $\gtrsim$ 100 KeV to several hundred KeV. While the cross sections for the primary reactions are reasonably well known, those of secondary reactions are not. There are no specific programs directed toward these areas at this time. The following data is needed:

1) Cross Sections -- The cross sections listed below are needed in the energy range from several hundred KeV to a few MeV. The desired accuracy is specified in Table II.

a) $^{11}B\ (p, n)\ ^{11}C$

b) $^{11}B\ (\alpha, p)\ ^{14}C$

c) $^{11}B\ (\alpha, n)\ ^{14}N$

d) $^{6}Li(^{3}He, p)\ 2\alpha$ or ^{8}Be

e) $^{6}Li\ (^{6}Li, X)\ \gamma$

2) Elastic Cross-Sections -- Elastic cross sections for the interactions between the suprathermal product ions from the reactions in A.3.b.1) above with the plasma fuel ions are needed in the energy range from several hundred KeV to a few MeV. The desired accuracy is specified in Table II.

c. Data Compilations -- Compilations of the types of data listed below are needed for the advanced fuels listed above, as well as for DT and TT. The energy ranges for which data is needed are as stated above and the desired accuracy is specified in Table II. (Note: There is no program to accomplish this task presently underway. This effort is needed in the early stages of collecting the data requested above to avoid duplication of efforts.)

1) σ vs E

2) $\langle \sigma v \rangle$ vs T

B. Priority II

1. Data for D-T Fusion Engineering Prototype and Demonstration Power Plant Designs:

a. Neutron emission spectra data is needed as a function of secondary angle and energy for selected incident neutron energies in the 9 MeV to 14 MeV range for the materials listed below. This data is needed for shielding, activation and neutron transport calculations. The accuracy required is $\pm$ 10%.

Material	Use
Al	Structure, Insulation
Be	Neutron Multiplier, Molten Salt Coolant
Ti	Structure
Nb	Coil Material, Refractory Structure
W	High Efficiency Shield
Sn	Coil Material
Mo	Structure, Refractory
N	Activation of Air
V	Refractory Structure
F	Molten Salt Coolant
^{10}B	Shield
O	Activation in Air or Water, Insulation

b. He and H production data is needed as a function of selected incident neutron energies in the 9 MeV to 14 MeV range for the materials listed below. This data is needed for radiation damage calculations. The material uses are as specified in B.1.a above. The accuracy required is specified in A.1.c above.

Al	Be	Ti	Nb	W	Sn
Mo	N	V	F	^{10}B	O

c. Data is needed to define the energy spectra of the charged particles resulting from (n, α) and (n, p) reactions for 14 MeV neutrons incident on the materials in items A.2.a, A.2.b, B.1.a and B.1.b avove. This data is required for radiation damage studies. The desired accuracy is to be determined.

B. 1. d. Data is needed to describe the breeding reactions in ^{7}Li and Th due to interactions with 11 MeV and 14 MeV neutrons, and in ^{6}Li due to interactions with 0.5 MeV to 5 MeV neutrons. The energy ranges specified above were chosen to cover bands where the current data is questioned and/or where the breeding cross section appears most significant. The desired accuracy is $\pm$ 10%. The Th data is for use in potential hybrid design work.

e. Secondary gamma production cross sections are needed as a function of selected incident neutron energies in the 9 MeV to 14 MeV range for ^{10}B, ^{11}B, and Ti. The desired accuracy is $\pm$ 10%. This data is used in blanket, shield and magnet heat deposition calculations. (OFE understands that gamma production cross sections for the other materials in items A.2.a, A.2.b, B.1.a, B.1.b, B.1.c and B.1.d above are already known.)

TABLE I

Incident Neutron Energy Range (MeV)	Desired Accuracy By Energy Group (%)
< 0.5	30 - 60
0.5 - 2	20 - 40
2 - 4	10 - 20
4 - 7	10 - 20
7 - 10	10 - 20
10 - 15	10 - 20
15 - 20	10 - 20
20 - 25	10 - 20
25 - 30	20 - 40
> 30	40 - 80

TABLE II

Absolute Accuracy	$\pm$ 30%
Relative Accuracy	$\pm$ 10%

INVITED PAPERS: SESSION A

NUCLEAR DATA REQUIREMENTS FOR FUSION REACTOR DESIGN

Nuclear Data Requirements for Fusion Reactor Design - Neutronics Design, Blanket Neutronics and Tritium Breeding

G. Constantine

Atomic Energy Research Establishment, Harwell, U.K.

Abstract

The neutronics problems encountered in fusion reactor blanket design are explored, with special reference to the tritium breeding requirement. The sensitivity of this parameter to cross section uncertainties is then considered and targets for accuracy requirements suggested against the background of a standard deviation of ±2% in the calculated tritium breeding. The role of integral assemblies and benchmark experiments in helping to achieve this by data adjustment is discussed.

1. Introduction

Recent years have witnessed an explosion in the number of studies carried out on a variety of types of fusion reactor blanket [1-6], each with their own constraints imposed primarily by plasma engineering demands. These demands broadly determine the disposition and composition of various components, first wall, tritium breeding zone, shielding for magnet coils and the coils themselves (if applicable) and biological shield. Many reactor designs encompass restrictions in the form of stabilising coils, insulators etc. close in to the plasma, penetrations for injectors, divertors, pump lines and in the case of inertial confinement fusion systems, pellet injection and laser/ion beam entry ports. Engineering and heat transfer considerations dictate the physical form of the combined tritium breeding/heat removal system, whether it be in the solid or liquid phase, with liquid or gaseous cooling, contained within tubular, cellular or annular structures. Materials limitations also exert a strong influence on the evolution of a design.

The major part of the energy released from the DT reaction, the only serious contender for fusion power generation, is invested in the neutron produced and it is in calculating the effects of this that neutronics plays its part in an interacting array of disciplines. Neutronics in the broadest sense covers the problems of neutron transport, the many types of interaction with the various nuclides in the components of the reactor, computation of neutron flux and energy spectrum distributions, reaction rates including activation, transmutation, secondary neutron production and gas formation, radiation damage and nuclear heating, not only that due to short range atom recoil local to the neutron interaction but also generation of gamma rays and their subsequent transport and energy deposition.

In considering the topic of nuclear data requirements, it is instructive to note briefly the three main areas in which neutronics has been applied in the past:

(a) Fission Reactor Calculations

(b) Shielding Calculations

(c) Fusion Reactor Blanket Calculations.

Of these, (a) is basically an eigenvalue problem, historically the area in which neutronics was developed; it encompasses the assessment of the reactivity of a multiplying medium and prediction of its critical parameters as well as fundamental flux distributions. Areas (b) and (c) are both source problems, in that the task is basically to calculate the spatial, energy and occasionally temporal distribution of neutrons through a physical assembly, arising from a known neutron source distribution. They differ only in emphasis, the term "shielding calculations" implying deep penetration, while a fusion reactor blanket calculation could be styled a "shallow penetration" problem. Inevitably there is overlap between (b) and (c). However, all three problem types differ in the

accuracy they set out to achieve and the demands they make on calculation methods and nuclear data. The task of calculating the critical size of a fissile assembly is undoubtedly the most exacting, not only because it is the most susceptible to verification but also because the consequences of wrong prediction can be serious. Fission reactor calculations have therefore always been backed up by a strong programme not only in basic data accumulation but also of experimental measurements in subcritical and zero energy critical assemblies.

Shielding calculations pose a very different set of problems. Firstly a much inferior order of accuracy is acceptable but because of the deep penetration involving attenuation by many orders of magnitude, the results are very sensitive to the cross section data used. The highly anisotropic flux distributions through a shield lead to great emphasis on the need for adequate representation of directional parameters both in the nuclear scattering processes and in the calculational methods used.

Fusion reactor blanket calculations share aspects in common with the other two areas. As in shielding, anisotropy effects play a large part since the neutron source is asymmetrically placed with respect to the reactor blanket. In a fission reactor biological shield, the small fraction of neutrons in the "tail" of the fission spectrum, extending up to ~20 MeV, exert a disproportionate influence due to their greater penetrating power. The data needs for the fusion reactor, therefore, with its 14 MeV source neutron energy, run in parallel with those of reactor shielding, whereas for fission reactor calculations neutrons of greater than say 5-8 MeV are of negligible significance. Of the many parameters that need to be calculated in fusion reactor blanket neutronics, that of the tritium breeding ratio stands out conspicuously above the rest in its accuracy requirements, although not to the same degree as that demanded for the reactivity parameter in fission reactor calculations.

2. Tritium Breeding Requirements

A self sustaining DT burning fusion reactor must breed tritium in the blanket to replace that burnt, by a margin to cover losses, diversion into inventory in an expanding power programme, and decay during the period between formation and use while it is either immobilised in blanket materials or forming part of the hold-up in separation plant. These allowances are all subject to considerable uncertainty at this stage, expressed directly as the uncertainty ΔB in the required breeding gain B. In the absence of uncertainties a breeding ratio T (defined as the number of tritium atoms produced per atom burnt) would just be sufficient to close the breeding cycle if $T = B + 1$. To design a reactor with a closed breeding cycle reliably we must aim at a breeding ratio higher than this basic value by a margin which covers both ΔB and the possible shortfall ΔT arising from the combined effects of nuclear data uncertainties on the neutronics calculations and the approximations used in the calculations themselves. Thus the aiming point for the tritium breeding ratio should be given by $T = 1 + B + \Delta B + \Delta T$. It is important to close the breeding cycle with a high degree of confidence - the allowances ΔB and ΔT should be adequate on this basis rather than representing one single standard deviation. Gerstl et al. [7] discuss the implications of this and make the point that to meet a design criterion such as an uncertainty ΔT in tritium breeding ratio to a given confidence level, one must specify a maximum allowable limit on the standard deviation in the calculated breeding ratio, arising from cross section and calculation method uncertainties. Since we are aiming at a safety margin corresponding to a combined uncertainty $\Delta B + \Delta T$, to achieve that at the same confidence level an upward relaxation in the calculated standard deviation in breeding ratio is possible. At this stage in fusion reactor development, however, both the breeding gain B required and the uncertainty ΔB in it are very ill-defined. In this context the aim of achieving a 1% standard deviation in T [8] probably appears over-optimistic. A figure of ±2% standard deviation in tritium breeding ratio puts the nuclear data/neutronics calculations in the position of being comfortably ahead at present, with some prospect that it can be achieved. It is to be expected that ΔB will diminish in due course as the specification of fusion reactor blanket systems tightens up.

Abdou [9] points out that the significance of uncertainties is very system dependent; the tritium breeding ratio potential ranges from high in

lithium blankets and less for most lithium compounds down to marginal for the molten salt "flibe" (Li_2BeF_4) . Uncertainty considerations could prevent the last from breeding. A practical blanket will be designed to have a tritium breeding ratio ($\Delta B + \Delta T$) above that required, to give an adequate safety margin. This could be as much as 10% depending on the confidence level criterion chosen. If the blanket turned out exactly as intended it would have a doubling time of ~150 days (assuming 10 Kg tritium inventory, 5 Gw (th)). There would be a 50% chance of a breeding margin greater than 10%. Even so the consequences of ending up with over production of tritium are far less serious than with under-production. In any case as Bachmann [10] emphasises, it is inconceivable that a fusion reactor would be built without a means of reducing the breeding ratio incorporated. Reduction of the lithium enrichment if appropriate, or substitution of a few non-breeding cells or modules (see for instance reference [11]) at some point when it becomes clear that the tritium inventory is increasing too rapidly, are two out of a variety of possible measures.

3. Neutronics Design

This topic covers the whole area of neutronics calculations for the fusion reactor and extensive surveys of methods have been carried out in the recent past [12,13]. In generating a fully fledged design there are two separate phases; firstly the scoping survey followed by the detailed neutronics study. The purpose of scoping surveys is to investigate the broad consequences of adopting a particular design philosophy and to examine effects of choice of materials, dimensions of first wall, breeding blanket, reflector and shield components, structure fraction, lithium enrichment, etc. Once the choice has been narrowed down on a mix of criteria such as tritium breeding, radiation damage limitations, activation etc. together with those imposed by other disciplines, such as plasma physics, engineering, heat transfer, maintainability, chemistry, resource limitations, etc., the more detailed study can proceed. The toroidal geometry encountered in most fusion reactor designs is difficult to model neutronically but a cylindrical approximation is usually considered adequate for scoping studies. Complex blanket structures can be represented by homogeneous approximations. Although the parameters of interest emerging from the survey may be in error on account of these approximations, it is still important to use the best available nuclear data so that relative values resulting from changes in materials will be valid.

Computational methods for survey calculations have for the most part been based on the Carlson Sn method [14] employed in the form of one-dimensional discrete ordinates codes such as ANISN [15] and DTF-IV [16]. Monte Carlo has its advocates on the grounds of computational cost even in 1-D scoping and optimisation surveys [17]. However, in studying the influence of small changes in blanket configuration, Monte Carlo is at a disadvantage because of the steeply rising cost of improving the statistical errors on the results.

In making a full neutronics assessment of a practical reactor blanket following the scoping survey stage, three major effects must be considered:

1. The toroidal geometry
2. The presence of penetrations through the blanket and shield.
3. The departure from a homogeneous representation of the blanket by its sub-division into modular form.

It is not in general practicable to do other than tackle all these problems independently.

(a) Toroidal Geometry

A number of workers have investigated the shortcomings of the cylindrical approximation to the toroid in respect of poloidal variation in wall loading [18,19] primary neutron flux [20] and spectra [21], gas production and displacement [19] and tritium breeding [22]. Various computational methods have been devised to tackle this specific problem including the possibility of utilising existing Sn codes [23], 2-D neutron transport codes with triangular meshes such as TRIDENT [24], Monte Carlo

[21], MCN [25] and an ingenious solution by Verschuur [26] involving calculations of differential neutron albedos by 1-D Sn code, followed by use of these in an iterative solution of the multiply reflected neutron fluxes within the torus.

(b) Penetrations

Essentially penetrations through the blanket/shield constitute more of a problem in shielding than in tritium breeding and they are routinely tackled by Monte Carlo methods [27,28] or 2-D discrete ordinates calculations [29]. In the latter reference Takahiro et al. calculate a 1.3% drop in tritium breeding for 12 injector ports 1m in diameter in their Tokamak reactor design, demonstrating that this is a non-negligible problem.

(c) Blanket inhomogeneities

The departure of practical blanket structures from a homogeneous so-called "onion skin" model comprising unbroken layers of first wall, breeding zone, reflector and shield has been the subject of several investigations, mostly by Monte Carlo methods [30,31]. The two-dimensional discrete ordinates code DOT [32] has been used as well in the FINTOR-D design. The approximations made in adapting this to the X-Y geometry of DOT led to unacceptably high differences (~23%) in tritium breeding ratio in the comparison with MORSE [33] calculations, once again emphasising the importance of adequate geometry description.

4. Data Requirements for Neutronics Codes

The many codes in existence for carrying out both scoping surveys and detailed design, either by 1 or 2 dimensional discrete ordinates or Monte Carlo methods, need as part of their input the neutronic data in appropriate form. This is derived from the basic nuclear data available in libraries such as UKNDL [34], ENDF/B [35] and ENDL [36]. The codes in general require the neutronic data in a different format (e.g. cross sections in a groupwise structure) from the basic data libraries. A host of processing codes including MINX [37], SUPERTOG [38], AMPX [39] has been developed to service the needs for neutron and gamma transport calculations, reaction rates including activation, transmutation, radiation damage and nuclear heating. The importance of these and the way in which they are used cannot be over-stressed, especially where simplifications are being made, for instance in minimising the order of quadrature or reducing the number of groups in a multi-group calculation for the sake of cost. In a shield calculation the former can introduce large errors because the highly anisotropic flux distribution is inadequately modelled. A fusion reactor blanket is a less stringent environment in this respect and P_3 Legendre expansion with S_8 or S_{16} quadrature is usually sufficient. Group structure requirements are more demanding, however, particularly for tritium breeding, and Evangelides and Lindstrom's account [40] is informative. They collapsed the DLC-2 100 group library to a 15 group set and found gross tritium breeding under-prediction with combinations of 1/E and either fission or fusion weighting. Agreement was improved to <2% when the 15 group structure was re-cast to give more groups when the breeding contribution was high, retaining a fusion + 1/E weighting. The best agreement was obtained using a many group diffusion or P1 calculation to provide space-dependent flux weighting for condensing to the few group data.

The problem of structure in cross sections that is finer than the energy group structure in the calculations is a familiar one in neutronics. Resonance self shielding effects and even steeply varying threshold reaction cross sections give rise to appreciable errors. Ostrow and Goldstein [41] discuss the application of a discrete energy version of the Sn code ANISN, known as MOMANS [42] to such problems. This is capable of rapid calculation of neutron transport in finely detailed energy grids. They instance the problem of the near Gaussian energy distribution due to thermal broadening of the nominal 14 MeV neutrons from the DT reaction. The $^{27}Al(n,2n)$ reaction which is of significance to neutron multiplication and tritium breeding in some reactor designs, has a threshold at 13.5 MeV and in a MOMANS discrete energy Sn treatment exhibits a 40% drop in reaction rate relative to a multigroup Sn calculation. Complex resonance structure in materials such as iron and niobium pose a serious challenge. The latter material is discussed in Section 7.

It is clear that great care is needed in vetting the methods and approximations used in carrying out neutronics calculations. Experience with collaborative programmes involving benchmark calculations by several laboratories (for example Steiner [43]) has shown that large discrepancies can occur, even using the same basic nuclear data. Further progress needs to be made in this department before the requirements can be met for CTR blanket design, particularly in respect of tritium breeding.

5. Basic Nuclear Data Requirements

The nuclear data base for neutronics calculations has been painstakingly assembled over a period of many years from cross section measurements by many workers, evaluated and cross checked by exposure to comparison between measurements and calculations of integral assemblies. That for CTR applications has grown by extension of the data bases for fission reactors and their shielding requirements, by inclusion of appropriate materials over the relevant energy range. Fortunately the CTR data base is much more advanced than that for fission reactors at an equivalent stage of their development.

The main requirements at present are to improve the accuracy of much of the basic nuclear data for fusion reactors in respect of materials in the blanket and shield. Table I below gives the range of data of relevance to calculations of the basic neutronics of the blanket, including neutron flux and spectra and tritium production distributions. Other effects, e.g. gamma production, nuclear heating, radiation damage etc. are the subjects of later papers at this meeting.

Table I. Nuclear data of importance to tritium breeding calculations

Component	Candidate Materials	Reactions	Remarks
Structure	Refractory materials/alloys) Nb, V, Mo, Ti. Steels Fe) Ni Cr Al)	Neutron absorbing reactions) elastic and) inelastic) scattering,) (n,2n))	Secondary neutron spectra and angular dependence
Breeder	^{6}Li ^{7}Li Be, F in flibe Li_2BeF_4 ceramic compounds (solid) blankets Li_2O, Li_2C_2 Aluminium compounds LiAl, $Li_2Al_2O_4$	$^{6}Li(n,\alpha)t$) $^{7}Li(n,n'\alpha)t$) absorption,) (n,2n) and) elastic and) inelastic) scattering)	Secondary neutron spectra and angular dependence
Neutron Multipliers	Be, Pb)	(n,2n)) inelastic and) elastic	Secondary neutron spectra and angular dependence
Moderators and Reflectors	C, Steel)	scattering,) neutron absorption	
Spectrum Shifters	C, Si (D,T in inertial confinement)		

6. Data Uncertainty Effects

The assessment of accuracy requirements in basic nuclear data has come to the fore over the past 3-5 years following a period in which a large variety of fusion reactor blanket studies were carried out. Techniques have evolved for the quantitative estimation of effects of data uncertainties on parameters of interest, in particular the tritium breeding. Bartine et al. [44] have calculated the changes in breeding ratio due to changes over specific energy ranges of various partial cross sections of ^{6}Li, ^{7}Li, Nb and C in the standard benchmark configuration devised by Steiner [43] comprising a graphite reflected, liquid lithium breeding blanket with 6% niobium structure, with a niobium first wall. Their method used linear perturbation theory and employed forward and adjoint transport

calculations, performed with the one-dimensional discrete-ordinates code ANISN [15] using P_3S_{12}. The perturbation calculations were carried out with the code SWANLAKE [45]. This calculates the percentage changes in parameters of interest such as tritium breeding in the lithium isotopes over specific regions of the blanket for a given percentage change in any given specified cross section over the whole or parts of the complete energy spectrum. Sensitivity of the tritium breeding to variations in the following cross sections were reported:- Σ total collision, $\Sigma(n\gamma)$, Σ elastic and $\Sigma(nn')\gamma$ for ^{6}Li, ^{7}Li, Nb and C, $\Sigma(n,2n)$ for ^{6}Li, ^{7}Li and Nb, $\Sigma(np)$ for ^{6}Li and Nb and the tritium breeding reactions ^{6}Li(n,α)t and ^{7}Li$(nn'\alpha)$t. Table II gives a brief summary of the total breeding sensitivity to these cross sections.

Table II. Sensitivity of total breeding to changes in cross sections in the Steiner [43] blanket, reported by Bartine et al. [44]

$\frac{1}{R}\left(\frac{\delta R^{6}\text{Li} + \delta R\ ^{7}\text{Li}}{\delta C}\right)$ where $\delta R\ ^6$Li and $\delta R\ ^7$Li are the changes in the ^{6}Li and ^{7}Li components of the total breeding ratio R. δC is the fractional change in the relevant cross section over the complete energy range.

Cross Section	^{6}Li	^{7}Li	Nb	C
Σtotal collision	1.23×10^{-1}	1.27×10^{-1}	-2.0×10^{-1}	6.31×10^{-2}
$\Sigma(n\gamma)$	-1.79×10^{-5}	-9.02×10^{-3}	-1.12×10^{-1}	-4.96×10^{-3}
Σelastic	-7.22×10^{-3}	-7.51×10^{-2}	-3.5×10^{-3}	6.49×10^{-2}
$\Sigma(nn')\gamma$	-1.38×10^{-2}	-1.70×10^{-2}	-9.2×10^{-2}	3.08×10^{-3}
$\Sigma(n2n')$	7.0×10^{-4}	5.5×10^{-3}	1.52×10^{-2}	-
$\Sigma(np)$	-1.22×10^{-3}	-	-5.4×10^{-3}	-
$\Sigma(n\alpha)$t	1.45×10^{-1}	-	-	-
$\Sigma(nn'\alpha)$t	-	2.23×10^{-1}	-	-

Table III

Comparison of Results Obtained from Perturbation Calculations and Discrete Ordinates Calculations with Perturbed Cross Sections

Element Perturbed	Cross-Section Type Perturbed	$\delta C \times 100\%$	Perturbation Calculation			Discrete Ordinates Calculation (Ref. 47)		
			$\frac{\delta R_{^6\text{Li}}}{R}\times100\%$	$\frac{\delta R_{^7\text{Li}}}{R}\times100\%$	$\frac{\delta R}{R}\times100\%$	$\frac{\delta R_{^6\text{Li}}}{R}\times100\%$	$\frac{\delta R_{^7\text{Li}}}{R}\times100\%$	$\frac{\delta R}{R}\times100\%$
Nb	$\Sigma_{(n,n')}$	25 at all energies	-0.28	-2.03	-2.31	-0.23	-1.92	-2.15
Nb	$\Sigma_{(n,n')}$	-25 at all energies	0.28	2.03	2.31	0.24	2.13	2.37
Nb	$\Sigma_{(n,2n')}$	25 at all energies	2.07	-1.69	0.38	2.09	-1.63	0.46
Nb	$\Sigma_{(n,2n')}$	-25 at all energies	-2.07	1.69	-0.38	-2.23	1.74	-0.49
^{7}Li	$\Sigma_{(n,n')\alpha,t}$	20 at all energies	-0.26	4.72	4.46	-0.21	4.31	4.10
^{7}Li	$\Sigma_{(n,n')\alpha,t}$	-20 at all energies	0.26	-4.72	-4.46	0.21	-4.94	-4.73
^{6}Li	$\Sigma_{(n,t)\alpha}$	3 for $E \le 0.01$ MeV 5 for $0.01 < E \le 2$ MeV 10 for $2 < E \le 14.9$ MeV	0.49	0.00	0.49	0.49	-0.01	0.48
^{6}Li	$\Sigma_{(n,t)\alpha}$	-3 for $E \le 0.01$ MeV -5 for $0.01 \le E \le 2$ MeV -10 for $2 \le E \le 14.9$ MeV	-0.49	0.00	-0.49	-0.51	0.01	-0.50

Perturbation methods are rapid and can give far more detail than that given here, including the variation in sensitivity to cross section changes across the neutron energy spectrum. These sensitivity profiles, of which Fig. 1 shows an example, are invaluable for assessing the areas in which improvements in cross section data should be sought. Doubt attaches to perturbation results in the case of large cross section disturbances. In a study of the same system by Steiner and Tobias [46,47] the sensitivity of the breeding ratio was evaluated by altering reference cross section

sets to reflect their estimated uncertainties. The XLACS code [48] was used to process the ENDF/B-3 data or its modified values into the form required for a discrete ordinates P_3S_4 calculation by XSDRN [49] in 100 groups. Both positive and negative changes were made to the cross sections. In the case of the ^6Li (n,α)t reaction the changes were energy dependent since the cross section is known with greater precision at lower energies. Table III shows the comparison with the perturbation results of Bartine et al. The agreement between them, even for appreciable cross section changes effectively validates the use of perturbation theory.

Alsmiller et al. [50] have extended perturbation theory to an intercomparison of various reactor designs and show that the sensitivities are very system dependent. The differences between sensitivities of the tritium breeding to changes in Li partial cross sections for two markedly differing concepts are shown in Table IV. The first is the ORNL concept proposed by Fraas [51] employing natural lithium metal as the breeder with either niobium or vanadium structure; the second is the LASL design, the Reference Theta Pinch Reactor [52] (RTPR) which is of the "thermal" type. Reliance is placed on (n,2n)neutron multiplication in a beryllium region close to the first wall, followed by a graphite moderator and enriched ^6Li, which utilises the neutrons at low energy. ^7Li is present in the natural lithium coolant but to a much lesser extent than in the ORNL design. This is seen in the much reduced sensitivity of the breeding ratio in the LASL concept to ^7Li cross section changes.

Table IV

Percent Change in Breeding Ratio Due to a 1% Increase at All Energies in the Indicated Partial Cross Sections of ^7Li

^7Li Cross-Section Type	Breeding Material j	$\frac{\delta R_j}{R}$ in Percent ($R = R_{^6Li} + R_{^7Li}$)		
		ORNL Design with Nb	ORNL Design with V	LASL Design
$\Sigma_{(n,n')\alpha,t}$	^6Li	1.7×10^{-2}	2.2×10^{-2}	3.1×10^{-3}
	^7Li	2.8×10^{-1}	2.7×10^{-1}	1.2×10^{-1}
	$^6Li + ^7Li$	3.0×10^{-1}	2.9×10^{-1}	1.2×10^{-1}
$\Sigma_{ABSORPTION}$	^6Li	-5.9×10^{-3}	-6.0×10^{-3}	-2.3×10^{-3}
	^7Li	-3.4×10^{-3}	-3.4×10^{-3}	-2.8×10^{-4}
	$^6Li + ^7Li$	-9.3×10^{-3}	-9.4×10^{-3}	-2.6×10^{-3}
$\Sigma_{ELASTIC}$	^6Li	1.8×10^{-2}	2.9×10^{-2}	6.4×10^{-3}
	^7Li	-1.8×10^{-2}	-1.9×10^{-2}	2.4×10^{-4}
	$^6Li + ^7Li$	0.0	1.0×10^{-2}	6.6×10^{-3}
$\Sigma_{INELASTIC}$	^6Li	4.3×10^{-3}	5.5×10^{-3}	1.3×10^{-3}
	^7Li	-1.1×10^{-2}	-1.1×10^{-2}	-3.9×10^{-4}
	$^6Li + ^7Li$	-6.7×10^{-3}	-5.5×10^{-3}	-6.5×10^{-3}
$\Sigma_{(n,2n)}$	^6Li	3.7×10^{-2}	3.9×10^{-2}	1.1×10^{-2}
	^7Li	-1.9×10^{-2}	-1.9×10^{-2}	-1.6×10^{-3}
	$^6Li + ^7Li$	1.8×10^{-2}	2.0×10^{-2}	9.4×10^{-3}
$\Sigma_{TOTAL\ COLLISION}$	^6Li	7.0×10^{-2}	9.0×10^{-2}	2.0×10^{-2}
	^7Li	2.3×10^{-1}	2.2×10^{-1}	1.1×10^{-1}
	$^6Li + ^7Li$	3.0×10^{-1}	3.1×10^{-1}	1.3×10^{-1}

In a later paper [53] Alsmiller et al extend their cross section sensitivity analysis to include the Princeton Plasma Physics Laboratory (PPPL) reference fusion power plant [54] based on flibe as the breeder and a broader range of materials. They compute breeding sensitivity profiles for the tritium producing reactions in ^6Li and ^7Li, Σ elastic for carbon, Σ (n,2n') for beryllium and identical changes in all the partial cross sections for fluorine and calculate the changes in breeding shown in Table VI resulting from the modifications to the cross sections given in Table V. In Table V, if a total cross section is specified in column 5, it is increased in accordance with the increases specified in the previous columns. If a partial cross section is specified, it is decreased in line with increases in the previous columns to retain a constant total cross section.

7. Data Uncertainties in Specific Materials

7.1 Niobium

The contribution of niobium data uncertainties to tritium breeding errors has been dealt with by Steiner [46][47], who used the Nordheim [55] method in his treatment of self-shielding in the niobium capture resonances. Gerstl and Henryson [56] employed the MC^2 -2 (57) code to generate group dependent self-shielding factors for niobium for use with the 100-group DLC-2D cross section set based on ENDF/B-III in ANISN (S_8P_3) calculations for assessment of the RTPR. This was used to carry out P_1, homogeneous, 2081-group fundamental mode calculations to give spectrum weighting for the shielded cross sections in the 100 group structure, varying the relative concentrations of the other constituents (^{6}Li, ^{7}Li, C, O, Al, Be) in the

Table V

Cross-Section Uncertainties Assumed for Various Partial Cross Sections

Element	Cross-Section Type Varied	Energy Range (MeV)	Percent Increase in Varied Cross Section δC	Cross-Section Type Varied to Compensate[a]
^{6}Li	$\Sigma_{(n,t)\alpha}$	$<1 \times 10^{-7}$	0.5	$\Sigma_{\text{total collision}}$
		$10^{-7} - 10^{-2}$	1.0	
		$10^{-2} - 10^{-1}$	1.0 - 2.0[b]	Σ_{elastic}
		$10^{-1} - 3 \times 10^{-1}$	5.0	
		$3 \times 10^{-1} - 5 \times 10^{-1}$	5.0 - 10[b]	
		$5 \times 10^{-1} - 7 \times 10^{-1}$	10 - 15	
		$7 \times 10^{-1} - 1 \times 10^{0}$	15	
		$1 \times 10^{0} - 1.7 \times 10^{0}$	15 - 10[b]	
		$1.7 \times 10^{0} - 1.4 \times 10^{1}$	10	
^{7}Li	$\Sigma_{(n,n't)\alpha,t}$	All energies	20	Σ_{elastic}
C	Σ_{elastic}	<4.8	3.0	$\Sigma_{\text{total collision}}$
		4.8 - 9.0	5.0	$\Sigma_{\text{inelastic}}$
		9.0 - 15	15	
Be	$\Sigma_{(n,2n')}$	1.85 - 6.4	10	Σ_{elastic}
		6.4 - 14	10 - 15[b]	
F	All partial cross sections	All energies	20	$\Sigma_{\text{total collision}}$

[a] See discussion in text.
[b] Linear interpolation was used between the values shown.

Table VI

Breeding-Ratio Uncertainties Due to the Cross-Section Variations Shown in Table IV

Element	Breeding Material j	$\delta R_j/R$ (%) ORNL Design with Nb	ORNL Design with V	LASL Design	PPPL Design
^{6}Li	^{6}Li	0.14	0.07	0.19	0.07
	^{7}Li	-0.01	-0.01	0.00	-0.04
	^{6}Li and ^{7}Li	0.13	0.06	0.19	0.03
^{7}Li	^{6}Li	0.26	0.35	0.02	0.00
	^{7}Li	5.60	5.56	2.42	1.95
	^{6}Li and ^{7}Li	5.86	5.91	2.44	1.95
C	^{6}Li			-0.82	
	^{7}Li			0.24	
	^{6}Li and ^{7}Li			-0.58	
Be	^{6}Li			2.51	1.33
	^{7}Li			-0.18	-0.10
	^{6}Li and ^{7}Li			2.33	1.23
F	^{6}Li				-1.02
	^{7}Li				-1.28
	^{6}Li and ^{7}Li				-2.30

mixture to represent various zones in the RTPR blanket. They found considerable spatial dependence of the self-shielded cross sections through the blanket and estimated a 10% enhancement in tritium breeding relative to the calculation carried out with infinite dilution cross section values. Investigations by Soran and Dudziak [58] who applied the Bondarenko formalism [59] showed that their treatment of the niobium resonances gave an increase of 7% in tritium breeding compared with unshielded cross sections for the TRPR. Clearly, choice of treatment of resonance self-shielding plays an important part in neutronics calculations, irrespective of uncertainties in the data.

Table III shows that niobium (nn') and (n,2n) data uncertainties can contribute considerably to tritium breeding errors in the Steiner model blanket, particularly the former; the (n,2n), due to partial cancellation of the breeding changes in ^{6}Li and ^{7}Li, less so. This may well not be true to the same extent in other blanket designs. In a later treatment [46] Steiner and Tobias vary the (n,2n) cross section together with the (nn') in such a way that the total inelastic cross section remains unchanged. Under these circumstances a much greater sensitivity to the (n,2n) cross section is noted (a change of -2.43% in T instead of -0.49% for a 25% reduction in σ(n,2n)). This is due predominantly to a large change in T6 caused by the loss in neutron multiplication, opposed by a rather small increase in T7. This arises because the (nn') reaction (which is increased) degrades the neutron spectrum less than the (n2n). Secondary neutrons from the (n2n) reaction (threshold ~9MeV), although more numerous by a factor 2, are very much less effective in exciting the $^{7}Li(nn'\alpha)t$ reaction, most of them falling completely below the reaction threshold. The effects of data uncertainties in total inelastic and (nn') and (n,2n) cross sections are obviously interlinked and an assessment of the requirements should take account of their interaction.*

---

* The problem of correlated cross sections and their uncertainties is dealt with in a more quantitative manner in the covariance formulation discussed by Gerstl et al [7]. In this they use first order perturbation theory to define a sensitivity profile P_{Σ_i} where $P_{\Sigma_i}\frac{\Delta\Sigma_i}{\Sigma_i}$ quantifies the relative change in a reaction rate R as a result of modifying the cross section Σi in the i^{th} energy group by $\Delta\Sigma i$. Gerstl et al define a covariance matrix $Cov(\Sigma i,\Sigma j)$, the elements of which link the cross section uncertainties in the i^{th} and j^{th} energy groups. The diagonal elements $Cov(\Sigma i,\Sigma i)$ are the usual uncorrelated cross section uncertainties expressed as the variance of Σi :-

$$Cov(\Sigma i,\Sigma i) = Var(\Sigma i) = E\{\delta\Sigma i^2\} = \Delta\Sigma i^2 \qquad (1)$$

The off-diagonal terms indicatecorrelations between the cross sections Σi and Σj. Thus the variance of the total reaction rate is given by

$$\left(\frac{\Delta R}{R}\right)^2 = \sum_{ij} P_{\Sigma i}P_{\Sigma j}\frac{Cov(\Sigma i,\Sigma j)}{\Sigma i\Sigma j} \qquad (2)$$

If the cross section uncertainties in all groups are uncorrelated, the variance of the total reaction rate will be at a minimum, given by:

$$\left(\frac{\Delta R}{R}\right)^2 = \sum_{i} \left(P_{\Sigma i}\frac{\Delta\Sigma i}{\Sigma i}\right)^2 \qquad (3)$$

while if they are fully correlated, as for example in the case where the cross section shape is known well, but the normalisation is in doubt, the variance reaches a maximum value of:-

$$\left(\frac{\Delta R}{R}\right)^2 = \left(\sum_{i} \left(P_{\Sigma i}\frac{\Delta\Sigma i}{\Sigma i}\right)\right)^2 \qquad (4)$$

Although the energy group covariances have been listed for a number of reactions [7] the problems of assigning correlations between separate reaction cross sections for a given element or isotope have not been addressed, much less the question of correlations between uncertainties for different elements that could arise for example through use of common standards or measuring techniques.

7.2 Lithium-6

Table III shows that the influence of the $^{6}Li(n,n'\alpha)t$ reaction cross section uncertainty is small. This is to be expected since the cross section is small in the high energy region where there are a lot of threshold reactions in other materials (including ^{7}Li) in competition. The ^{6}Li breeding reaction is essentially 1/V below 0.3MeV and absorbs a high fraction of the available neutrons below the MeV region, and any variation in cross section does not materially alter this fact. Downscattering offers no competition to the $^{6}Li(n\alpha)t$ reaction because the scattered neutrons remain available to it. In addition the cross section is well known because of its use as a standard.

7.3 Lithium-7

Since tritium breeding in ^{7}Li is accomplished via the threshold reaction $^{7}Li(nn'\alpha)t$, in a fusion reactor spectrum it finds itself in competition with other high energy neutron absorbing reactions and elastic scattering, (n,2n) and (nn') reactions. Table III shows that the breeding in ^{7}Li is a very strong function of the reaction cross section uncertainty in the Steiner benchmark blanket. To aim for a tritium breeding ratio uncertainty (standard deviation) of 2% due to this cause alone would demand an accuracy of ±9% in the cross section. This must be reduced considerably to achieve a given tritium breeding ratio to an accuracy of 2% against a background of uncertainties due to other causes. These will be uncertainties for other materials - Table IV shows that the uncertainties in other reactions in ^{7}Li do not affect breeding to any great extent. The request for 5% accuracy in WRENDA 76/77 [60] will barely meet this criterion. It can also be seen in Table IV that for "thermal" reactor concepts where tritium breeding in ^{7}Li is subdued in favour of neutron multiplication in beryllium [61] or lead [62] [63] the need for such accuracy in the $^{7}Li(n,n'\alpha)t$ cross section is reduced. It is of course replaced by the need for accurate beryllium or lead (n,2n) data.

7.4 Carbon Cross Section Data

Table VI (from Alsmiller et al [53] shows that in the "thermal" design the graphite elastic cross section gives opposing effects in the ^{6}Li and ^{7}Li breeding components, leaving a net effect of 0.58% change in total breeding sensitivity to the cross section changes set out in Table V. More detailed consideration of the shape of the sensitivity profile is necessary to make quantitative recommendations on the required accuracy improvements across the spectrum. An additional concern at high energy is the $C(n,n'3\alpha)$ reaction, which gives rise to tritium breeding uncertainty on account of uncertainties in both the cross section and secondary neutron parameters.

7.5 Beryllium (n,2n) Reaction Data

The two beryllium-containing designs examined by Alsmiller et al show basically similar behaviour in that the ^{6}Li $(n\alpha)t$ reaction rate is the more sensitive to changes in Be(n,2n) cross section, the ^{7}Li tritium breeding ratio showing a negative correlation due to the fact that the reactions are in competition with each other for neutrons of high energy. The effect is small in Alsmiller's analysis because as the (n,2n) cross section is increased, the elastic cross section is decreased. Once again in making a realistic appraisal of the sensitivity profiles one should critically examine the effects of the restriction indicated in Table V that the beryllium total cross section should remain constant. (See footnote on previous page)

7.6 Lead (n,2n) and (nn') data

Lead has been used in conceptual design studies by Gulf Atomic [62] and a Harwell/Culham study of a Reverse Field Pinch Reactor [63] though no data uncertainty assessments were made in either case. Lead shows considerable promise for neutron multiplication in DT fusion reactors on account of its high (n,2n) cross section which can lead to a thin blanket of the "thermal" type. The high reaction threshold energy of ~7MeV precludes further multiplication by the secondary neutrons by the same reaction starting from an initial reaction with a 14MeV neutron, but they are still efficient at promoting the $^{7}Li(nn'\alpha)t$ reaction. There is therefore a need to keep under

Table VII

Comparison of the Tritium Breeding Ratio, Neutron Multiplication, and Parasitic Reaction Rate for Niobium, Type 304 Stainless-Steel, and Nimonic-105 Structures

	Type 304 Stainless Steel	Niobium	Nimonic-105
Tritium breeding ratio			
$R_{^6Li}$	0.600	0.598	0.605
$R_{^7Li}$	0.927	0.920	0.858
R^a	1.53	1.52	1.46
Neutron multiplication	0.0277	0.0498	0.0176
Parasitic reaction rate	0.0305	0.0691	0.0881

[a] $R = R_{^6Li} + R_{^7Li}$ = total breeding ratio.

review not only the (n,2n) and the competing (n,n') reaction cross sections but also their secondary neutron energy and angular distributions.

7.7 Fluorine Data

In the PPPL flibe design [54] the fluorine cross section uncertainty shows a large negative influence on both ^{6}Li and ^{7}Li tritium breeding. To force the uncertainty in total tritium breeding to the 2% level (one standard deviation) would require ~17% accuracy in the total collision cross section, assuming that all the contributing partial cross sections were positively correlated across the whole spectrum. A more realistic figure of ~10% is necessary to ensure that the overall net standard deviation in tritium breeding due to this and other uncertainties falls within our specification.

7.8 Structural Materials

Various authors have carried out comparative studies of the nuclear performance of different structural materials in breeding blankets, including tritium breeding, neutron absorption and multiplication. Steiner [64] intercompares vanadium and niobium, Williams et al [65] niobium, nimonic-105 and type 304 stainless steel, while Cheng and Conn [66] report on tritium breeding with stainless steel, niobium, molybdenum, vanadium and aluminium in the UWMAK I blanket. Cross section uncertainties are not considered but it is possible to observe a meaningful correlation between tritium breeding ratio and neutron multiplication via (n,2n) reaction and parasitic reaction rate in the structural materials in Table VII, reproduced from reference 65.

Here the net absorption rate, comprising the difference between the parasitic absorption rate in the components of the structural material (the sum of the (n,p), (n,α) and (n,γ) reactions) and the multiplication rate via the (n,2n) reactions are directly correlated with the tritium breeding ratio,R. It can be seen that R+ parasitic reaction rate - neutron multiplication $\approx$1.53 for each material. The main differences are felt in tritium breeding from ^{7}Li. More detailed scrutiny of the contributions of the individual reactions will lead to estimates of improvements in cross section uncertainties required to reduce the uncertainty in tritium breeding. Although these will of course be composition dependent and therefore specific to a particular material choice and design, in carrying out a scoping survey, comparison between materials for tritium breeding ratio is only meaningful if the data uncertainties lead to the required minimum imprecision. Two points should be made:-

(i) The natural lithium/graphite blanket model described by Williams et al [65] has a very low structure fraction, of the order 2% overall. A more realistic structure fraction, while still giving an adequate tritium breeding ratio, will increase the parasitic absorption and neutron multiplication and consequently also the differences in tritium breeding between materials as a result of cross section uncertainties.

(ii) Uncertainties need to be reduced on the basis of the error in tritium breeding they lead to. Thus a lower percentage error should be sought in a large cross section. As before, the sensitivity profile gives a measure of the energy regions in which improvements are most profitable.

7.9 Spectrum Shifters

The term spectrum shifter is normally applied to a layer of material located between the front wall and the plasma, whose purpose is to prolong the life of the first wall by bearing the brunt of the charged particle and soft X-ray flux and soften the neutron energy spectrum. The ISSEC (Internal Spectral Shifter and Energy Converters)[67] concept achieves a tritium breeding ratio in excess of unity in spite of the soft spectrum it induces by including either beryllium- or lithium-containing materials within the ISSEC itself. Apart from silicon (in the form of SiC) all the other candidate materials for issecs have already been considered above.

An analogous effect on neutron spectra is noted for inertial confinement fusion, in that neutron moderation by elastic scattering and some multiplication via (n,2n) reactions on D and T can take place in the compressed pellet during the burn phase. Although this may prove a useful bootstrapping effect in complementing the alpha particle heating, it has been shown that considerable changes will occur in the neutron spectrum incident on the first wall [68]. The effects of these on tritium breeding and neutron heating have been considered by Beynon and Bryant [69] for a variety of breeding and structural materials. For a typical pellet size, the spectrum softening led in the worst case of a Li_7Pb_2 blanket to a 4.3% drop in tritium breeding ratio. The great majority of the neutrons suffer at most only a single interaction in the pellet, so an uncertainty in the elastic and (n2n) cross sections for D and T of 20%, even if they were all correlated would lead to a tritium breeding uncertainty below 1%.

8. Secondary Neutron Uncertainties

The problem of secondary neutron generation is a prominent one in fusion reactor neutronics because the high energy of the source neutrons makes (n,2n) and (n,n'xy) reactions energetically possible. The influence of the nuclear data describing the energy spectrum and to a lesser extent the angular correlation of the emerging neutrons is considerable on such parameters as the tritium breeding in ^7Li. The secondary neutron spectrum also determines the possibility of further (n,2n) and (n,nxy) reactions etc. The sensitivity analysis methods developed for examining the effect of cross section uncertainties on fusion reactor parameters have been extended by Gerstl [70] to include sensitivity profiles for secondary energy and angular distributions. He makes the point that these data are much less well known that the cross sections for secondary neutron production and the resulting uncertainties in tritium breeding could be correspondingly greater. So far there are no well formatted error files for secondary distributions. In addition to the secondary neutron energy and angular distributions, both of them double differential, the correlation between energy and angle would be highly desirable in the long term. It is clearly not possible to consider the effects of data uncertainties in such a scheme before it exists, and our quantitative appreciation of the influence of secondary neutron effects is limited to comparing data library treatments or making arbitrary changes in distribution temperature in evaporation models, etc.

8.1 Secondary Neutrons from the $^7Li(n,n'\alpha)t$ Reaction

Steiner [46][71] discusses the effect of the assumptions in the evaporation model used for the secondary neutron energy distribution. In this $\Theta(E)$ is the nuclear temperature expressed as a function of E, the incident neutron energy. He perturbs $\Theta(E)$ by ±50%, the increased value yielding a harder secondary spectrum. The most significant effect is that the fraction of the tritium breeding in ^7Li contributed by secondary neutrons from that reaction varies markedly, from 0.18 with the hard spectrum, 0.15 in the reference case and 0.09 in the softened spectrum with the low value of $\Theta(E)$. The differences between data sets has been investigated by Markovskii et al [72] who have carried out studies on the ETRT reactor (which is basically similar to Steiner's) using UKNDL [34] and ENDF/B - III [35]. They found that the difference in secondary neutron spectrum was responsible for a 7% difference in tritium breeding ratio. The probabilities of inducing a second tritium breeding reaction in ^7Li by neutrons generated by a first event at 14MeV are respectively 0.36 and 0.44 for UKNDL and ENDF/B - III. Markovskii et al varied the hardness of the ENDF/B evaporation spectrum by multiplying the distribution temperature by a coefficient K_v. The dependence of the tritium breeding ratio on K_v is shown in Fig. 2.

8.2 Beryllium Secondary Neutron Energy and Angular Distributions

The "thermal" reactor blankets and those containing flibe make use of beryllium as a neutron multiplier. Not only the actual (n,2n) cross section but also the energy and angular dependence of the emergent neutrons play a large part in determining the tritium breeding. Since beryllium exhibits a threshold energy of 2.8MeV the secondary neutrons from the Be(n,2n) reaction caused by a 14MeV neutron have enough energy to be able to repeat the interaction with another beryllium nucleus. In the case of flibe the secondary neutrons may alternatively have the opportunity to undergo the $^{7}Li(n,n'\alpha)t$ threshold reaction. That the enhancement in neutron availability and hence tritium breeding are very sensitive to the energy spectrum is demonstrated by Soran et al [73] in their intercomparison of ENDF/B - II and - III data in analysing the Reference Theta Pinch Reactor. The mean energy of secondary neutrons is ~3MeV lower in the latter data set (~4MeV cf ~7MeV). While the relevant processing codes gave the same integral cross sections from the two sets, DTF-IV [16] transport calculations on RTPR gave a 6% reduction in tritium breeding with the ENDF/B - III derived data. This is due to three effects:-

(i) reduction in number of $^{7}Li(n,n'\alpha)t$ reactions induced by the secondary neutrons

(ii) reduction in the number of additional Be(n2n) reactions caused by the secondaries. With ENDF/B - III data the total Be(n,2n) reaction rate is reduced by 15%

(iii) preferential forward emission leading to greater leakage of secondary neutrons directly through the blanket.

More recently Howerton and Perkins [74] have commented on the shortcomings of the latest ENDF/B format, in which it is not possible to describe the break-up modes for the $^{9}Be(n,2n)$ reaction recently evaluated by them. Their evaluation used 5 levels in ^{9}Be, 4 of them wide, while the ENDF/B - IV format permits only up to 4 narrow levels.

8.3 The Role of Integral Assemblies and Benchmark Experiments

In the development of fission reactor neutronics capability, subcritical and low power critical assemblies have been instrumental in checking both methods and nuclear data and similar experiments are likely to be equally valuable for fusion systems. In particular, validation of neutron spectrum and tritium breeding calculations will play an essential part in blanket development. Experiments fall into two categories according to purpose. Both usually comprise a 14MeV neutron source within an assembly of materials. In the first the object is to investigate as far as possible a single material in as uncomplicated a geometry as possible to simplify calculations to determine the consistency between calculated and measured parameters such as reaction rates, spectra etc. and point to possible data shortcomings. In the second a more determined attempt is made to simulate a reactor blanket design or features thereof, and generate more representative neutron spectra.

In the first category a number of experiments have been performed and analyses carried out on lithium [75-78] as spheres or cylinders and a wide variety of other materials, including LiD[79], LiF[80], Al, Ti, Fe, C and O [81] and beryllium [82][83]. Leonard [77] gives a comprehensive survey. Among the measurements made for comparison with calculations, have been the following:-

(i) reaction rate measurements in (n,p), (n,α) and (n,2n) threshold indicators

(ii) fission reaction rates and reaction rate ratios in fertile and fissile nuclides (^{238}U, ^{235}U, ^{237}Np, ^{232}Th, ^{239}Pu)

(iii) spectrum measurements using nuclear emulsions, proton recoil (liquid scintillation, gas proportional), ^{6}Li scintillation spectrometers and time-of-flight

(iv) spatial distribution of tritium production rates using β-counting techniques, including estimates of production in each lithium isotope by using samples highly enriched in either ^{6}Li or ^{7}Li.

Kuijpers [84] gives a useful discussion on unfolding neutron spectra in respect of the sensitivity to cross section uncertainties in the detectors.

The second category includes shielding experiments, obviously of great value for blanket/shield penetrations, and attempts to simulate the blanket configuration, of which an example is the work of Herzing et al[85]. In this they extended their Li metal sphere experiments[75] by cladding it in graphite and measured the altered T6 and T7 distributions for comparison with calculations. A full simulation of a CTR blanket is obviously out of the question and in designing an integral assembly consideration must be given at an early stage to the way in which the results are to be applied in adjusting the cross section data for the materials investigated. Beynon[86] points out that in the many bare lithium systems the mean neutron energy is ~4MeV while in lithium blanket systems with a reflector it is ~1MeV. He develops arguments to show that this mismatch must be avoided by proper design of the assembly. He makes use of the concept of the sensitivity profile[44] discussed briefly in section 7 and shows that if the integral assembly exhibits a similar profile to the CTR blanket of interest then it will be of optimum value for data adjustment. He illustrates this with comparative sensitivity profiles for the LiF spherical assembly experiment at Birmingham , UK[80] and the Harwell/Culham blanket model based on the Culham Conceptual Tokamak Reactor[87]. Fig. 3 shows the sensitivity profiles of breeding in ^{6}Li to the $^{6}Li(n\alpha)t$ reaction in each case while Fig. 4 shows the sensitivity profiles of total breeding to the iron total cross section, if the integral assembly has a 5mm thick spherical steel shell around the source to represent the first wall in its location between the plasma and the blanket. The poor match in sensitivity profiles shows that the steel shell does not adequately represent the 6% steel structure fraction distributed through the blanket model.

Adjustment in the iron data made by forcing agreement in the integral assembly will not ensure prediction accuracy for total tritium breeding in the blanket.

Reupke and Muir [88] express a similar viewpoint as a result of experience with their consistency analysis code ALVIN. Using this they carry out a minimum variance fit between calculated and measured $^{7}Li(n,n'\alpha)t$ tritium breeding rate distributions through a 14MeV neutron-driven LiD assembly, permitting variations in the $^{7}Li(n,n'\alpha)t$ cross section in attempts to improve the fit. Although the value of χ^2 for the fit improved considerably, they concluded that additional integral experiments with improved design are necessary to determine the sources of inconsistencies in the combined differential and integral data.

9. Conclusions

The accuracy target for blanket neutronics parameters such as tritium breeding rate cannot be rigidly decided. Any figure such as the 2% standard deviation suggested here, can be argued for and against - no doubt in the course of time closer limits on uncertainty will be demanded. An important point in choosing a value is that it enables us to pinpoint the worst sources of errors so that attention can be directed towards them. Fusion reactor blanket technologists are still in the process of evaluating many concepts, each with its own mix of materials range of neutron spectra etc, and if these are to be judged fairly on neutronics grounds, adequate data is needed followed at a later stage by more accurate data for those materials selected. At present lithium is the only material which is certain to be included in a breeding blanket.

Two main points have emerged in this review; firstly that to the old adage that a calculation is only as good as the data put into it, one must also add the warning that the accuracy may well be the victim of the approximations used; and secondly that the sensitivity of estimated parameters such as tritium breeding to nuclear data uncertainties is very system dependent. In the high energy neutron spectra of fusion reactor blankets, the effects of competing threshold reactions, (n,2n) and (nn'),including $^{7}Li(n,n'\alpha)t$ in producing secondary neutrons that can still take part in subsequent threshold reactions, are very important. The influence of uncertainties, not only in the cross-section data but also in the secondary neutron energy and angular distributions and correlations between these uncertainties has not been adequately studied yet, even for lithium-7, let alone for possibly important materials such as beryllium and lead and a wide range of candidate materials for the blanket structure.

REFERENCES

[1] BADGER, B., et al. UWMAK-III, High-Performance, Non-Circular Tokamak Power Reactor Design. UWFDM-150 (Dec. 1975).

[2] MILLS, R.G. (Ed.), A Fusion Power Plant. MATT-1051 (Aug. 1974).

[3] SEKI, Y., et al. Tritium Breeding in Ceramic Lithium Compound Blankets. Conf. 74042, pp 77-86.

[4] POWELL, J.R., et al. Studies of Fusion Reactor Blankets with Minimum Radioactive Inventory and with Tritium Breeding in Solid Lithium Compounds. BNL-18236 (June 1973).

[5] VERSCHUUR, K.A., BROCKMANN, H. Neutronic and Photonic Studies on Fusion Reactor Blankets with Low Lithium and Tritium Inventories. Jül-1261/RCN-236 (Dec. 1975).

[6] HANCOX, R., et al. A 600 MW(e) reversed field pinch reactor study. IAEA Workshop on Fusion Reactor Design, Madison, 10-21 October 1977.

[7] GERSTL, S.A.W., DUDZIAK, D.J. and MUIR, D.W. Application of Sensitivity Analysis to a Quantitative Assessment of Neutron Cross-Section Requirements for the TFTR. LA-6118-MS (1975).

[8] CROCKER, V.S., BLOW, S., WATSON, C.J.H. Nuclear Cross-Section Requirements for Fusion Reactors CLM-P240 (1970).

[9] ABDOU, M.A., CONN, R.W. Nucl. Sci. Eng. 55 3 (1974) 256.

[10] BACHMANN, H., et al. Nucl. Sci. Eng. 67 1 (1978) 74.

[11] SANTORO, R.T., et al. Nucl. Technol. 37 3 (1978) 274.

[12] DUDZIAK, D.J. An Assessment of Nucleonic Methods and Data for Fusion Reactors, LA-UR-76-2086.

[13] MAYNARD, C.W. Trans. Am. Nucl. Soc. 23 (1976) 11.

[14] CARLSON, B.G. Solution of the Transport Equation by S_n Approximations, LA-1599 (1953).

[15] ENGLE, W.W. Jr. A User's Manual for ANISN, A One-Dimensional Discrete Ordinates Code with Anisotropic Scattering, K-1963, Computing Technology Centre, Union Carbide Corp. (1967).

[16] LATHROP, K.D. DTF-IV, a FORTRAN-IV Program for Solving the Multigroup Transport Equation with Anisotropic Scattering, LA-3373 (1965).

[17] RAGHEB, M.M.H., et al. Atomkernenergie 31 3 (1978) 192.

[18] CHAPIN, D.L. A Comparison of the DT Neutron Wall Loading Distributions in several Tokamak Designs, MATT-1186.

[19] ABDOU, M.A., JUNG, J. Nucl. Technol. 35 1 (1977) 51.

[20] DAENNER, W. Neutron Flux Asymmetry in Toroidal Geometry. IPP 4/101 (Sept. 1972).

[21] CONSTANTINE, G., PICKETT, D. A Neutronic Study of the Culham Conceptual Tokamak Reactor Mk II, Proceedings of the 9th Symposium on Fusion Technology, Garmisch Partenkirchen (June 1976) pp 649-655.

[22] CHAPIN, D.L. Comparative Analysis of a Fusion Breeder Reactor in Cylindrical and Toroidal Geometry using Monte Carlo, MATT-1234.

[23] CONN, R.W., et al. Trans. Am. Nucl. Soc. 23 (1976) 12.

[24] SEED, T.J., et al. TRIDENT: A Discrete Ordinates Code with Toroidal Geometry Capabilities, Trans. Am. Nucl. Soc. 23 (1976) 12.

[25] CASHWELL, E.D., et al. MCN: A Neutron Monte Carlo Code, LA-4571 (1972).

[26] VERSCHUUR, K.A. Neutronics in the Toroidal Belt Geometry of a Screw-Pinch Reactor, presented at the 10th Symposium on Fusion Technology, Padova, (Sept. 1978).

[27] SANTORO, R.T., et al. Nucl. Technol. 37 1 (1978) 65.

[28] EL-GUEBALY, L.A., MAYNARD, C.W. Monte Carlo Calculations for a Fusion Reactor Blanket and Shield, FDM79, University of Wisconsin (Jan. 1974).

[29] TAKAHIRO, I.D.E., et al. Evaluation of Neutron Streaming through Injection Ports in a Tokamak, JAERI M6475.

[30] CONSTANTINE, G., et al. UKAEA Research Group Report, CLM-R136 (1975).

[31] CONSTANTINE, G. Possible Improvements to a Basic Cellular Thin Blanket Fusion Reactor Configuration, presented at the 10th Symposium on Fusion Technology, Padova (Sept. 1978).

[32] RHODES, W.A., MYNATT, F.R. The DOT-III Two Dimensional Discrete Ordinates Transport Code ORNL-TM-4280 (1973).

[33] STRAKER, E.A., et al. The MORSE Code - A Multigroup Neutron and Gamma Ray Monte Carlo Transport Code, ORNL-4585 (1970).

[34] PARKER, K. AWRE 0-70163 (1963).

[35] OZER, O., GARBER, D. ENDF/B Summary Documentation, BNL-17541 and ENDF-201 Brookhaven National Laboratory (1973).

[36] HOWERTON, R.J., et al. Evaluated Nuclear Cross Section Library, UCRL 50400, Vol. 4, Lawrence Livermore Laboratory (1971).

[37] WEISBIN, C.R., et al. MINX - A Multigroup Interpretation of Nuclear Cross Sections. Trans. Am. Nucl. Soc. 16 (1973) 127.

[38] WRIGHT, R.Q., et al. SUPERTOG: A Program to Generate Fine Group Constants and P_n Scattering Matrices from ENDF/B, ORNL-TM-2679 (1969).

[39] GREENE, N.M., et al. AMPX - A Modular Code System for Generating Coupled Multigroup Neutron-Gamma Libraries from ENDF/B, ORNL-TM-3706 (1976).

[40] EVANGELIDES, G., LINDSTROM, D. Trans. Am. Nucl. Soc. 23 (1976) 19.

[41] ALSMILLER, J.R., et al. Trans. Am. Nucl. Soc. 19 (1974) 463.

[42] STEINER, D. Nucl. Fusion 14 (1974) 33.

[43] STEINER, D. Analysis of a Benchmark Calculation of Tritium Breeding in a Fusion Reactor Blanket: the United States Contribution. ORNL-TM-4177 (Apr. 1973).

[44] BARTINE, D.E., et al. Cross Section Sensitivity of Breeding Ratio in a Fusion-Reactor Blanket, Nucl. Sci. Eng. 53 3 (1974) 304.

[45] BARTINE, D.E., et al. SWANLAKE, A Computer Code Utilising ANISN Transport Calculations for Cross Section Sensitivity Analysis, ORNL-TM-3809 (1973).

[46] STEINER, D., TOBIAS, M. Nucl. Fusion 14 2 (1974) 153.

[47] STEINER, D. ORNL-TM-4200.

[48] GREENE, N.M., et al. XLACS: A Program to Produce Weighted Multigroup Neutron Cross Sections from ENDF/B, ORNL-TM-3646 (1972).

[49] GREENE, N.M., CRAVEN, C.W. Jr. XSDRN: A Discrete Ordinates Spectral Averaging Code, ORNL-TM-2500 (1969).

[50] ALSMILLER, R.G., et al. Trans. Am. Nuc. Soc. 19 (1974) 463.

[51] FRAAS, A.P. ORNL-TM-3096 (1973).

[52] DUDZIAK, D.J. Discrete Ordinates Neutronic Analysis of a Reference Theta Pinch Reactor (RTPR) LA-DC-72-1427 (1972).

[53] ALSMILLER, R.G., et al. Comparison of the Cross Section Sensitivity of the Tritium Breeding Ratio in Various Fusion Reactor Blankets, Nucl. Sci. Eng. 57 2 (1975) 122.

[54] GREENSPAN, E., PRICE, W.G. Jr. Tritium Breeding Potential of the Princeton Reference Fusion Power Plant. Conf. 740402-P2, San Diego (1974).

[55] NORDHEIM, L.W. Symp. Appl. Math. XI (1961) 58.

[56] GERSTL, S.A.W., HENRYSON, H., II, Trans. Am. Nucl. Soc. 18 (1974) 25.

[57] TOPPEL, B.J., HENRYSON, H., II, Trans. Am. Nucl. Soc. 16 (1973) 126.

[58] SORAN, P.D., DUDZIAK, D.J. Application of Bondarenko Formalism to Fusion Reactors LA-UR 75-351 (1975).

[59] BONDARENKO, I.I., et al. Group Constants for Nuclear Reactor Calculators, Consultants Bureau Enterprises, Inc., New York (1974).

[60] LESSLER, R.M. (Ed). WRENDA 76/77 INDC (Sec)-55/URSF.

[61] DARVAS, J. A Design with Low Lithium and Tritium Inventories, Nucl. Fusion, Special Supplement on Fusion Reactor Design Problems (1974) 377.

[62] - Conceptual Design Study of a Non-circular Tokamak Demonstration Fusion Power Reactor, Gulf Atomic, GA-13992, (Nov. 1976).

[63] BAKER, L.J. Some Implications of a Cellular Structure in Minimum Thickness Fusion Reactor Blankets, presented at the 10th Symposium on Fusion Technology, Padova (Sept. 1978).

[64] STEINER, D. Nucl. Fusion 14 1 (1974) 25.

[65] WILLIAMS, M.L., et al. Nucl. Technol. 29 3 (1976) 384.

[66] CHENG, E.T., CONN, R.W. Nucl. Sci. Eng. 62 4 (1977) 601.

[67] CONN, R.W., et al. New Concepts for Controlled Fusion Reactor Blanket Design, UWFDM-115 (1974).

[68] BEYNON, T.D., CONSTANTINE, G. A Study of Fusion Neutron Heating in Laser Compressed DT Spheres, J. Phys. G: Nuclear Physics 3 (1977) 81.

[69] BEYNON, T.D., BRYANT, R. To be published.

[70] GERSTL, S.A.W. Sensitivity Profiles for Secondary Energy and Angular Distributions LA-UR 77-917.

[71] TOBIAS, M., STEINER, D. Cross Section Sensitivity of Tritium Breeding in Fusion Reactor Blankets, Conf. 740402, San Diego (1974) 185.

[72] MARKOVSKII, D.V., et al. Influence of Neutron Constants on the Behaviour of a Thermonuclear Reactor Blanket, IAE 2579 (1975).

[73] SORAN, P.D., et al. Effect of Be (n,2n) Multigroup Treatment on Theta Pinch Blanket Neutronics, Conf. 740402, San Diego (1974) 172.

[74] HOWERTON, R.J., PERKINS, S.T. Comments on Beryllium (n,2n) Cross Sections in ENDF/B- -IV and -V, Nucl. Sci. Eng. 65 1 (1978) 201.

[75] HERZING, R., et al. Nucl. Sci. Eng. 60 2 (1976) 169.

[76] BACHMANN, H., et al. Nucl. Sci. Eng. 67 1 (1978) 74.

[77] LEONARD, B.R. A Compendium of 14MeV Neutron Source Experiments, Proc. Magnetic Fusion Energy Blanket and Shield Technology, March 29-April 2, 1976, Brookhaven National Laboratory, ERDA-76-117-1 (1976) p66.

[78] FRITSCHER, U., et al. Determination of Neutron Spectra and Cross Section Sensitivity of Tritium Production in a Lithium Sphere, presented at 10th Symp. on Fusion Technology, Padova, 1978.

[79] WYMAN, M. An Integral Experiment to Measure the Tritium Production from ^{7}Li by 14MeV Neutrons in a Lithium Deuteride Sphere, LA-2234, (1972).

[80] SCOTT, M.C. (Birmingham University) to be published.

[81] HANSEN, L.F., et al. Nucl. Sci. Eng. 60 1 (1976) 27.

[82] BASU, T.K., et al. Experimental Studies of Neutron Multiplication from Beryllium (n,2n) Reaction in CTR Blankets, presented at 10th Symp. on Fusion Technology, Padova, (1978).

[83] DRAKE, D.M., et al. Nucl. Sci. Eng. 63 4 (1977) 401.

[84] KUIJPERS, L.J.M. Spectrum Unfolding from Activation Measurements in a CTR Model Blanket Experiment: Comparisons and Sensitivity Analysis, Jül-1435, July 1977.

[85] HERZING, R., et al. Nucl. Sci. Eng. 63 3 (1977) 341.

[86] BEYNON, T.D., et al. The Design and Analysis of Integral Assembly Experiments for CTR Neutronics. IAEA Specialists' Mtg. on Shielding and Integral Experiments, Vienna, Oct. 1976.

[87] MITCHELL, J.T.D., HOLLIS, A.A. A Tokamak Reactor with Servicing Capability Proc., 9th Symp. on Fusion Technology, Garmisch Partenkirchen, (1976).

[88] REUPKE, W.A. Consistency Analysis of Fusion Reactor Neutronics Data; Tritium Production, Trans. Am. Nucl. Soc. 23 (1976) 21.

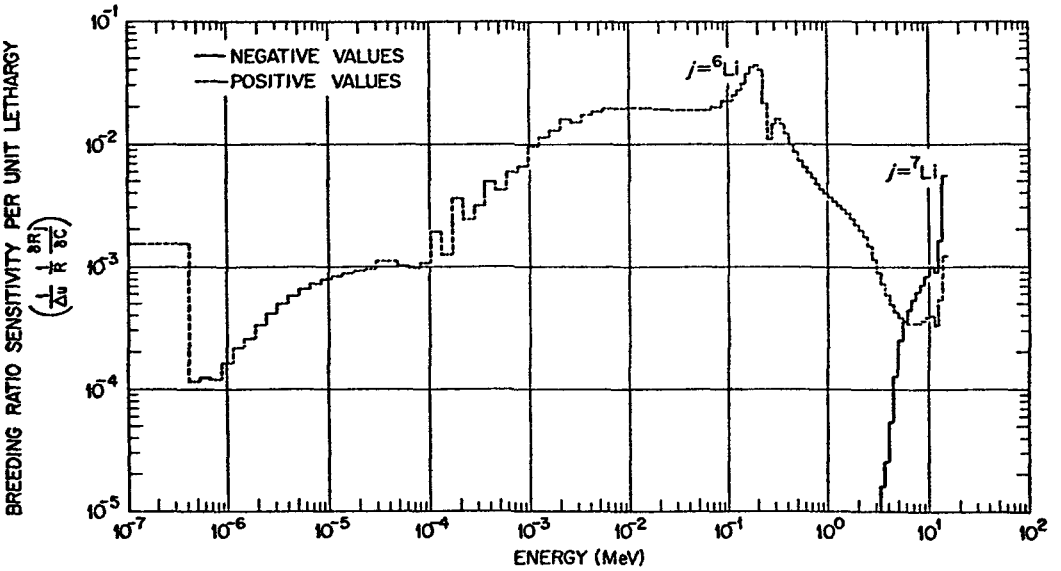

Fig. 1 **Breeding ratio sensitivity per unit lethargy versus energy for the ^{6}Li$(n,t)\alpha$ cross section.**

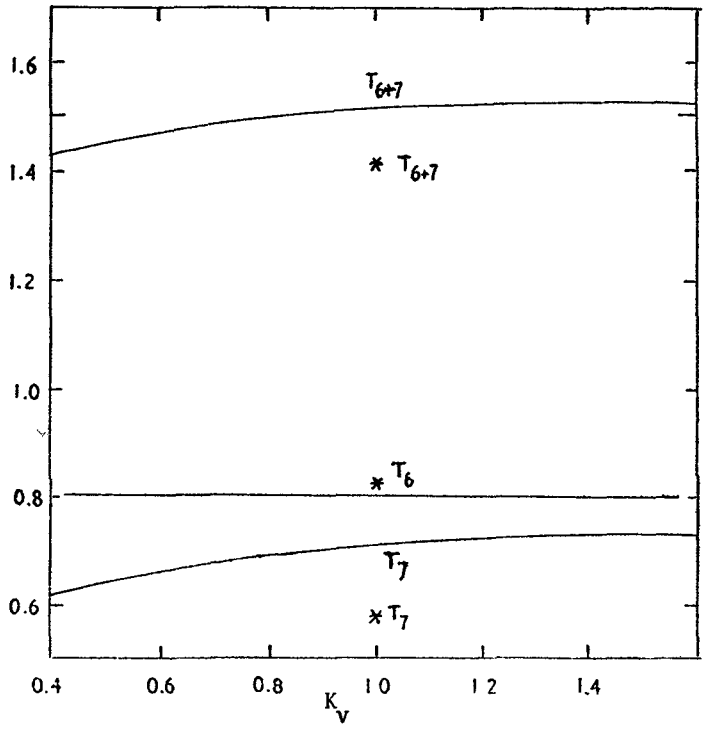

Fig. 2 Dependence of tritium breeding in blanket of ETRT reactor on hardness of neutron spectrum of $^{7}Li(n,n'\alpha)T$.
*- calculation with UKNDLconstants for ^{7}Li.

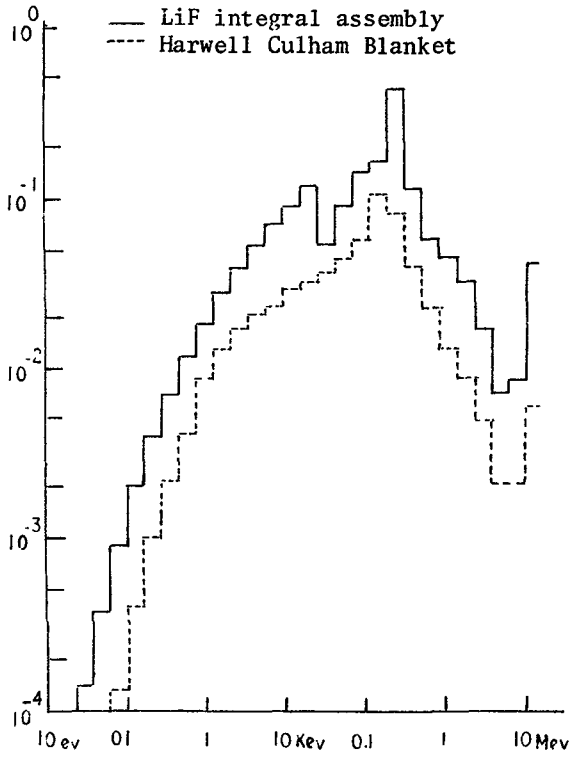

Fig. 3 Comparisons of sensitivity profiles of breeding in ^{6}Li to the $^{6}Li(n,\alpha)T$ reaction for the Birmingham LiF experiment and a Harwell-Culham conceptual design.

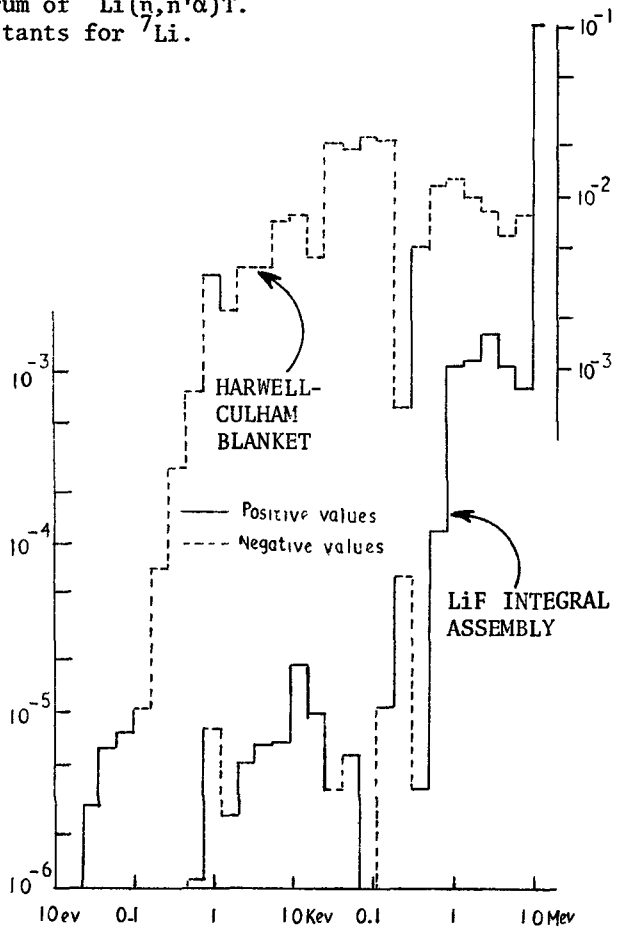

Fig. 4 Sensitivity of the total tritium breeding to iron total cross sections in the HC design and in the Birmingham LiF experiment.

Review of Nuclear Heating in Fusion Reactors

AG-159/A2
Review Paper

Yasushi Seki
Japan Atomic Energy Research Institute
Tokai-mura, Ibaraki-ken, Japan

ABSTRACT

The mechanism, calculational method, required types of data for nuclear heating calculation are briefly reviewed. The proposed materials in the blanket and shield of fusion reactors for which the nuclear data are required for heating calculations are enumerated. The significance and related problems of nuclear heating in various components of fusion reactors are described. Nuclear data requirements for the nuclear heating calculations and required experiments for the data testing are presented.

I. INTRODUCTION

The scientific feasibilities of both magnetically and inertially confined D-T fusion reactors are expected to be demonstrated within several years. This review will be focused on nuclear heating in Tokamak fusion reactors as they are in the most advanced design stage and the reviewer has the experience in the nuclear heating calculations for two Tokamak type reactors.[1],[2] However, except for some differences caused by variations in the materials and subcomponents involved in each reactor type, many problems related to nuclear heating are common in all fusion reactor types. Therefore, most of the discussions presented here will be applicable to other types of reactors with little modifications.

Nuclear heating in the blanket of a fusion power reactor will be utilized for generating electricity. In the rest of the reactor components, the nuclear heat generated is considered useless or a nuisance because its removal is required in most cases. The heat removal becomes a serious problem particularly in the components where liquid helium temperature must be maintained (e.g., superconducting magnets and cryopumps). The total refrigeration power required for these components must be lower than allowed from economical balance which is usually represented as less than a certain fraction of the net electrical power output of the reactor. Therefore, one of the most important considerations in the blanket and shield design of a

fusion power reactor will be enhancing the nuclear heat deposition in the blanket while reducing that to other components and especially suppressing that in cryogenic components to the practical minimum.

The uncertainty in the calculated nuclear heating rate at various parts of a reactor is caused by

1) the uncertainty in nuclear data for a) radiation transport calculation, and b) kerma factor* calculations,
2) the error introduced in processing nuclear data into multigroup cross section sets which may be used in transport calculations**,
3) the error in kerma factor calculations, and
4) the deficiency in radiation transport calculations.

The required accuracy for the spatial distribution of the nuclear heating rate is suggested to be ± 10 ∿ 20% in fission reactor design in general. The requirement should be less stringent for fusion reactor blankets with lower power density.+ At present, the lack of experimental data on nuclear heating in fusion reactor systems precludes one from stating anything definite, but it seems quite apparent that the state-of-the-art for the nuclear heating calculation is far from satisfying the suggested requirement. For instance, there is a report showing that the uncertainty in the neutron transport cross sections alone may cause ∿ 100% error in the calculated nuclear heating in the superconducting toroidal field coil of an experimental power reactor.(3) The uncertainty study of Ref. 3 was conducted using a one-dimensional calculational model. Similar studies to see the effect of nuclear data uncertainties upon nuclear heating in fusion reactors have been conducted.(4)-(7) In the case where more realistic and hence more complex configurations with various penetrations through blanket and shield are treated(24)-(27), the deficiency in the particle transport calculation method may cause additional large errors in the calculated nuclear heating. Since the nuclear data requirements for the radiation transport calculations will be treated by other reviewers, this review

---

*Kerma stands for Kinetic Energy Released in Materials.

**Multigroup processing may be omitted when continuous energy Monte Carlo method is employed.

+ A target accuracy of 10∼20% was suggested also for fusion shielding in Ref. 41.

will deal mainly with the nuclear data directly related to nuclear heating calculations, namely, kerma factor calculations.

The mechanism, the required types of nuclear data and the method for the calculation of nuclear heating in fusion reactors will be briefly reviewed in Section II. In Section III, the proposed materials in various types of blanket and shield for which the nuclear data are required are given. The significance of nuclear heating in the blanket and shield is also described in this section. In Section IV, nuclear heating in other components which may become critical in the reactor design is treated. Finally, nuclear data requirements for the nuclear heating calculations and related experiment proposals are given in Section V.

II. NUCLEAR HEATING CALCULATION

II.1. Mechanism of Nuclear Heating

The mechanism of nuclear heating in a fusion reactor[2] is shown in Fig. 1. As a result of the D-T fusion reaction, a 14-MeV neutron and a 3.5-MeV alpha particle are created. The alpha particles are mostly confined in the plasma until most of their energies are given to heating plasma particles and the energies will eventually be deposited on the first wall surface in the form of electromagnetic radiation and particle diffusion. If a diverter is present, only the particles are diverted away from the first wall to the diverter region.

On the other hand, the 14-MeV neutrons without any electric charge will mostly penetrate through the first wall and interact with the materials in the blanket producing charged particles and/or some more neutrons and/or gamma rays depending on which reaction the neutron will undergo. The emitted charged particle will deposit most of its energy in the immediate vicinity (compared to neutron mean-free path) of the neutron reaction. The secondary gamma rays produced will transport longer distance in the blanket, but ultimately transfer most of their energy to atoms of the blanket elements through photoelectric absorption, Compton scattering, and pair production processes. The secondary neutrons produced will undergo similar processes as the source neutrons, generating further charged particles, gamma rays and neutrons. All these heat depositions originating from the 14-MeV neutron are defined here as the nuclear heating. Total energy deposited per incident neutron in a blanket will depend on the numbers and types of exothermic and

endothermic reactions occurring in the blanket and also on the energies carried away by the neutrons and gamma rays escaping from the blanket. In many of the Tokamak reactor designs, the nuclear heating in a blanket is calculated to be around 17 MeV per incident source neutron[5] which usually amounts to more than 95% of the total nuclear heating for the whole reactor system.

II.2. Required Nuclear Data

As described in II.1, neutrons and gamma rays transport before they deposit energy in the blanket. Hence, the nuclear heating calculation is generally carried out in two steps. Firstly, the radiation transport in a fusion reactor is calculated resulting in spatially and energy-dependent neutron and gamma ray fluxes. Secondly, kerma factors are multiplied to the neutron and gamma ray fluxes to obtain nuclear heating rate. Accordingly, required nuclear data for nuclear heating calculation may also be classified as those for radiation transport calculation and those for kerma factor calculation. Since the former will be described in detail by other reviewers, the nuclear data required for kerma factors are mainly described here.

The 14-MeV neutrons will go through wider variety of reactions in the blanket than fission neutrons because of their higher energy. In order to calculate kerma factors accurately, extensive nuclear data information for each of the reactions are necessary. Beside the cross sections, the emission probability and energy distribution of every emitted particle and gamma ray, the energy resulting from mass conversion in the reaction and the average decay energy per reaction are required for each reaction.

II.3. Kerma Factor Calculation

The concept of kerma factors was originally introduced in the field of health physics for calculating biological radiation dose. Kerma is defined as the total kinetic energy of the charged particles that are produced by neutrons and gamma rays, per unit mass of the irradiated material. In the course of calculating nuclear heating in fusion reactor blankets[8], the kerma factors for some elements of interest in blankets have been generated for the first time by Ritts et al.[9] The calculational method for obtaining kerma factors introduced in the Ritts' work was not general enough to permit accurate calculations of nuclear heating for the large number of materials required in fusion reactors. To solve this situation,

Abdou et al. have produced a computer code MACK[10] which calculates neutron kerma factors using ENDF/B data. As fusion reactor neutronics calculations were carried out in many places, this code came to enjoy a wide distribution since it was included in the RSIC code collection[11] of the Oak Ridge National Laboratory.

The evaluation of gamma ray kerma factors is relatively easy and is normally performed by modifying the codes which generate photon-interaction multigroup cross sections, such as MUG[12] and GAMLEG.[13] The most recent version is the code SMUG which is one of the modules in the AMPX code system[14] for generating coupled multigroup neutron-gamma ray libraries from ENDF/B. It may be of some interest to note that similar code systems for calculating nuclear heating has been developed at the Los Alamos Scientific Laboratory[15], the Casaccia Laboratory in Italy[16], the Institute of Plasma Physics, Garching[38], and the Japan Atomic Energy Research Institute[17].

It was pointed out by Abdou and Maynard[18] that the gamma ray production data employed for nuclear heating calculations were sometimes not consistent with the neutron nuclear data as to energy conservation. They showed the error in the calculated nuclear heating in some fusion reactor systems caused by the above inconsistency by applying the so-called direct energy balance method.[19] This method, based on the kinematic equations of all nuclear reactions for every element in a blanket, gives total nuclear heating in a blanket accurately, but not the spatial distribution of nuclear heating rate. The method was developed to serve as a validation tool for the accuracy of the calculated total nuclear heating.

Recently, the improved version of the MACK code, MACK-IV[20] has been developed. Also, a comprehensive ENDF/B processing system NJOY[21] has been made which includes kerma factor calculation module based completely on ENDF/B-IV data. Both of these new codes attempt to solve the inconsistency problem arising from the lack of energy-conserving gamma production data in ENDF/B-IV. There seems to be still some problem remaining which precludes completely automatic generation of neutron kerma factors without some knowledge of ENDF/B-IV data status related to gamma production. MACK-IV provides for the choice of two calculational paths to avoid this problem, while NJOY gives out warning messages requesting reexamination of obtained kerma factors when the problem arises.

III. NUCLEAR HEATING IN BLANKET AND SHIELD

III.1. Materials Employed in Blanket and Shield

In a typical Tokamak reactor, more than 95% of nuclear heating is deposited in the blankets. It is a well known fact that if a D-T fusion reactor is to be self-sustaining in tritium cycle, the blanket of the fusion reactor must have lithium in one form or another. Accordingly, the use of lithium in the form of liquid metal, the molten salt FLIBE, alloys (LiAl, Li_4Pb, etc.) and solid compounds (Li_2O, Li_2AlO_3, etc.) have been proposed. Nuclear heating in each of these materials has been calculated in the corresponding fusion reactor design employing these materials. Beside these lithium bearing materials, breeding blankets usually consist of neutron reflectors (graphite, stainless steel), structural materials (stainless steel, Mo, Nb, Al, etc.), primary coolants if necessary (He, water, etc.) and in some cases neutron multipliers (Be, Pb, etc.) In the case of fusion-fission hybrid reactors, fissile materials are also introduced into the blanket.

In addition to these tritium breeding blankets, separate shield is generally required between the blankets and superconducting toroidal field coils (TFC) to further reduce radiation damage to the sensitive components of superconducting magnets (SCM). When a shielding was made to satisfy the requirement imposed by the radiation damage to superinsulation and copper (or aluminum) stabilizer of SCM, the nuclear heating in the TFC was shown to be reduced to insignificant level for an experimental reactor with a low neutron wall loading (0.17 MW/m^2) and a high duty factor (50%)[1]. For the additional magnet shield, more or less conventional shielding materials familiar in fission reactors such as concrete, borated graphite and lead have been proposed. In cases when hands-on maintenance of the reactor is requested, the shielding materials must be selected taking into account their induced activation.

On the other hand, the nonbreeding blankets used solely for the purpose of efficient radiation shielding have been proposed for the near term fusion facilities with low tritium consumption not requiring tritium production. In almost every recent tokamak reactor design, nonbreeding blankets are partially placed in the inner toroidal section of the blanket so as to make the reactor compact and hence economical at the cost of reduced tritium production. As the shielding material for nonbreeding blankets, the use of

stainless steel, boron carbide, borated water, lead, ordinary and heavy concrete, etc., has been proposed. The use of effective, but expensive, shield material such as tungsten or tantalum alloys may be justified[39] in the inner toroidal blanket because the reduction of inner blanket thickness results in large capital cost reduction.

III.2. Nuclear Heating in Blanket and Shield

Nuclear heating rate in the blanket and shield is generally the largest at the first wall and it decreases almost exponentially with the distance from the first wall as may be seen in an example in Fig. 2 for JAERI experimental fusion reactor (JXFR)[1]. In the regions where exothermal reactions with 1/v characteristics at low neutron energy such as $^{6}Li(n,\alpha)$ reactions are dominant, the nuclear heating rate tends to decrease more slowly than exponential. Only about 10% of the total nuclear heating is deposited in the stainless steel first wall due to the penetrability of neutrons as shown in Table I.[1] On the other hand, ions, neutral atoms and electromagnetic radiation from the plasma deposit most of their energy on the surface of the first wall, diverter or limiter. This causes the high heat load on the first wall and localized high temperature spots which make the heat removal from the first wall the most difficult task.

The total energy of the electromagnetic radiation and particle diffusion from the plasma is 3.5 MeV per fusion reaction. In the absence of a diverter, all this energy will be deposited on the first wall resulting in a surface heating of 0.25 P_w where P_w is the neutron wall loading caused by a 14-MeV neutron per fusion reaction. On the other hand, for typical first wall materials, the total nuclear heating per unit area of the first wall is $\sim f P_w \Delta x$ where f is $\sim$ 0.05 to 0.1 and Δx is the thickness of the first wall which is typically $\sim$ 0.2 to 1 cm. Therefore, the surface heat load can be 3 to 25 times higher than the nuclear heating in the first wall.

The total amount of nuclear heating is more than 80% of the total energy recovered per fusion reaction. However, the energy deposited by neutron-induced reactions and secondary gamma rays is distributed in a large blanket volume. Therefore, the power density and the heat removal problem in the blanket are much less than those in the first wall. One may also note that the power density in a fusion reactor blanket is approximately an order of magnitude lower than that in a fission reactor.

IV. NUCLEAR HEATING IN OTHER COMPONENTS

Nuclear heating rates in the components outside the magnet shield will be generally less than 10^{-4} W/cm^3 which will be insignificant in most cases. When the component must be maintained at the liquid helium temperature and/or the existence of some penetration in the shield does not attenuate the radiation as anticipated, nuclear heating in those components outside the shield must be closely examined.

The large amount of electricity required for the refrigeration to deal with the nuclear heating in the superconducting toroidal field coil has been recognized from the early days of fusion reactor design.[22],[23] Containment of higher than 10^8K plasma using $\sim$ 4K superconducting magnets has been a favorite topic often quoted as an example to demonstrate the difficulty of fusion reactor technology. It has been said on some occasions that the thickness of the magnet shield must be optimized to yield the best trade off between the capital cost gain obtained by the compactness of the reactor and the reduction of the required refrigeration power for the magnets. This optimization is valid for a low duty cycle, high instantaneous power producing facilities such as TNS and ignition test reactors which are envisioned as near term machines to be built before the experimental reactor. However, even for an experimental reactor with 50% load factor[1] it has been shown that the limiting factor for determining the minimum blanket thickness is not the instantaneous flux effect such as nuclear heating, but the cumulative fluence effects such as the long life induced activity accumulation and the radiation damage. In the case of a commercial fusion power reactor with higher load factor it seems to be certain that when adequate shield is provided to cope with the fluence effects, the nuclear heating in the magnet becomes negligibly small in comparison with other heat sources. In the detailed design of toroidal field coil magnets for JXFR[1] the nuclear heating in TFC amounted to less than 15% of the total heat load in TFC.

The nuclear heating in the cryopanels of cryosorption or cryocondensation pumps for evacuating the main vacuum vessel and/or neutral beam injector has been recently calculated.[24],[25],[40] In contrast to the superconducting magnets which can be shielded from radiation, there always exists streaming paths from the plasma to these vacuum pumps through which neutrons and gamma rays can penetrate. There are some ideas to plug these paths when

the plasma is in ignited mode.[26] The feasibility of moving heavy shield plugs at high speed twice for every burn pulse seems questionable to the reviewer. The nuclear heating in the cryopanels of the neutral beam injectors in TFTR has been found to be sufficiently small.[25] It was also found to be allowable in the case of JXFR for the nuclear heating in the cryopanels of main and injector vacuum pumps.[24] But the problem of nuclear heating calculations by radiation through penetrations involve complex geometry which is strictly dependent on each reactor design and on the operating conditions of each reactor that the results thus obtained are difficult to generalize.

Radiation streaming through diagnostic penetrations in TFTR has been recently calculated[27], which should also be problem dependent. There may be some troublesome effects created by nuclear heating to the heat sensitive semiconductors used in the instrumentations. But the accumulation of long life induced activity seems to be more problematic also for this case.

V. NUCLEAR DATA REQUIREMENTS

In order to specify the nuclear data requirements for nuclear heating calculations for fusion reactors with their required accuracies and priorities, sensitivity studies to study the effect of nuclear data uncertainties on nuclear heating such as by Steiner[4], Abdou and Conn[5], Alsmiller et al.,[3] Simmons et al.,[6] and Arcipiani et al.,[7] are required. As of today, too few and too specific results of such studies are available to draw any definite or general statement on data requirements. However, Ref. (3) states that the uncertainty in the calculated nuclear heating at a toroidal field coil due to uncertainty in neutron transport cross sections is $\sim$ 100%, which seems to be clearly too large for general acceptance. Moreover, in the neutronics calculation for fusion reactors with 14-MeV neutrons, the energy and angular distribution data for secondary neutrons should become very important.[28] The energy and angular distributions are not only important for neutron transport calculations but as shown in Ref. (18), they are also important for accurate calculations of kerma factors. A sensitivity analysis method to calculate the sensitivity to the energy and angular distribution data of secondary neutrons and gamma rays has been developed and the importance of these data in fusion reactor application has been demonstrated by Gerstl.[29]

The role of gamma-ray heating is far greater in fusion reactors than in fission reactors where almost all energy comes out of neutron induced fissions. In fact, the gamma-ray heating often exceeds neutron heating in some of the critical reactor components such as TFC and the first wall material if it is made mostly of high atomic number elements. Hence, gamma-ray production cross sections which had been regarded as not very significant in fission reactor application have become important. It is timely that more gamma-ray production data have come to be available in ENDF/B-IV and V, but it is believed not to be sufficient and further efforts are requested in this field.

On the other hand, experimental verifications of the nuclear data and radiation transport methods employed for nuclear heating calculations in fusion reactors are also required. There are several integral experiments on fusion blanket assembly conducted to date, but aside from a few of neutron and gamma-ray spectra measurements[30]-[33] which should be useful for the testing of radiation transport calculations, most of them placed the verification of tritium production as their primary objective.[32],[34] An experiment employing calorimeter, TLD[35] or some other detector to measure nuclear heating more or less directly should be conducted.

There is a proposal[36] to conduct a nuclear heating calculation on a benchmark problem and through intercomparison of the results evaluate the state-of-the-art of the calculational methods. Such a comparison for gamma-production codes have already been carried out in the USA[37]. This kind of intercomparison of benchmark calculations on an appropriate integral experiment, using the same nuclear data should be useful in clarifying the errors in the nuclear data processing and radiation transport calculations, thus making clear the uncertainty due to nuclear data.

ACKNOWLEDGEMENTS

The author would like to thank Dr. R. G. Alsmiller, Jr. of the Oak Ridge National Laboratory, Dr. Mohamed A. Abdou of Georgia Institute of Technology, and Dr. Hiroshi Maekawa of Japan Atomic Energy Research Institute for the valuable comments in preparing this review.

References

1. K. Sako et al., "First Preliminary Design of an Experimental Fusion Reactor," JAERI-7300, (1977) in Japanese.
2. K. Sako et al., "Conceptual Design of the JAERI Demonstration Fusion Reactor," Proc. 2nd Topical Meeting on the Technology of Controlled Nuclear Fusion, Richland, WA, CONF-760935-P2, 607 (1976).
3. R. G. Alsmiller, Jr., J. Barish, and C. R. Weisbin, "Uncertainties in Calculated Heating and Radiation Damage in the Toroidal Field Coil of a Tokamak Expeimental Power Reactor Due to Neutron Cross Section Errors," Nucl. Technol. 34, 376 (1977).
4. D. Steiner, "The Nuclear Performance of Fusion Reactor Blankets," Nucl. Appl. Technol. 9, 83 (1970).
5. M. A. Abdou and R. W. Conn, "A Comparative Study of Several Fusion Reactor Blanket Designs," Nucl. Sci. Eng. 55, 256 (1974).
6. E. L. Simmons, S. A. W. Gerstl, Donald J. Dudziak, "Cross-Section Sensitivity Analysis for a Tokamak Experimental Power Reactor," LA-6943-MS (1977).
7. B. Arcipiani, G. Palmiotti and M. Salvatores, "Neutron Heating Sensitivity to Cross Section Variations in a Controlled Thermonuclear Blanket," Nucl. Sci. and Eng., 65, 540 (1978).
8. D. Steiner, "Neutronics Behavior of Two Fusion Reactor Blanket Designs," ORNL/TM-2648 (1969).
9. J. J. Ritts, M. Solomito and D. Steiner, "Kerma Factors and Secondary Gamma-Ray Sources for Some Elements of Interest in Thermonuclear Blanket Assemblies," ORNL/TM-2564 (1970).
10. M. A. Abdou, C. W. Maynard and R. Q. Wright, "MACK: A Computer Program to Calculate Neutron Energy Release Parameter and Multigroup Neutron Reaction Cross Sections from Nuclear Data in ENDF Format," ORNL/TM-3995 (1973).
11. RSIC Computer Code Collection, Abstracts of Peripheral Shielding Routines (PSR) Packaged by the Radiation Sheilding Information Center, ORNL-RSIC-31 (1976).
12. J. R. Wright and F. R. Mynatt, "MUG: A Program for Generating Multigroup Photon Cross Sections," CTC-17 (1970).
13. K. D. Lathrop, "GAMLEG - A Fortran Code to Produce Multigroup Cross Sections for Photon Transport Calculations," LA-3267, Los Alamos Scientific Laboratory (1965).

14. N. M. Greene et al., "AMPX: A Modular Code System for Generating Multigroup Neutron-Gamma Libraries from ENDF/B," ORNL/TM-3706, Oak Ridge National Laboratory (1976).

15. D. J. Dudziak, "Transmutation and Atom Displacement Rates in a Reference Theta-Pinch Reactor," Proceedings of the First Topical Meeting on the Technology of Controlled Nuclear Fusion, San Diego, CA, April 16-18, 1974, CONF-740402-P2 (1974) p. 114.

16. G. Casini and R. Cuniberti, "Nuclear Blanket and Shielding Problems in Demonstration Fusion Reactors," ibid, (1974) p. 238.

17. S. Miyasaka et al., "Code System for the Radiation Heating Calculation on a Nuclear Reactor, RADHEAT, JAERI-M 5794 (1974) (in Japanese).

18. M. A. Abdou and C. W. Maynard, "Calculational Methods for Nuclear Heating. Part II. Application to Fusion Reactor Blanket and Shields," Nucl. Sci. Eng. 56, 381 (1975).

19. M. A. Abdou and C. W. Maynard, "Calculational Methods for Nuclear Heating. Part I. Theory and Computational Algorithms," Nucl. Sci. Eng. 56, 360 (1975).

20. M. A. Abdou, Y. M. Gohar and R. Q. Wright, "MACK-IV, A New Version of MACK: A Program to Calculate Nuclear Response Functions from Data in ENDF/B Format," ANL/FPP-77-5 (1978).

21. R. E. MacFarlane et al., "NJOY: A Comprehensive ENDF/B Processing System, Proc. of Multigroup Nuclear Cross-Section Preparation and Data Library Manipulation Techniques Seminar Workshop, Oak Ridge, TN, March 14-16, 1978, to be published as ORNL-RSIC-41.

22. G. M. McCracken and S. Blow, "The Shielding of Superconducting Magnets in a Fusion Reactor," CLM-R120 (1972).

23. J. T. Kriese and D. Steiner, "Magnet Shield Design for Fusion Reactors," ORNL/TM-4256 (1973).

24. H. Iida, T. Ide and Y. Seki, "Nuclear Heat Deposition in Cryosorption Pumps of a Fusion Reactor," Proceedings of the Seventh Symposium on Engineering Problems of Fusion Research, Vol. II, 1658, Knoxville, October 25-28, 1977 (1977).

25. R. T. Santoro, R. A. Lillie, R. G. Alsmiller, Jr. and J. M. Barnes, "Multi-Dimensional Neutronics Analyses of the Tokamak Fusion Test Reactor Neutral Beam Injectors," ORNL/TM-6354 (1978).

26. J. Jung and M. A. Abdou, "Radiation Shielding of Major Penetrations in Tokamak Reactors," ANL/FPP/TM-107 (1978).

27. L. C. Pwu and V. C. Baker, "Neutron Streaming Study for the Diagnostic Penetrations of the TFTR," Trans. Am. Nucl. Soc., Vol. 27, 798 (1977).

28. Y. Seki and H. Maekawa, "Cross-Section Sensitivity Analysis of ^{235}U and ^{238}U Fission Rates Measured in a Graphite-Reflected Lithium Assembly," Nucl. Sci. Eng., 66, 243 (1978).

29. S. A. W. Gerstl, "Sensitivity Profiles for Secondary Energy and Angular Distributions," Proc. Fifth International Conference on Reactor Shielding, 101, Knoxville, April 17-23 (1977).

30. L. F. Hansen, C. Wong, T. Komoto and J. D. Anderson, "Measurements of the Neutron Spectra from Materials Used in Fusion Reactors and Calculations Using the ENDF/B-III and -IV Neutron Libraries," Nucl. Sci. Eng. 60, 27 (1976).

31. H. Bachmann, U. Fritcher, F. W. Kappler, D. Rusch, H. Werle, and H. W. Wiese, "Neutron Spectra and Tritium Production Measurements in a Lithium Sphere to Check Fusion Reactor Blanket Calculations," Nucl. Sci. Eng. 67, 74 (1978).

32. R. Herzing, L. Kuypers, P. Cloth, D. Filges, R. Hecker, and N. Kirch, "Experimental and Theoretical Investigations of Tritium Production in a Controlled Thermonuclear Reactor Blanket Model," Nucl. Sci. Eng. 60, 169 (1976).

33. S. Itoh, Y. Seki and H. Maekawa, "Measurements and Calculations of Fast Neutron Spectra in a Graphite-Reflected Lithium Assembly," Proc. Third Topical Meeting on the Technology of Controlled Nuclear Fusion, May 9-11, 1978, Santa Fe, NM, to be published.

34. M. E. Wyman, "An Integral Experiment to Measure the Tritium Production from ^{7}Li by 14 MeV Neutrons in a Lithium Deuteride Sphere, LA-2234 (Rev) (1972).

35. H. Maekawa, J. Kusano and Y. Seki, "Response Distributions of ^{6}LiF and ^{7}LiF Thermoluminescence Dosimeters in Lithium Blanket Assemblies," NEACRP-L-165 published as JAERI-M 6811 (1976).

36. R. H. Curtis, private communication.

37. W. E. Ford, III, private communication.

38. R. T. Perry, H. Gorenflo, W. Daenner, "INDRA: A Program System for Calculating the Neutronics and Photonics Characteristics of a Fusion Reactor Blanket," IPP 4/137, January (1976).

39. M. A. Abdou, "Nuclear Design of the Blanket/Shield System for a Tokamak Experimental Power Reactor," Nucl. Technol. 29, 7 (1976).

40. M. A. Abdou and J. Jung, "Nuclear Analysis of a Tokamak Experimental Power Reactor Conceptual Design," Nucl. Technol. 35, 51 (1977).

41. "Differential and Integral Nuclear Data Requirements for Shielding Calculations," Proc. of a specialists' meeting (Vienna, 1976), IAEA-207 (1978).

Table I. Region integrated nuclear heating in the blanket, shield and TFC of JXFR.[1]

Zone No. (k)	Regions	Radiation heating (MeV/D-T neutron)		
		Neutron $\int H_n \phi_n dV_k$	Gamma-ray $\int H_\gamma \phi_\gamma dV_k$	Total $\int H_n \phi_n + H_\gamma \phi_\gamma dV_k$
1	Plasma*	1.56×10^{-8}	1.93×10^{-10}	1.58×10^{-8}
2	Vacuum*	4.40×10^{-9}	7.37×10^{-11}	4.47×10^{-9}
3	Carbon coating	3.38×10^{-1}	8.80×10^{-2}	4.27×10^{-1}
4	Stainless steel (SS)	5.52×10^{-1}	9.61×10^{-1}	1.51
5	Li_2O(24%)+SS(9%)+He(27%)	3.66	2.02	5.68
6	Li_2O(72%)+SS(17%)+He(11%)	5.93	2.82	8.75
7	SS(90%)+He(10%)	3.03×10^{-2}	3.24×10^{-1}	3.54×10^{-1}
8	SS	1.24×10^{-3}	2.05×10^{-2}	2.17×10^{-2}
1∿8	Blanket total	10.51	6.23	16.74(99.7%)
9	Vacuum*	2.63×10^{-11}	1.11×10^{-12}	2.74×10^{-11}
10	Heavy concrete (90%)+	2.32×10^{-2}	2.83×10^{-2}	5.15×10^{-2}
11	Lead	7.20×10^{-9}	1.18×10^{-6}	1.19×10^{-6}
12	Air	1.71×10^{-10}	7.73×10^{-11}	2.48×10^{-10}
13	Insulator	3.65×10^{-8}	5.73×10^{-8}	9.38×10^{-8}
14	SCM	8.82×10^{-8}	8.13×10^{-7}	9.02×10^{-7}
15	Insulator	8.44×10^{-15}	5.70×10^{-14}	6.54×10^{-14}
9∿15	Shield and TFC	0.02	0.03	0.05 (0.3%)
1∿15	Total	10.53 (63%)	6.26 (37%)	16.79 (100%)

* Plasma and vacuum regions are filled with 10^{13} atoms·cm^{-3} of hydrogen.

\+ Heavy concrete is cooled by borated water.

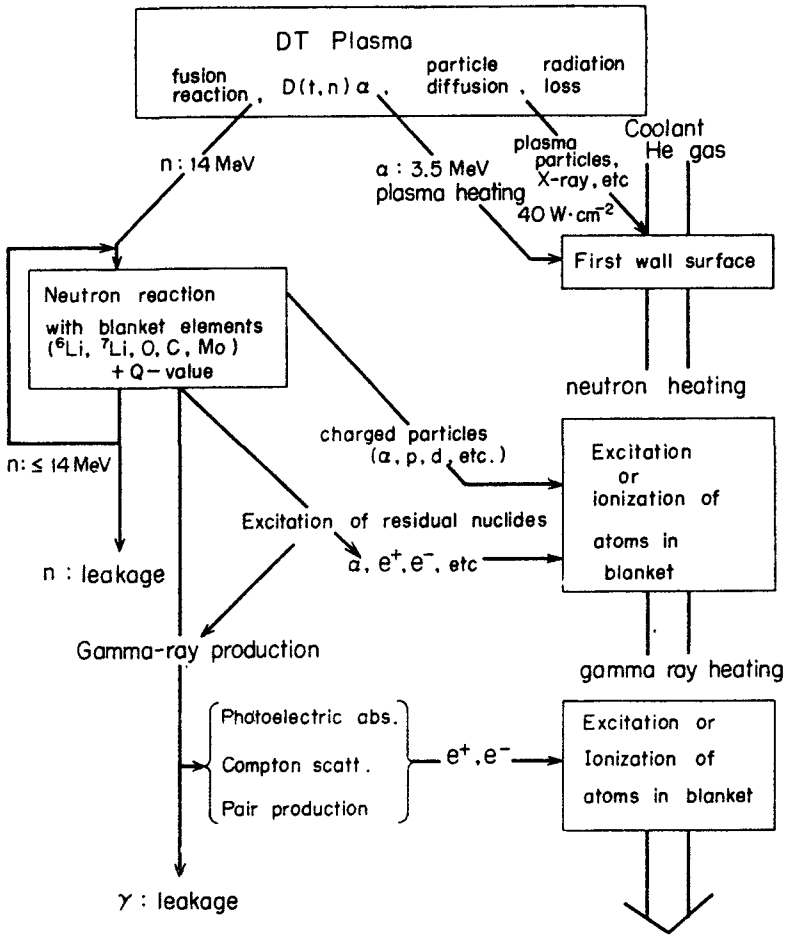

Fig. 1. Nuclear heating mechanism in a D-T fusion reactor.[2]

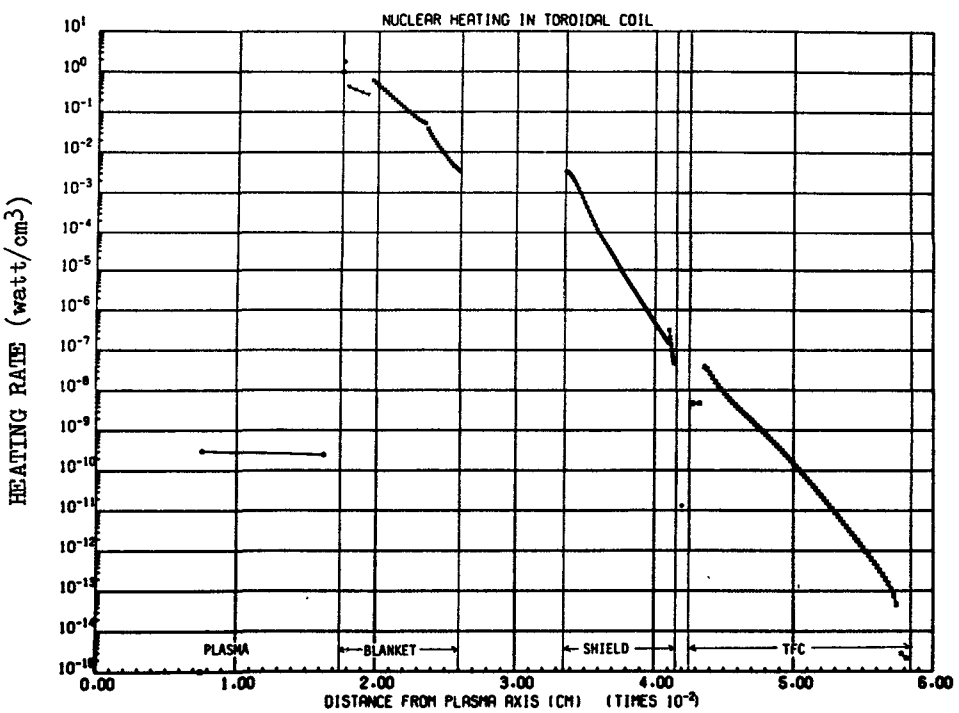

Fig. 2. Nuclear heating rate in the blanket, shield and TFC of JXFR[1].

Nuclear Data Requirements for Transmutation and Activation of Reactor Wall and Structural Materials

AG-159/A3
Review Paper

O.N. Jarvis, A.E.R.E. Harwell, U.K.

Abstract

This paper details the extent of the nuclear data needed for inclusion in a data library to be used for general assessments of fusion reactor structure activation and transmutation problems, describes the sources of data available, reviews the published literature and explores the reliability of current calculations by providing an independent assessment of the activity inventory to be expected for five structural materials in a simple blanket design for comparison with the results of other workers. An indication of the nuclear reactions which make important contributions to the activity, transmutation and gas production rates for these structural materials is presented.

1. Introduction

In the present review we are concerned mainly with substantiating and assimilating the activation and transmutation calculations which have been published in the open literature, with a special interest in the nuclear cross-section and decay chain data employed. Most of the published calculations assume that the fusion reactor of the future will operate on the D-T fuel cycle. "Advanced" fusion operating on the D-D or D-^{3}He cycles will be very much more difficult to achieve than D-T fusion and will not be entirely free from the 14 MeV neutron component; indeed, as was pointed out by Kulcinski[1], the radioactivity of structures associated with D-D fusion will be only marginally less than that for D-T fusion. Accordingly, the scope of the present review is restricted to D-T fusion.

Estimates of activation and transmutation of the first wall and structure of a fusion reactor may differ considerably between conceptual reactors embodying different plasma confinement techniques since their neutron blanket designs are subject to different constraints. Thus, the blanket must be provided with adequate cooling but in the magnetic confinement approach[2] the presence of strong magnetic fields will inhibit the free flow of the (liquid) lithium needed for tritium breeding whereas for inertial confinement[3] the impulsive nature of the energy deposition requires a "first-wall" of liquid lithium in several designs. Even when we consider a particular type the various designs of the blanket can differ considerably, with significant effects on the activation properties.

The major aim in the design of the primary blanket is to obtain a sufficiently large tritium breeding factor per incident 14 MeV neutron from the ^{6}Li(n,α) and ^{7}Li(n,n'α) reactions that the initial tritium inventory is maintained, not forgetting the existence of penetrations through the blanket for vacuum pumps, beam injection equipment, etc. A secondary aim is to make the blanket and magnet shield regions as compact as possible to minimize the capital cost of the reactor. The neutronics calculational methods used to obtain the neutron fluxes and spectra at various locations in the reactor lie outside the scope of the present paper. It should be noted that although such calculations generally provide first-order transmutation and activation estimates they take into account only the strong reactions involving the original constituents of the blanket. It is customary to use a separate activation code to take into account all the improbable reactions which, nevertheless, may make an important contribution to the total activity and also to discover the importance of the non-linear effects which arise in high fluence irradiations. In addition, because the neutron fluxes and spectra are not very sensitive to the structural materials adopted, the activation code can be used to obtain valuable comparisons between different materials without requiring the neutronics calculations to be repeated.

2. The Data Base for Activation/Transmutation Calculations

2.1 Computer codes for activation/transmutation calculations

Before activation calculations can be made three major requirements must be met: (i) the activation and radioactive decay chains of the nuclides involved must be specified, (ii) group averaged cross-sections for

all participating reactions must be obained, and (iii) the differential equations must be set up and a suitable method[4] of solving them invoked. The early assessments of fusion reactor blanket activity used codes built around the particular restricted set of nuclides of interest. This is reasonably straightforward for a monoisotopic structural element such as niobium but is much more complex for stainless steel, which involves 14 stable isotopes, unless simplified calculations such as those of Nigg and Davidson[5] are considered adequate. After a certain level of complexity has been passed it becomes advantageous to develop more general computer codes in which the particular problem of interest is specified as data input: this implies the existence of very extensive activation and decay chain data and cross-section data libraries. The Garching code AKTIV[6] and the Wisconsin code DKR[7] provide good examples of this approach.

Alternatively, it may be considered expedient to take advantage of the existence of codes written for fission reactor applications. These can handle heavy isotope and fission product inventories in addition to the structural elements. Two codes of this type merit special mention; these are the U.K.A.E.A. code FISPIN[8] and the Oak Ridge code ORIGEN[9]. An extended version of the code ORIGEN was used for illustrative purposes in preparing the present review. For both codes it is necessary for the fusion oriented user to provide a group-averaged reaction cross-section data library (although data libraries for fission reactor applications are available with both codes). Evidently, the use of fission reactor codes and the availability of fission data libraries greatly facilitates comparisons between fusion and fission reactor situations.

2.2 Nuclide library specification

The specification of a nuclear data library intended for general applications involving the structural materials and their major impurities starts with a listing of all the isotopes in the constituent elements - these are the zero generation nuclides. The scope is then enlarged by considering all the reactions involving the zero generation nuclides which are energetically possible, and so obtaining the first generation reaction products. If these first generation nuclides are stable or possess lifetimes in excess of some lower limit T_ℓ then their (second generation) reaction products are considered next, and the process is continued as far as is considered necessary. It is vital that complete decay chains for all the radioactive nuclides are included in the library; this may introduce further long-lived and stable nuclides which should also be considered as parents for nuclear reactions. The extensive nuclear library listed in Appendix I was constructed in this fashion, with the reaction chains being truncated when it was found that members could only be reached after several successive reactions.

The reaction types permitted must include the four reactions (n,γ), (n,2n) (n,p) and (n,α) which are of importance for fission reactors but in addition the 14 MeV neutron energy requires (n,d), (n,t) (n,n'α) and (n,n') to be included. For present purposes we are interested mainly in the reaction product and not the emitted particle so that, for example, (n,t) includes (n,nd), (n,npn), etc. The inelastic scattering cross-section (n,n') is of practical interest only when a long-lived isomeric state is populated. The other reactions may also lead to the population of isomeric states which must be permitted by the library specification; this is particularly important in cases where the isomers do not decay to their ground states. The above list of reaction types omits reactions which generally have threshold energies above 14 MeV; this exclusion may not always prove satisfactory - e.g. the (n,^{3}He) reaction is occasionally of significance.

The lifetime limit T_ℓ which determines whether or not nuclear reactions involving unstable nuclides as parents should be considered can be determined in relation to the minimum level of impurity elements which we feel should be taken into account in the activity calculations. A simple argument shows that when only impurities and minor constituents above 100 ppm are considered then the lower limit to the lifetime can be set at about 10^2 days. This result applies mainly to activation calculations involving a significant period of irradiation at high flux levels. For very short irradiations it will be sufficient to consider only those reactions involving the original constituents which lead to unstable decay products; however, as the half-lives and decay characteristics vary considerably from nucleus

to nucleus it should not be assumed that the major constituents are necessarily of greater importance than the minor constituents.

2.3 Decay chain data

Essentially all of the radioactive decay data is well established and can be taken from the "Table of Isotopes" compiled by Lederer, Hollander and Perlman[10]. Only for a few medium weight metastable nuclides is there any uncertainty regarding the nature of their radioactive decays.

In computing the decay power the energy release in each radioactive decay is required but for β-decay it is not appropriate to adopt the energy release quoted in the "Table of Isotopes" as this includes the neutrino energy. Only between 1/3 and 1/2 of the total β-decay energy is carried by the charged particle; a good estimate of the actual fraction can be obtained from the work of Stamatelatos et al[11]. For γ-dose rate calculations the γ-spectrum associated with each radionuclide will be needed. Convenient libraries of γ-lines available on magnetic tape are those of Erdtmann and Soyka[12] and of Bowman and MacMurdo[13].

2.4 Reaction cross-section data

An assessment of the availability of reaction cross-section data for fusion reactor activation calculations shows that the majority of the reactions have been investigated only at a single energy (14 MeV) and that the data often refers to the element rather than to its constituent isotopes as required for activation calculations. Also, with just a few isolated exceptions, the data is restricted to the stable nuclides only. It follows that the generation of synthetic nuclear cross-sections through the use of nuclear models, adjusted to reproduce existing data, is of particular importance for fusion work.

It is obvious that the construction of a multigroup nuclear cross-section library from the original literature would require a vast effort. Fortunately, the neutron data field is of great importance for fission reactor design and an excellent index[14] to the literature is maintained (CINDA). Nevertheless, reference to the original literature need be made only as a last resort. Undoubtedly the most satisfactory source of data is one of the evaluated nuclear data files; for a summary of the 1973 contents of these files reference should be made to the IAEA technical report No146[15].

The evaluated files are available on magnetic tape but the wealth of data encompassed is such that special processing codes are needed to put the data needed for activation calculations into a convenient multigroup form. The processing code SUPERTOG[16] is used in connection with the ENDF/B files and the transport code ANISN[17]; the 100 group GAM-II[18] energy structure is used. For activation calculations a 100-group structure provides unnecessary detail and more compact structures are sometimes preferred[7]; as a pointer into the future it should be noted that the d-Li neutron source[19] proposed for materials testing purposes will provide neutrons with energies peaked at 14 MeV but with a high energy tail reaching to 30 or 40 MeV so that an extended energy format may be required[20,21].

A list of data collections of value in cross-section library construction for activation applications is provided in Table 1. An up-to-date compilation of neutron data handbooks and other data sources is provided in CINDA. Of especial interest is the compilation of 14 MeV neutron cross-sections prepared by Tsukada[22] which proves of singular value for normalizing modelled data.

2.5 Nuclear models for cross-section estimation

The use of nuclear models in the evaluation of nuclear data has been reviewed by Prince[23], who has provided detailed information on the nuclear model codes which have been described in the literature, their applicability and availability. Perhaps invidiously, we select just three of these as being of particular relevance here - THRESH[24], FISPRO[25] and GNASH[26]:

(i) THRESH is a statistical model code which computes the particle emission reaction cross-sections induced by neutrons in the

Table 1

List of Data Collections for Activation/Transmutation calculations

1. The Evaluated Data Files: (See IAEA tech. report 146)
   UKNDL (U.K.)
   ENDF (U.S.)
   LLL (U.S.)
   KEDAK (Germany)
   "Benzi" - Italian fission product library
   "Cook" - Australian fission product library

2. ENDF/B-IV Dosimetry File. ed. by B.A. Magurno. BNL-NCS-50446 (1975)

3. UCRL-50400 Vol 18 (1977) "ACTL-Evaluated Neutron Activation Cross-section library"

4. BNL-325, supplement 2 (1966)

5. W.E. Alley and R.M. Lessler, "Neutron Activation Cross-Sections", Nuclear Data Tables 11 (1973) No's 8 & 9.

6. "Handbook on nuclear activation cross-sections", IAEA technical report 156 (1974)

7. "Compilation of Threshold Reaction Neutron Cross-Sections", A. Schett, K. Okamoto, L. Lesca, F.H. Frohner, H. Liskien and A. Paulsen, EANDC 95 U, Centre de Compilation de Donnees Neutroniques, Saclay (1974).

8. "Evaluated reference cross-section library", R.L. Simons and W.N. McElroy, BNWL-1312 (1970).

9. "Multigroup reaction cross-sections for FTR application", R.B. Kidman, HEDL-TME-72-135 (1972).

10. "Table of Nuclear reactions and subsequent radioactive decays induced by 14 MeV neutrons" K. Tsukada JAERI 1252 (1977).

11. DLC-33/Montage 400. "100 Group neutron activation cross-section data for fusion reactor structure and coolant materials" R.S.I.C. Oak Ridge (1976).

energy range 0-20 MeV. A number of adjustable parameters permit normalization of prediction to measurement. The more recent version of the code, THRESH-2, is suitable for nuclei in the range Z=21 to 83 Attractive features of the code are its simplicity and speed of execution. The accuracy of the predictions can be assessed in part by comparing predicted cross-sections with those contained in the ENDF/B evaluations for the energy range 8-14 MeV, which is an important region for CTR activation calculations and coincides with the region where the important reactions (n,2n), (n,p) and (n,α) are approaching their maximum values; the ratios of prediction/evaluation were 1.2 ± 0.2, 1.4 ± 1.0 and 0.8 ± 0.5 respectively. Since the THRESH parameters were doubtless derived from these same data the good agreement is predictable. No such test is available for the less strong reactions (n,d), (n,t), (n,nα) etc owing to lack of ENDF/B data. However, a comparison with 14 MeV cross-section tabulations[22] shows most cross-sections to be within a factor of 3 of the tabulated values except for (n,t) for which the prediction is often 10 to 30 times high; the explanation of this probably lies in the prediction including (n,nd) and (n,2np) whereas the measured values often refer to triton emission only.

(ii) FISPRO-II has been used to compute radiative capture cross-sections for fission product nuclides over the neutron energy range 1 keV to 10 MeV. It is a fairly simple program using the Hauser-Feshbach formalism but, of necessity, requires spins and parities for low-lying levels, level density parameters, radiation widths

and transmission coefficients for each nucleus treated. The fission product library "Benzi" of Table 1 is based on FISPRO calculations. Cross-sections for the missing energy region 0-1keV can be estimated approximately from the thermal neutron (2200 m/s) cross-section and the resonance integral: the ORIGEN data library ORYX-E[27] provides a convenient source for this information.

(iii) GNASH is a modern code incorporating pre-compound emission followed by a multi-step Hauser-Feshbach calculation. A considerable quantity of input data is required for each case treated but the performance of the code is most impressive. Not only are all the particle emission reactions treated as well as radiative capture but GNASH also yields isomer ratios (the relative population of metastable and ground states of the daughter nucleus following a neutron induced reaction). A complete library of cross-section data for CTR applications generated using the GNASH code would be most welcome.

2.6 The composition of a neutron nuclear data library

The neutron cross-section library specified in the Appendix to ref 67 (and used here for the calculations reported in section 4) exemplifies the manner in which the data sources listed in Table 1 can be utilized. Not all the relevant material held in the evaluated files has yet been incorporated. Whenever possible the particle emission cross-sections calculated using THRESH-2 have been normalized at 14 MeV to the most credible entry listed in the compilation by Tsukada[22].

In principle, the multigroup cross-sections for reactions leading to a metastable state are needed in addition to those for reactions leading to the ground state, but it is most unusual for both sets of data to be available. Therefore it is convenient to assume that the ratio of populations of isomeric and ground states - the isomer ratio - is independent of energy. Estimates of isomer ratios for thermal neutrons can be found in the ORIGEN data library [27] but comprehensive coverage is also provided for 14 MeV cross-sections by Tsukada[22].

The only multigroup cross-section data library intended specifically for activation calculations for fusion reactor structures which is readily available is the 100-group (GAM-II) library DLC-33 B constructed by D. Muir[28] from point cross-section data derived from ENDF/B3, UKNDL, Cook, Benzi and other sources, heavily supplemented with THRESH calculated cross-sections, made available by the Brookhaven National Laboratory[29]. DLC-33B contains only cross-sections leading to radionuclides. The library discussed above used DLC-33B for its foundation.

2.7 Activation with 14 MeV neutrons

As a significant proportion of the activation and transmutation effects in fusion reactor structures are caused by the high energy neutron flux an approximate appreciation of the importance of these effects can be obtained, independently of reactor blanket design, from an examination of the effects induced by monokinetic 14 MeV neutrons. The Tsukada compilation is useful here, for not only are the 14 MeV cross-sections listed, but also the half-lives of any daughter radionuclides and also the initial activities following a 4 month irradiation with 10^{15} n/cm^{2}s for each isotope. To estimate the total activity for a structural material the many activities associated with the constituent nuclides must be summed. This has been done by Kamykowski[30] who has provided a graphical presentation of the decay activity for 19 elements irradiated for a period of 7 days in a 14 MeV neutron flux of intensity 10^{15} n/cm^2.s.

3. Review of the published literature on activation

The first published account of the activation and afterheat of the structure of a fusion reactor was that made by Fraas and Postma[31] in connection with a study of the hazards associated with a D-T fusion power plant. The preferred structural material was niobium which, although expensive, is still considered a suitable material provided an industry can be built up around it by the time that series ordering of fusion power stations becomes possible. This early choice of niobium was unfortunate because, although niobium is a monoisotopic element

which superficially indicates a simple activation calculation, there are in fact a plague of long-lived isomeric states which can be reached from ^{93}Nb through (n,n'), (n,2n) and (n,γ) reactions for which the isomer/ground state branching ratios are -even now - only approximately known. Because Fraas and Postma considered the formation of ^{94}Nb to yield the dominant activity they found that the total activity for a 5GW(th) reactor at shut-down would be 5 x 10^5 Ci and the decay power to be only 5kW. Dudziak[32] pointed out that inclusion of ^{92m}Nb and ^{94m}Nb would alone raise the activity to 10^{10}Ci and the decay power to 30MW; he also noted that molybdenum should offer similar properties to niobium. Blow[33] examined the activation chains for niobium more carefully, obtained theoretical estimates for reactions for which data was lacking, and performed calculations for the "first" wall of a simple blanket design. Steiner calculated the total activity for this same blanket to be 2 x 10^{10} Ci and the decay power to be 50MW when normalized to a 5GW(th) reactor. Comparison of the results of Blow with those of Steiner shows that about 25% of the saturation activity of the blanket (and 30% of the afterheat) must be attributed to the first wall: this comparison makes allowance for the omission of the 6.3 minute isomer ^{94m}Nb from Blow's calculations. These results are proportionally reasonable since the "first wall" contains 19% of the bulk of the structure. Blow[33,35] also performed preliminary calculations for the Nimonic alloy PE16, which exhibits activity and decay power values of about 40% those for niobium, and also for molybdenum for which the decay power falls off appreciably more rapidly than for either PE16 or niobium. Steiner and Fraas[36] then showed that the choice of vanadium as a structural material results in a blanket for which the activity falls off with such rapidity that recycle of the material might be possible, whereas niobium would have to be deposited in a long-term storage area; this feature encouraged Steiner[37] to perform a detailed investigation of the use of vanadium in a neutron blanket, relative to niobium as a standard material.

The pioneering phase of induced activation calculations can be considered to have been concluded by the work of Nigg and Davidson[5] who studied 316 stainless steel using the blanket model of Blow[33] and Steiner[34]. The calculations of Nigg and Davidson were relatively comprehensive (but nevertheless approximate) as they included some 39 nuclear reactions; they concluded that the activity and decay power for SS316 was comparable with that for niobium.

With the importance of activation calculations established it has become obligatory for all complete design studies of fusion test rigs and conceptual power reactors to include an assessment of the structural activation. These studies are generally presented in report form only[38-47]. More readily accessible are the proceedings of specialist conferences in which outlines of the proposed designs are presented together (e.g. see ref 48). Of greater interest, perhaps, are the publications in which the performance of different structural materials and/or different blanket designs are compared. Thus Vogelsang, Kulcinski, Lott and Sung[49] compared the activation and afterheat of 316 stainless steel with a niobium alloy (Nb-1%Zr) and a vanadium alloy (V-20% Ti) when employed in the blanket of the University of Wisconsin Tokamak Reactor (UWMAK-I). Their calculations identified the major contributing radioisotopes and are in general agreement with the results to be presented in the following section. In particular, they noted that after 10 years of operation at a neutron wall loading of 1.25 MW/m^2 the 316 SS first wall induced activity (afterheat) was 30% (25%) of the bulk blanket values and that after just 2 years operation these values were 80% (90%) of those for 10 years. The first wall: bulk blanket ratios are much as would be expected if only the portion of the blanket at smaller radius than the reflector becomes significantly active. Dudziak and Krakowski[50] considered the use of the niobium and vanadium alloys (Nb-1Zr and V-20Ti) in a reference theta-pinch reactor design (RTPR); this is a most detailed study which includes activation of the magnet coils as well as the blanket and also compares the activity, afterheat and Biological Hazard Potentials with Tokamak reactor designs and with fission reactors.

The conceptual reactor design studies include two schemes of particular relevance since they lead to reduced structural activation. The first is the Brookhaven National Laboratory (BNL) design[39,40] which incorporates a minimum activity blanket using a sintered aluminium product (SAP) for the structure and a LiAl compound for the breeding material (since SAP is incompatible with liquid lithium). The second scheme, that of the Wisconsin group[51], suggested that the radiation damage suffered by any first wall material should be reduced by shielding it with a graphite screen to soften the incident neutron flux. Although this second concept may be of considerable value the implications are not pursued in the present review.

Conn, Sung and Abdou[52] have performed the useful service of bringing together five major blanket designs for intercomparison. These designs include the ORNL model of Fraas[38], the UWMAK-I design[45] employed by Vogelsang et al [49], the Princeton Plasma Physics Laboratory (PPPL) design[41] which employs flibe ($LiF-BeF_2$) as a moderating and breeding material, the Lawrence Livermore Laboratory (LLL) mirror reactor blanket[42] using lithium depleted to 4.0% in ^6Li and the BNL minimum activity blanket[39] which employs lithium enriched to 90% ^6Li. Despite the differences in designs and materials, Conn et al [52] found that at shutdown following a 2 year operation at a neutron wall loading of $1MW/m^2$ the induced activities in the blankets were within a factor of 4 and clustered at 1000 Ci/kW(th) whilst the afterheat levels lay between 0.5 and 5% of the thermal operating powers, with a maximum afterheat power density of only $\sim 0.2W/cm^3$. They also quoted the specific activities of the various first walls (in disintegrations/ $sec.cm^3$): the two stainless steel structures (LLL and PPPL) give similar results despite the very different blanket designs.

Effectively in continuation of earlier work by Steiner[37] for niobium and vanadium, Williams, Santoro and Gabriel[53] further intercompared niobium, 304 stainless steel and nimonic 105 using the blanket configuration of Fraas[38] and concluded that 304SS offers the best neutronic responses of these materials. Similarly, Vogelsang[54] extended the earlier work with the UWMAK-I blanket[45] to an investigation of five alloys based on molybdenum (TZM), steel(316SS), vanadium (V-20Ti), niobium (Nb-1Zr) and aluminium (Al2024). The article by Kessler and Kulcinski[55] provides a valuable tabulation of the data presented graphically by Vogelsang and also compares the environmental damage potential for fusion with that for the fast reactor. These studies are adopted as the model for the activation calculations presented in the following section.

More recently, Rovner and Hopkins[56] have considered the use of ceramic materials such as silicon carbide and carbon as potential first wall materials: the activation of such structures is negligible - indeed, it is probably determined by impurities - but the technology requires much development. Finally, Gruber[57] has broken new ground by investigating the effect of impurities in beryllia, graphite, 316 stainless steel and the alloy V-10Cr-10Ti using an unusual blanket designed to minimize the lithium inventory by breeding with thermal and epithermal neutrons only. Since the strong thermal neutron flux generates more long-lived radionuclides than in a conventional blanket design the activity falls off relatively slowly.

To conclude this section we note that the fusion reactor blanket activity and afterheat are strongly dependent on blanket design and operating conditions, including

(i) the choice of structural material

(ii) the general design principle (minimum activity, minimum Li inventory, etc)

(iii) the choice of moderating material (graphite or stainless steel) and its location relative to the first wall

(iv) the volume percent of structural material in the blanket.

Nevertheless, for a particular structural material, a standard neutron wall loading (say, 1 MW/m^2) and a standard operating period (say, 2 years) it is found that the specific activity and afterheat of the first walls are little dependent on blanket design and that extant designs lead to surprisingly similar activity and afterheat values for the bulk blankets.

4. Detailed calculations for a typical blanket

In the present review our primary interest lies in assessing the accuracy and completeness of the nuclear cross-section data and decay schemes and not in discussing the merits of different blanket designs with regard to operational or environmental hazards associated with the activation of the structure. It is for this reason that we have chosen a very simple blanket model with which to compare different structural materials by a straight volume for volume substitution, assuming any changes in the neutron spectra resulting from the substitution to be negligible. In our model[58] the first wall thickness is taken to be 1cm, with a 73.6cm lithium breeding zone (5% structure by volume) and a 45.8cm reflector. This corresponds to the design chosen for the Culham Conceptual Tokamak Mark II[59].

The neutron fluxes and spectra have been calculated[60] using the transport code ANISN[17] for a large number of blanket segments or intervals. The first wall neutron spectrum[58] is insensitive to design detail and is essentially the same as that listed by Gabriel et al[61]. Strictly, the gross activity of the blanket should be determined by computing the activity of each interval and summing. However, the neutron spectrum does not alter drastically within the breeding blanket, although the flux falls about an order of magnitude, so that for low to moderate fluence irradiations it is probably adequate to sum the neutron spectra, suitably weighted by the appropriate flux and volume of the region, and to perform a single activation calculation. This approximation is strictly valid only when the constituent nuclides of the structure are essentially undepleted and the burn-up of reactions products is negligible.

For the present calculations the irradiation period was chosen to be 2 years and the neutron wall loading to be 1.25MW/m^2 to facilitate direct comparison with the presentations of Vogelsang[54] and of Kessler and Kulcinski[55] which relate to the UWMAK-I blanket (being reasonably similar to the Culham blanket). It is evident that the larger portion of the blanket activity will be contained within the first walls and breeding zones of these two blanket designs. We would thus predict the specific activities in the first walls to be closely similar for the two blankets, and would not expect the bulk blanket activities to differ by as much as a factor of two. Thus, whilst small discrepancies between the two sets of calculations could be attributed to differences in blanket design, the cause of any major discrepancies is most likely to be found following a comparison of the quality and extent of the nuclear data libraries on which the calculations are based.

Table 2: Comparison of Induced Activities (Ci/kW(th) for five CTR structural materials at shutdown after 2 years operation at a neutron wall loading of 1.25 MW/m^2

Isotope	Half-life	SS316	TZM	V-Ti	Al-2024	Nb-1Zr
H3	12.3 y	2.2	0.58	4.01	0.15	1.6
Na24	15.0 h				240	
Mg27	9.5 m	0.11			182	
Al26	7.4 10^5 y				1.10^{-4}	
Al28	2.3 m	15.0			47.6	
Ca45	165 d	$2.10^{-4}\ell^2$	0.56	10.3		
Sc46	83.9 d	$2.10^{-4}\ell^2$	0.56	10.4		
Sc47	3.43d	$2.10^{-3}\ell^2$	0.44	13.9		
Sc48	1.83d	2.10^{-3}	0.84	42.1		
Sc49	58 m	7.10^{-4}	0.03	0.56		
Ti45	3.09h	4.10^{-6}	0.02	0.41		
Ti51	5.8 m	0.16	0.02	72.9	3.10^{-4}	
V49	330 d	3.0		1.8	5.10^{-3}	
V^{52}	3.75m	54.6		284	0.37	
Cr51	27.8 d	103		0.041	0.187	
Mn53	$1.9.10^6$y	9.10^{-6}			2.10^{-8}	
Mn54	303 d	80.9			3.82	
Mn56	2.58h	244			4.02ℓ	
Mn57	1.7 m	2.55			7.10^{-3}	
Fe55	2.6 y	266			0.70	
Fe59	45.6 d	3.72 h			0.01	
Co56	77 d	5.2				
Co57	270 d	141 h				
Co58	71.3 d	114				
Co58m	8.9 h	51				
Co60	5.26y	3.85			0.26	
Co60m	10.5 m	1.68ℓ			0.46	
Ni57	36 h	4.01				
Ni59	8.10^4y	1.10^{-3}				
Ni63	92 y	0.07			0.07	
Cu64	12.8 h	3.10^{-4}			42.1	
Zn65	245 d				0.73	
Sr89	52.7 d	$5.10^{-6}\ell^2$				0.025
Sr90	27.7 y	$7.10^{-8}\ell^2$	6.10^{-3}			5.10^{-4}
Y90	64 h	2.10^{-5}	0.05			16.7
Y91	58.8 d	3.10^{-5}	0.02			0.25

Table 2: cont.

Isotope	Half-life	SS316	TZM	V-Ti	Al2024	Nb-1Zr
Zr89	78.4 h	0.17	6.30			4.09
Zr95	65.5 d	0.09	3.04			1.20
Zr97	17.0 h	0.09	2.93			0.25
Nb91m	62.0d	0.11	3.76			0.16
Nb92m	10.2 d	0.33	10.7			576
Nb93m	13.6 y	5.10^{-5} h	2.10^{-3} h			46.3 h
Nb94	2.10^{4}y	9.10^{-6}	3.10^{-4}			0.31h
Nb94m	6.3 m	0.06	1.83			4100
Nb95	35 d	0.59	19.6			10.1
Nb95m	90 h	$2.10^{-3}\ell^2$	$0.07\ell^2$			$0.20\ell^2$
Nb96	23.4 h	0.27	9.03			2.10^{-3}
Nb97	72m	0.35 h	11.5 h			0.25
Mo91	15.5 m	1.79	59.0			
Mo93	1.10^{4}y	1.10^{-3}	0.04ℓ			
Mo93m	6.9 h	2.60	85.5			3.10^{-3}
Mo99	66.7 h	27.7	910			
Mo101	14.6 m	7.88	259			
Tc99	2.10^{5}y	2.10^{-4}	6.10^{-3}			
Tc99m	6.0 h	24.1	791			
Tc101	14 m	7.88	259			
Totals		1191	2460	441	603	4770
(Kessler & Kulcinski)		(1062)	(4120)	(1261)	(884)	(5155)

Notes: 1 The primary blanket includes the first wall, breeding zone and manifold space of the CCTR-II design. Reactor first wall area is nearly 1000 m^2.

2 The assumed compositions are listed in Table 4. The masses of the primary blanket structural materials per m^2 of first wall are: SS316, 1.39 tonnes; TZM, 1.58 tonnes; V-20Ti, 0.96 tonnes; Al2024, 0.49 tonnes; and Nb-1Zr, 1.47 tonnes.

3 To convert activity from Ci/kW(th) to Ci/m^2 multiply by 1.78×10^3.

Comparing the activities quoted in Table 2 with those given in Table V-XV of ref. 55 shows that, true to expectation, the majority of the nuclide activities are indeed well within a factor of 2 of each other for all five materials investigated. Where large differences occur (greater than a factor of 5) the offending activity is marked in Table 2 according to whether it is higher (h) or lower (l) than the ref. 55 value. For very large differences an obvious possibility is that a particular reaction path has been neglected in one set of calculations. We note that most of the cases where we find the activity to be lower are examples of nuclide production through successive neutron reactions with the nuclide abundance varying with the square of the irradiation period: these cases are accordingly marked ℓ^2. For lesser differences (factor between 2 and 5, say) the discrepancy is probably no more than a reflection of the uncertainty in a particular cross-section or branching ratio.

An example of a potentially important reaction cross-section which has been the subject of some discussion is afforded by the production of ^{95}Nb and ^{95m}Nb from ^{93}Nb by successive neutron capture reactions. Because the thermal and resonance cross-sections of ^{94}Nb are 15 times the cross-sections of ^{93}Nb it has been assumed[33,34] that the same factor is applicable over the whole energy range; it was further assumed that 90% of all captures in ^{94}Nb lead to ^{95m}Nb. The apparent importance of this reaction was discussed by Persiani et al[62] who proposed an integral measurement to determine the capture cross-section in a fast fission spectrum. This experiment was later performed by Turk and Harker[63] who found the ^{94}Nb capture cross-section to be 236 ± 18mb, rather similar to that for ^{93}Nb in such a spectrum; they further found the branching ratio to ^{95m}Nb to be only 2%. These results support the statistical model calculations of Poenitz[64] which predicted a high energy ^{94}Nb capture cross-section of less than half the ^{93}Nb cross-section, and a branching ratio

Table 3. First wall radioactivity following a 2 years irradiation at 1.25 MW/m^2

Alloy	Specific activity (Ci/cm^3) for decay period T				First wall activity at T=0 / Blanket activity
	T=0	1 day	1yr	300yrs	
SS316	101	68	28	8×10^{-4}	48%
V-20Ti	20	6.3	0.77	4×10^{-8}	25%
Nb-1Zr	144	56	2.9	6×10^{-3}	17%
TZM	101	59	0.10	5×10^{-3}	23%
Al2024	48	7.0	0.26	6×10^{-4}	45%
Natural Uranium	6×10^{-6}				

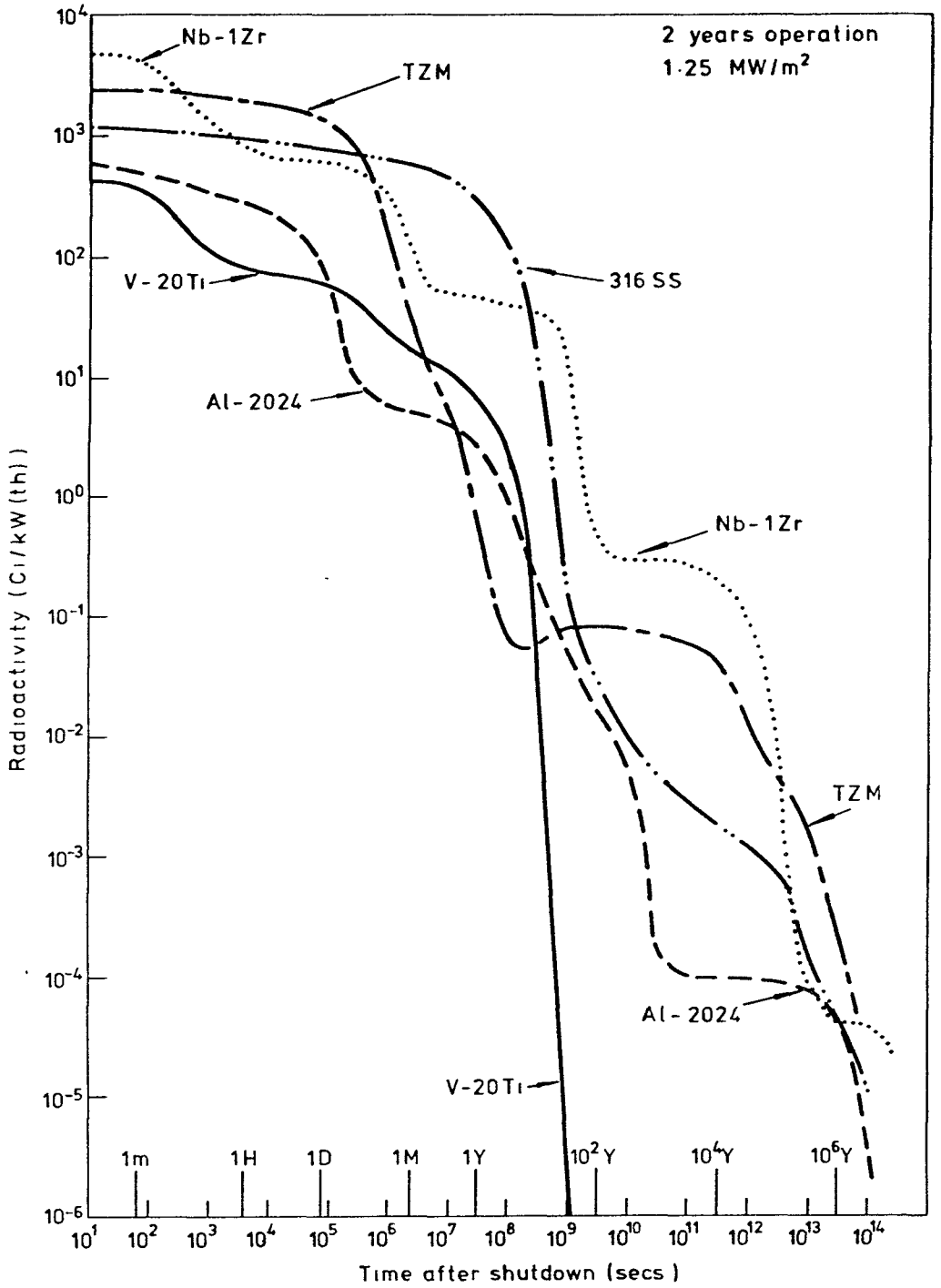

Fig. 1. Decay of induced radioactivity of the CCTRII blanket.

of 10%. Accordingly, we have taken the $^{94}Nb(n,\gamma)$ cross-section to be equal to that of ^{93}Nb for energies above 1 keV, with a 2% branching ratio. The ^{95m}Nb production is now clearly unimportant. A reaction which is important for niobium is $^{93}Nb(n,n')^{93m}Nb$, for which the cross-sections are taken from the work of Hegedus[65].

4.1 Discussion of activity calculations

The blanket activity builds up very rapidly, reaching 10% of its saturation level within an hour from start-up for all five structural materials. Only 316SS fails to achieve 90% of its equilibrium level within a month (316SS actually takes 6 years). The effects of blanket depletion become apparent after 100 years of operation at 1.25 MW/m^2.

The specific activities of the first wall materials following a 2 year irradiation at 1.25 MW/m^2 are indicated in Table 3 for several decay periods; the activity for natural uranium is provided for comparison. Also indicated are the first wall activities expressed as a fraction of the corresponding bulk blanket value. These fractions fall in the range 17 to 48%, demonstrating how the major contribution to the activity is due to the inner portion of the breeding blanket only. The front wall activities for each individual nuclide mostly bear the same ratio to the bulk blanket values as for the total activities although for a few nuclides produced by high Q-values reactions the front wall activity closely approximates the total.

The rate at which the induced activity in the blanket decays is illustrated in fig 1. There are four time scales of particular interest; (i) from shut-down to 1 day, of relevance for possible accident situations, (ii) from 1 day to 1 month, of relevance for maintenance and repair operations, (iii) from a few years to a few tens of years, where consideration may be given to recycling the structural materials or to depositing them in short-term storage prior to permanent disposal, and (iv) for decay times of 100 years or more for considerations of eventual releases of activity to the environment by leaching by ground water, etc. The relative activities of the three alloys 316SS Nb-1Zr and TZM fluctuate with decay period such that there is no preference for any one at all times. As expected, the aluminium and vanadium alloys possess a clear advantage with the vanadium activity essentially vanishing after a decade or so - a feature which could, of course, be modified by the presence of minor impurities. In principle the activity of certain materials (e.g. molybdenum) can be reduced by the futuristic device of isotopic tailoring[66].

Whilst the listing of nuclide activities for the several alloys (Table 2) represents the primary result of our calculations it does not provide the best measure of the relative hazards expected. Of greater relevance are the structural afterheat, γ-dose rates and biological hazard potentials: for a full presentation of these responses see ref 67. In general, the agreement between the results obtained in the present calculations with those given by Kessler and Kulcinski[55] is entirely adequate for current purposes although a detailed comparison does uncover a number of discrepancies.

4.2 Transmutation in structural materials

It is obvious that the progressive transmutation of a metal or alloy into elements not originally present must ultimately have a disastrous effect on the mechanical properties of the metal or alloy. Since the addition of an alloying element at the level of 1% or less has an observable effect on the behaviour of many materials it is likely that the permitted level of transmutant impurities may be even lower. Transmutation damage may be apparent at modest fluences if the new elements form an alloy possessing a different crystal structure from the parent metal whereas if they merely go into solid solution with the parent metal the effects may not be important until very high fluences have been attained.

The transmutation rates exhibited by the structure depend on the location within the blanket. Usually the first wall is most at risk but in some blanket designs[57] the important transmutation products result from (n,γ) reactions which are important in the interior of the blanket where an appreciable thermal neutron component is found. Beyond the primary blanket the effects of transmutation on the insulation properties of electrical insulators and on the resistivity of super-conducting materials have to be considered: the

Table 4. Major Transmutation Effects in First Wall Materials

Element	Initial Composition (at. %)	Composition change rate[a] (appm per MW-yr/m^2)	Composition (at %)[b] 2 yr	10yr	30yr
Type 316 stainless steel[c]					
Fe	62.9	-334 (-1224)	62.9	62.5	60.9
Cr	19.0	+ 57	19.0	19.1	19.4
Ni	12.0	-343 (-177)	11.9	11.6	10.8
Mn	2.0	+411 (+1160)	2.0	2.5	4.0
Mo	2.0	- 17	2.0	2.0	1.93
Si	2.0	- 17	1.99	1.98	1.94
Ti	-	+ 52 (+45)	0.012	0.065	0.20
V	-	+126 (+177)	0.031	0.16	0.46
Co	-	+ 38	0.029	0.47	0.072
V-20 Ti					
V	84.0	-415 (-162)	83.8	83.4	82.2
Ti	16.0	+298 (+53)	16.1	16.4	17.3
Cr	-	+ 86 (+99)	0.022	0.11	0.31
Sc	-	+ 20 (+9)	0.005	0.024	0.073
Ca	-	+ 11	0.004	0.013	0.039
Nb-1Zr					
Nb	99.25	-1274 (-1485)	98.9	97.7	94.4
Zr	0.75	+1238 (+1473)	1.06	2.30	5.35
Y	-	+ 15 (+ 12)	0.004	0.019	0.066
Mo	-	+ 21	0.002	0.026	0.19
TZM					
Mo	98.9	- 926	98.4	97.7	95.6
Ti	1.0	- 2	1.0	0.99	0.99
Zr	0.10	+ 63	0.11	0.18	0.34
Y	-	+ 10	0.003	0.012	0.036
Nb	-	+ 181	0.046	0.227	0.67
Tc	-	+ 583	0.15	0.73	1.98
Ru	-	+ 91	0.02	0.11	0.41
Al 2024					
Al	93.52	- 420	93.3	93.0	91.9
Mg	3.02	+ 372	3.1	3.5	4.38
Si	0.48	+ 15	0.48	0.50	0.53
Cr	0.046	+ 9	0.048	0.058	0.080
Mn	0.45	- 8	0.45	0.44	0.42
Fe	0.24	- 2	0.24	0.24	0.23
Ni	-	+ 51	0.013	0.064	0.18
Cu	2.15	- 57	2.14	2.08	1.92
Zn	0.098	+ 10	0.10	0.11	0.13

a) Averaged over first 10 years

b) Wall loading 1.25 MW/m^2

c) Values in parentheses are from Vogelsang et al [49]

magnitudes of these effects are highly dependent on the details of the blanket and shield design and fall outside the scope of this review.

It is to be expected that transmutation will be more serious for a monoisotopic element (such as niobium) than for an element (such as molybdenum) which possesses several stable isotopes since for many of these isotopes the (n,γ) and (n,2n) reactions merely lead to another stable isotope and the physical and chemical properties of the material are not thereby altered.

Furthermore, as it is likely that any material chosen for structural purposes will be an alloy (often comprised of neighbouring elements), the influence of transmutations may be less than appears initially to be the case.

Transmutation rates in first wall materials have been calculated by Blow[35] (Nb, Mo, PE16), Steiner[37] (Nb, V), Vogelsang et al[49] (SS316, V-20Ti and Nb-1Zr) and Rovner and Hopkins[56] (ceramic materials, including SiC and Al_2O_3). We restrict our present concern to the five alloys considered earlier (Nb-1Zr, TZM, V-20Ti, Al2024 and SS316). The transmutation effects computed with our library are tabulated in Table 4 in a manner permitting direct comparison for SS316, V-20Ti and Nb-1Zr with the results of Vogelsang et al[49]. The agreement between the two sets of calculations is rather poor: the reason for this is not obvious.

As expected, the largest transmutation rate we observe is for Nb-1Zr, where the Zr composition increases to 5.3% after 37.5 MW-yr/m^2. The increased concentration of Zr reduces the ductility of the metal The solubility limit for Zr in Nb is about 15 at.% for temperatures below 600°C, implying a useful lifetime wall loading not exceeding about 100 MW-yr/m^2. The production of Mo is evidently negligible: even with the very large $^{94}Nb(n,\gamma)$ cross-section used by Blow[33] and Steiner[37] the production of molybdenum, through the reactions $^{93}Nb(n,\gamma)$ $^{94}Nb(n\gamma) \xrightarrow{\beta-}$ ^{95}Mo was small compared with the production of zirconium through the more direct route $^{93}Nb(n,2n)$ $^{92m}Nb \xrightarrow{E.C}$ ^{92}Zr. Similar lifetime estimates can be associated with the other materials provided the relevant solubility limits are known.

4.3 Gas production

The generation of hydrogen and helium gases by transmutation reactions induced by neutrons is of great importance in determining the useful lifetime of structural materials in a fusion reactor. In the absence of gas production the lifetime is determined by the number of displacements suffered by each atom due to neutron scattering and reactions; the migration of the lattice vacancies and interstitials results in a volume swelling and loss of valuable physical properties such as ductility, creep resistance, crystal form and alignment, hardness, etc. The addition of gas production, primarily dependent on the presence of the high energy component of the neutron flux, facilitates void nucleation and enhances the swelling. Thus, a knowledge of both displacement and gas production rates is essential in characterizing the radiation damage suffered by a material: the latter effect is of far greater importance for fusion reactors than for fission reactors.

Displacement rates calculations involve an appeal to a model in order to relate the calculable primary knock-on atom (PKA) energy spectrum to the production of atomic displacements. Such calculations fall outside the scope of the present review although certain results are included for completeness. Gas production estimates, on the other hand, can be made directly from a nuclear data library prepared for activation calculations. Alternatively, one could utilize the library of nuclear scattering events compiled by Gabriel, Amburgey and Green[68] (RECOIL) to derive displacement and gas production rates for any desired neutron spectrum. Gabriel, Bishop and Wiffen[61] used this procedure to obtain dpa and gas production estimates for several alloys and for a number of pure elements for a first wall neutron spectrum very similar to that for the CCTR II first wall. Their results are reproduced in Table 5, together with gas production rates obtained from our nuclear data library.

Comparison of the two sets of gas production figures in Table 5 shows that good agreement is rarely found. This cannot be attributed to differences between the neutron spectra. The source of any large differences must therefore be sought in the nuclear cross-sections. The RECOIL data base possesses a significant advantage in that it can use cross-sections appropriate to the element (for which precise measurements are most likely to be available) whereas an activation library contains only isotopic data which, when summed to simulate the elemental data, is likely to be less accurate. On the other hand, the RECOIL library contains only data held in ENDF/B4 whereas the activation library provides estimates for all contributing reactions as required; consequently, it is not surprising that the activation library hydrogen production estimates are generally the higher. It is evident that a careful study of all contributing reactions and an assessment of the cross-section uncertainties is required before a definitive set of gas production rates can be obtained.

Table 5. Estimates of dpa and Gas Production Rates for a fusion reactor first wall with a wall loading of $1 MW/m^2$.

	Displacement Damage (dpa/s) ($x10^{-7}$) (from ref 61)	Helium (appm per MW-s/m^2) ($x10^{-7}$)		Hydrogen (appm per MW-s/m^2) ($x10^{-7}$)	
		ref 61	This work	ref 61	This work
^{6}Li	-	3081	2370	3071	2370
^{7}Li	-	360	365	367	365
^{10}B	-	8980	6680	28.7	213
^{11}B	-	23.6	26.7	12.5	14.2
C	-	604	-	-	-
N	-	205	167	144	120
O	-	118	126	41.0	47.9
Mg	2.80	147	281	148	146
Al	4.63	101	112	94.5	104
Si	4.61	159	244	298	255
Ti	5.03	33.5	49.3	49.7	100
V	3.63	15.0	17.0	78.2	144
Cr	3.58	32.6	74.7	100	135
Mn	3.58	26.7	34.9	100	230
Fe	3.62	34.9	51.1	151	153
Co	3.60	23.1	38.9	73.7	210
Cu	4.88	31.8	45.3	173	239
Nb	2.31	9.18	9.83	33.3	85.5
Mo	2.38	-	21	-	53
Ni	3.87	130	69	397	801

Table 6. Reported Gas Production Rates for Various Materials (appm per MW-yr/m^2)

Material	Helium		Hydrogen Isotopes	
	Fusion First wall	PFR[a)]	Fusion First Wall	PFR[a)]
SiC	1595		440	
SAP	409		779	
Al2024 (Al)	319-344 (365)	29	298-306 (347)	145
V-20Ti (V)	59 (73)	41	229 (429)	100
PE16	199-240		783-1149	
SS316	144-238 (195)		405-611 (713)	554
Nb-1Zr (Nb)	24-32 (32)	2.8	76-114 (275)	20
TZM (Mo)	47 (66)	5.3	95 (167)	34

a) Fast Reactor flux (FD5 spectrum) $\phi = 8.45 \times 10^{15}$ n/cm^2 sec.

Estimates of gas production rates for a variety of first wall materials and blanket designs are available in the literature. The range of estimates for several alloys is illustrated in Table 6, together with our activation library estimates (in parentheses). These are seen to be generally high. An interesting test of our library is available through comparison with the gas production measurements on 316 steel in a 15 MeV neutron flux by Haight et al[69]: we predict a cross-section for helium of 54mb and for hydrogen of 263 mb, compared with measured values 48 $\pm$ 7mb and 260 $\pm$ 38 mb, respectively.

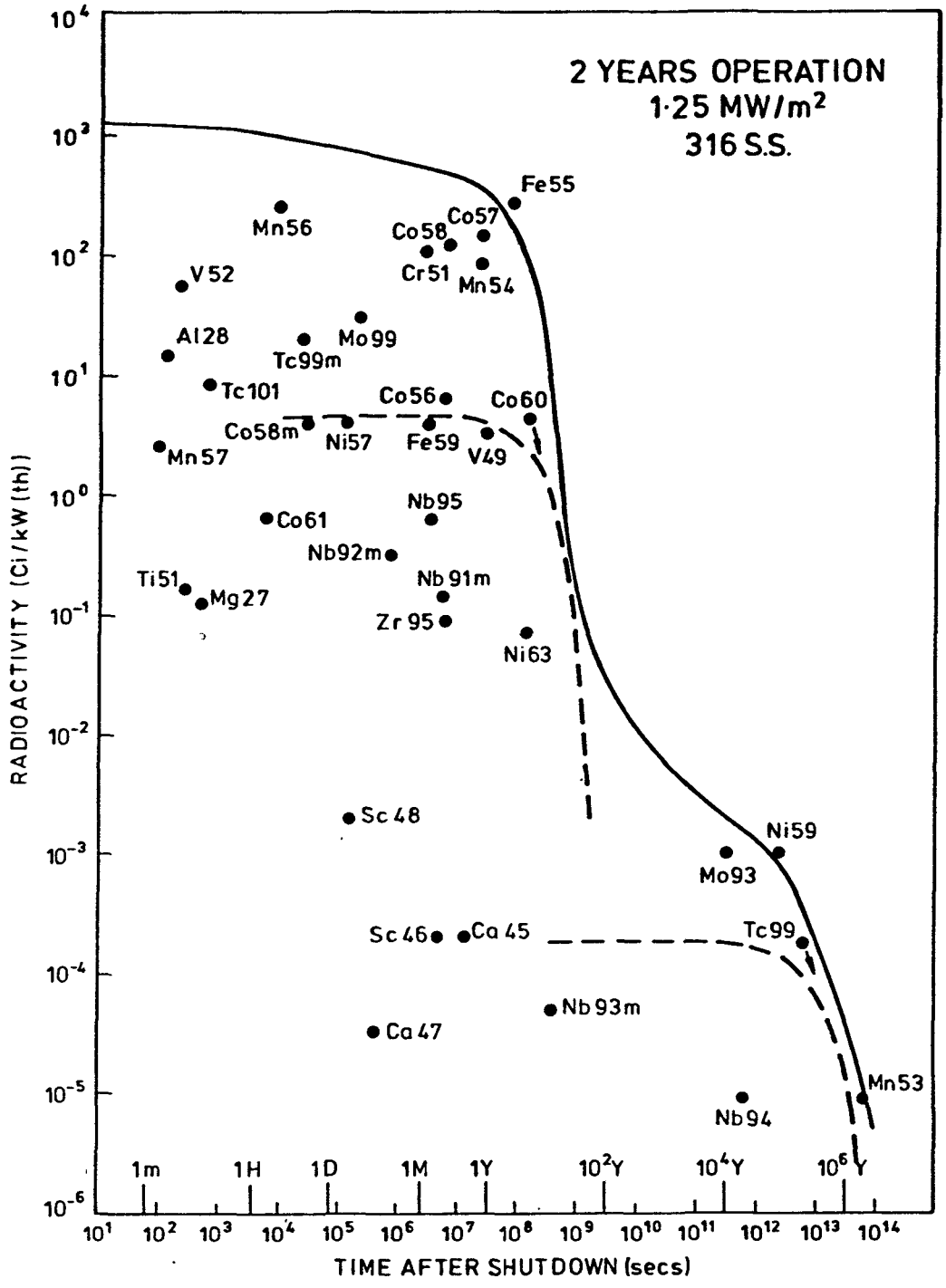

Fig 2. Illustrating the individual nuclide contribution to the activity of a 316 S.S. primary blanket.

The gas production rates considered above refer exclusively to first wall irradiations with no prior neutron moderation. The effects of spectral shifting have been considered by Conn et al[51] and the variations of gas production rates with depth have been considered by Santoro, Baker and Barnes[70].

5. Identification of important reactions

An assessment of the nuclear data requirements and indications of the precision needed can be obtained by inspecting the relative contributions of the many nuclides to the major responses described in section 2. This assessment is appropriate to the group-averaged cross-sections only. A first attempt at producing lists of data requirements is presented below for the five alloys with compositions as presented in Table 4, taking the induced

activity in the primary blanket, and the major transmutation products and gas production rates in the first wall to be the three responses of greatest interest.

5.1 Structural activation

The basic information with respect to structural activation was presented in Table 2 but can be assimilated more readily from figures such as fig. 2 in which the total activity for 316 S.S. is plotted against decay time as before but, in addition - as suggested by Gruber[57] - a point is plotted for each radionuclide corresponding to its initial activity (at shutdown) at a decay time equal to its decay half-life. The decay curves for all individual radionuclides on this log-log plot are of the same shape and pass below the corresponding plotted points since the activities will have decayed to half their shut-down values in the decay period equal to the half-lives, provided there is no generation of the chosen nuclide due to the decay of others. The relative importance of all the nuclides can now

Table 7: Cross-section requirements for primary blanket activity calculations

Radionuclide a)	Maximum Contribution to activity (%)	Reaction c)	Accuracy factor b)
316 S.S.			
V52	5	Cr52(n,p)	5
Mn56	10	Mn55 (n,γ)	2.5
Mo99	3	Mo98 (n,γ)	8
Cr51	10	Cr52 (n,2n)	2.5
Co58	15	Ni58 (n,γ)	1.7
Co57	20	Ni58 (nd)	1.2
Mn54	12	Mn55 (n,2n)	2
Fe55	86	Fe56 (n,2n)	0.25
		Fe54 (n,γ)	2
Co60	10	Ni60 (n,p)	2.5
Mo93	30	Mo94 (n,2n)	1.3 *
		Mo92 (n,γ)	2.2 *
Ni59	80	Ni58 (n,γ)	0.4
		Ni60 (n,2n)	1.0
Tc99	40	Mo98 (n,γ)	1.6
		Mo100(n,2n)	1.7
Mn53	97	Fe54 (n,d)	0.25 *
Nb-1Zr			
Nb94m	85	Nb93(n,γ)Nb94m	0.3
Nb92m	85	Nb93(n,2n)Nb92m	0.3
Nb95	5	Nb94(n,γ)	5 (d)
Nb93m	95	Nb93(n,n')Nb93m	0.25 *
Nb94	100	Nb93(n,γ)	0.25
Zr93	40	Nb93(n,p)	0.6 *
		Zr94(n,2n)	10
Nb92	100	Nb93(n,2n)	0.25
V-20Ti			
V52	64	V51(n,γ)	0.4
Ti51	17	V51 (n,p)	1.6
Sc48	49	V51 (n,α)	0.5
		Ti48(n,p)	10
Sc47	17	Ti47(n,p)	3
		V51 (n,n'α)	3
Sc46	35	Ti46(n,p)	0.7
		Ti47(n,d)	10
Ca45	41	Ti48(n,α)	0.6
V49	90	V50 (n,2n)	0.3 *

Table 7 (continued)

Radionuclide[a]	Maximum Contribution to activity (%)	Reaction[c]	Accuracy factor[b]
		TZM	
Mo101	10	Mo100 (n,γ)	2.5
Tc99m	32	Mo98(n,γ)Mo99 ⟶ Tc99m	1.3 *
Mo93m	4	Mo94(n,2n)Mo93m	6
Mo99	50	Mo98(n,γ)	0.5 *
		Mo100(n,2n)	2
Nb92m	5	Mo92(n,p)Nb92m	5
Nb95	60	Mo95(n,p)	0.4
		Mo96 (n,d)	8
		Mo97 (n,t)	7 *
Nb91m	16	Mo92 (n,d)Mo91m	1.6
Ca45	12	Ti48(n,α)	2
Zr95	15	Mo98(n,α)	1.2
Sc46	3	Ti46 (n,p)	8
Nb93m	40	Mo93 decay	
Mo93	50	Mo94 (n,2n)Mo93 (⟶ Nb93m)	0.5 *
		Mo92 (n,γ)	1.0 *
Tc99	100	Mo98(n,γ)	0.25 *
		Al 2024	
Al28	8	Al27(n,γ)	3
Mg27	32	Al27(n,p)	0.8
Cu64	14	Cu63(n,γ)	2
		Cu65(n2n)	6
Na24	82	Al27(n,α)	0.3
		Mg24(n,p)	7
Zn65	12	Zn64(n,γ)	2 *
		Zn66(n,2n)	5
Mn54	64	Mn55(n,2n)	0.4
		Fe54(n,p)	10
Fe55	30	Fe56(n,2n)	0.8
		Fe54(n,γ)	7
Co60	17	Cu63(n,α)	1.5
Ni63	99	Cu63(n,p)	0.25 *
		Cu65(n,t)	4 *
Al26	120	Al27(n,2n)	0.25

Notes a) Radionuclide listed in order of half-life (shortest at top of table)
b) Accuracy needed is tabulated cross-section X accuracy factor; the star * indicates reactions where desired accuracy may not yet be available.
c) (n,d) implies (n,n'p) + (n,d), (n,t) implies (n,npn) + (n,n'd) + (n,t)
d) Target unstable (Nb 94 only).

be appreciated immediately. Assuming the total activity is required for all decay periods to an accuracy of 25% then the production of the nuclides listed in Table 7 should be known with the accuracies specified. It is assumed, perhaps optimistically, that all reaction cross-sections have been measured or estimated to within a factor of ten or their true values so that radio-nuclides contributing less than 2.5% to the aggregate activity have been excluded. For simplicity each radionuclide is considered as if it alone contributed to the uncertainty in the total activity.

Because the neutron flux and irradiation period are rather modest it is found that, with one exception, only reactions involving the constituent nuclides of the alloys contribute significantly to the total activities. For each alloy only four or five reaction cross-sections are needed to the highest accuracy (∿25%). Those reactions for which measurements or estimates appear, at first sight, not to provide the desired precision are indicated

in Table 7. A more careful study of the literature is needed before any recommendations regarding the need for further measurements can be made.

5.2 Transmutation

Only those reactions which are important for determining the transmutation effects in first wall materials as summarized in Table 4 are considered here. Each composition change rate entered in Table 4 is the aggregate of a number of reactions which may lead to either a gain or a loss for the selected element. In order to restrict the list of notable reactions to manageable form we adopt a selection level of 10% or more of the net transmutation rate for each element, and assume that the net rate is required to an accuracy of 10%, i.e. minor elements for which the composition increases by less than 10% of the change rate for the major constituent are omitted. Whether or not the transmutation products are important depends on metallurgical considerations which are not discussed here. The major transmutation reactions are listed in Table 8; each reaction may appear twice - once as a loss and once as a gain. The desired accuracy is listed for each reaction. The selection of reactions for inclusion in Table 8 is dependent on the time-scale considered for the irradiation period: we have adopted a period of several years, this is longer than the decay periods of the majority of the radionuclides formed.

Table 8. Major first-wall transmutation reactions

Element	Gain/loss (+/-)	Reaction	Accuracy factor
		316SS	
Fe	-	Fe56(n,2n)Fe55⟶ Mn55	0.2
	-	Fe56(n,α)Cr53	0.5
	+	Ni58(n,p)Co58⟶ Fe58	0.6
	+	Ni58(n,d)Co57⟶ Fe57	0.4*
Cr	-	Cr52(n,2n)Cr51⟶ V51	0.2 *
	-	Cr52(n,α)Ti49	0.5
	+	Fe56(n,α)Cr53	0.5
Ni	-	Ni58(n,p)Co58	0.3
	-	Ni58(n,d)Co57⟶ Fe57	0.2 *
Mn	-	Mn55(n,γ)Mn56⟶ Fe56	0.5
	-	Mn55(n,2n)Mn54⟶ Cr54	1.0
	+	Fe56(n,2n)Fe55⟶ Mn55	0.1 *
Ti	+	Cr52(n,α)Ti49	0.2 *
	+	Cr52(n,nα)Ti50	0.5 *
V	+	Cr52(n,2n)Cr51⟶ V51	0.13 *
Co	+	Ni60(n,p)Co60⟶ Ni60	0.2
	+	Ni60(n,d)Co59	0.5
	+	Ni62(n,α)Fe59⟶ Co59	0.3 *
		V-20Ti	
Ti	+	V51(n,α)Sc48⟶ Ti48	0.7
	+	V51(n,d)Ti50	0.1 *
V	-	V51(n,γ)V52⟶ Cr52	0.5
	-	V51(n,α)Sc48⟶ Ti48	1.0
	-	V51(n,d)Ti50	0.2 *
Cr	+	V51(n,γ)V52⟶ Cr52	0.1 *

Table 8 cont.

Element	Gain/loss (+/-)	Reaction	Accuracy factor
		Nb - 1Zr	
Nb	-	Nb93(n,2n)Nb92m⟶ Zr92	0.1
	-	Nb93(n,d)Zr92	0.4 *
Zr	+	Nb93(n,2n)Nb92m⟶ Zr92	0.1
	+	Nb93(n,d)Zr92	0.4 *
		TZM	
Mo	-	Mo100(n,2n)Mo99⟶ Tc99	0.25
	-	Mo98(n,γ)Mo99⟶ Tc99	0.3 *
	-	Mo92(n,2n)Nb91	1.0
	-	Mo100(n,γ)Mo101⟶ Tc101⟶ Ru101	1.0
Zr	+	Mo94(n,α)Zr91	0.3 *
	+	Mo95(n,n'α)Zr91	0.5 *
	+	Mo98(n,n'α)Zr94	1.0 *
	+	Mo97(n,α)Zr94	1.0 *
Nb	+	Mo92(n,2n)Nb91	0.25
	+	Mo92(n,p)Nb92	0.5
	+	Mo94(n,d)Nb91	0.7
Tc	+	Mo98(n,γ)Mo99⟶ Tc99	0.25 *
	+	Mo100(n,2n)Mo99⟶ Tc99	0.16 *
		Al 2024	
Al	-	Al27(n,α)Na24⟶ Mg24	0.1
	-	Al27(n,d)Mg26	0.6
Mg	+	Al27(n,α)Na24⟶ Mg24	0.1
	+	Al27(n,d)Mg26	0.6
Ni	+	Cu63(n,2n)Cu62⟶ Ni62	0.3
	+	Cu65(n,2n)Cu64⟶ Ni64	0.5
	+	Cu63(n,γ) Cu64⟶ Ni64	1.0
	+	Cu63(n,p)Ni63	1.0
	+	Cu63(n,d)Ni62	1.0
Cu	-	Cu63(n,2n)Cu62⟶ Ni62	0.3
	-	Cu63(n,γ)Cr64⟶ Ni64+Zn64	0.6
	-	Cu65(n,2n)Cu64⟶ Ni64+Zn64	0.5
	-	Cu63(n,p)Ni63	1.0
	-	Cu63(n,d)Ni62	1.0

5.3 Gas production

In Table 9 the reactions contributing significantly to the total hydrogen and helium gas production rates are tabulated for the five alloys. We have chosen to list those reactions which contribute 2% or more of the gas production for each alloy and give accuracy factors for each reaction appropriate to a 10% uncertainty in the total. The contributions from impurity constituents, notably ^{14}N in stainless steel, have not been included. For precise estimates of gas production the summation of isotopic contributions is likely to be less preferable than summation of elemental contributions, since direct experimental measurements are more readily available for elements than for isotopes. Nevertheless, for high fluence irradiations some isotopic cross-section data may be needed if successive reaction sequences are likely to be important. As an example we refer to the sequence $^{58}Ni(n,\gamma)^{59}Ni(n,\alpha)^{56}Fe$ which provides an important source of helium in irradiations of stainless steel.

Table 9. First-Wall gas Production

Material	Reaction (helium)	Accuracy	Reaction (hydrogen)	Accuracy
316 S.S.	Fe54(n,α)	5	Fe54(n,p)	1
	Fe56(n,α)	0.3	Fe54(n,d)	5
	Fe56(n,n'α)	1	Fe56(n,p)	0.3
	Ni58(n,α)	2	Ni58(n,p)	0.7
	Ni58(n,n'α)	3	Ni58(n,d)	0.4
	Ni60(n,α)	5	Ni60(n,p)	5
	Cr50(n,α)	5	Cr52(n,p)	1.5
	Cr52(n,α)	0.6	Si28(n,p)	5
	Cr52(n,n'α)	2 *		
	Cr53(n,α)	5		
	Si28(n,α)	1		
Nb-1Zr	Zr91(n,α)	5	Nb93(n,p)	0.3 *
	Nb93(n,α)	0.13 *	Nb93(n,d)	0.18 *
	Nb93(n,n'α)	0.2	Nb93(n,t)	1 *
TZM	Mo92(n,α)	0.7	Mo92(n,p)	0.3
	Mo94(n,α)	0.6*	Mo92(n,d)	0.5 *
	Mo94(n,n'α)	3 *	Mo94(n,d)	2 *
	Mo95(n,n'α)	1 *	Mo95(n,p)	0.8
	Mo96(n,α)	1.3*	Mo95(n,d)	0.5 *
	Mo96(n,n'α)	2 *	Mo95(n,t)	4 *
	Mo97(n,α)	1 *	Mo96	1.4
	Mo97(n,n'α)	2 *	Mo98(n,p)	2
	Mo98(n,α)	1 *	Mo100(n,p)	5
	Mo98(n,n'α)	1 *		
	Mo100(n,α)	2		
V-20Ti	Ti46(n,α)	1	Ti46(n,p)	3
	Ti47(n,α)	4	Ti47(n,p)	5
	Ti48(n,α)	0.5	Ti48(n,p)	2
	V51(n,α)	0.2	V51(n,p)	0.5
	V51(n,n'α)	1	V51(n,d)	0.16*
Al 2024	Mg(n,α)	1.4	Al27(n,p)	0.14
	Al27(n,α)	0.11	Al27(n,d)	0.5
			Cu63(n,p)	1
			Cu63(n,d)	1

6. Conclusion

In the present review we have considered the availability of nuclear data and computational methods for calculations of structural activation, transmutation and gas production in a fusion reactor. It is clear that the situation in both respects is perfectly adequate for current purposes, where uncertainties of a factor of two are acceptable. However, in the future design of a prototype fusion power reactor there will be strong economic incentives to obtain more precise estimates - an accuracy of ± 10% being a reasonable goal. Before this goal can be attained there will need to be a considerable improvement in much of the nuclear reaction cross-section data.

References

[1] KULCINSKI, G.L., "The Potential of D-D Reactions in Future Fusion Devices" p459 in "Fusion and Fast Breeder Reactors", RR-77-8, International Institute for Applied Systems Analysis (1977).

[2] RIBE, F.L. "Fusion Reactor Systems", Rev. Mod. Phys. 47(1975)7.

[3] RIBE, F.L. "Recent Developments in the Design of Conceptual Fusion Reactors", Nuclear Technology. 34(1977)179.

[4] BALL, S.J. and ADAMS, R.K. "MATEXP. A General Purpose Digital Computer Program for Solving Ordinary Differential Equations by the Matrix Exponential Method", ORNL-TM-1933(1967).

[5] NIGG, D.W. and DAVIDSON, J.N., "The Induced Activity and Decay Power of the Structure of a Stainless Steel Fusion Reactor Blanket", Proceedings of the 1st Topical Meeting on the Technology of Controlled Nuclear Fusion, Dan Diego - CONF - 740402 - 1(1974)578.

[6] ODENTHAL, H.J., DANNER, W. and GORENFLO, H. "AKTIV. A Computer Code for Evaluating the Activity, Afterheat, and Biological Hazard Potential of Stainless Steel Structures in Fusion Reactor Blankets", Max-Planck-Institut fur Plasmaphysik, Garching, Munchen, FDR. Report IPP 4/154 (1977).

[7] SUNG, T.Y. and VOGELSANG, W.F., "DKR - A Radioactivity Calculation Code for Fusion Reactors", University of Wisconsin report UWFDM-170(1976), and "Decay Chain Data Library for Radioactivity Calculations", University of Wisconsin Report UWFDM-171(1976).

[8] RICHARDSON, B.L. "FISPIN-4. A Computer Programme to Calculate the Heavy Isotope and Fission Product Inventories of Irradiated Reactor Fuels", UKAEA Reactor Group, TRG Memorandum 6907 (1976).

[9] BELL, M.J. "ORIGEN - The ORNL Isotope Generation and Depletion Code" ORNL-4628 (1973). Available from the Radiation Shielding Information Centre Computer Code Collection (Oak Ridge) as CC-217.

[10] LEDERER, C.M., HOLLANDER, J.M. and PERLMAN, I. "Table of Isotopes", John Wiley and Sons, Inc. (1968).

[11] STAMATELATOS M.G. and ENGLAND, T.R. "Accurate Approximations to Average Beta-Particle Energies and Spectra", Nucl. Sci and Eng. 63 (1977) 204.

[12] ERDTMANN, G.E. and SOYKA, W., "A Table of the γ-Rays of all known Radionuclides", Nucl. Instr. and Methods 121(1974)197.

[13] BOWMAN, W.W. and MacMURDO, K.W., "Radioactive-Decay Gammas", Atomic Data and Nuclear Data Tables 13(1974)89.

[14] "CINDA - An Index to the Literature on Microscopic Neutron Data", IAEA Vienna.

[15] "Neutron Nuclear Data Evaluations", I.A.E.A. Technical Report 146(1973).

[16] WRIGHT, R.Q. et al, "SUPERTOG: A Program to Generate Fine Group Constants and P_n Scattering Matrics from ENDF/B", ORNL-TM-2679(1969).

[17] ENGLE, W.W. "A Users Manual for ANISN. A one-Dimensional Discrete Ordinates Transport Code with Anisotropic Scattering", K-1693, Oak Ridge National Laboratory (1967).

[18] GREENE, N.M. et al, "AMPX: A Modular Code System for Generating Coupled Multigroup Neutron Gamma Libraries from ENDF/B". ORNL-TM-3706(1976).

[19] "Fusion Materials Irradiation Testing Facility, Hanford Reservation Richland, Washington", DOE/EIS-0017 (1978).

[20] GABRIEL, T.A., AMBURGEY, J.D. and GREENE, N.M. "Radiation-Damage Calculations, Primary Knock-on Atom Spectra, Displacement Rates and Gas Production Rates" Nucl. Sci. and Eng. 61 (1976)21.

[21] "Symposium on Neutron Cross-Sections from 10 to 40 MeV", Brookhaven 1977, BNL-NCS-50681.

[22] TSUKADA, K., "Table of Nuclear Reactions and Subsequent Radioactive Decays Induced by 14 MeV Neutrons". JAERI 1252 (1977).

[23] PRINCE, A. in "Nuclear Theory in Neutron Nuclear Data Evaluation", IAEA-190 Vol 1 (1976).

[24] PEARLSTEIN, S. "Neutron Induced Reactions in Medium Mass Nuclei", J. Nucl. Energy 27 (1973)81.

[25] BENZI, V. and REFFO, G., "Fast Neutron Radiative Capture Cross-Sections of Stable Nuclei with 32 < Z < 66", E.N.E.A. Neutron Data Compilation Centre CCDN NW/10 (1969).

[26] YOUNG, P.G. and ARTHUR, E.D. "GNASH: A Pre-equilibrium, Statistical Nuclear Model Code for Calculations of Cross-Sections and Emission Spectra", LA-6947(1977).

[27] KEE, C.W. "A Revised Light Element Library for the ORIGEN Code", ORNL-TM-4896(1975), available from RSIC Oak Ridge as DLC-38/ORYX-E.

[28] DLC-33/Montage-400, "100 Group Neutron Activation Cross-Section Data for Fusion Reactor Structure and Coolant Materials", R.S.I.C. Oak Ridge (1976)

[29] M.R. BHAT, B.A. MAGURNO, S. PEARLSTEIN and F.M. SCHEFFEL, "Nuclear Data for CTR Related Projects", BNL19344 (1974).

[30] KAMYKOWSKI, E.A., "Fast Neutron Induced Activity of Elements Relevant to Fusion Reactor Structural Design", Grumman Aerospace Corp. Bethpage NY. AD-A040 430 (1977).

[31] FRAAS, A.P. and POSTMA, H. "Preliminary Appraisal of the Hazards Problems of a D-T Fusion Reactor Power Plant", ORNL-TM-2822(1970).

[32] DUDZIAK, D.J., "A Technical Note on D-T Fusion Reactor Afterheat", Nucl. Technol. 10(1971)391.

[33] BLOW, S. "Transmutation, Activity and Afterheat in a Fusion Reactor Blanket", U.K.A.E.A. Report A.E.R.E. R-6581(1971).

[34] STEINER, D. "The neutron Induced Activity and Decay Power of the Niobium Structure of a D-T Fusion Reactor Blanket", ORNL-TM-3094 (1970).

[35] BLOW, S. "Some Features of the Behaviour of Structural Materials in a Possible Fusion Reactor Blanket", U.K.A.E.A. Report A.E.R.E. R-6845 (1971).

[36] STEINER, D. and FRAAS, A.P. "Preliminary Observations on the Radiological Implications of Fusion Power", Nuclear Safety 13 (1972)353.

[37] STEINER, D. "The Nuclear Performance of Vanadium as a Structural Material in Fusion Reactor Blankets", Nuclear Fusion 14 (1974)33.

[38] FRAAS, A.P., "Conceptual Design of the Blanket and Shield Region and Related Systems for a full scale Toroidal Fusion Reactor". ORNL-M-3096 (1973).

[39] POWELL, J.R. et al, "Studies of Fusion Reactor Blankets with Minimum Radioactive Inventory and with Tritium Breeding in Solid Lithium Compounds", BNL-18236(1973).

[40] POWELL, J.R. et al, "Minimum Activity Blankets for Commercial and Experimental Power Reactors", BNL-18439 (1973).

[41] PRICE, W.G. Jr., "Blanket Neutron Studies for a Fusion Power Reactor", Trans. Am. Nucl. Soc. 17 (1973)35.

[42] LEE, J.D., "Geometry and Heterogeneous Effects on the Neutronic Performances of a Yin-Yang Mirror Reactor Blanket", UCRL-75141, Lawrence Livermore Laboratory (1973).

[43] MILLS, R.G. et al, "A Fusion Power Plant" MATT-1050, Princeton Plasma Physics Laboratory, Princeton, N.J. (1974).

[44] "An Engineering Design Study of a Reference Theta-Pinch Reactor (RTPR)". LA-5336, ANL-8019, Joint Report of Los Alamos Scientific Laboratory and Argonne National Laboratory (1974).

[45] BADGER, B., KULCINSKI, G.L., CONN, R.W. et al, "UWMAK-I, A Wisconsin Toroidal Fusion Reactor Design", UWFDM-68, University of Wisconsin, Madison, (1975)

[46] BADGER, B., CONN, R.W. KULCINSKI, G.L. et al, "UWMAK-II, A Conceptual Tokamak Power Reactor Design", UWFDM-112, University of Wisconsin, Madison (1975).

[47] BADGER, B., CONN, R.W., KULCINSKI, G.L. et al, "UWMAK-III, A High-Performance, Non-Circular Tokamak Power Reactor Design", UWFDM-150, University of Wisconsin, Madison (1975).

[48] Proceedings of the First Topical Meeting on the Technology of Controlled Nuclear Fusion, San Diego, California, April 16-18, 1974, CONF-740402-P1 and P2 (1974).

[49] VOGELSANG, W.F., KULCINSKI, G.L., LOTT, R.G. and SUNG, T.Y. "Transmutations, Radioactivity and Afterheat in a Deuterium-Tritium Tokamak Fusion Reactor", Nucl. Technol. 22 (1974)329.

[50] DUDZIAK, D.J. and KRAKOWSKI, R.A., "Radioactivity Induced in a Theta-Pinch Fusion Reactor", Nuclear Technol. 26 (1975)125.

[51] CONN, R.W., KULCINSKI, G.L., AVCI, H., EL MAGHRABI, M. "New Concepts for Controlled Fusion Reactor Blanket Design", Nucl. Technol. 26 (1975)125.

[52] CONN, R.W., SUNG, T.Y., and ABDOU, M.A. "Comparative Study of Radioactivity and Afterheat in Several Fusion Reactor Blanket Designs", Nucl. Technol. 26 (1975)391.

[53] WILLIAMS, M.L., SANTORO, R.T. and GABRIEL, T.A. "The Calculated Performance of Various Structural Materials in Fusion Reactor Blankets", Nucl. Technol. 29 (1976)384.

[54] VOGELSANG, W.F. "Radioactivity and Associated Problems in Thermonuclear Reactors", UWFDM-178, University of Wisconsin, Madison (1976)

[55] KESSLER, G. & KULCINSKI, G.L. "Radioactive Inventories of Reactor Economies", p181 in "Fusion and Fast Breeder Reactors", RR-77-8, International Institute for Applied Systems Analysis (1977).

[56] ROVNER, L.H., and HOPKINS, G.R., "Ceramic Materials for Fusion," Nucl. Technol. 29(1976)274.

[57] GRUBER, J. "Evaluation of the Activity Levels in Fusion Reactor Blankets", HMI-B202, Hahn-Meitner-Institut fur Kernforschung, Berlin (1977)

[58] JARVIS, O.N., "Nuclear data for fusion reactors", Int. Conference on Neutron Physics and Nuclear Data for Reactors and other Applied Purposes, Harwell, U.K. 25 to 29 September 1978.

[59] MITCHELL, J.T.D. and HOLLIS, A., "A Tokamak Reactor with Servicing Capability", Proceedings of the 9th Symposium on Fusion Technology, Garmisch-Partenkirchen (1976). Pergamon Press.

[60] BAKER, I.J. (private communication)

[61] GABRIEL, T.A., BISHOP, B.L., and WIFFEN, F.W. "Calculated Atom Displacement and Gas Production Rates of Materials using a Fusion Reactor First Wall Neutron Spectrum". Nucl. Technol. 38 (1978)427.

[62] PERSIANI, P.J., PENNINGTON E.M., HARKER, Y.D. and HEATH, R.L. "The $^{94}Nb(n,\gamma)^{95m}Nb$ Reaction for the CTR Reactor Technology Program", NBS spec. publ. 425, Vol 2 p708 (1975).

[63] TURK, E.H., and HARKER, Y.D. p.17 in ERDA-NCS-3/U(1976).

[64] POENITZ, W.P., P21, in USNDC-11 (1974).

[65] HEGEDUS, F. "Detecteur de Fluence de Neutrons Rapides Utilisant la Reaction $^{93}Nb(n,n')^{93m}Nb$", FRNC-TH-228, U.S.A.E.C. (1972).

[66] CONN, R.W., OKULA, K. JOHNSON, W., "Minimizing Long-Term Radioactivity in Fusion Reactors by Isotopic Tailoring", Trans. Am. Nucl. Soc. 26 (1977)27.

[67] JARVIS, O.N., "Transmutation and activation of fusion reactor first wall and structural materials". UKAEA report AERE-R9298 (in preparation).

[68] GABRIEL, T.A., AMBURGEY, J.D. and GREENE, N.M. "Radiation Damage Spectra, Displacement Rates and Gas Production Rates", Nucl. Sci. and Eng. 61(1976)21.

[69] HAIGHT, R.C., GRIMES, S.M. and ANDERSON, J.D., "Hydrogen and Helium production Cross-Section for 15 MeV Neutrons on Types 316 and 304 Stainless Steel", Nucl. Sci. and Eng. 63(1977)200.

[70] SANTORO, R.T., V.C. BAKER and J.M. BARNES, "Neutronics and Photonics Calculations for the Tokamak Experimental Power Reactor", Nucl. Technol. 37 (1978)274.

APPENDIX I

SPECIFICATION OF NUCLEAR CROSS-SECTION LIBRARY FOR ACTIVATION, TRANSMUTATION AND AFTER-HEAT CALCULATIONS

EXPLANATION OF SYMBOLS:-

NUCL	NUCLIDE, SYMBOL AND ATOMIC NUMBER (M=METASTABLE)
(N,G)	N,GAMMA CROSS-SECTION
(N,2N)	N,2N CROSS-SECTION
(N,A)	SUM OF N,A AND N,N3HE CROSS-SECTIONS
(N,P)	N,P CROSS-SECTION
(N,D)	SUM OF N,D AND N,NP CROSS-SECTIONS
(N,T)	SUM OF N,T AND N,ND AND N,NNP CROSS-SECTIONS
(N,NA)	SUM OF N,NA AND N,AN CROSS-SECTIONS
(N,N*)	EXCITATION OF ISOMERIC STATE
T	LIFETIME
	* - STABLE
	S,M,H,D,Y - SECONDS, MINUTES, HOURS, DAYS, YEARS
ABUND	NATURAL ABUNDANCE(%)

--	DATA NOT WANTED, REACTION PRODUCT NOT IN LIBRARY
**	DATA WANTED FOR LIBRARY, BUT POSSIBLY UNIMPORTANT
ORIG.F	DATA ALREADY AVERAGED FOR AN LMFBR SPECTRUM
ESTIM.	ESTIMATED CROSS-SECTIONS.
THRESH	DATA GENERATED FROM NUCLEAR MODEL (NOT N,G)
T2	IMPROVED MODEL THRESH2 (STILL NOT FOR N,G)
T2.NRM	T2 X-SECTIONS NORMALIZED TO TSUKADA 14MEV DATA.
BENZI	ITALIAN (NUCLEAR MODEL) DATA FOR (N,G)
COOK	AUSTRALIAN (NUCLEAR MODEL) DATA FOR (N,G)
ALLEY	CROSS-SECTIONS TAKEN FROM ALLEY AND LESSLER.
BNL-32	BNL-325
UKAEA	UKAEA DATA FILES
ENDF/B	ENDF/B3 OR B4 DATA FILES

NOTE: ORIG.F TYPICALLY UNDER-ESTIMATES N,G FOR A FUSION REACTOR FIRST-WALL SPECTRUM BY A FACTOR OF ABOUT 3, BUT IS COMPLETELY UNTRUSTWORTHY FOR PARTICLE EMITTING REACTIONS.

NUCL.	(N,G)	(N,2N)	(N,A)	(N,P)	(N,D)	(N,T)	(N,NA)	(N,N*)	T	ABUND
H 1	ENDF/B	—	—	—	—	—	—	—	*	100.0
H 2	ENDF/B	ENDF/B	—	—	—	—	—	—	*	0.0
H 3	**	**	—	—	—	—	—	—	Y	0.0
H 4	—	—	—	—	—	—	—	—	*	0.0
HE 3	ORIG.F	—	—	ENDF/B	**	—	—	—	*	0.0
HE 4	—	—	—	ENDF/B	—	—	—	—	*	100.0
HE 6	—	—	—	—	—	—	—	—	S	0.0
LI 6	ENDF/B	—	ENDF/B	ENDF/B	—	—	**	—	*	7.4
LI 7	ENDF/B	ENDF/B	—	—	ENDF/B	—	ALLEY	—	*	92.6
LI 8	—	—	—	—	—	—	—	—	S	0.0
LI 9	—	—	—	—	—	—	—	—	S	0.0
BE 8	—	—	—	—	—	—	—	—	S	0.0
BE 9	ENDF/B	ENDF/B	ENDF/B	ENDF/B	—	ENDF/B	—	—	*	100.0
BE 10	**	ORIG.F	ORIG.F	—	—	—	—	—	Y	0.0
BE 11	—	—	—	—	—	—	—	—	S	0.0
B 10	**	—	ENDF/B	UKAEA	ENDF/B	ENDF/B	**	—	*	19.8
B 11	ENDF/B	ORIG.F	ENDF/B	ENDF/B	**	ENDF/B	**	—	*	80.2
B 12	—	—	—	—	—	—	—	—	S	0.0
B 13	—	—	—	—	—	—	—	—	S	0.0
C 12	ENDF/B	—	ENDF/B	ORIG.F	**	—	**	—	*	98.9
C 13	ALLEY	ORIG.F	ALLEY	**	—	**	**	—	*	1.1
C 14	ORIG.F	**	ORIG.F	—	—	—	—	—	Y	0.0
C 15	—	—	—	—	—	—	—	—	S	0.0
N 13	—	—	—	—	—	—	—	—	M	0.0
N 14	**	ENDF/B	HEDL	ENDF/B	**	ALLEY	**	—	*	99.6
N 15	**	ORIG.F	ORIG.F	ORIG.F	**	**	**	—	*	0.4
N 16	—	—	—	—	—	—	—	—	S	0.0
O 16	ENDF/B	—	ENDF/B	ENDF/B	ENDF/B	—	**	—	*	99.8
O 17	**	ORIG.F	THRESH	—	**	**	**	—	*	0.0
O 18	ORIG.F	ORIG.F	ORIG.F	—	—	—	**	—	*	0.2
O 19	—	—	—	—	—	—	—	—	S	0.0
F 18	—	—	—	—	—	—	—	—	M	0.0
F 19	ORIG.F	UKAEA	ALLEY	ORIG.F	**	ALLEY	**	—	*	100.0
F 20	—	—	—	—	—	—	—	—	S	0.0
NE 20	**	—	ORIG.F	ORIG.F	**	—	**	—	*	90.9
NE 21	**	ORIG.F	ORIG.F	—	**	**	**	—	*	0.3
NE 22	**	ORIG.F	ORIG.F	—	—	—	**	—	*	8.8
NE 23	—	—	—	—	—	—	—	—	S	0.0
NA 22	ORIG.F	—	**	**	**	**	**	—	Y	0.0
NA 23	ENDF/B	ENDF/B	ENDF/B	ENDF/B	**	**	**	—	*	100.0
NA 24	ORIG.F	**	ORIG.F	—	**	**	**	**	H	0.0
NA 24M	—	—	—	—	—	—	—	—	S	0.0
NA 25	—	—	—	—	—	—	—	—	S	0.0
MG 24	ENDF/B	—	ENDF/B	ENDF/B	**	—	**	—	*	78.7
MG 25	ORIG.F	ORIG.F	ORIG.F	ORIG.F	**	**	**	—	*	10.1
MG 26	ALLEY	ORIG.F	ORIG.F	—	**	—	**	—	*	11.2
MG 27	—	—	—	—	—	—	—	—	M	0.0
MG 28	—	—	—	—	—	—	—	—	H	0.0
AL 26	**	—	**	**	**	**	**	—	Y	0.0
AL 26M	—	—	—	—	—	—	—	—	S	0.0
AL 27	ENDF/B	ENDF/B	ENDF/B	ENDF/B	ENDF/B	ENDF/B	**	—	*	100.0
AL 28	—	—	—	—	—	—	—	—	M	0.0
AL 29	—	—	—	—	—	—	—	—	M	0.0
AL 30	—	—	—	—	—	—	—	—	S	0.0
SI 28	ENDF/B	—	ENDF/B	ENDF/B	ENDF/B	—	**	—	*	92.2
SI 29	**	ORIG.F	ESTIM.	ALLEY	**	**	**	—	*	4.7
SI 30	ALLEY	ORIG.F	ESTIM.	ESTIM.	**	—	**	—	*	3.1

NUCL.	(N,G)	(N,2N)	(N,A)	(N,P)	(N,D)	(N,T)	(N,NA)	(N,N*)	T	ABUND
SI 31	—	—	—	—	—	—	—	—	H	0.0
SI 32	—	**	—	—	—	**	**	—	Y	0.0
P 31	—	—	—	—	—	—	—	—	*	100.0
P 32	ORIG.F	**	**	**	**	**	**	—	D	0.0
P 33	ORIG.F	**	**	—	**	**	**	—	D	0.0
P 34	—	—	—	—	—	—	—	—	S	0.0
S 32	ORIG.F	—	ORIG.F	ALLEY	T2.NRM	—	**	—	*	95.0
S 33	**	ORIG.F	ORIG.F	ALLEY	**	**	**	—	*	0.8
S 34	ALLEY	T2.NRM	ALLEY	T2.NRM	**	**	**	—	*	4.2
S 35	**	**	**	—	**	**	**	—	D	0.0
S 36	ALLEY	ALLEY	—	—	—	**	**	—	*	0.0
S 37	—	—	—	—	—	—	—	—	M	0.0
CL 34	—	—	—	—	—	—	—	—	S	0.0
CL 35	BNL-32	T2.NRM	T2.NRM	BNL-32	T2	T2	T2	—	*	75.5
CL 36	**	T2	T2	T2	**	**	T2	—	Y	0.0
CL 37	ALLEY	T2.NRM	T2.NRM	T2.NRM	T2	T2	T2	—	*	24.5
CL 38	—	T2	—	—	T2	T2	T2	—	M	0.0
CL 38M	—	—	—	—	—	—	—	—	S	0.0
AR 36	**	—	T2.NRM	T2.NRM	T2	T2	T2	—	*	0.3
AR 37	**	T2	T2	T2	T2	T2	T2	—	D	0.0
AR 38	**	T2	T2.NRM	T2.NRM	T2	T2	T2	—	*	0.1
AR 39	**	T2	T2	—	T2	T2	T2	—	Y	0.0
AR 40	ORIG.F	T2.NRM	T2.NRM	—	—	T2	T2	—	*	99.6
AR 41	—	—	—	—	—	—	—	—	H	0.0
AR 42	—	T2	—	—	—	—	—	—	Y	0.0
K 38	—	—	—	—	—	—	—	—	M	0.0
K 39	ENDF/B	ENDF/B	ENDF/B	ENDF/B	T2.NRM	T2.NRM	ENDF/B	—	*	93.1
K 40	**	T2	T2	T2	T2	T2	T2	—	Y	0.1
K 41	BNL-32	T2.NRM	T2.NRM	T2.NRM	T2	T2	T2	—	*	6.8
K 42	—	—	—	—	—	—	—	—	H	0.0
K 43	—	—	—	—	—	—	—	—	H	0.0
K 44	—	—	—	—	—	—	—	—	M	0.0
CA 40	BNL-32	—	T2.NRM	T2.NRM	T2.NRM	T2.NRM	T2.NRM	—	*	97.0
CA 41	**	T2	T2	T2	T2	T2	T2	—	Y	0.0
CA 42	**	T2.NRM	T2.NRM	T2.NRM	T2	T2	T2	—	*	0.6
CA 43	**	T2.NRM	T2.NRM	T2.NRM	T2.NRM	T2	T2	—	*	0.1
CA 44	BNL-32	T2.NRM	T2.NRM	T2.NRM	T2	T2	T2	—	*	2.1
CA 45	**	T2	T2	—	T2	T2	T2	—	D	0.0
CA 46	BNL-32	T2.NRM	—	—	—	**	T2	—	*	0.0
CA 47	—	—	—	—	—	—	—	—	D	0.0
CA 48	ALLEY	T2	—	—	—	—	—	—	*	0.2
CA 49	—	—	—	—	—	—	—	—	M	0.0
SC 44	—	—	—	—	—	—	—	—	H	0.0
SC 44M	—	—	—	—	—	—	—	—	D	0.0
SC 45	BNL-32	T2.NRM	T2.NRM	T2.NRM	T2	T2	T2	—	*	100.0
SC 46	ORIG.F	T2	T2	T2	T2	T2	T2	—	D	0.0
SC 46M	—	—	—	—	—	—	—	—	S	0.0
SC 47	—	—	—	—	—	—	—	—	D	0.0
SC 48	—	—	—	—	—	—	—	—	D	0.0
SC 49	—	—	—	—	—	—	—	—	M	0.0
SC 50	—	—	—	—	—	—	—	—	M	0.0
TI 45	—	—	—	—	—	—	—	—	H	0.0
TI 46	ORIG.F	T2.NRM	T2.NRM	ENDF/B	T2	T2.NRM	T2	—	*	7.9
TI 47	ORIG.F	T2.NRM	T2	ENDF/B	T2.NRM	T2	T2	—	*	7.3
TI 48	ORIG.F	T2.NRM	BNL-32	ENDF/B	T2.NRM	T2	T2	—	*	73.9
TI 49	ORIG.F	T2.NRM	T2.NRM	T2.NRM	T2.NRM	T2	T2	—	*	5.5
TI 50	BNL-32	T2.NRM	T2.NRM	T2.NRM	T2.NRM	T2	T2	—	*	5.3

NUCL.	(N,G)	(N,2N)	(N,A)	(N,P)	(N,D)	(N,T)	(N,NA)	(N,N*)	T	ABUND
TI 51	--	--	--	--	--	--	--	--	M	0.0
V 48	**	--	T2	T2	T2	T2	T2	--	D	0.0
V 49	ORIG.F	T2	T2	T2	T2	T2	T2	--	D	0.0
V 50	ORIG.F	T2.NRM	T2.NRM	T2	T2	T2	T2	--	Y	0.2
V 51	ENDF/B	T2.NRM	T2.NRM	T2.NRM	T2	T2	T2.NRM	--	*	99.8
V 52	--	--	--	--	--	--	--	--	M	0.0
V 53	--	--	--	--	--	--	--	--	M	0.0
V 54	--	--	--	--	--	--	--	--	S	0.0
CR 49	--	--	--	--	--	--	--	--	M	0.0
CR 50	BNL-32	BNL-32	T2.NRM	T2.NRM	T2.NRM	T2	T2	--	*	4.3
CR 51	ORIG.F	T2	T2.NRM	T2.NRM	T2	T2	T2	--	D	0.0
CR 52	ENDF/B	ENDF/B	ENDF/B	ENDF/B	T2.NRM	T2	T2	--	*	83.8
CR 53	ORIG.F	T2.NRM	T2.NRM	T2.NRM	T2.NRM	T2	T2	--	*	9.6
CR 54	ALLEY	T2.NRM	T2.NRM	T2.NRM	T2.NRM	T2	T2	--	*	2.4
CR 55	--	--	--	--	--	--	--	--	M	0.0
MN 52	--	--	--	--	--	--	--	--	D	0.0
MN 53	**	T2	T2	T2	T2	T2	T2	--	Y	0.0
MN 54	ORIG.F	T2	T2.NRM	T2.NRM	T2	T2	T2	--	D	0.0
MN 55	ALLEY	ENDF/B	ENDF/B	ENDF/B	T2	T2	T2	--	*	100.0
MN 56	--	--	--	--	--	--	--	--	H	0.0
MN 57	--	--	--	--	--	--	--	--	M	0.0
MN 58	--	--	--	--	--	--	--	--	M	0.0
FE 53	--	--	--	--	--	--	--	--	M	0.0
FE 54	BNL-32	T2.NRM	BNL-32	UKAEA2	T2.NRM	T2.NRM	T2	--	*	5.8
FE 55	ORIG.F	T2	T2.NRM	T2.NRM	T2	T2	T2	--	Y	0.0
FE 56	ENDF/B	ENDF/B	ENDF/B	ENDF/B	T2.NRM	T2	T2	--	*	91.7
FE 57	ORIG.F	T2.NRM	T2.NRM	T2.NRM	T2.NRM	T2	T2	--	*	2.2
FE 58	BNL-32	T2.NRM	T2.NRM	T2.NRM	T2	T2	T2	--	*	0.3
FE 59	ORIG.F	T2	--	--	T2	T2	T2	--	D	0.0
FE 60	**	T2	--	--	--	T2	--	--	Y	0.0
FE 61	--	--	--	--	--	--	--	--	M	0.0
CO 55	--	--	--	--	--	--	--	--	H	0.0
CO 56	**	T2	T2	T2	T2	T2	T2	--	D	0.0
CO 57	**	T2	T2	T2	T2	T2	T2	--	D	0.0
CO 58	**	T2	T2.NRM	T2.NRM	T2	T2	T2	**	D	0.0
CO 58M	--	--	--	--	--	--	--	--	H	0.0
CO 59	ALLEY	ENDF/B	ENDF/B	ENDF/B	T2	T2.NRM	T2	--	*	100.0
CO 60	**	T2	T2.NRM	T2.NRM	T2	T2	T2	**	Y	0.0
CO 60M	--	--	--	--	--	--	--	--	M	0.0
CO 61	--	--	--	--	--	--	--	--	M	0.0
CO 62	--	--	--	--	--	--	--	--	M	0.0
CO 63	--	--	--	--	--	--	--	--	S	0.0
CO 64	--	--	--	--	--	--	--	--	S	0.0
NI 57	--	--	--	--	--	--	--	--	H	0.0
NI 58	ENDF/B	ENDF/B	ENDF/B	ENDF/B	T2.NRM	T2	T2.NRM	--	*	67.8
NI 59	ORIG.F	T2	T2.NRM	T2.NRM	T2	T2	T2	--	Y	0.0
NI 60	ORIG.F	T2.NRM	T2.NRM	BNL-32	T2.NRM	T2	T2	--	*	26.2
NI 61	ORIG.F	T2.NRM	T2.NRM	T2.NRM	T2.NRM	T2	T2	--	*	1.2
NI 62	BNL-32	T2.NRM	T2.NRM	T2.NRM	T2.NRM	T2	T2	--	*	3.7
NI 63	ORIG.F	T2	T2	T2	T2	T2	T2	--	Y	0.0
NI 64	ALLEY	T2.NRM	T2.NRM	T2.NRM	T2.NRM	T2	T2	--	*	1.1
NI 65	--	--	--	--	--	--	--	--	H	0.0
NI 66	--	--	--	--	--	--	--	--	H	0.0
CU 62	--	--	--	--	--	--	--	--	M	0.0
CU 63	ENDF/B	ENDF/B	ENDF/B	ENDF/B	T2.NRM	T2	T2	--	*	69.1
CU 64	--	--	--	--	--	--	--	--	H	0.0
CU 65	ENDF/B	ENDF/B	ENDF/B	ENDF/B	T2	T2	T2.NRM	--	*	30.9

NUCL.	(N,G)	(N,2N)	(N,A)	(N,P)	(N,D)	(N,T)	(N,NA)	(N,N*)	T	ABUND
CU 66	--	--	--	--	--	--	--	--	M	0.0
CU 67	--	--	--	--	--	--	--	--	H	0.0
ZN 64	ALLEY	--	T2.NRM	T2.NRM	T2.NRM	T2	T2	--	*	48.9
ZN 65	**	T2	T2	T2	T2	T2	T2	--	D	0.0
ZN 66	**	T2.NRM	T2.NRM	T2.NRM	T2.NRM	T2	T2	--	*	27.8
ZN 67	**	T2.NRM	T2.NRM	T2.NRM	T2.NRM	T2	T2	--	*	4.1
ZN 68	ALLEY	T2.NRM	T2.NRM	--	T2.NRM	T2	T2	--	*	18.6
ZN 69	--	--	--	--	--	--	--	--	M	0.0
ZN 69M	--	--	--	--	--	--	--	--	H	0.0
ZN 70	ALLEY	T2.NRM	--	--	--	--	--	--	*	0.6
ZN 71	--	--	--	--	--	--	--	--	M	0.0
ZN 71M	--	--	--	--	--	--	--	--	H	0.0
GA 69	--	--	T2.NRM	T2.NRM	T2	T2	T2	--	*	60.2
GA 71	--	--	--	T2.NRM	T2	T2	T2.NRM	--	*	39.8
SR 84	ALLEY	--	--	--	--	--	--	--	*	0.6
SR 85	**	T2	--	--	--	--	--	**	D	0.0
SR 85M	--	--	--	--	--	--	--	--	M	0.0
SR 86	BENZI	T2.NRM	--	--	--	--	--	--	*	9.9
SR 87	BENZI	T2	--	--	--	--	--	--	*	7.0
SR 87M	--	--	--	--	--	--	--	--	H	0.0
SR 88	ALLEY	T2	--	--	--	--	--	--	*	82.5
SR 89	ORIG.F	T2	--	--	--	--	--	--	D	0.0
SR 90	ORIG.F	T2	--	--	--	--	--	--	Y	0.0
SR 91	--	--	--	--	--	--	--	--	H	0.0
SR 92	--	--	--	--	--	--	--	--	H	0.0
SR 93	--	--	--	--	--	--	--	--	M	0.0
Y 88	**	--	--	--	--	--	--	--	D	0.0
Y 89	COOK	T2.NRM	--	T2.NRM	T2	T2	--	--	*	100.0
Y 89M	--	--	--	--	--	--	--	--	S	0.0
Y 90	--	--	--	--	--	--	--	--	H	0.0
Y 90M	--	--	--	--	--	--	--	--	H	0.0
Y 91	COOK	T2	--	T2	T2	T2	--	**	D	0.0
Y 91M	--	--	--	--	--	--	--	--	M	0.0
Y 92	--	--	--	--	--	--	--	--	H	0.0
Y 93	--	--	--	--	--	--	--	--	H	0.0
Y 94	--	--	--	--	--	--	--	--	M	0.0
Y 95	--	--	--	--	--	--	--	--	M	0.0
Y 96	--	--	--	--	--	--	--	--	M	0.0
ZR 89	--	--	--	--	--	--	--	--	H	0.0
ZR 90	BENZI	T2.NRM	T2	T2.NRM	T2.NRM	T2	T2	--	*	51.5
ZR 91	BENZI	T2.NRM	T2	T2.NRM	T2.NRM	T2	T2	--	*	11.2
ZR 92	COOK	T2.NRM	BNL-32	T2.NRM	T2.NRM	T2	T2	--	*	17.1
ZR 93	ORIG.F	T2	T2	T2	T2	T2	T2	--	Y	0.0
ZR 94	ALLEY	T2.NRM	T2.NRM	T2.NRM	T2.NRM	T2	T2	--	*	17.4
ZR 95	ORIG.F	T2	T2	T2	T2	T2	T2	--	D	0.0
ZR 96	COOK	T2.NRM	T2.NRM	T2.NRM	T2	T2	T2.NRM	--	*	2.8
ZR 97	--	--	--	--	--	--	--	--	H	0.0
NB 91	**	--	T2	T2	T2	T2	--	**	*	0.0
NB 91M	**	--	T2	T2	T2	T2	--	--	D	0.0
NB 92	**	T2	T2	T2.NRM	T2.NRM	T2	T2	**	Y	0.0
NB 92M	**	T2	T2	T2.NRM	T2.NRM	T2	T2	--	D	0.0
NB 93	ENDF/B	ENDF/B	ENDF/B	ENDF/B	T2	T2	T2.NRM	FRNC-T	*	100.0
NB 93M	ENDF/B	ENDF/B	ENDF/B	ENDF/B	T2	T2	T2.NRM	--	Y	0.0
NB 94	ESTIM.	T2	T2	T2.NRM	T2	T2	T2	**	Y	0.0
NB 94M	--	--	--	--	--	--	--	--	M	0.0
NB 95	ORIG.F	T2	T2	T2	T2	T2	T2	**	D	0.0
NB 95M	--	--	--	--	--	--	--	--	H	0.0

NUCL.	(N,G)	(N,2N)	(N,A)	(N,P)	(N,D)	(N,T)	(N,NA)	(N,N*)	T	ABUND
NB 96	—	—	—	—	—	—	—	—	H	0.0
NB 97	—	—	—	—	—	—	—	—	M	0.0
NB 97M	—	—	—	—	—	—	—	—	M	0.0
NB 98	—	—	—	—	—	—	—	—	M	0.0
NB 99	—	—	—	—	—	—	—	—	M	0.0
NB100	—	—	—	—	—	—	—	—	M	0.0
MO 91	—	—	—	—	—	—	—	—	M	0.0
MO 92	BENZI	T2.NRM	T2.NRM	T2.NRM	T2.NRM	—	—	—	*	15.8
MO 93	ORIG.F	T2	T2	T2.NRM	T2	T2	T2	**	Y	0.0
MO 93M	—	—	—	—	—	—	—	—	H	0.0
MO 94	BENZI	T2.NRM	T2.NRM	T2.NRM	T2	T2	T2	—	*	9.0
MO 95	BENZI	T2.NRM	T2.NRM	T2.NRM	T2.NRM	T2	T2	—	*	15.7
MO 96	BENZI	T2.NRM	T2.NRM	T2.NRM	T2.NRM	T2	T2	—	*	16.5
MO 97	BENZI	T2.NRM	T2	T2.NRM	T2.NRM	T2	T2	—	*	9.5
MO 98	COOK	T2.NRM	T2.NRM	T2.NRM	T2.NRM	T2	T2	—	*	23.8
MO 99	—	—	—	—	—	—	—	—	H	0.0
MO100	COOK	T2.NRM	T2.NRM	T2	T2	T2	T2	—	*	9.6
MO101	—	—	—	—	—	—	—	—	M	0.0
TC 96	—	—	—	—	—	—	—	—	D	0.0
TC 97	**	T2	T2	T2	T2	T2	T2	**	Y	0.0
TC 97M	**	T2	T2	T2	T2	T2	T2	—	D	0.0
TC 98	**	T2	T2	T2	T2	T2	T2	—	Y	0.0
TC 99	COOK	T2.NRM	T2.NRM	T2.NRM	T2	T2	T2.NRM	**	Y	0.0
TC 99M	—	—	—	—	—	—	—	—	H	0.0
TC100	—	—	—	—	—	—	—	—	S	0.0
TC101	—	—	—	—	—	—	—	—	M	0.0
RU 96	—	—	—	—	—	—	—	—	*	5.5
RU 97	—	—	—	—	—	—	—	—	D	0.0
RU 98	—	—	—	—	—	—	—	—	*	1.9
RU 99	—	—	—	—	—	—	—	—	*	12:7
RU100	—	—	—	—	—	—	—	—	*	12.6
RU101	—	—	—	—	—	—	—	—	*	17.1
RU102	—	—	—	—	—	—	—	—	*	31.6
RU103	—	—	—	—	—	—	—	—	D	0.0
RU104	—	—	—	—	—	—	—	—	*	18.6
RU105	—	—	—	—	—	—	—	—	H	0.0
RU106	—	—	—	—	—	—	—	—	D	0.0
RU107	—	—	—	—	—	—	—	—	M	0.0
RH103	—	—	—	—	—	—	—	—	*	100.0
RH104	—	—	—	—	—	—	—	—	S	0.0
RH104M	—	—	—	—	—	—	—	—	M	0.0
RH105	—	—	—	—	—	—	—	—	H	0.0
RH105M	—	—	—	—	—	—	—	—	S	0.0
RH106	—	—	—	—	—	—	—	—	S	0.0
RH106M	—	—	—	—	—	—	—	—	M	0.0
RH107	—	—	—	—	—	—	—	—	M	0.0
PD102	—	—	—	—	—	—	—	—	*	1.0
PD103	—	—	—	—	—	—	—	—	D	0.0
PD104	—	—	—	—	—	—	—	—	*	11.0
PD105	—	—	—	—	—	—	—	—	*	22.2
PD106	—	—	—	—	—	—	—	—	*	27.3
PD107	—	—	—	—	—	—	—	—	Y	0.0
PD107M	—	—	—	—	—	—	—	—	S	0.0
PD108	—	—	—	—	—	—	—	—	*	26.7
PD109	—	—	—	—	—	—	—	—	H	0.0
PD109M	—	—	—	—	—	—	—	—	M	0.0
PD110	—	—	—	—	—	—	—	—	*	11.8

NUCL.	(N,G)	(N,2N)	(N,A)	(N,P)	(N,D)	(N,T)	(N,NA)	(N,N*)	T	ABUND
PD111	—	—	—	—	—	—	—	—	M	0.0
PD111M	—	—	—	—	—	—	—	—	H	0.0
AG107	ALLEY	—	T2.NRM	T2.NRM	T2	T2	T2.NRM	—	*	51.8
AG108	—	—	—	—	—	—	—	—	M	0.0
AG108M	—	—	—	—	—	—	—	—	Y	0.0
AG109	ALLEY	T2.NRM	T2.NRM	T2.NRM	T2	T2	T2.NRM	**	*	48.2
AG109M	—	—	—	—	—	—	—	—	S	0.0
AG110	—	—	—	—	—	—	—	—	S	0.0
AG110M	—	—	—	—	—	—	—	—	D	0.0
AG111	—	—	—	—	—	—	—	—	D	0.0
AG111M	—	—	—	—	—	—	—	—	S	0.0
AG112	—	—	—	—	—	—	—	—	H	0.0
CD106	BENZI	—	T2	—	—	—	T2	—	*	1.2
CD107	—	—	—	—	—	—	—	—	H	0.0
CD108	ALLEY	T2.NRM	T2	T2.NRM	T2	—	T2	—	*	0.9
CD109	**	T2	T2	T2	T2	T2	T2	—	D	0.0
CD110	BENZI	T2.NRM	T2	T2.NRM	T2	T2	T2	—	*	12.4
CD111	BENZI	T2.NRM	T2	T2.NRM	T2	T2	T2	**	*	12.8
CD111M	—	—	—	—	—	—	—	—	M	0.0
CD112	BENZI	T2	T2.NRM	T2.NRM	T2	T2	T2	—	*	24.1
CD113	BENZI	T2.NRM	T2	—	T2	T2	T2	—	*	12.3
CD114	ALLEY	T2	T2.NRM	—	—	T2	T2	—	*	28.9
CD115	—	—	—	—	—	—	—	—	H	0.0
CD115M	—	—	—	—	—	—	—	—	D	0.0
CD116	ALLEY	T2.NRM	—	—	—	—	—	—	*	7.6
CD117	—	—	—	—	—	—	—	—	H	0.0
CD117M	—	—	—	—	—	—	—	—	H	0.0
CD118	—	—	—	—	—	—	—	—	M	0.0
CD119	—	—	—	—	—	—	—	—	M	0.0
CD120	—	—	—	—	—	—	—	—	S	0.0
CD121	—	—	—	—	—	—	—	—	S	0.0
IN111	—	—	—	—	—	—	—	—	D	0.0
IN112	—	—	—	—	—	—	—	—	M	0.0
IN113	ALLEY	T2.NRM	T2	T2.NRM	T2	T2	T2	**	*	4.3
IN113M	—	—	—	—	—	—	—	—	M	0.0
IN114	—	—	—	—	—	—	—	—	S	0.0
IN114M	—	—	—	—	—	—	—	—	D	0.0
IN115	ALLEY	T2.NRM	T2.NRM	T2.NRM	T2	T2	T2	**	Y	95.7
IN115M	—	—	—	—	—	—	—	—	H	0.0
IN116	—	—	—	—	—	—	—	—	S	0.0
IN116M	—	—	—	—	—	—	—	—	M	0.0
IN117	—	—	—	—	—	—	—	—	M	0.0
IN117M	—	—	—	—	—	—	—	—	H	0.0
IN118	—	—	—	—	—	—	—	—	M	0.0
IN119	—	—	—	—	—	—	—	—	M	0.0
IN119M	—	—	—	—	—	—	—	—	M	0.0
IN120	—	—	—	—	—	—	—	—	S	0.0
IN120M	—	—	—	—	—	—	—	—	S	0.0
IN121	—	—	—	—	—	—	—	—	M	0.0
IN122	—	—	—	—	—	—	—	—	S	0.0
IN123	—	—	—	—	—	—	—	—	S	0.0
IN124	—	—	—	—	—	—	—	—	S	0.0
SN111	—	—	—	—	—	—	—	—	M	0.0
SN112	BENZI	T2.NRM	T2.NRM	T2.NRM	T2.NRM	—	T2	—	*	1.0
SN113	**	T2	T2	T2	T2	T2	T2	**	D	0.0
SN113M	—	—	—	—	—	—	—	—	M	0.0
SN114	BENZI	T2.NRM	T2	T2.NRM	T2	T2	T2	—	*	0.7

NUCL.	(N,G)	(N,2N)	(N,A)	(N,P)	(N,D)	(N,T)	(N,NA)	(N,N*)	T	ABUND
SN115	BENZI	T2	T2	T2	T2	T2	T2	—	*	0.4
SN116	COOK	T2.NRM	T2.NRM	T2.NRM	T2	T2	T2	—	*	14.3
SN117	BENZI	T2.NRM	T2.NRM	T2.NRM	T2	T2	T2	**	*	7.6
SN117M	BENZI	T2.NRM	T2.NRM	T2.NRM	T2	T2	T2	—	D	0.0
SN118	COOK	T2	T2.NRM	T2	T2.NRM	T2	T2	—	*	24.0
SN119	BENZI	T2.NRM	T2	T2.NRM	T2	T2	T2	**	*	8.6
SN119M	BENZI	T2.NRM	T2	T2.NRM	T2	T2	T2	—	D	0.0
SN120	ALLEY	T2	T2	T2.NRM	T2	T2	T2	—	*	32.9
SN121	—	—	—	—	—	—	—	—	H	0.0
SN121M	—	—	—	—	—	—	—	—	Y	0.0
SN122	COOK	T2.NRM	T2	T2.NRM	T2	T2	T2	—	*	4.7
SN123	ORIG.F	T2	T2	T2	T2	T2	T2	**	D	0.0
SN123M	—	—	—	—	—	—	—	—	M	0.0
SN124	ALLEY	T2.NRM	T2	T2	T2	T2	T2	—	*	5.9
SN125	—	—	—	—	—	—	—	—	D	0.0
SN125M	—	—	—	—	—	—	—	—	M	0.0
SB121	—	—	T2	T2.NRM	T2	T2	T2	—	*	57.3
SB123	—	—	T2	T2.NRM	T2	T2	T2	—	*	42.8
SB125	—	—	T2	T2	T2	T2	T2	—	Y	0.0
HF173	—	—	—	—	—	—	—	—	H	0.0
HF174	ENDF/B	T2.NRM	—	—	—	—	—	—	*	0.2
HF175	**	T2	—	—	—	—	—	—	D	0.0
HF176	**	ENDF/B	—	—	—	—	—	—	*	5.2
HF177	**	T2.NRM	—	—	—	—	—	—	*	18.5
HF178	**	T2.NRM	—	—	—	—	—	—	*	27.1
HF178M	—	—	—	—	—	—	—	—	S	0.0
HF179	ALLEY	T2	—	—	—	—	—	—	*	13.8
HF179M	—	—	—	—	—	—	—	—	S	0.0
HF180	ENDF/B	T2	—	—	—	—	—	**	*	35.2
HF180M	—	—	—	—	—	—	—	—	H	0.0
HF181	**	T2	—	—	—	—	—	—	D	0.0
HF182	—	T2	—	—	—	—	—	—	Y	0.0
TA180	**	—	—	T2	T2	T2	—	—	Y	0.0
TA181	ENDF/B	ENDF/B	—	T2.NRM	T2	T2	—	—	*	100.0
TA182	**	T2	—	T2	T2	T2	—	**	D	0.0
TA182M	—	—	—	—	—	—	—	—	M	0.0
TA183	—	—	—	—	—	—	—	—	D	0.0
W180	ALLEY	—	T2	T2	—	—	T2	—	*	0.1
W181	**	T2	T2	T2	T2	—	T2	—	D	0.0
W182	**	ENDF/B	T2.NRM	ENDF/B	T2	T2	T2	—	*	26.4
W183	**	T2.NRM	T2	ENDF/B	T2.NRM	T2	T2	—	*	14.4
W184	ENDF/B	T2	ENDF/B	—	T2.NRM	T2	T2	—	*	30.6
W185	**	T2	T2	—	—	T2	T2	—	D	0.0
W185M	—	—	—	—	—	—	—	—	M	0.0
W186	ENDF/B	ENDF/B	—	—	—	—	T2	—	*	28.4
W187	—	—	—	—	—	—	—	—	H	0.0
RE185	—	—	T2	T2	T2	T2	T2	—	*	37.1
RE187	—	—	—	T2.NRM	T2	T2	—	—	Y	62.9
HG196	ALLEY	—	—	—	—	—	—	—	*	0.1
HG197	—	—	—	—	—	—	—	—	H	0.0
HG197M	—	—	—	—	—	—	—	—	H	0.0
HG198	ALLEY	T2.NRM	—	—	—	—	—	—	*	10.0
HG199	**	T2.NRM	—	—	—	—	—	**	*	16.8
HG199M	—	—	—	—	—	—	—	—	M	0.0
HG200	**	T2	—	—	—	—	—	—	*	23.1
HG201	**	T2.NRM	—	—	—	—	—	—	*	13.2
HG202	ALLEY	T2.NRM	—	—	—	—	—	—	*	29.8

NUCL.	(N,G)	(N,2N)	(N,A)	(N,P)	(N,D)	(N,T)	(N,NA)	(N,N*)	T	ABUND
HG203	**	T2	—	—	—	—	—	—	D	0.0
HG204	ALLEY	T2.NRM	—	—	—	—	—	—	*	6.9
HG205	—	—	—	—	—	—	—	—	M	0.0
TL202	**	—	—	T2	T2	T2	—	—	D	0.0
TL203	ALLEY	T2.NRM	—	T2.NRM	T2	T2	—	—	*	29.5
TL204	**	T2	—	T2	T2	T2	—	—	Y	0.0
TL205	ALLEY	T2.NRM	—	T2.NRM	T2	T2	—	—	*	70.5
TL206	—	—	—	—	—	—	—	—	M	0.0
TL207	—	—	—	—	—	—	—	—	M	0.0
TL208	—	—	—	—	—	—	—	—	M	0.0
PB203	—	—	—	—	—	—	—	—	H	0.0
PB204	ALLEY	T2.NRM	T2	T2	T2	T2	T2	—	Y	1.5
PB205	**	T2	T2	T2	T2	T2	T2	—	Y	0.0
PB206	**	T2.NRM	T2.NRM	T2	T2	T2	T2	—	*	23.6
PB207	**	T2.NRM	T2	T2	T2	T2	T2	—	*	22.6
PB208	ENDF/B	ENDF/B	T2.NRM	T2.NRM	T2	T2	T2	—	*	52.3
PB209	—	—	—	—	—	—	—	—	H	0.0
BI209	—	—	T2.NRM	T2.NRM	T2	T2	T2	—	*	100.0

NUCLEAR DATA NEEDS FOR RADIATION DAMAGE STUDIES RELEVANT TO FUSION REACTOR TECHNOLOGY

AG-159/A4

Review Paper

S.M. QAIM
Institut für Chemie 1 (Nuklearchemie)
Kernforschungsanlage Jülich GmbH
D-517 Jülich, Federal Republic of Germany

Abstract

Radiation damage problem is of vital significance for fusion reactor design and originates from displacement of atoms from their normal lattice sites as well as from nuclear transmutations, especially those leading to the formation of hydrogen and helium. An outline of the radiation damage effects resulting in bulk property changes is given and their relation to nuclear data is discussed. The available methods for studying radiation damage in metals are briefly mentioned. The nuclear data needs relevant to radiation damage studies are discussed. Data are needed primarily for neutron dosimetry, for calculating displacement cross sections and for gas production. A brief review of the status of available data is given and the areas needing further experimental work are described.

INTRODUCTION

It is now well known that in a fusion reactor the first wall separating the vacuum zone around the confined plasma from the blanket would receive a heavy energy load, somewhere between 1 and 10 MW/m^2, depending on the conceptual reactor design. This heavy load would originate primarily from the presence of fast neutrons and α-particles, both generated in the fusion of deuterium and tritium, and would place more stringent demands on the structural materials than in fast reactors. In a fusion reactor higher radiation damage effects are expected, although the total neutron flux at the first wall may be lower than that in the core of a fast reactor. The anticipated neutron energy spectrum at the first wall of a fusion reactor, involving the fusion of deuterium and tritium, is shown [1] in Fig. 1. For comparison the spectra for a fast reactor and a thermal reactor are also shown. Evidently the neutron spectrum in a fusion reactor will be appreciably harder than that in a fast reactor; this is manifested more clearly if the high energy parts of the spectra are plotted on a linear scale [2,3].

The present demands on nuclear data for fusion technology are primarily for design calculations pertaining to various areas like tritium production and breeding, nuclear heating, radiation damage, radiation shielding, etc. Nuclear data needs for fusion have been discussed in general terms in several review articles [1-4]. The present review deals with the specific topic of data for radiation damage. Since several aspects of nuclear data needs for radiation damage have already been discussed [5], the emphasis in the present report is on newer information and most recent trends in data needs.

RADIATION DAMAGE STUDIES

Sources of Radiation Damage

There are two main sources of radiation damage in metals, viz., displacement of atoms from their normal lattice sites and the formation of foreign atoms via nuclear transmutations. We discuss the two sources below.

Displacement of atoms: The displacement damage in a metal under the influence of radiation is usually specified by the

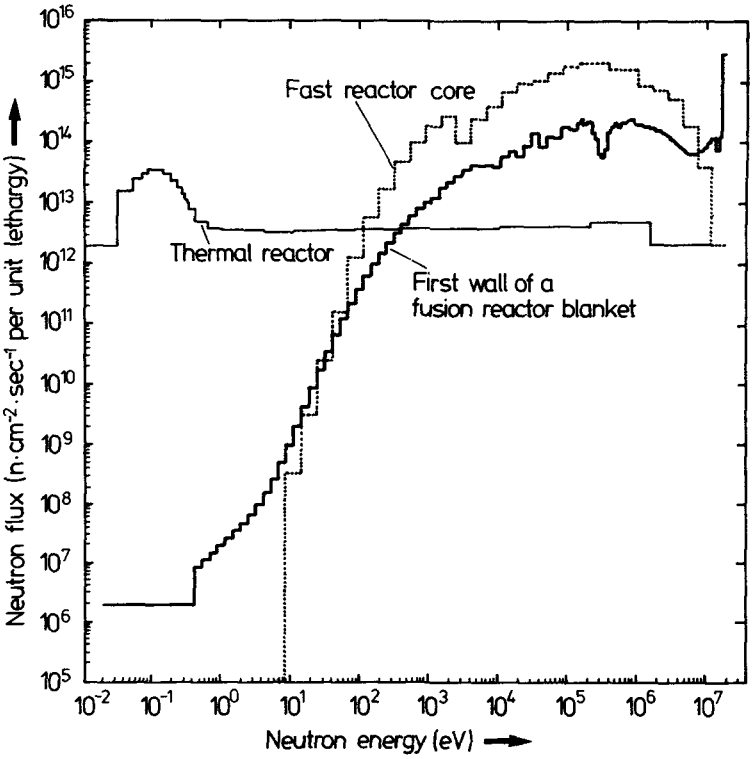

Fig. 1 Neutron energy spectrum at the first wall of a fusion reactor compared with neutron spectra for fast and thermal reactors (After Jarvis [1]).

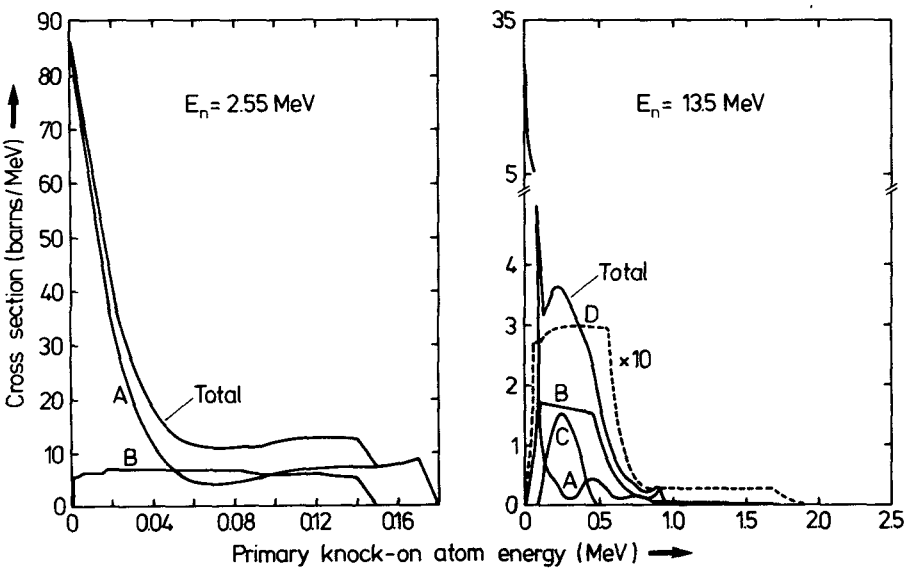

Fig. 2 PKA spectra for iron at incident neutron energies of 2.55 and 13.5 MeV. The various contributions are indicated by A (n,n), B (n,n'), C (n,2n) and D (n,charged particle). The (n,charged particle) contribution has been increased tenfold for clarity (After Doran et al [5]).

number of displacement events per lattice atom (dpa). It is described by damage energy cross sections whose calculation (cf., e.g. [6,7]) involves two steps:

a) determination of the primary knock-on atom (PKA) energy spectrum, and
b) determination of how the PKA energy is partitioned in the form of kinetic energy given to atoms and excitation energy given to electrons.

For calculating the PKA spectrum in a material it is essential to know the cross sections of all the nuclear reactions in which the target atom receives a kinetic energy > E_d, where E_d is an effective displacement threshold energy. PKA spectra have been calculated using ENDF/B-IV data for a range of atomic weights at several neutron energies. Typical PKA spectra for iron [5] are shown in Fig. 2 for two incident neutron energies. It is apparent that at low energies (n,n) and (n,n') are the only contributing processes whereas at higher energies (n,2n) and (n, charged particle) processes also make some contributions. A solid state model is employed to give the number of atoms displaced from their lattice positions by the primary knock-on. The original cross section is multiplied by the number of displacements and on summing over all collision types, the displacement cross section is obtained. Typical displacement cross sections [4] for several structural materials are shown in Fig. 3 as a function of

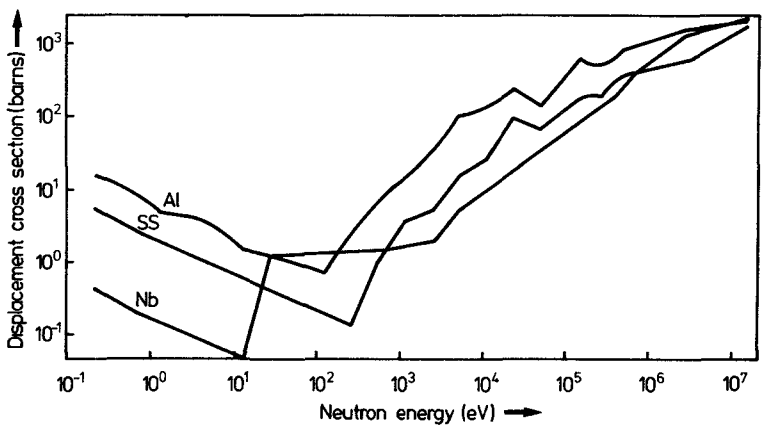

Fig. 3 Displacement cross sections for Al, stainless steel and Nb as a function of incident neutron energy (After Maynard [4]).

neutron energy. After an initial decrease in the cross section with energy, it increases again with energy due to the increase in the reaction cross section. Each displacement cross section is composed of several contributing processes. This is illustrated by the displacement cross-section curve for aluminium [5] shown in Fig. 4. Evidently the (n,n) and (n,n') processes are most important, but (n,2n) and (n, charged particle) reactions also contribute appreciably.

Nuclear transmutations: In addition to the displacement damage, fast neutrons bring about nuclear transmutations as a result of which certain foreign elements are created within the lattice and exist as dilute impurities (cf. [8]). These foreign elements may or may not occupy the same sites as the original niobium atoms and may strongly influence the development of the damage microstructure leading thereby to property changes. There is another aspect of nuclear transmutations too, which is quite serious and involves the foramtion of gases like hydrogen and helium via (n,xp) and (n,xα) reactions, respectively.

Nuclear transmutation, and especially gas production, is normally not a very serious phenomenon at relatively low neutron energies but is expected to be one of the major sources

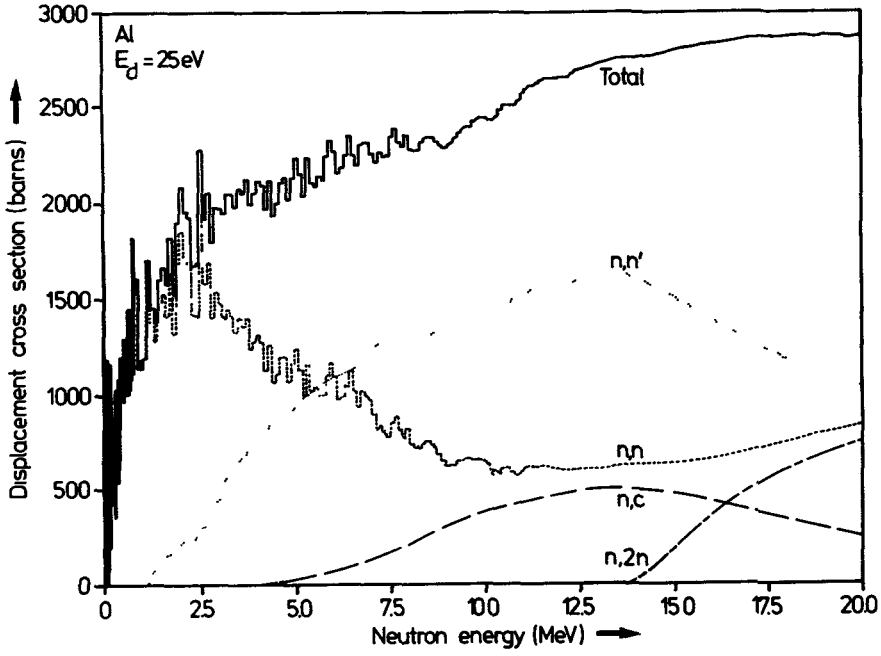

Fig. 4 Displacement cross section for aluminium showing contributions from various reactions, e.g. (n,n), (n,n'), (n,2n) and (n, charged particle) processes (After Doran et al [5]).

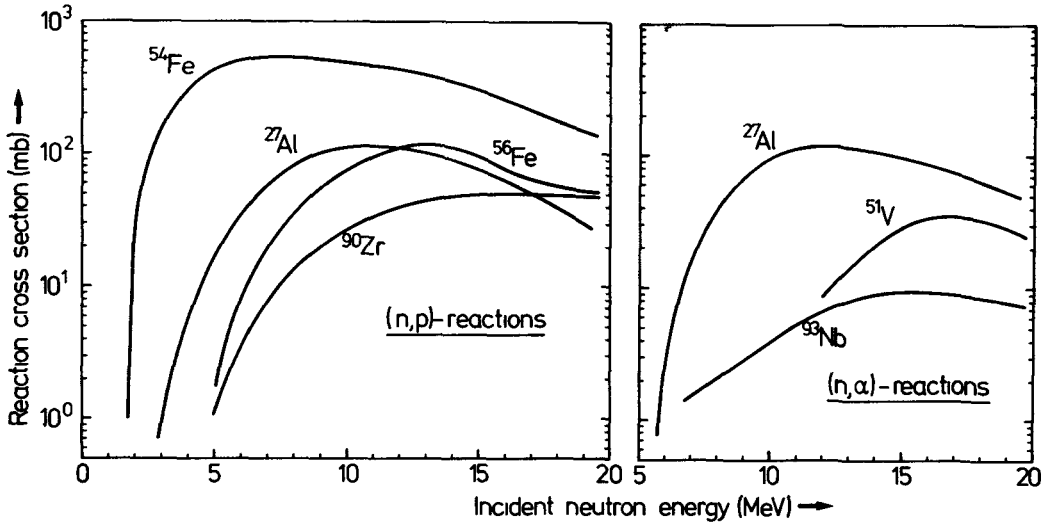

Fig. 5 Excitation functions for (n,p) and (n,α) reactions on some structural materials (Data taken from ref. [9]).

of radiation damage in the case of fast neutrons such as those anticipated in a fusion reactor. As can be seen in Fig. 5, which has been constructed on the basis of data given in ref. [9], the (n,p) and (n,α) cross sections steeply increase with increasing neutron energy and have appreciable values in the region around 14 MeV; the expected transmutation rates in a fusion reactor will therefore be much higher than those in a fast reactor.

The expected displacement and gas production rates for a fast breeder reactor and a fusion reactor are given in Table I.

TABLE I: RADIATION DAMAGE EFFECTS IN STRUCTURAL MATERIALS*

Parameter	Fast breeder core	Fusion reactor first wall
Neutron flux or loading	8.5×10^{15} n/cm^2·sec	3.5 MW/m^2
Temperature	600 °C	530 °C (SS 316) 1000 °C (Nb)
Atomic displacement rate (dpa/yr)	60	40 (SS 316) 29 (Nb)
Hydrogen gas production (at.ppm/yr)	700	2000 (SS 316) 400 (Nb)
Helium gas production (at.ppm/yr)	30	660 (SS 316) 110 (Nb)

* After O.N. Jarvis, ref. [1]

Effects of Radiation Damage

In a thermal reactor the radiation damage effects manifest themselves (cf. e.g. [10]) in two important phenomena, viz., bulk swelling of the sample due to void formation and their growth, and radiation enhanced creep of the material. In fast breeder reactors, and especially in fusion reactors, on the other hand, radiation enhanced diffusion and gas produced embrittlement are also important. Irradiation of structural materials with high energy neutrons leads to considerable concentrations of point defects at all temperatures and therefore lowers the temperature up to which a material is metallurgically stable.

It is known [10] that gas production leads to high temperature embrittlement of structural materials. Due to the higher cross sections of the (n,xp) reactions as compared to the (n,xα) reactions hydrogen production in a fusion reactor would be higher than the helium production. However, hydrogen production is the lesser problem since it diffuses rapidly out of structural materials at the elevated temperatures of interest (500 - 900 °C). Helium production, on the other hand, may greatly facilitate void formation by nucleation and thereby enhance swelling. Furthermore, helium bubbles located in the

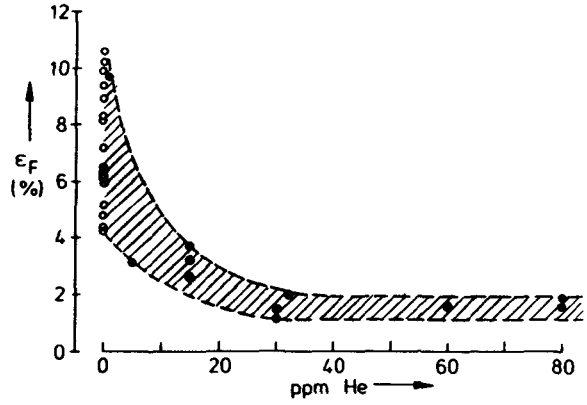

Fig. 6 Total creep elongation to fracture, ε_F, for stainless steel as a function of helium concentration; open circles: helium-free samples, full circles: helium-implanted samples (After Ullmaier et al [10,11]).

grain boundaries greatly influence the structural properties of the material. Since grain boundary diffusion usually dominates bulk diffusion, bubbles in the grain boundaries grow particularly fast. At elevated temperatures this effect may lead to intergranular fracture. This fracture mode is usually coupled with a drastic decrease of the strain to fracture as compared with helium free samples of the same material which break by transcrystalline fracture.

A typical example describing the effect of helium concentration on the mechanical properties of stainless steel [10,11] is shown in Fig. 6. The total creep elongation to fracture, ε_F, decreases as a function of helium concentration till a very low value is reached. Helium embrittlement is a very serious phenomenon and is often regarded to be virtually the life time limiting effect for the first wall of a fusion reactor.

Study of Radiation Damage Effects

Radiation damage studies are carried out from two rather independent appraoches, namely, application oriented materials research and fundamental investigations. The former appraoch is more empirical and consists of irradiating reactor materials for sufficiently long periods followed by investigations of the changes in bulk properties such as swelling, enhanced creep and embrittlement. Since the damage rates are rather low ($\sim 10^{-6}$ dpa/sec), the data needed for engineering design can be obtained only after several years of reactor irradiations which are not only expensive but also produce highly radioactive specimens that are difficult to handle. Furthermore, since there is a great complexity of simultaneously occurring processes that contribute to the manifestation of the technologically important macroscopic property changes, in such irradiations it is virtually impossible to separate and describe the different mechanisms involved.

The second approach consists of studying radiation damage by simulation techniques where the effects of the neutrons are simulated by high energy charged particle bombardment. Fig. 7, taken from ref. [10], gives a comparison of the displacement rates produced by neutrons, α-particles and heavy ions. Recently dual beam irradiation has also been suggested [1]. The metal under investigation is bombarded with the same metal ions of an energy carefully selected to duplicate the fusion reactor neutron PKA energy spectrum, and helium production is simulated by implanting low-energy He ions. It has also been demonstrated that 16 MeV protons, produce very similar damage effects to 14 MeV neutrons [12]; however, with only equal effectiveness so that in the case of protons as well long irradiations are necessary.

Simulation experiments involving irradiations with charged particles can lead to a fundamental understanding of some radiation damage phenomena. They, however, do not necessarily give the same total effect as the neutrons. Ideally, first wall materials selected on the basis of simulation experiments should be subjected to life time tests in a 14 MeV neutron flux before their use as structural materials in a fusion reactor. Unfortunately present day 14 MeV neutron sources do not have high enough intensity for high damage studies. However, during the last few years an appreciable effort has been invested towards the development of intense neutron sources. Solid and gas target systems, deuteron stripping, spallation as well as plasma sources are being developed. The state of the art information has been summed up recently [13]. Among all those systems the Li(d,n) and Be(d,n) neutron sources appear to be very promising. The interpretation of radiation damage effects observed using those sources, however, will need an extensive nuclear data base covering the energy region up to 40 MeV. Those needs are discussed below.

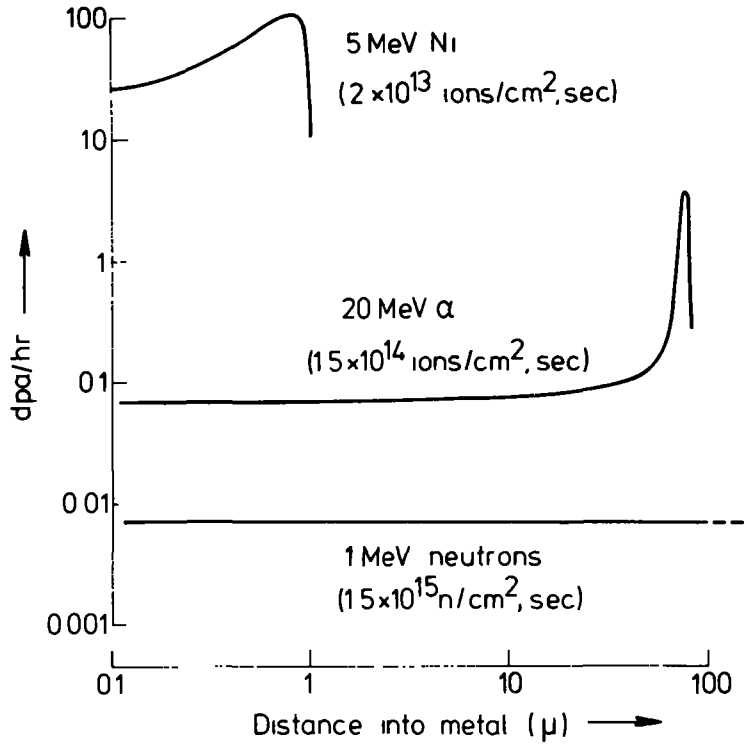

Fig. 7 Comparison of damage effectiveness and range of different particle beams used in radiation damage experiments. The quoted particle fluxes are maximum values which are attainable with present-day sources (After Ullmaier and Schilling [10]).

NUCLEAR DATA NEEDS AND STATUS OF AVAILABLE DATA

From the above discussion it is evident that the radiation damage problem is much more severe for fusion reactor design than for fast breeder reactors. Furthermore, due to the corrosive nature of lithium used for tritium breeding as well as due to the high working temperature for the reactor to be economical, the demands on structural materials become still more stringent. To date only a few materials like V, Ti, stainless steel, Nb, Mo, W, etc. appear to meet the criteria for selecting first wall materials [14]; eventually some suitable alloys will have to be developed. A technical assessment of some alloys has been carried out [15] but a strong research and development programme is necessary.

For radiation damage studies with fast neutrons it is essential in the first place to establish well characterized reference spectra [16] for 14 MeV and deuteron-break-up sources so that materials scientists can correlate their experimental data. Correlation will require integral testing of nuclear data to establish uniform dosimetry practices. Furthermore, broad-based sensitivity studies [16] are needed to determine the sensitivity of materials damage parameters to variations in cross-section data and nuclear models used.

The nuclear data needs for radiation damage studies fall into three main groups:

1) Data for the characterization of the radiation environment
2) Data for calculating displacement cross sections and related defect parameters, and
3) Data for quantitative estimation of transmutation products, especially gases.

Measurements and evaluations are essential [16] in the first place for C, Al, Si, Ti, V, Cr, Mn, Fe, Co, Ni, Cu, Zr, Nb, Mo, Sn, W, Pb, etc. up to 30 MeV, and if possible up to 40 MeV. In many cases existing data and theoretical calculations would meet the data needs but in others precision measurements may be necessary. Furthermore, for a semi-quantitative estimate of the radiation damage effects, a knowledge of nuclear data for elements present as impurity will also be necessary. Similarly, for neutron dosimetry cross sections for many more elements shall be required. It may be pointed out that whereas elemental evaluations may be adequate for use in displacement damage calculations, isotopic evaluations are necessary for dosimetry and transmutation product determinations. The advantage of evaluating the data for a series of stable isotopes is that the reaction Q-value effect can be well investigated and the unknown cross sections can be predicted, including those for some long-lived transmuted species [17].

We discuss each of the above three areas of nuclear data needs in detail below.

Data for the Characterization of Radiation Environment

The objective of neutron dosimetry is to provide a base for characterizing a variety of test and fusion reactor neutron environments [5] in terms of flux, fluence and neutron energy distribution averaged over the duration of the irradiation. For this purpose both instrumental dosimetry techniques (such as time-of-flight (TOF) and ^{6}Li spectrometry) and multiple foil spectrum analysis technique (MFA) have been used.

The TOF method requires accurate scattering and reaction cross sections of carbon in order to calculate detector efficiencies above 15 MeV. The ^{6}Li coincidence spectrometry technique, on the other hand, demands an accurate knowledge of the $^{6}Li(n,\alpha)T$ reaction. This cross section is well-known.

The technique of MFA is relatively simple [18] and consists of identification of a number of reaction products following irradiations of suitable monitor foils in the neutron

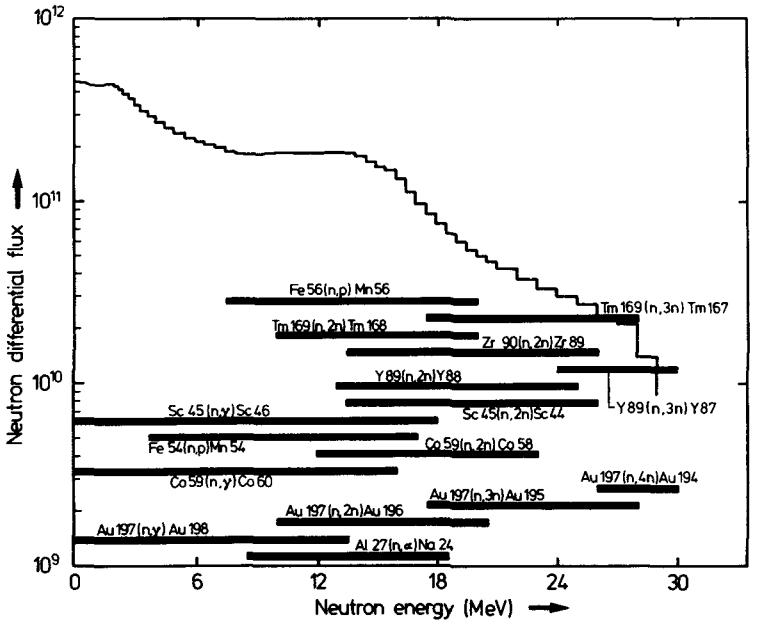

Fig. 8 Differential neutron flux (n/MeV/cm^2•sec) for 30 MeV deuterons on ^{9}Be at 20 μA beam current. The nuclear reactions used for spectrum unfolding are given together with the energy range of their applicability (After Nethaway et al [19]).

environment under investigation; the products may be radioactive or stable and may be detected by gamma counting, mass spectrometry, track recording, etc. From the characteristic energy dependence of each reaction cross section, the fluence and energy spectrum can be unfolded. The fluence results are of high accuracy since they are derived from spectrum-averaged cross sections. Spectrum definition, however, is not of high quality since the energy resolution of the technique is not high. Nonetheless, because of its simplicity the technique is advantageous.

Presently the MFA technique is applied to a large extent using radiometric assay of the activation products. Most of the reactions of current interest have been recently reviewed [5,16]. In all about fifty nuclear reactions having different threshold energies have been suggested. The characteristic energy ranges of some of them are shown in Fig. 8 in connection with an analysis of the neutron spectrum produced in the break-up of 30 MeV deuterons on Be-target [19]. The desired accuracy of the monitor reaction cross-section data in the energy range from thermal to 14 MeV is 5 - 8 % and that in the range of 14 to 40 MeV between 10 and 20 %. For some of the suggested monitor reactions data are available up to 30 MeV; however, the accuracy is not sufficient. Beyond 30 MeV practically no data exist.

The existing ENDF/B-IV Dosimetry Cross-Section File [20] includes data for some forty nuclear reactions, useful or potentially useful, to meet the needs of the breeder reactor programme. The emphasis therefore lies on the energy range below 10 MeV. Although the File now extends to 20 MeV, little data testing has been done above 10 MeV. Extension of the File by incorporating some or all of the proposed [5,16] monitor reactions has been recommended [16] and standardization of the data up to 40 MeV is urged.

Data for Calculating Displacement Cross Sections

For displacement radiation damage calculations extensive cross-section data are needed. The calculation of recoil energy spectra demands detailed information on differential angular cross sections for elastic and inelastic scattering as well as on energy distribution of emitted particles in nonelastic events. In the case of fission reactors the major reactions of interest are elastic and inelastic scattering and, except for the question of accuracy in some cases, the existing data base is reasonably complete. For applications to fusion reactors, however, calculations must extend to 14 MeV and contributions from other nonelastic reactions like (n,xn), (n, charged particle) etc. must also be taken into account. Furthermore, if instead of a DT neutron source a high energy deuteron break-up neutron source were to be used for materials tests, for an understanding of the radiation damage effects nuclear data sets up to 40 MeV will be needed.

The status of fast neutron data has been reviewed [21] and the most recent advances in the study of neutron threshold reactions have been recently discussed [22]. In the present review therefore only a brief discussion is given. For a few structural materials high resolution total cross sections have been measured for neutron energies up to 40 MeV but for many others further accurate measurements are necessary. As far as elastic and differential elastic scattering cross sections are concerned, at 14 MeV data with errors of 3 to 5 % are available for most of the structural materials. At higher energies, however, data are scanty. Many measurements of total nonelastic cross sections have been carried out near 14 MeV but few at other energies in the range of 10 to 40 MeV. It is, nonetheless, possible to calculate nonelastic cross sections with reasonable accuracies using the optical model.

In contrast to the total nonelastic cross section, the various partial nonelastic cross sections are not known with the same accuracy. Furthermore, other than at 14 MeV the data are scanty. The (n,γ) reaction, for example, though constituting only a small fraction of the nonelastic cross section for neutrons between 10 and 40 MeV has not been measured above 15 MeV. The status of the inelastic neutron scattering data between 10 and 40 MeV is the same as for elastic neutron scattering; investigations in neutron energy ranges other than the 14 MeV area have been only recently initiated. Among the (n,xn) processes the (n,2n) and (n,3n) reactions are most important. At 14 MeV for nuclei in the medium and heavy mass regions the (n,2n) reaction is by far the most dominating process. Most of the measurements on (n,xn) reactions, extending up to neutron energies of about 28 MeV, have been carried out using the activation technique, often in combination with radiochemical methods (cf. e.g. [23,24]); in recent years, however, large liquid scintillator method has also been employed [25,26]. The data obtained using the two techniques are generally in agreement within 10 %. Both the techniques, however, yield no information on the energy distribution of the emitted neutrons.

Some part of the nonelastic cross section is also constituted by reactions in which charged particles are emitted. These include processes like (n,p), (n,n'p), (n,d), (n,t), (n,2p), (n,^{3}He), (n,α), (n,n'α), etc. and may cause considerable displacement radiation damage, especially when the recoil energy of the emitted charged particle is high. Out of all those processes the (n,p) and (n,α) reactions have been extensively investigated at 14 MeV (cf., e.g. [22,23,27]), mainly using the activation technique. In many cases, however, the data are still discrepant. At other energies between 8 and 40 MeV the data are relatively scarce. Many of the data needs, however, could be met by theoretical calculations. The (n,n'p) and (n,n'α) reactions were studied systematically at 14 MeV for the first time at Jülich [17] and it was shown that their cross sections are high enough to necessitate their inclusion in

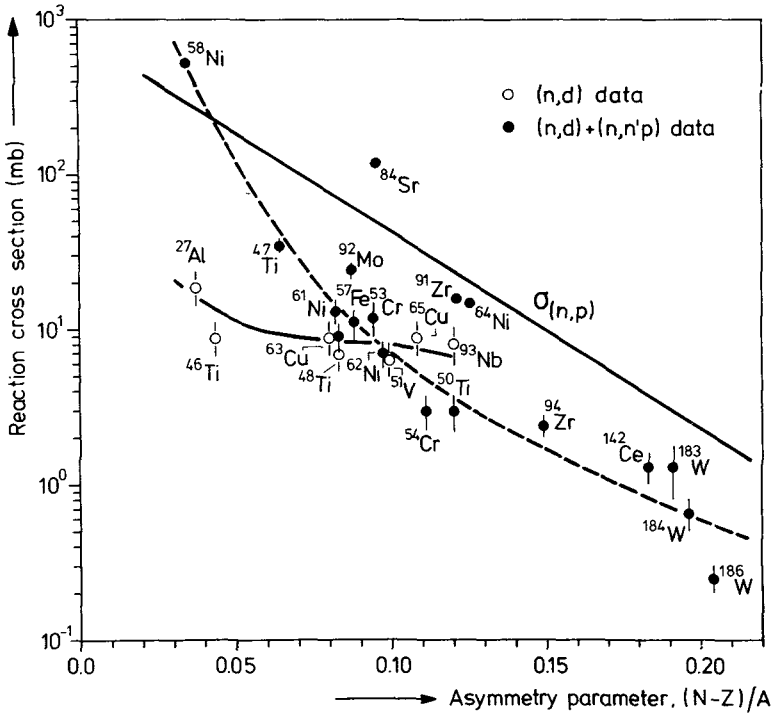

Fig. 9 Trends in (n,p), (n,d) and [(n,d) + (n,n'p)] reaction cross sections; the data for (n,d) reactions are based on measurements done at Livermore, those for (n,p) and [(n,d) + (n,n'p)] reactions at Jülich (After Qaim [22]).

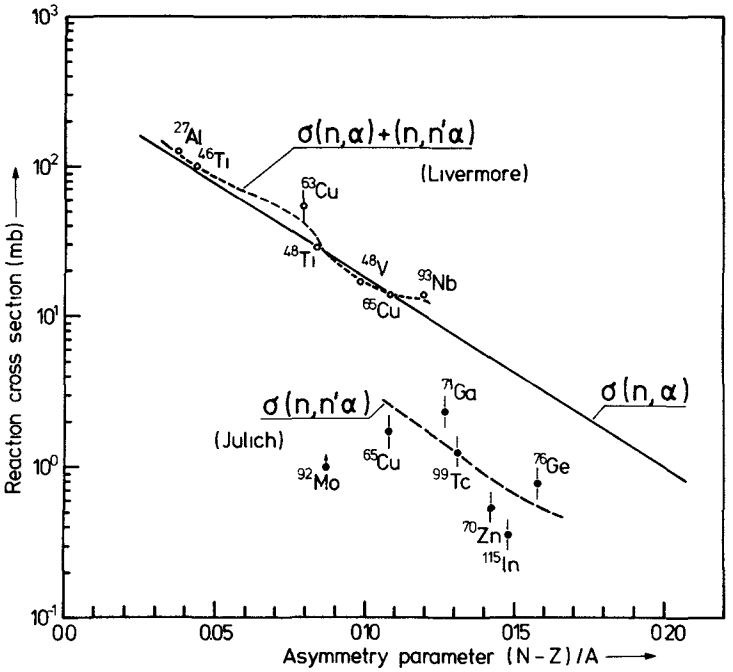

Fig. 10 Trend in (n,n'α) reaction cross sections and comparison with the gross trends in the (n,α) and (n,xα) cross-section data (After Qaim [22]).

radiation damage calculations. In spite of many more investigations in recent years [28,29] the data base is still weak. A study of the (n,d) reactions at 14 MeV is underway at Livermore [29]. The (n,2p), (n,t) and (n,^{3}He) reactions are rare. Extensive studies on the latter two reactions have been carried out at Jülich using radiochemical techniques (cf., e.g. [22,30,31]). Because of their extremely low cross sections the latter reactions are of little importance in the context of displacement damage effects.

In addition to the cross-section data of the (n,xn) and (n, charged particle) reactions, detailed information on the angular and energy distribution of the emitted particles is also needed. So far such data have been scarcely available. Though the situation is improving [29], still extensive measurement programmes are needed.

A recent radiation damage experiment carried out using neutrons produced by 30 MeV deuterons on a thick Be target has shown [32] that for dilute alloys of V, Nb and Mo the resistivity damage rates are about 2/3 those produced by 14 MeV. Evidently for a correlation of the damages produced by the two types of neutron sources, a strong nuclear data base will be needed. Some integral cross-section measurements using the break-up neutron spectrum have been initiated [28,32] but further extensive work is needed.

Data for Estimating Transmutation Products

Transmutation reactions are important not only for their contribution to the displacement damage effects but also due to the reason that the transmuted species may strongly influence the development of damage microstructure that leads to property changes. As discussed above gas production is of particular interest for fusion reactors. The status of gas producing reactions in structural materials for fast reactors has been recently reviewed [33]; additional reactions important in the case of fusion reactors are discussed here. Of all the (n, charged particle) reactions leading to gas formation, the (n,t), (n,^{3}He) and (n,2p) reactions are unimportant because of low

cross sections. The major contributing reactions are thus (n,p), (n,n'p), (n,d), (n,α) and (n,n'α).

Most of the (n,p) cross-section data exist for 14 MeV neutrons [22,27], though in some cases lower and higher energy regions have also been investigated with varying degrees of accuracy [9]. Since the first systematic report on [(n,n'p) + (n,d)] reactions from Jülich [17], studies have been carried out exclusively at 14 MeV at two laboratories, at Jülich using radiochemical techniques and at Livermore using a high-precision magnetic quadrupole spectrometer. In those cases where the same nuclides have been investigated at both the laboratories, the agreement is generally good. The results are summarized [22] in Fig. 9. It is evident that in the light mass region the (n,d) cross section is small compared with the [(n,n'p) + (n,d)] cross section. The sequential emission of a neutron and a proton is therefore more favoured than the emission of a deuteron. In the medium mass region, however, the (n,d) cross section almost approaches the sum of the (n,d) and (n,n'p) cross sections. Evidently the available data are still scarce. Due to the interest in estimating the equilibrium hydrogen concentration, which is of importance for understanding the phenomenon of hydrogen embrittlement, the need of (n,xp) cross-section measurements at 14 MeV and in other energy regions is imminent.

The production of helium via (n,α) and (n,n'α) reactions is currently believed to be one of the major damage mechanisms in fusion reactors. The status of the cross-section data for those reactions is similar to that for the (n,p) and (n,n'p) reactions, respectively. The cross sections for some (n,n'α) reactions at 14 MeV measured at Jülich are shown in Fig. 10 and compared with the trend in the (n,α) cross sections [22]. It is apparent that the contribution of the (n,n'α) reaction in the investigated mass region amounts to between 10 and 15 % of the (n,α) reaction. The data on (n,xα) reactions obtained at Livermore using the magnetic quadrupole spectrometer are also shown in Fig. 10. Evidently a greater part of the measured cross section is furnished by the (n,α) reaction, the contribution of the other α-emitting processes (e.g., (n,n'α)) is < 20 %. In addition to radiochemical and magnetic quadrupole spectrometer techniques, the use of mass spectrometric method for measurement of total helium production has also been initiated [34,35].

The existing calculational methods may be used with varying degrees of success for estimating (n,p) and (n,α) reaction cross sections up to 40 MeV. However, the recently proposed calculational methods for the (n,n'p) and (n,n'α) reactions are highly empirical and unsupported by experimental data. At energies higher than 14 MeV, such as those encountered in Be(d,n) or Li(d,n) neutron radiation test facilities, the (n,n'p) and (n,n'α) reaction cross sections are unpredictable and therefore total hydrogen and helium production rates are highly uncertain. Furthermore, reactions like (n,t) and (n,^{3}He) which have very low cross sections at 14 MeV would also contribute appreciably [28,36] at higher energies. It is therefore suggested that extensive investigations on hydrogen and helium producing reactions be carried out up to neutron energies of 40 MeV, and an extra File on gas production covering the energy region up to 40 MeV be maintained and reviewed periodically.

CONCLUSIONS

The radiation damage problem is of vital importance for fusion reactor design. Although both displacement effects and nuclear transmutations are expected to contribute to the total radiation damage, the latter phenomenon leading to the formation of hydrogen and helium gases will be more critical. For displacement calculations differential angular cross sections for elastic and inelastic scattering are needed. Those needs can be met by the existing data and theoretical calculations.

On the other hand data are also needed on the energy distribution of the emitted particles. Such data are scanty and further experimental work is needed. For calculations of radiation damage due to nuclear transmutations, total cross sections of many reactions, especially those contributing to hydrogen and helium formation, are needed. The data base, in particular between 6 and 13 MeV and beyond 14 MeV, is very weak. Though (n,p) and (n,α) cross sections can be calculated in many cases with sufficient accuracy using nuclear models, in the case of (n,n'p) and (n,n'α) reactions extensive experimental work is needed. The high energy neutron sources to be used for radiation damage studies require careful characterization. For neutron dosimetry multiple foil analysis has great potential but data are seriously lacking. In view of the increasing importance of deuteron-break-up neutron sources for radiation damage studies, the nuclear data base should be extended up to 40 MeV.

Acknowledgements: It is a pleasure to thank Prof. G. Stöcklin for his active support of the Nuclear Data Research Programme at Jülich and for stimulating discussions. Acknowledgement is made to Dr. H. Ullmaier and Dr. J. Darvas for their comments on the manuscript of this paper.

REFERENCES

[1] JARVIS, O.N., "Nuclear data for fusion reactors", Proc.Int. Conf. on Neutron Physics and Nuclear Data for Reactors and other Applied Purposes, Harwell, September 1978, in press.

[2] STEINER, D., "Nuclear data needs for fusion reactor design", Proc.Conf.Nuclear Cross Sections and Technology, Washington, D.C., March 1975, NBS-Special Publication 425 (1975) 646.

[3] QAIM, S.M., WÖLFLE, R., STÖCKLIN, G., "Nuclear data for fusion reactors", Proc.Symp.Fast Neutron Interactions and the Problems of High Current Neutron Generators, Debrecen, August 1975, Atomki Közlemények 18 (1976) 335.

[4] MAYNARD, C.W., "Neutrons and fusion", Proc.Int.Conf. on the Interactions of Neutrons with Nuclei, Lowell, July 1976, Conf.-760715-P1(1976)789.

[5] DORAN, D.G., HEINRICH, R.R., GREENWOOD, L.R., FARRAR IV, H., "MFE damage analysis program nuclear data needs", Proc. Symp.Neutron Cross Sections from 10 to 40 MeV, Brookhaven National Laboratory, May 1977, BNL-NCS-50681 (1977) 323.

[6] ODETTE, G.R., DOIRON, D.R., "Neutron energy dependent defect production cross sections for fission and fusion applications", Nucl.Tech. 29 (1976) 346.

[7] GABRIEL, T.A., AMBURGEY, J.D., GREENE, N.M., "Radiation damage calculations: primary knock-on atom spectra, displacement rates, and gas production rates", Nucl.Sci.Eng. 61 (1976) 21.

[8] BLOW, S., "Transmutation, activity, and after-heat in a fusion reactor blanket", AERE-R6581 (1971).

[9] GARBER, D.S., KINSEY, R.R., "Neutron cross sections, Vol. II, Curves", BNL 325, Physics, Nuclear-TID-4500 (1976).

[10] ULLMAIER, H., SCHILLING, W., "Radiation damage in metallic reactor materials", Proc.Int.Course on Physics of Modern Materials, ICTP Trieste, June 1978 (IAEA Publication 1979).

[11] SAGÜES, A.A., SCHROEDER, H., KESTERNICH, W., ULLMAIER, H., "The influence of helium on the mechanical properties of DIN 1.4970 austenitic steel", Proc.Radiation Effects in Breeder Reactor Structural Materials, Scottsdale, Arizona, June 1977, Amer.Met.Soc. of AIME, New York (1977) 367.

[12] MITCHELL, J.B., LOGAN, C.M., ECHER, C.H., "Comparison of 16 MeV protons, 14 MeV neutrons, and fission neutron damage in copper", J.Nucl.Materials 48(1973) 139.

[13] ULLMAIER, H. (Editor), "High energy and high intensity neutron sources", Special Issue of Nucl.Instr.Methods 145 (1977) 1.

[14] CONN, R.W., "First wall and divertor plate material selection in fusion reactors", J.Nucl.Materials 76 and 77 (1978) 103.
[15] "Alloys for the fusion reactor environment: A technical assessment", DOE, Div. of Magnetic Fusion Energy, Washington, D.C., DOE/ET-0007 (1978).
[16] Workshop Report on "Materials damage studies", Proc.Symp. Neutron Cross Sections from 10 to 40 MeV, Brookhaven National Laboratory, May 1977, BNL-NCS-50681 (1977) 29.
[17] QAIM, S.M., STÖCKLIN, G., "Measurement and systematics of cross sections for common and low-yield 14 MeV neutron induced nuclear reactions on FR-material and transmuted species", Proc. 8th Symp.Fusion Technology, Noordwijkerhout, June 1974, EUR 5182e (1974) 939.
[18] McELROY, W.N., KELLOGG, L.S., "Fuels and materials fast-reactor dosimetry data development and testing", Nucl. Tech. 25 (1975) 189.
[19] NETHAWAY, D.R., VAN KONYNENBURG, R.A., GUINAN, M.W., GREENWOOD, L.R., "Neutron spectra from 30 MeV deuterons on a thick beryllium target", Proc.Symp. Neutron Cross Sections from 10 to 40 MeV, Brookhaven National Laboratory, May 1977, BNL-NCS-50681 (1977) 135.
[20] MAGURNO, B.A. (Editor), "ENDF/B-IV dosimetry file", BNL-NCS-50446 (1975).
[21] HAIGHT, R.C., "Review of neutron data: 10 to 40 MeV", Proc.Symp.Neutron Cross Sections from 10 to 40 MeV, Brookhaven National Laboratory, May 1977, BNL-NCS-50681 (1977) 201.
[22] QAIM, S.M., "Recent advances in the study of some neutron threshold reactions", Proc.Int.Conf. Neutron Physics and Nuclear Data for Reactors and other Applied Purposes, Harwell, September 1978, in press.
[23] QAIM, S.M., "A survey of fast-neutron induced reaction cross-section data", Proc.Conf. Nuclear Cross Sections and Technology, Washington, D.C., March 1975, NBS-Special Publication 425 (1975) 664.
[24] BAYHURST, B.P., GILMORE, J.S., PRESTWOOD, R.J., WILHELMY, J.B., JARMIE, N., ERKKILA, B.H., HARDEKOPF, R.A., "Cross sections for (n,xn) reactions between 7.5 and 28 MeV", Phys.Rev. C12 (1975) 451.
[25] FREHAUT, J., MOSINSKI, G., "Measurement of (n,2n) and (n,3n) cross sections for incident energies between 6 and 15 MeV", Proc.Conf. Nuclear Cross Sections and Technology, Washington, D.C., March 1975, NBS-Special Publication 425 (1975) 855.
[26] VEESER, L.R., ARTHUR, E.D., YOUNG, P.G., "Cross sections for (n,2n) and (n,3n) reactions above 14 MeV", Phys.Rev. C16 (1977) 1792.
[27] MOLLA, N.I., QAIM, S.M., "A systematic study of (n,p) reactions at 14.7 MeV", Nucl.Phys. A283 (1977) 269.
[28] QAIM, S.M., MOLLA, N.I., "Nuclear data measurements for FR-wall and structural materials", Proc. 9th Symp. on Fusion Technology, Garmisch-Partenkirchen, June 1976, EUR 5602 (1976) 589.
[29] GRIMES, S.M., HAIGHT, R.C., ANDERSON, J.D., ALVAR, K.R., BORCHERS, R.R., "Development of a spectrometer for the measurement of (n,xp), (n,xd), and (n,xα) cross sections, angular distributions and spectra at E_n = 15 MeV", Proc. Symp. Neutron Cross Sections from 10 to 40 MeV, Brookhaven National Laboratory, May 1977, BNL-NCS-50681 (1977) 297.
[30] QAIM, S.M., STÖCKLIN, G., "Investigation of (n,t) reactions at 14.6 MeV and an analysis of some systematic trends in the cross-section data", Nucl.Phys. A257 (1976) 233.
[31] QAIM, S.M., "A systematic investigation of (n,^{3}He) reactions at 14.6 MeV and an analysis of the gross trend in the cross-section data", Radiochim.Acta 25 (1978) 13.
[32] GUINAN, M.W., VIOLET, C.E., "Initial damage rates in Nb, V and Mo from 30 MeV D-Be neutrons", Proc.Symp.Neutron Cross Sections from 10 to 40 MeV, Brookhaven National Laboratory, May 1977, BNL-NCS-50681 (1977) 361.

[33] PAULSEN, A., "Status report about some activation, hydrogen and helium producing cross sections of structural materials", Proc.Specialist Meeting on Neutron Data of Structural Materials for Fast Reactors, Geel, December 1977, Pergamon Press (1979) 261.
[34] FARRAR IV, H., KNEFF, D.W., "Helium generation in fusion reactor materials", Tech.Prog.Report A.I.-ERDA-13201 (1977).
[35] QAIM, S.M., WU, C.H., WÖLFLE, R., to be published.
[36] QAIM, S.M., WÖLFLE, R., "Triton emission in the interactions of fast neutrons with nuclei", Nucl.Phys. A295 (1978) 150.

Nuclear Data Requirements For Fusion Reactor Shielding

AG-159/A5
Review Paper

Mohamed A. Abdou
Georgia Institute of Technology
Atlanta, Georgia

Abstract

The nuclear data requirements for experimental, demonstration and commercial fusion reactors are reviewed. Particular emphasis is given to the shield as well as major reactor components of concern to the nuclear performance. The nuclear data requirements are defined as a result of analyzing four key areas. These are the most likely candidate materials, energy range, types of needed nuclear data, and the required accuracy in the data. Deducing the latter from the target goals for the accuracy in prediction is also discussed. A specific proposal of measurements is recommended. Priorities for acquisition of data are also assigned.

1. Introduction

The function of the shielding system in any nuclear reactor is: 1) to protect reactor components from intolerable levels of (a) radiation damage, (b) nuclear heating, and (c) induced activation that may result in maintainability and disposal problems; and 2) to protect workers as well as the general public from intolerable radiation exposure at all times during operation, shutdown, scheduled maintenance, and unscheduled failures.

Shielding calculations require methods and data to predict the nuclear performance parameters of interest. An extensive base of methods and data exists in the highly-developed fission field. However, the specific nature of fusion reactor systems and the high neutron energy range of interest make it necessary to pursue a research and development program to extend and improve the methods and nuclear data. The purpose of this paper is to detail the nuclear data requirements for experimental, demonstration, and the first generation of commercial fusion power reactors.

The scope of the paper is limited to fusion reactors operated with the D-T cycle. However, since roughly half the energy of the neutrons in the D-D cycle is carried away with 14 MeV neutrons, almost all general results and conclusions are also applicable for reactors operated on the D-D cycle with modest modifications. Both magnetic and inertial-confinement reactors are discussed, but most of the details are focused on the former with particular emphasis on tokamak-type reactors.

For convenience of the reader, the discussion of the nuclear data requirements in Sec. 3 is preceeded by a brief description of the fusion reactor shield components in Sec. 2. In addition, a rather comprehensive list of references is given at the end of the paper to cover publications related to fusion reactor shield. References 1-25 cover the general problems of the technological requirements for fusion power development. Some of these are conceptual designs for fusion power plants and include detailed discussions of the shielding problems. References 26-45 address the problems of the bulk shield. References 51-58 focus on the radiation streaming problems in fusion reactors.

It is useful to conclude this introductory section by underlying both the importance and difficulty of shielding fusion reactors. This may best be accomplished by comparing the problems of fusion reactor shielding in reference to those of the more familiar systems of fission reactors. The following items explain the key points of comparison:

(1) The blanket and bulk shield in fusion reactors are penetrated by many more large-size holes than are fission reactors. Fusion reactor penetrations are directly exposed to the energetic source neutrons

and the functional requirements of some of them exclude making any significant bends in the penetration ducts.

(2) The 14 MeV neutrons produced in the D-T cycle are much more capable of deep penetration than are the fission neutrons whose average energy is ~2 MeV. Furthermore, the high energy neutrons induce a variety of nuclear reactions, with many radioactive residual nuclei, that are inaccessible to lower energy neutrons.

(3) The recoverable energy per fission reaction is ~9-10 times larger than that of a fusion reaction. Therefore, for the same power, a fusion reactor has ~4-5 times more neutrons than in a fission reactor.

(4) The interrelations between the shield and the components of the reactor are much more complicated in fusion compared to fission reactors. In addition, there are many major components of fusion reactors that are very sensitive to radiation and require extensive measures of radiation protection.

(5) Most fusion reactor concepts call for major scheduled maintenance tasks that require more time and manpower than in any of the fission reactors. This fact together with those in 1-4 make the problems of radiation exposure and maintainability in fusion reactors extremely important.

Nothing in the above points suggests that fusion reactor shielding problems cannot be solved at a reasonable cost. They do suggest, however, that the problems are difficult and prudent economically viable solutions need to be worked out early in the fusion reactor development. Obviously, the availability of a good base of methods and nuclear data is crucial to acccomplishing this goal.

2. Fusion Reactor Shield Components

Fusion reactors can be classified into two types according to the plasma confinement scheme: a) magnetic-confinement reactors (MCR), and b) inertial confinement reactors (ICR). Many of the shielding problems in MCR's and ICR's are similar, but there are several key differences. This section provides an overview of the shield components and their functions in the two types.

The shield system in fusion reactors consists generally of the following components: 1) blanket, 2) primary bulk shield, 3) penetration shield, 4) component shield, and 5) biological shield. Figures 1 and 2 demonstrate the physical relationship among these components and other reactor subsystems in the two leading magnetic-confinement schemes of tokamaks and mirrors. Figure 3 displays this relationship for a laser driven reactor, a leading contender among inertial confinement schemes.

The primary function of the blanket is to convert the kinetic energy of fusion neutrons and secondary gamma-rays into heat. It provides, of course, a significant amount of radiation attenuation. The neutron source strength in the fusion core is 0.625×10^{19} P/E_f neutrons/sec where P is the reactor thermal power in MW and E_f is the recoverable energy per fusion reaction in MeV. In the absence of energy multiplication by fissionable materials, E_f in reactors operated on the DT cycle is ~20 MeV. Thus, the neutron source strength is ~3×10^{20} neutrons/sec for every 1000 MW of thermal power. Tokamaks and mirrors are operated at quasi-steady state, and steady-state while ICR's are operated with repetitive short pulses. The above source strength is a time-average. In ICR's and MCR's the blanket must contain lithium in one form or another to regenerate tritium. The magnitude of radiation attenuation provided by the blanket in both types of reactors is roughly the same as the blanket must extract ~95-99% of the energy of the neutrons and secondary gammas.

The primary bulk shield[26-45] circumscribes the blanket. The basic function of the bulk shield is to protect reactor components exterior to the blanket from

intolerable levels of nuclear heating, radiation damage and activation. The largest difference in shielding ICR's and MCR's comes from the markedly different boundary conditions for the primary shields in the two-types of reactors.

In magnetic-confinement reactors the primary magnetic field for plasma confinement is normally provided by superconducting magnets. Removal of heat from superconducting magnets at ~4°K is a powerconsuming process; about 300 watt of electric power is required to remove one watt of heat deposited in the magnets. Furthermore, heat generated in the magnets create distortions and stresses in the magnet particularly if the heat is generated non-uniformly. The components of a superconducting magnet are overly sensitive to radiation and the irradiation effects in these components strongly affect the design, operation, stability and safety of the magnets. Therefore, considerations of protecting the main superconducting (S.C.) magnets dominate the design criteria for the primary bulk shield in magnetic-confinement fusion reactors.

The trade-offs in the design of the bulk shield and the main magnets strongly impact the performance and economics of magnetic confinement reactors. Keeping the thickness of the bulk shield small results in unacceptably large power losses to run the S.C. magnet refrigerators as well as intolerable levels of radiation damage. Increasing the thickness of the primary bulk shield require displacing the magnets further from the plasma. This results in a reduction in the strength of the magnetic field in the plasma region and the reactor power in addition to an increase in the size of the magnets and the reactor. These considerations are discussed in Ref. 31.

Since inertial confinement fusion reactors do not require magnets the design considerations for the primary shield are very similar to those in fission reactors. Space restrictions remain as important shield design considerations, but they are much more relaxed compared to those in magnetic-confinement reactors.

Present conceptual designs for fusion reactors call for many largesize holes to penetrate the blanket and bulk shield. The most troublesome of all these penetrations are those for supplementary plasma (or pellet) heating and vacuum pumping in MCR's and ICR's in addition to impurity control penetrations in MCR's. Shielding these penetrations represents a new challenge that no other nuclear system had to cope with before. The challenge can best be understood by recalling some of the characteristics of these penetrations: 1) large size, the cross section area varies from ~0.4 to 3 m^2, 2) these penetrations have openings in the first wall directly visible to the source neutrons generated in the fusion core; they pass through the blanket and bulk shield and extend to the reactor exterior leading to large size expensive equipment, and 3) the functional requirements of some of these penetrations do not permit significant bends in the penetration ducts.

The presence of penetrations makes it impossible for the bulk shield alone to satisfy the functional requirements of the primary shield. Penetration shields are, therefore, required as a necessary part of the primary shield and reactor design. A penetration shield is a mixture of attenuating materials that completely surrounds the penetration as it emerges from the bulk shield and extends to the penetration functional equipment (e.g., injector for neutral beams, pump for vacuum pumping, laser building for laser beams, etc.). Radiation streaming and penetration shielding is discussed in Refs. 51-58.

Two types of component shields are required. The first is to attenuate the radiation that streams through the component. Examples are the shields around the beam injector chamber and the vacuum pumps (see Fig. 1). The second type is the shield provided locally to protect a component that is overly sensitive to radiation such as some of the instrumentation equipment.

The primary shield which consists of the bulk, penetration and component shield provides for protection of components during reactor operation. Its biological shielding function is limited only to reducing the induced activation to appropriate levels as required by maintenance tasks during shutdown. The biological dose outside the reactor during operation is several million rems/hr. Therefore, a biological shield is necessary. Since the reactor building is required to be ~2-3 m of concrete to satisfy the structural containment function, the walls of the reactor building are presently conceived to serve the dual purpose of providing the necessary containment as well as biological shielding. It appears unlikely that practical designs to permit any type of personnel access into the reactor building during operation can be developed. On the other hand, fusion reactors require periodic major component replacement and maintenance tasks and the need for some personnel access into the reactor building after shutdown is unavoidable even with remote maintenance planned for. These considerations are discussed in Ref. 92.

3. Nuclear Data Needs

Commercialization of fusion power requires an aggressive research and development program in a large number of technical areas.[1-25] In the nuclear design area, we are very fortunate to have the extensive methods and data information base that has been developed over the past thirty years in the fission and weapons programs. Up to the present, the nuclear analysis of fusion reactors has relied almost entirely on this information base. It must be realized, however, that a nuclear design of an actual fusion reactor requires[77] some research and development (R&D). These R&D requirements can be characterized as low risk extensions and improvements to the state-of-the-art. However, they are also indespensible as they serve critical needs related to the reactor performance as well as economic, environmental and safety considerations. Much of these needs will have to be satisfied before building the next generation of experimental power reactors planned for the midto late 1980's.

The nuclear aspects of a fusion reactor can be classified into methods and data. The state-of-the-art and required developments in calculational methods were reviewed in Refs. 74, 75 and 92. In this section, the attention is focused on nuclear data needs; the subject of this meeting. Although our main concern is shielding, the data requirements for general fusion neutronics are covered as well.

As a first step, one needs to define the materials of concern. Table 1 gives a summary of materials being considered for the blanket and shield excluding hybrid applications. Table 1 shows the actual form of material to be used, but Table 2 shows the elemental materials of potential use in the blanket, shield and other fusion reactor components. The reason the list is long is that at this stage there is a diversity of design concepts and a number of reactor types for which the appropriate selection of materials vary widely. There is presently no committment to a specific reactor design with a definite material selection. This represents one of the serious difficulties in establishing the priorities in a nuclear data measurements program. Nuclear data is, of course, required for all these materials as a part of the input to the comparative technical evaluations necessary to select design concepts and materials. However, most of the requirements for this purpose can generally be satisfied by presently available data with a modest effort of data evaluation.[78] The major concern is the nuclear data measurements. Because of cost and limitations on available experimental facilities these measurements must be kept to a minimum. An important consideration, however, is the long time that these measurements consume. In order to ensure timely availability of important data needs, one is forced to make judgements now about the material selection. To satisfy this purpose, we have indicated a qualitative judgement in Table 2 on the probability of using each material in 1) the next generation of experimental power reactors, and 2) the demonstration and commerical power plants. These are careful judgements, but as our knowledge deepens and expands some of them may change.

The second area of concern in identifying the nuclear data needs is the energy range of interest. In fusion design application, this energy range extends from thermal energies to at least the average energy of the D-T neutrons, i.e. 14 MeV. It should also be noticed that there is a considerable width in the spectrum of the source neutrons emitted from DT plasmas significantly heated or driven by injecting energetic deutrons. Therefore, the high energy limit for nuclear data should extend to ~16 MeV. There are other fusion-related applications, such as materials irradiation facilities with D-Li neutron source, that require extending the data base to ~30 MeV, but these are not covered here as our concern is focused in this paper on reactor design applications. The fact that the energy range of the greatest importance in fusion extends to 16 MeV while there has been only a nominal interest above 5 MeV in fission suggests that most of the new nuclear data measurements needed for fusion is in the energy range 5-16 MeV.

The third area of concern is the type of nuclear data required in fusion design applications. Table 3 shows these data types. The nuclear designer needs to calculate: 1) Tritium breeding in the blanket and tritium production that may contaminate other regions, 2) nuclear heating, 3) radiation damage indicators (atomic displacement, gas production and transmutations), 4) induced activation and related parameters such as the decay heat and biological dose, and 5) neutron and gamma-ray shielding attenuation characteristics. To evaluate these quantities one needs a variety of nuclear data that can be broadly classified into three areas: a) neutronics, b) γ-ray production, and c) gamma-ray interactions. The nuetronics data consist of cross sections for individual neutron reactions and secondary neutron energy and angular distributions. The reactions of importance are most affected by the energy range of interest which extends to ~16 MeV. For example, high energy neutrons are capable of inducing a variety of important reactions that are inaccessible to lower energy neutrons. Therefore, in fusion design one needs cross sections for reactions such as (n,α), (n,n$'\alpha$), (n,p) and (n,n$'$p) for which there is presently no or little information for several important materials.[79-81] It should be emphasized that while lumped cross sections such as the total helium production cross section may be suitable for radiation damage calculations, induced activation requires cross sections for individual reactions. Furthermore, accurate calculation of induced activation requires the nuclear data for each individual isotope. It has also been shown[79,80] that although nuclear heating calculations can be made directly from lumped data for a mixture of isotopes, the correct averaging of data, e.g., energy dependent Q-values, implicitly assumes that the isotopic data is known.

Since shielding plays a major role in fusion design, the data requirements for shielding must be emphasized. These requirements are generally different from those for the blanket. In shielding, the main interest is neutron and gamma attenuation, deep penetration and streaming. This requires emphasizing the 1) accuracy of basic cross sections such as total and elastic and inelastic scattering, 2) gamma-ray production and interaction, 3) energy and angular distribution of secondary neutrons and gammas; scattering anisotropy is generally crucial to streaming and deep penetration problems, and 4) good resolution of cross section minima.

Gamma-ray production data is very crucial to nuclear heating and radiation shielding application. The status of nuclear data in this area is particularly serious despite significant recent improvements reflected in the latest ENDF/B version.[82] For example, there is presently no reliable gamma production data for important materials such as ^{11}B and tungsten. The data measurements and evaluation for gamma production can actually be simplified by recognizing that only two types of information are required: a) the total gamma production cross section as a function of the incident neutron energy, and b) the energy distribution of emitted gammas as a function of the incident neutron energy. The angular distribution of emitted gammas is also required, but at a lower priority since the nature of the volumetric source distribution tends to largely

compensate the modest anisotropies in emission. Measuring or identifying gamma production by reaction and isotope is of secondary importance except in special cases.

Nuclear data for gamma-ray interaction is generally the best known of all types of data. Only modest revisions are required in this area.

The fourth area of concern in defining the nuclear data needs is the required accuracy in the data. This is a difficult area and is a part of the more general question of the required accuracy in predicting the nuclear performance characteristics. The errors in nuclear calculations come from a variety of errors and approximations such as those in data measurements, data representation in evaluated files such as those of ENDF/B, data processing, multigroup energy representation, geometric representation of the system, transport calculations and response function evaluation. Therefore, a knowledge of the target accuracy in the estimated nuclear parameters is necessary but not sufficient to define the accuracy goal for the basic nuclear data.

The desirable accuracy in predicting the nuclear performance characteristics can be determined from an elaborate cost-benefit analysis. The cost is principally that of the research and development, the man and computer-time for performing the calculations and verification experiments. The benefits are the economic gains realized by reducing the degree of conservatism usually necessary to assure satisfactory operation and safety of the power plant. For example, overpredicting radiation attenuation in the shield has very serious consequences of impairing operation of many fusion reactor components, increasing the number of unscheduled failures, reducing plant availability and increasing the potential of radiation exposure. The seriousness of the situation is compounded by the fact that there is normally no space for shield improvement after the reactor has been built. Therefore, shielding calculations are always required to be conservative. The larger the uncertainties in prediction the higher the safety margin and the degree of conservatism have to be. A high degree of conservatism in shield design can be an unacceptable burden on the reactor economics.

It is very doubtful that a reliable cost-benefit analysis of the type referred to above can be performed for fusion reactors for many years, and perhaps decades, to come. Quantifying the costs and benefits is extremely difficult in practice. It appears, therefore, that the fusion community has to be content with only evaluating the penalties resulting from uncertainties in prediction or the benefits that can be derived from improving the accurancy of prediction. This is still a difficult task, but some effort in this area is definitely required as a part of fusion reactor research and development program. For our purpose here let us qualitatively discuss an elementary example. Figure 4 shows[31] the cost of energy in a tokamak reactor as a function of the blanket/shield thickness, Δ^{i}_{BS}, on the inner side of the torus with stainless steel and boron carbide as the constituents of the blanket/shield. The results are shown for several sizes of the major radius. At present, the tokamak design effort is focused on small size reactors of major radius R = 6 m or less for better economics. From Fig. 4 one notices the great sensitivity of the cost of energy to the value of Δ^{i}_{BS} at $R \leq 6$ m. The optimum value of Δ^{i}_{BS} is ~1 m. Using smaller values of Δ^{i}_{BS} will result in a sharp increase in the cost of energy due to the large increase in the power required to run the superconducting magnet refrigerators and the large increase in the magnet cost necessary to accomodate higher radiation levels. At these small values of Δ^{i}_{BS} there are risks associated with the reliability of the operation and safety of the magnets. Therefore, it appears now that the design value for Δ^{i}_{BS} must be greater than the optimum value of 1 m. Figure 4 indicates the penalty in the cost of energy resulting from using larger Δ^{i}_{BS}.

One should carefully note here that the penalty as shown in Fig. 4 is due to the increase in Δ^{i}_{BS} with the shield actually performing as calculated. The penalty from increasing Δ^{i}_{BS} and the shield providing less attenuation than

calculated is much larger than that in Fig. 4. To provide a more realistic indication of this penalty we have plotted in Fig. 5 the cost of power as a function of the additional non-shield increase, δ, in Δ^i_{BS}. This is roughly the effect of the actual thickness of the blanket/shield built as $\Delta^i_{BS} + \delta$ while its attenuation is only that predicted by the present calculation for a thickness Δ^i_{BS}. The results in Fig. 5 suggest that for small-size tokamaks the penalty of the increased cost of power can be as high as 1% (for a 1000 MWe this is ~20 million dollars) for every loss of attenuation equivalent to that provided by only 1 cm (in this example, 1 cm is 1% of Δ^i_{BS}) of shielding. This is a very large penalty and serves to demonstrate that very good accuracies will be required for most of the shielding calculations in fusion reactors.

In Table 4, we attempt to define some target accuracies in predicting the important nuclear parameters in the blanket, shield and other reactor components where radiation is of concern. As in many instances in this section, these must be viewed as careful judgements some of which may change as our experience and knowledge of fusion reactors deepen and expand. A few notes on the accuracies defined in Table 4 are in order. Generally, very good accuracies are required in the blanket where primary energy conversion, tritium production and severe radiation damage occur. The target accuracies for calculating the nuclear responses in the shield can be much less than those in the blanket. However, the need for relatively high accuracies in predicting the nuclear responses in the superconducting magnets in MCR's requires that the characteristics of the radiation emerging from the bulk shield (and penetration shields) be known to an appropriately good accuracy. Only a factor of 2-3 has been set as the target accuracy for the biological dose in the reactor floor (outside the bulk shield) and outside the reactor building. Better accuracies are, of course, desirable, but they are not practically achievable because of the large number of decades of radiation attenuation involved.

The most difficult question is to define the accuracy goals for each type of basic nuclear data measurement for each material. These goals must, of course, be consistent with the target accuracies for predicting the nuclear design parameters discussed above and shown in Table 4. But two key questions arise. One is how much of the tolerance in design calculation accuracy can be permitted for nuclear data. The second is how much inaccuracy in estimating a nuclear performance parameter results from an error in a particular part of nuclear data in a specific energy range for a given material.

Sensitivity analysis[83] is generally resorted to for defining the nuclear data accuracy needs. The general purpose of the sensitivity analysis is to determine the sensitivity of calculated parameters for a nuclear system to the information used. Thus, sensitivity analysis can be utilized to examine the effects of uncertainties in nuclear data as well as variations in materials and geometry on the calculated parameters of interest. In the past few years, there has been a very significant progress in developing theoretical formalisms and computer codes for sensitivity analysis.[84,85] The lastest of these developments is the channel theory[86] which makes it possible to determine the "channels" in space and energy that contribute most to the radiation field in a particular location. A number[87-90] of sensitivity studies for fusion applications have also been recently performed.

The sensitivity analysis is of considerable value in many problem areas. Unfortunately, at this stage of fusion reactor development, it cannot be used as the primary tool for defining the nuclear data needs. A principal difficulty with the sensitivity studies is that the information they yield are highly system, geometry, response, material and reaction specific. For example, radiation streaming in complex geometry changes substantially from one design to another and the relative importance of particular pieces of nuclear data can be widely different. At present, there is a diversity of reactor types, design concepts and materials being considered for fusion reactors. Furthermore, sensitivity studies require part of the input information to be the uncertainties in the cross sections and the correlations between the various cross

section errors. These are available only for very few materials. Some of the cross sections needed for fusion application have never been measured and a sensitivity analysis for these cross sections is obviously meaningless. It is desirable, however, to provide realistic estimates of the carefully evaluated data in the data files for future use in sensitivity studies.

Table 5 shows the recommended nuclear data measurements needed for fusion reactors. These are not limited to the shield requirements, but they cover also the blanket and reactor components where the radiation field is of concern. The needs indicated in Table 5 are for measurements and do not include data for which evaluation or theoretical estimates can suffice. The priorities of the data needs are assigned as follows: (1) urgent, (2) high priority, (3) needed, and (4) low priority. These priorities were assigned based on careful judgements[91] of (a) the probability that the isotope or element will be used in fusion reactors particularly in the next generation of experimental machines; (b) the significance of the reaction to neutron transport, energy deposition, radiation damage, tritium production and induced activation; (c) accuracy of currently available data; and (d) the variety of considerations that have been discussed in this section.

4. Summary

Valuable extensive experience and a broad base of methods and data is available to the fusion reactor shield designer from the highly developed field of fission. However, fusion reactor shielding presents new, interesting and sometimes challenging problems above and beyond those familiar in fission reactors. Furthermore, the specific nature of fusion reactor systems and the high neutron energy range of interest in the D-T cycle make it necessary to pursue a nuclear research and development program.

No technical systematic method exists for rigorously quantifying the specific nuclear data requirements. Nor is it likely that such a method would become available in the near future for reasons discussed in the paper. Therefore, only a framework of nuclear data requirements can be developed at present with heavy reliance on the experienced judgement of researchers in the field to fill in the specific details. Flexibility is necessary to modify these judgements as our knowledge and experience deepen and expand. Close interaction among experimentalists, evaluators and reactor designers is crucial to any prudent data acquisition program.

An attempt was made to define the specific nuclear data requirements, as we see them today, for fusion reactors with particular emphasis on those for the shielding. Six key areas were analyzed: (1) materials, (2) energy range, (3) specific types of nuclear data, (4) accuracy of data, (5) priority, and (6) time scale needed for acquisition of data. The presence of a diversity of design concepts and the lack of a committment to any material at present poses the most serious obstacle to defining the nuclear data needs. Assigning a probability of using potential materials was resorted to as shown in Table 2. For near-term experimental reactors, it appears that the use of the following materials is very likely: iron-based alloys (Fe, Cr, Ni, Mn) in the shield and blanket and magnet structure, boron-carbide (B, C) and lead in the shield, copper in the magnets, aluminum in a variety of components, and H, C and O in insulators. Tungsten is an exception in that the decision on using it will depend on verifying its apparent benefits by new differential and integral experiments. Lithium is probably the only material whose use in commercial reactors is almost certain.

Most of the new measurements needed are in the energy range of 5-16 MeV. This high energy range of interest dictates the need for knowledge of data for virtually all the variety of reactions that are energetically possible up to ~16

MeV; albeit a wide variation in accuracy requirements. The need for data by isotope and reaction has been shown. In shielding, the main interest is neutron and gamma attenuation, deep penetration and streaming. This requires emphasizing the (a) accuracy of basic cross sections such as total, elastic and inelastic scattering, (b) gamma-ray production and interaction, (c) accuracy of neutron emission spectra and angular distributions; scattering anisotropy is generally crucial to streaming and deep penetration problems, and (d) good resolution of cross section minima.

Specifying the needed accuracy in data was shown to be extremely difficult at this stage of fusion reactor development. An attempt was made to define target accuracies for predicting the various responses in several reactor components. These are shown in Table 4.

Table 5 shows the nuclear data measurements needs for fusion reactors as derived in this work. It should be clear that some of the items in this table will very likely require revisions as a result of future work. The table, however, should serve as a useful guide for developing a nuclear data measurement program to serve the needs of fusion reactors; particularly the near-term experimental power reactors.

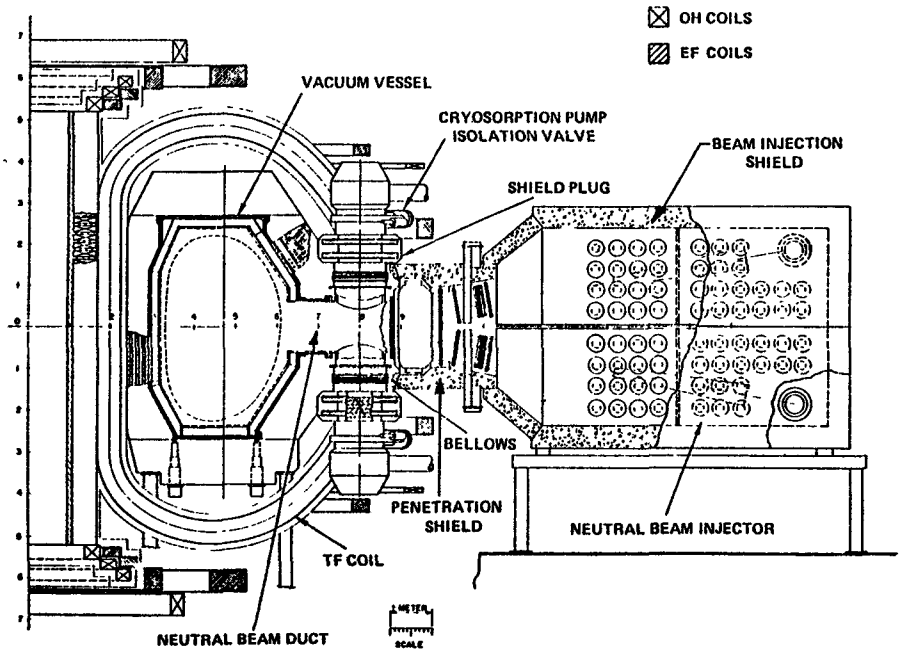

Fig. 1 Vertical cross section of a tokamak reactor design.

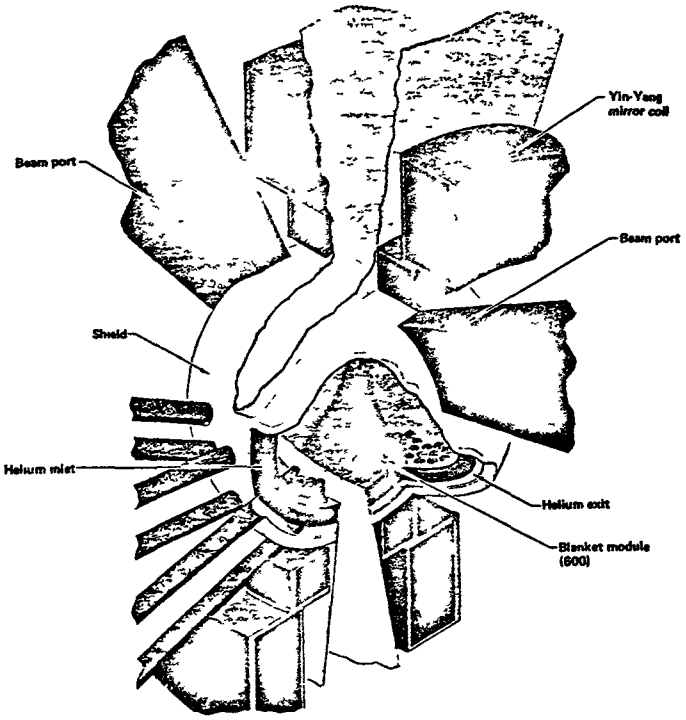

Fig. 2 Cutaway view of the blanket and bulk shield in a mirror reactor design.

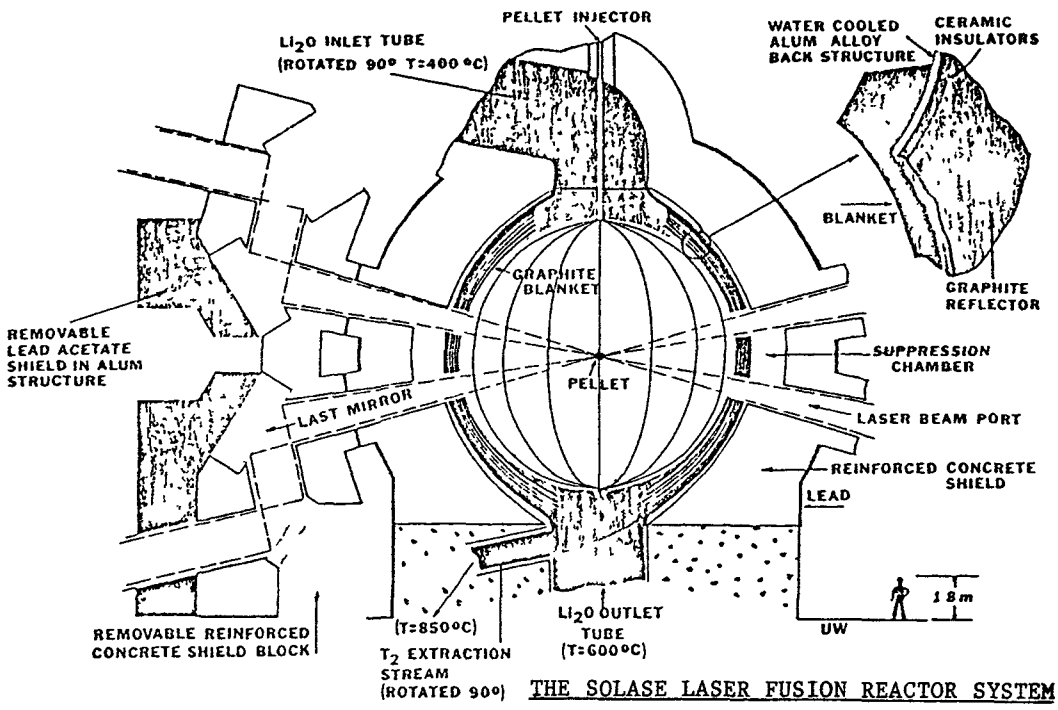

Fig. 3 A schematic of the Univ. of Wisconsin design,[10] SOLASE, for a laser fusion reactor.

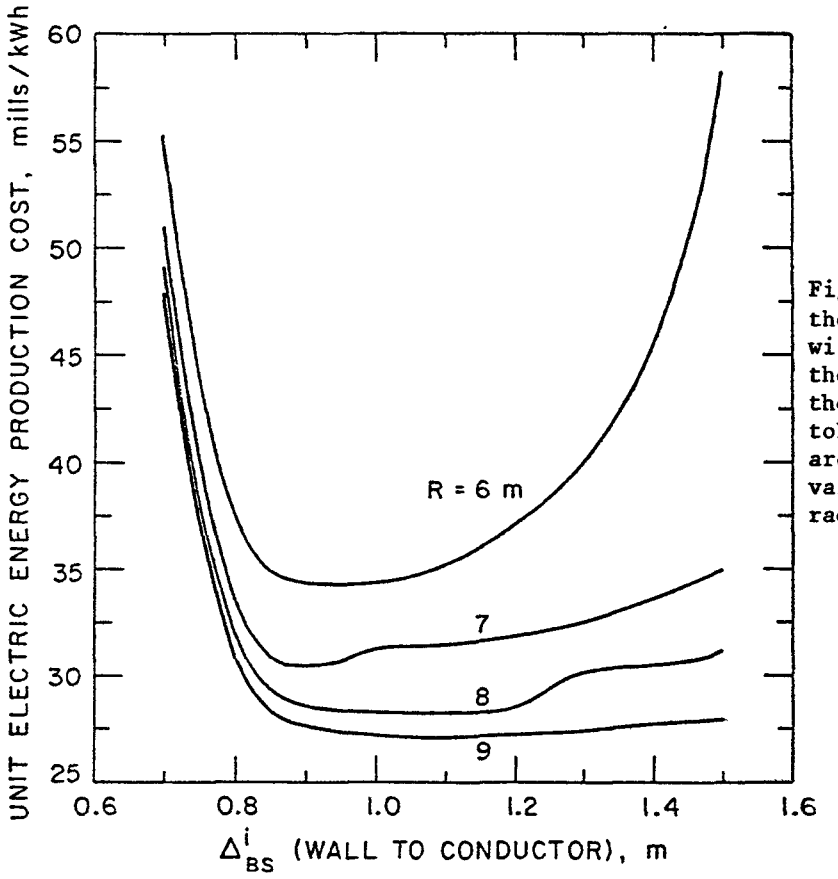

Fig. 4 Variation of the cost of energy with the thickness of the blanket/shield on the inner side of tokamaks. Results are shown for four values of the major radius.

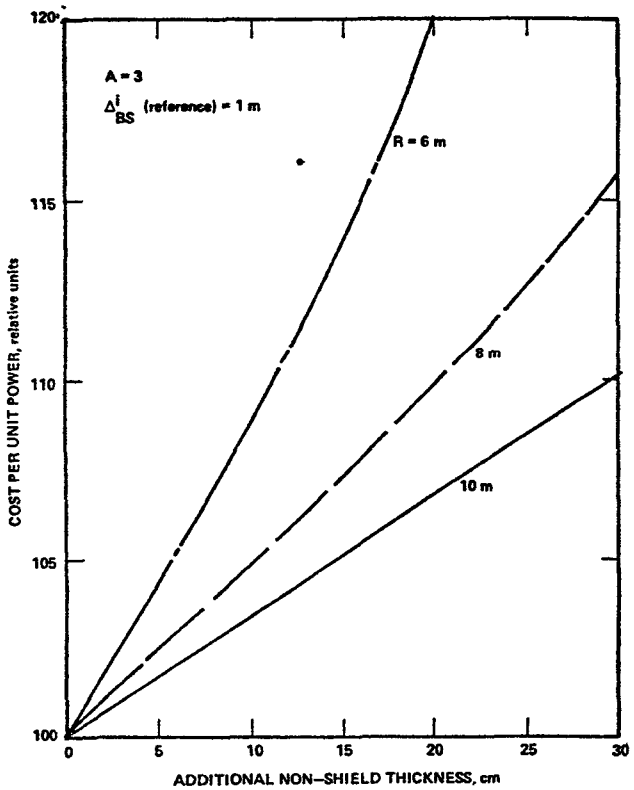

Fig. 5 Sensitivity of the cost of power in tokamak reactors to any non-attenuating increment in the blanket/shield thickness on the inner side of the torus.

Table 1

Summary of Material Proposed
for Blanket and Shield.

Application	Material
Tritium Breeding	Liquid Lithium Molten salts (Li_2BeF_4) Aluminum Compounds (LiAl, $Li_2Al_2O_4$) Ceramic Compounds (Li_2O, Li_2C_2) Lithium-Lead eutectic
Structural Material	Iron-Based Alloys Nickel-Based Alloys Refractory-Based Alloys (V, Nb, Mo) Titanium Aluminum-Based Alloys
Coolant	Liquid Lithium Molten salts Helium, Water
Neutron Multiplication	Beryllium, Lead
Reflector	Graphite, Stainless steel
Shield	Stainless steel, Tungsten Lead, Lead Mortar, Lead Acetate Boron Carbide (B_4C) Borated Water Iron Mortar, Concrete LiH, LiD

Table 2

Elementary Materials of Potential Use in Fusion Reactors
A qualitative judgement on the probability of using the material is shown
(H = high, M = average, L = Low)

	Demo and Commercial			Experimental Reactors			
Material	Blanket	Shield	Others	Blanket	Shield	Others	Comments
Hydrogen	M	H	H		H	H	plasma, H_2O, in organic insulators
Helium	M	M	H		M	H	coolant, also in S.C. magnets
Lithium	H	M		L			tritium breeding, neutron absorption
Beryllium	M						neutron and energy multiplication
Boron		H		M	H		probably in B_4C form
Carbon	L	H			H	H	B_4C, reflector, wall coating, in insulators
Nitrogen			M		M		reactor building atmosphere, insulators
Oxygen		H			H		H_2O, reactor building atmosphere
Flourine	L						in molten salts
Sodium			M				secondary coolant
Aluminum	L	L	H	L	L	H	S.C. magnet stabilizer and structure
Silicon	M	M	M				SiC, Stainless steel
Argon			M			M	reactor building atmosphere
Titanium	M	L		L			structural material
Vanadium	M	L		L			structural material
Chromium	H	H	H	H	H	H	in steel and super alloys
Manganese	H	H	H	H	H	H	in " " " "
Iron	H	H	H	H	H	H	in " " " "
Nickel	H	H	H	H	H	H	in " " " "
Copper			H			H	normal and superconducting magnets
Niobium	M		H				structural material, also in superconductor
Molybdenum	L	L					
Tin			M			L	in Nb_3Sn superconductor
Tantalum		L			L		
Tungsten		H			H		in space-restricted shield region
Lead	M	H			H		in lithium-lead compounds and lead shield
Bismuth		L					

Table 3
Types of Nuclear Data Required in Fusion Nuclear Design

Application	Tritium Breeding	Nuclear Heating	Radiation Damage Indicators	Induced Activation	Radiation Shielding
Data Type					
Total	X	X	X		X
Elastic	X	X	X		X
Inelastic	X	X	X		X
Neutron Emission	X	X	X		X
(σ_{em}, $d\sigma/d\Omega$, $P(E')$)					
(n,2n), (n,3n)	X	X		X	X
(n,α), (n; n'2)		X	X	X	
(n,p), (n; n'p)		X	X	X	
(n,d), (n; n'd)		X	X	X	
(n,t), (n; n't)	X	X	X	X	
(n, γ), (n; n'γ), (n; xγ)		X		X	X
Gamma Production		X			X
(σ^P, $d\sigma/d\Omega$, $P(E_n \rightarrow E_\gamma)$)					

Table 4
Some Required Accuracies[a] in Fusion Reactor Shielding

Location/Response	Desired Accuracy
First Wall/Blanket	
Nuclear Heating	total 2%, spatial distribution 10%
Tritium Producing	breeding ratio 5%, local 10%
Atomic Displacements	10%
Helium Production	10%
Transmutations	20%
Induced Activation	50%
Bulk Shield	
Nuclear Heating	gross 20%, local 30%
dpa and He and H production	factor of 2
Activation	factor of 2
Tritium Production	factor of 3
Main (Superconducting) Magnets	
Nuclear Heating	gross 10%, local 20%
dpa	gross 10%, local 20%
H, He production	gross 40%, local 80%
Activation	factor of 2
Penetration Duct Walls	
Nuclear Heating	local 20%
dpa and He and H production	local 50%
Penetration Functional Equipment (e.g. vacuum pumps, neutral beam injectors)	
Nuclear Heating	gross 30%, local 50%
dpa and He and H production	50%
Activation	factor of 2
Tritium production	factor of 2
Reactor Floor (outside the shield and inside the containment building)	
Biological Dose during operation	factor of 3
Biological Dose after shutdown	factor of 2
Coolant Manifolds and Heat Exchangers	
Biological Dose after shutdown	factor of 2
Containment Building	
Nuclear Heating	factor of 2
dpa and He and H production	local factor of 4
External Biological Dose (outside containment building)	factor of 3

a - These accuracies are approximate and they may change as our knowledge and experience deepen and expand. Some of these accuracies (e.g. that for the nuclear heating in the blanket) may be relaxed for near-term experimental machines.

Table 5

Nuclear Data Measurements Needs for Fusion Reactors

Reaction	Type of Measurement	Incident Energy (MeV)	Accuracy Goal (%)	Priority[a]	Comments
^{6}Li elastic scattering	$\sigma_{n,n}$, $d\sigma/d\Omega$	2-16	10	2	Reaction is important for good interpretation of other reactions.
^{6}Li inelastic scattering	$\sigma_{n,n'}$, $d\sigma/d\Omega$	2-16	10-20	2	
^{6}Li(n,α)t	$\sigma_{n,\alpha}$	0.3-16	5	2	
^{6}Li(n,2n')	$\sigma_{n,2n'}$, $P\left(E_{n'}\right)^{*}$	6-16	10-20	2	Source of helium and hydrogen production.
^{6}Li(n,n'p), ^{6}Li(n,n'α)	$\sigma_{n,n'p}$, $\sigma_{n,n'\alpha}$	5-16	30	4	Cross sections may be small but need to be examined.
^{6}Li(n,n'd)	$\sigma_{n,n'd}$, $P\left(E_{n'}\right)$	3-16	10-20	2	
^{6}Li neutron emission	$\sigma^{\dagger}_{n,em.}$	3-16	5	2	
^{7}Li(n;n't)	$\sigma_{n,n't}$, $P\left(E_{n'}\right)$	3-16	5	1	
^{7}Li elastic	$\sigma_{n,n}$	2-16	10	2	Elastic scattering is essential to interpreting important reactions such as (n;n',t).
^{7}Li inelastic scattering	$\sigma_{n,n'}$	-16	10-20	2	
^{7}Li neutron emission	$\sigma^{\dagger}_{n,em.}$	2-16	5	1	
Boron eleastic scattering	$\sigma_{n,n}$	6-16	5-15	2	Isotopic values needed; reaction affects the interpretation of other reactions.
B neutron emission	$\sigma_{n,em.}$	6-16	10	1	
^{10}B(n,t)	$\sigma_{n,t}$	1.2-16	20%	1	
^{11}B(n,t)	$\sigma_{n,t}$	12-16			
^{10}B(n,p)	$\sigma_{n,p}$	0.01-16	20	2	
^{10}B(n,2n)	$\sigma_{n,2n}$, $P\left(E_{n'}\right)$	9-16	20	2	$^{10}B(n,2n)^{9}B \rightarrow 2\alpha + P$
^{10}B(n;n'p)	$\sigma_{n;n'p}$, $P\left(E_{n'}\right)$	7-16	30	2	
^{11}B(n,α)	$\sigma_{n,\alpha}$	7-16	30	2	The decay product is 2α.
^{11}B(n,2n)	σ_{n2n}, $P\left(E_{n'}\right)$	12-16	30	2	
Boron gamma production	$\sigma_{n,x\gamma}$, $P\left(E_{\gamma}\right)$	10^{-6}-16	20	1	
C(n,xα)	$\sigma_{n,x\alpha}$	6.5-16	10	2	
C(n,α)	$\sigma_{\alpha_0}, \sigma_{\alpha_1}, \ldots$	6.5-16	20	3	Energy distribution of the charged particles is useful.
C(n;n'3α)	$\sigma_{n;n'3\alpha}$, $P\left(E_{n'}\right)$	8-16	10	1	Total helium production, heating and neutron transport in carbon is very sensitive to this reaction.
C neutron emission	$\sigma_{n,em.}$	6-15	10	1	
Fe neutron emission	$\sigma_{n,em.}$	8-16	10	1	
^{54}Fe, ^{56}Fe(n,α)	$\sigma_{n,\alpha}$	10^{-6}-16	20	2	Energy distributions of emitted alphas are very useful.
	$\sigma_{\alpha_0}, \sigma_{\alpha_1}, \sigma_{\alpha_2}, \ldots$		40	3	
^{54}Fe(n;n',p)	$\sigma_{n,n'p}$, $P\left(E_{n'}\right)$	~9.5-16	20	2	
Cr neutron emission	$\sigma_{n,em.}$	8-16	10	1	
Cr(n,xα)	$\sigma_{n,x\alpha}$	Threshold-16	20	2	
Cr(n,xp)	$\sigma_{n,xp}$	Threshold-16	20	2	
^{52}Cr(n,p)	$\sigma_{n,p}$, $\sigma_{np_0}, \sigma_{np_1}, \ldots$	Threshold-16	30	2	
^{53}Cr(n,p)				2	
^{54}Cr(n,p)				4	
^{50}Cr(n,p)				4	
^{52}Cr(n,2n)	$\sigma_{n,2n}$, $P\left(E_{n'}\right)$	~12-16	20	2	
^{52}Cr(n,d)	$\sigma_{n,d}, \sigma_{nd_0}, \sigma_{nd_1}, \ldots$	~9-16	30	3	
^{58}Ni inelastic scattering	$\sigma_{n,n'}$	4-16	10-20	2	
(level and continuum)	Angular and energy distributions	6-16	20-30		
^{60}Ni inelastic scattering	$\sigma_{n,n'}$	8-16	10-20	2	
(level and continuum)	Angular and energy distributions	6-16	20-30		
^{58}Ni(n;n',p)	$\sigma_{n,n'p}$, $P\left(E_{n'}\right)$	Threshold-16	20	1	Current uncertainity ~200%.
^{60}Ni(n;n',p)					
^{58}Ni(n,2n)	$\sigma_{n,2n}$, $P\left(E_{n'}\right)$	Threshold-16	10	3	Data currently available but there are some discrepancies at high energies.
^{60}Ni(n,2n)	$\sigma_{n,2n}$, $P\left(E_{n'}\right)$	Threshold-16	10	2	Currently, no data.

$^{58}Ni(n,\alpha)$ $^{60}Ni(n,\alpha)$	$\sigma_{n\alpha}, \sigma_{\alpha_0}, \sigma_{\alpha_1}, \ldots$	10^{-6}-16	10	1	
$^{58}Ni(n;n'\alpha)$ $^{60}Ni(n;n'\alpha)$	$\sigma_{n,n'\alpha}\ P\left(E_{n'}\right)$	7-16	20	4	
Nickel, neutron emission	$\sigma_{n,em.}$	Threshold-16	10-20	2	Angular distribution required where significantly anisotropic.
Cu neutron emission	$\sigma_{n,em.}$	2-16	10	1	
$^{63}Cu(n,p)$	$\sigma_{n,p}, \sigma_{np_0}, \sigma_{np_1}, \ldots$	1-16	20	1	
$^{63}Cu(n,d), ^{65}Cu(n,d)$	$\sigma_{n,d}, \sigma_{nd_0}, \sigma_{nd_1}, \ldots$	10-16	30	2	
$^{63}Cu(n;n'p)$	$\sigma_{n,n'p},\ P\left(E_{n'}\right)$	9-16	20	1	
Cu gamma production	$\sigma_{n,x\gamma},\ P\left(E_{\gamma}\right)$	10^{-6}-16	20	1	
V inelastic scattering	$\sigma_{n,n'}$, angular and energy distributions	7-16	10-20	3	
V neutron emission	$\sigma_{n,em.}$	7-16	10-20	2	Angular distribution is of interest.
V(n,p)	$\sigma_{np}, \sigma_{p_0}, \sigma_{p_1}, \ldots$	2-16	20	3	
V(n,α)	$\sigma_{n\alpha}, \sigma_{\alpha_0}, \sigma_{\alpha_1}, \ldots$	3-16	20	3	
V(n,2n)	$\sigma_{n2n},\ P\left(E_{n'}\right)$	12-16	10	2	
V(n;n'p) V(n;n'α)	$\sigma_{\gamma},\ P\left(E_{n'}\right)$	8-16	20	4	
Ti elemental total cross section	Total cross section	1-20	2	2	
^{46}Ti inelastic ^{48}Ti scattering	$\sigma_{n,n'}$	4-16	10	2	
$^{47}Ti(n,p)$	$\sigma_{np}, \sigma_{p_0}, \sigma_{p_1}, \ldots$	1-16	20	2	
$^{47}Ti(n,\alpha)$	$\sigma_{n\alpha}, \sigma_{\alpha_0}, \sigma_{\alpha_1}, \ldots$	10^{-6}-16	20	2	
$^{47}Ti(n,2n)$	$\sigma_{n,2n},\ P\left(E_{n'}\right)$	9-16	20	3	
$^{48}Ti(n,2n)$	$\sigma_{n,2n},\ P\left(E_{n'}\right)$	12-16	20	2	
$^{48}Ti(n,\alpha)$	$\sigma_{n\alpha}, \sigma_{\alpha_0}, \sigma_{\alpha_1}, \ldots$	Threshold-16	20	3	
Lead neutron emission	$\sigma_{n,em.}$	6-16	20	2	
Lead (n,n')	Discrete inelastic scattering	8-16	20	2	
$^{55}Mn(n,2n)$	$\sigma_{n,2n}$	12-16	20	2	
$^{55}Mn(n,p)$	$\sigma_{n,p}$	2-16	20	3	
$^{55}Mn(n,\alpha)$	$\sigma_{n,\alpha}$	1-16	20	3	
$^{55}Mn(n;n',p)$	$\sigma_{n,n'p}$	6-16	30	3	
$^{55}Mn(n;n',\alpha)$	$\sigma_{n,n'\alpha}$	8-16	30	3	
W inelastic scattering	$\sigma_{n,n'}$	1.5-4	10	4	
W elastic scattering	$\sigma_{n,n},\ d\sigma/d\Omega$	2-6 8-16	10	4	
W neutron emission	$\sigma_{n,em.}$	4-16	20	3	
W gamma production	$\sigma_{n,x\gamma},\ P\left(E_{\gamma}\right)$	10^{-6}-16	20	1	
Al(n,2n)	$\sigma_{n,2n}$	13.5-18	20	2	Cross section to the isomers ^{26}Al (positron emitter) is major concern for induced activation.
Al(n,p)	$\sigma_{n,p}$	14-16	20	2	
Al neutron emission	$\sigma_{n,em.}$	5-16	20	2	
$^{9}Be(n,2n)$	$\sigma_{n,2n}$	1.8-16	10	3	
^{9}Be neutron emission	$\sigma_{n,em.}$	1.8-16	10	3	
$^{40}Ar(n,2n)$	$\sigma_{n,2n}$	Threshold-15	20	2	
O Neutron emission	$\sigma_{n,em}$	5-16	10	2	

*$P\left(E_{n'}\right)$ refers to the energy distribution of secondary neutrons.

† For all entries in the table, $\sigma_{n,em.}$ refers to the neutron emission spectra and angular distribution, $\sigma_{n,Nem}(\theta_{n'}, E_{n'})$ generally required at several angles with outgoing neutrons recorded down to a few hundred KeV.

a. Priorities are assigned as follows: (1) Urgent, (2) high priority, (3) needed, (4) low priority.

References

1. STEINER, D., "The Technological Requirements for Power by Fusion," Nucl. Sci. Eng., 58, 107 (1975).

2. STACEY, W. M. and M. A. Abdou, "Tokamak Fusion Power Reactors," Nucl. Tech., 37, 29 (1978).

3. HANCOX, R., "The Euratom Fusion Technology Programme," CONF-760935-P2 (1976).

4. MORI, S., "The Fusion Technology Program in Japan," CONF-760935.

5. SCHRIVER, R. L., "U.S. Laser Fusion Technology Program," CONF-760935.

6. ABDOU, M. A. et al., "ANL Parametric Systems Studies," ANL/FPP/TM-100, Argonne National Laboratory (1977).

7. KULCINSKI, G. L., "Critical Issues Facing the Long Term Deployment of Fission and Fusion Breeder Reactors," Univ. of Wisconsin report UWFDM-234 (1978).

8. RIBE, F. L., "Recent Development in the Design of Conceptual Fusion Reactors," Nucl. Tech., 34, 179 (1977).

9. DEAN, S. O. et al., "Status and Objectives of Tokamak Systems for Fusion Research," WASH-1295, U.S. Atomic Energy Commission (1974).

10. CONN, R. W. et al., "SOLASE, A Laser Fusion Reactor Study," UWFDM-220, Univ. of Wisconsin (1978).

11. CONN, R. W., "What is Past is Prologue: Future Directions in Tokamak Power Reactor Design Research," CONF-760935-P2 (1976).

12. CARLSON, G. A. and R. W. Moir, "Mirror Machine Reactors," CONF-760935-P2 (1976).

13. KRAKOWSKI, R. A., "A Survey of Linear Magnetic Fusion Reactor Concepts," Proc. of the 3rd Topical Meeting on the Technology of Controlled Nuclear Fusion, Santa Fe, NM, May 9-11 (1978), to be published.

14. STEINER, Don, "Tokamak Reactor Design Studies: Progress and Prognosis," ibid.

15. CONN, R. W., G. L. Kulcinski and C. W. Maynard, "NUMAK, An Attractive Reactor for the Main Line of Tokamaks," ibid.

16. STACEY, W. M. et al., "Tokamak Experimental Power Reactor Conceptual Design," ANL/CTR-76-3, Argonne National Laboratory (Aug. 1976); also, W. M. Stacey, Jr. et al., "Tokamak Experimental Power Reactor Studies," ANL/CTR-75-2, Argonne National Laboratory (June 1975).

17. BAKER, C. et al., "Experimental Power Reactor Conceptual Design Study," GA-A14000, General Atomic Co. (July 1976); also, "Experimental Power Reactor Conceptual Design Study," GA-A13534, General Atomic Co. (July 1975).

18. ROBERTS, M. et al., "Oak Ridge Tokamak Experimental Power Reactor Study," ORNL/TM-5572 thru ORNL/TM-5577, Oak Ridge National Laboratory (1976).

19. CONN, R. W. et al., "UWMAK-III, A Noncircular Tokamak Power Reactor Design," UWFDM-150, Univ. of Wisconsin (July 1976).

20. KEARNEY, D. W. et al., "Conceptual Design Study of a Noncircular Tokamak Demonstration Fusion Power Reactors," GA-A13992, General Atomic Co. (1976).

21. STEINER, D. et al., "ORNL Fusion Power Demonstration Study: Interim Report," ORNL/TM-5813, Oak Ridge National Laboratory (1977).

22. COHN, D. R. et al., "High Field Compact Tokamak Reactor (HFCTR) Conceptual Design," RR-78-2, MIT Plasma Fusion Center (1978).

23. SAKO, K. et al., "Conceptual Design of the JAERI Demonstration Fusion Reactor," CONF-760935-P2 (1976).

24. BENDER, D. J. et al., "Reference Design for the Standard Mirror Hybrid Reactor," UCRL-52478, Lawrence Livermore Laboratory (1978).

25. CASALI et al., "FINTOR-1, A Minimum Size Tokamak DT Experimental Reactor," Commission of the European Communities Joint Research Centre, Ispra Establishment.

26. ABDOU, M. A. and C. W. Maynard, "Nuclear Design of the Magnet Shield for Fusion Reactors," CONF-740402-P1, Vol. 1, p. 685 (1974).

27. KRIESE, J. T. and D. Steiner, "Magnet Shield Design for Fusion Reactors," ORNL-TM-4256, Oak Ridge National Laboratory (1973).

28. McCRACKEN, G. M. and S. Blow, in CLM-R 120, Culham Laboratory (1972).

29. SANTORO, R. T., T. S. Tang, R. G. Alsmiller, Jr., and J. M. Barnes, ORNL/TM-5874, Oak Ridge National Laboratory.

30. ABDOU, M. A., "Nuclear Design of the Blanket/Shield System for a Tokamak Experimental Power Reactor," Nucl. Tech, 29, 7 (1976).

31. ABDOU, M. A., "Radiation Considerations for Superconducting Fusion Magnets," J. of Nucl. Materials, 72, 147 (1978).

32. GERSTL, S. A. W., "A Minimum Thickness Blanket/Shield with Optimum Tritium Breeding and Shielding Effectiveness," Proc. of the 3rd Topical Meeting on the Technology of Controlled Nuclear Fusion, Santa Fe, NM, May 9-11, 1978, to be published.

33. LEE, J. D., "TMR Nucleonics," in UCRL-52302 by R. W. Moir et al., (1977).

34. GOHAR, Y., C. W. Maynard and E. Cheng, "Neutronic and Photonic Analysis of UWMAK-III Blanket and Shield in Non-circular Geometry," CONF-760935-P3 (1976).

35. CHENG, E. T. et al., "Nucleonic Design for a Compact Tokamak Fusion Reactor Blanket and Shield," to be published in Nucl. Tech.

36. CASINI G. and R. Cuniberti, "Nuclear Blanket and Shielding Problems in Demonstration Fusion Reactors," CONF-740402-P2 (1974).

37. GABRIEL, T. A., R. T. Santoro and W. W. Engle, Jr., "Shield Design Calculations for ORMAK-F/BX," ORNL/TM-4619, Oak Ridge National Laboratory (1974).

38. DUDZIAK, D. J., "Selected Problems of Fusion Reactor Shielding," Trans. Am. Nucl. Soc., 23, 626 (1976).

39. AVERY, A. F. and M. M. Chesnutt, "Shield Design for the Joint European Torus," Proc. 5th Int. Conf. on Reactor Shielding (1977) Science Press.

40. SINGH, M. S., "Radiological Safety Design Considerations for a Laser-Fusion Facility," ibid.

41. JEDRUCH, J., "Design of Shielding for the Tokamak Fusion Test Reactor," Trans. Am. Nucl. Soc., 23, 628 (1976).

42. ALSMILLER, R. G., Jr., J. Barish and C. R. Weisbin, "Uncertainties in Calculated Heating and Radiation Damage in the Toroidal-Field Coil of a Tokamak Experimental Power Reactor Due to Cross Section Errors," ORNL/TM-4198 (1976).

43. VOGELSANG, W. F. and E. Ramer, "The Gamma-Ray Dose Rate After Shutdown from a Tokamak Reactor," Trans. Am. Nucl. Soc., 23, 628 (1976).

44. ABDOU, M. A., "Important Aspects of Radiation Shielding for Fusion Reactor Tokamaks," ATOMKERNERGIE, Bd. 30 (1977), Lfg4.

45. KULCINSKI, G. L. et al., "A Wisconsin Toroidal Fusion Reactor Design, UWMAK-1," UWFDM-68, Univ. of Wisconsin (1974).

46. AVERY, A. F., "Radiation Streaming - The Continuing Problem of Shield Design," Proc. 5th Int. Conf. on Reactor Shielding, R. W. Roussin, Editor (1977) Science Press.

47. MYNATT, F. R., "Shielding Methods Development in the United States," ibid.

48. MAIENSCHEIN, F. C., "Where Are We and Where Are We Going in Reactor Shielding," ibid.

49. MIYAKOSHI, J. et al., "Radiation Streaming of N. S. Mutsu and Its Repair Plan," ibid.

50. FARINELLI, U. and R. Nicks, "Shielding Problems in Fast Reactors," a chapter in the NEACRP Monograph: "NEACRP Review on The Status of Fast Reactor Physics," to be published.

51. ABDOU, M. A., L. Milton, J. Jung and E. M. Gelbard, "Multidimensional Neutronics Analysis of Major Penetrations in Tokamaks," Proc. 2nd Topical Mtg. on Tech. of Controlled Nucl. Fusion, CONF-760935-P3, p. 845 (1976).

52. ABDOU, M. A. and J. Jung, "Nuclear Analysis of a Tokamak Experimental Power Reactor Conceptual Design," Nucl. Tech., 35, 51 (1977).

53. JUNG, J. and M. A. Abdou, "Radiation Shielding of Major Penetrations in Tokamak Reactors," Nucl. Tech., 41, 71 (1978).

54. IDE, T., Y. Seki and H. Iida, "Effects of Neutron Streaming Through Injection Parts on Neutronics Characteristics of a Fusion Reactor," Proc. 2nd Topical Mtg. on Tech. of Cont. Nucl. Fusion, CONF-760935-P3, p. 395 (1976).

55. SANTORO, R. T. et al., "Monte Carlo Analysis of the Effects of a Blanket-Shield Penetration on the Performance of a Tokamak Fusion Reactor," ORNL/TM-5874 (1977).

56. SANTORO, R. T. et al., "Two and Three-Dimensional Neutronics Calculations for the TFTR Neutral Beam Injectors," ORNL/TM-6354 (1978).

57. NICKS, R., C. Ponti, G. Realini and H. Van Heusden, "Shielding Problems in the FINTOR Design," Proc. 5th Int. Conf. on Reactor Shielding (1977), Science Press.

58. RAGHEB, M. M., A. C. Klein and C. W. Maynard, "Three Dimensional Neutronics Analysis of the Mirrors-Beam Duct-Shield System for a Laser-Driven Power Reactor," UWFDM-239, Univ. of Wisconsin (1978).

59. ROUSSIN, R. W., Editor, 5th Int. Conf. on Reactor Shielding, Science Press (1977); See for example, Papers 2-8 in the Occupational Exposure Session, Session E.

60. POWELL, J. et al., Editors, "Proceedings of the Magnetic Fusion Energy Blanket and Shield Workshop; A Technical Assessment," ERDA-76/117/1; also CONF-760343 (1975).

61. ZAHN, H. S., et al., "Developing Maintainability for Tokamak Fusion Power Systems," COO-4184-4, McDonnel Douglas Astronautics Co. (1977).

62. Code of Federal Regulations, Title to, U. S. Government Printing Office, Washington, D.C. 20402.

63. VERNA, B. J., "Radiation Exposure and Protection Problems in Nuclear Power Plants - U. S. Overview," Proc. 5th Int. Conf. on Reactor Shielding, Science Press (1977).

64. CLEMMER, R. G., "TCODE - A Computer Code for Analysis of Tritium and Vacuum Systems for Tokamak Fusion Reactors," ANL/FPP/TM-110, Argonne National Laboratory (1978).

65. ENGLE, W. W., "A User's Manual for ANISN," K-1693, Oak Ridge National Laboratory (1976).

66. LATHROP, K. D., "DTF-IV, A Fortran-IV Program for Solving the Multigroup Transport Equation with Anisotropic Scattering," LA-3373 (1965).

67. HILL, T. R., "ONETRAN: A Discrete Ordinates Finite Element Code for the Solution of the One-Dimensional-Multigroup Transport Equation," LA-5990-MS (1975).

68. RHOADES, W. A. and F. R. Mynatt, "The DOT-III, Two-Dimensional Discrete Ordinates Transport Code," ORNL/TM-1880 (1973).

69. LATHROP K., and F. W. Brindley, "TWOTRAN-II, An Interfaced Exportable Version of the TWOTRAN Code for Two Dimensional Transport," LA-4848-MS (1973).

70. SEED, T. J., W. F. Miller, Jr., and F. W. Brinkley, "TRIDENT - A Two-Dimensional Triangular Mesh Discrete Ordinates, Explicit Neutron Transport Code," LA-6735-M, Los Alamos Scientific Laboratory (1977).

71. JUNG, J., "Finite Difference Equations for Transport Equations in Toroidal-Geometry," Nucl. Sci. eng., 60, 74 (1976).

72. CHAPIN, D. L. and W. G. Price, Jr., "A Comparison of the D-T Neutron Wall Load Distributions in Several Tokamak Fusion Reactor Designs," MATT-1186, Princeton Plasma Physics Laboratory (1975).

73. RHOADS, W. A., "The DOT IV Variable Mesh Discrete Ordinates Transport Code," Proc. 5th Int. Conf. on Reactor Shielding, Science Press (1977).

74. DUDZIAK, D. J., "An Assessment of Nucleonic Methods and Data for Fusion Reactors," CONF-760935-P3, p. 819 (1976).

75. MAYNARD, C. W., "Overview of Methods and Codes for Fusion Reactor Nuclear Analysis," Trans. Am. Nucl. Soc., 23, 11 (1976).

76. LATHROP, K. D., "THREETRAN: A Program to Solve the Multigroup Discrete Ordinates Transport Equation in (x,y,z) Geometry," LA-6333-MS (1976).

77. TWINING, B. G. and J. R. Powell, "An Assessment of Blanket and Shield Technology," CONF-760935-P4, p. 1433 (1976).

78. STEINER, D., "Nuclear Data Needs in Fusion Reactor Design," Proc. of Conf. on Nuclear Cross Sections and Technology, NBS Special Publication 425.

79. ABDOU, M. A. and C. W. Maynard, "Calculational Methods for Nuclear Heating - Part I: Theoretical and Computational Algorithms," Nucl. Sci. Eng., 56, 360 (1975).

80. ABDOU, M. A. and C. W. Maynard, "Calculational Methods for Nuclear Heating - Part II: Applications to Fusion Reactor Blankets and Shields," Nucl. Sci. Eng., 56, 381 (1975).

81. BHAT, M., Brookhaven National Laboratory, private communications.

82. GARBER, D., C. Dunford and S. Pearlstein, "Data Formats and Procedures for the Evaluated Nuclear Data File, ENDF," BNL-NES-50496, Brookhaven National Laboratory (1975).

83. GOLDSTEIN, H., "A Survey of Cross-Section Sensitivity Analysis as Applied to Radiation Shielding," 5th Int. Conf. on Reactor Shielding, Science Press (1977).

84. BARTINE, D. E., E. M. Oblow and F. R. Mynatt, "Radiation Transport Cross-Section Sensitivity Analysis - A General Approach Illustrated for a Thermonuclear Source in Air," Nucl. Sci, Eng. 55, 147 (1974).

85. WEISBIN, C. R. et al., "Cross Section and Method Uncertainties: The Application of Sensitivity Analysis to Study Their Relationship in Calculational Benchmark Problems," Proc. Conf. Nuclear Cross Sections and Technology, March 3-7, 1975, Washington, D.C., NBS Special Publication 425 (1975).

86. WILLIAMS, M. L. and W. W. Engle, Jr., "Spatial Channel Theory - A Technique for Determining the Directional Flow of Radiation Through Reacgor Systems," 5th Int. Conf. on Reactor Shielding, Science Press (1977).

87. GERSTL, S. A. W., D. J. Dudziak, and D. W. Muir, "Cross Section Sensitivity and Uncertainty Analysis with Application to a Fusion Reactor," Nucl. Sci. Eng., 62, 137 (1977).

88. ALSMILLER, R. G., Jr., J. Barish, and C. R. Weisbin, "Uncertainties in Calculated Heating and Radiation Damage in the Toroidal Field Coil and of a Tokamak Experimental Power Reactor Due to Neutron Cross Section Errors," Oak Ridge National Laboratory, ORNL/TM-4198 (1976).

89. GERSTL, S. A. W., "The Application of Perturbation Methods to Shield and Blanket Design Sensitivity Analysis," ANL/AP/CTR/TM-28, Argonne National Laboratory (1974).

90. ALSMILLER, R. G. et al., "Comparison of the Cross Section Sensitivity of the Tritium Breeding Ratio in Fusion Reactor Blankets," Nucl. Sci. Eng., 57, 122 (1975).

91. Table 13 was developed in collaboration with Dr. A. Smith, Argonne National Laboratory, Argonne, IL.

92. ABDOU, M. A., "Review of Fusion Reactor Shielding," to be published.

NEUTRON DATA FOR HYBRID REACTOR CALCULATIONS

AG-159/A6
Review Paper

D.V. MARKOVSKII, G.E. SHATALOV

I.V. Kurchatov Atomic Energy Institute, Moscow, USSR

ABSTRACT

A brief review of high-energy neutron integral experiments and their comparison with calculations is presented, taking into account the requirements for neutron data in hybrid blanket design. Some considerations concerning this data improvement are given.

INTRODUCTION

Current interest in hybrid reactors, fusion reactors with fissile material in the blanket, originates from two main considerations. On the one hand, such a system simplifies appreciably a number of current problems of "pure" thermonuclear reactors, such as attainment of favorable plasma parameters and making the first wall stable against radiation. On the other hand, it is possible to get economic benefits from a combined energy system making use of light-water, fast and hybrid reactors, where a relatively small number of hybrid reactors with high plutonium production could strongly affect the fuel balance [1]. Recently the concept of a fast subcritical blanket has been preferred, where the high energy of thermonuclear neutrons is most effectively used for neutron production in fission and nonelastic reactions in fissile materials. Also, better thermal performance and faster accumulation of secondary fissile material are achieved for natural or depleted uranium. This concept is being developed in the USSR in the hybrid thermonuclear Tokamak reactor project (HTTR) [2].

The objective of neutronic calculations of hybrid reactor blankets is to provide the project with detailed information on parameters such as the following: power distribution in the blanket, fissile-material and tritium-production rates, attenuation of neutron and gamma-ray fluxes in the shield, blanket and shield activation, radiation damage rates, gaseous-product generation rates and the time-dependent change of the isotopic composition of fuel.

In most cases the calculation is made in two separate stages: estimation of the detailed space-energy distribution of neutrons in the blanket and shield, followed by calculations of various flux functionals corresponding to the above parameters. This will require a library of input data for calculations of neutron fluxes, as well as data for calculations of the functionals in a format corresponding to the flux formats: KERMA factors, gamma-ray sources, activation cross sections, radiation damage cross sections, cross sections of the reactions with charged particle yield, yields and cross sections of fission products and elements in the chain of nuclear transformations of the fissile material.

In the present work only the data required for neutron flux calculation are considered in detail. A brief review of some integral experiments with pure materials, as well as comparison with BLANK code calculations [3], is presented below.

EXPERIMENTS WITH ^{238}U

The key functional for the hybrid reactor is the composite source, equal to the sum of the number of D-T reaction neutrons and the number of additional neutrons born in the (n,f), (n,2n) and (n,3n) reactions.

For the contribution to the fission rate and neutron multiplication, the most important are the (n,f) and (n,2n) reactions, from which secondary neutrons can induce subsequent fissions of ^{238}U. At present the cross sections of these reactions with energies close to 14 MeV are known to an accuracy of 2-5%, which seems to be sufficient for the calculations. The information about secondary neutron spectra is also of great importance since the probability of fission depends strongly on the fraction of neutrons with energies above the ^{238}U fission threshold. The spectra of secondary neutrons produced in the

interaction of neutrons with ^{238}U at energies of 14.3 and 9.1 MeV have been recently measured by Baryba et al. [4,5]. The total spectrum measured was divided into two components: the fission spectrum and the evaporation spectrum of neutrons from the equilibrium and pre-equilibrium states. Fig. 1 shows comparison of the spectra for E = 14.3 MeV [4], approximating the total evaporation spectrum and its equilibrium and pre-equilibrium components in accordance with the data of the ^{238}U files from the UKNDL [6] and ENDL [7] libraries and a domestic file [8]. The parameters proposed in Ref. 4 give a harder spectrum of secondary neutrons than those in the evaluated data files, particularly UKNDL.

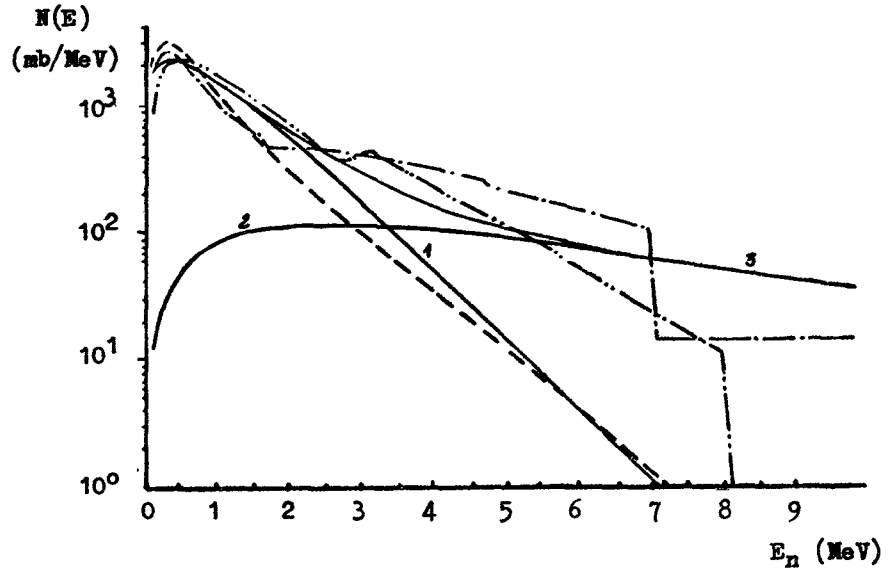

Fig. 1 ^{238}U secondary neutron spectra for E_0 = 11 MeV. Curves labelled 1, 2 and 3 show the equilibrium, pre-equilibrium and total spectra, respectively, from Ref. 4. The remaining curves are based on UKNDL (---), ENDL (-.-) and the domestic file (- . . -).

The integral experiments which can be used for the analysis of the ^{238}U spectra were performed by J.W. Weale et al. [10] and C. Wong et al. [9]. In Ref. 9 the neutron leakage spectra from uranium spheres with radii 3.63 and 10.91 cm, measured over the energy range from 10 keV to 14 MeV, are compared with calculations based on the ENDL and ENDF/B-IV data. It is noted that the spectrum within the 10 keV - 1 MeV range is described better with the ENDF/B-IV, while within the range 2-14 MeV the ENDL data give better results. Unfortunately, the spectra measured in this work are given in the units of the detector counts, which prevents their comparison with other calculations.

The experiment by Weale et al. [10], whose results were reported in 1961, is so far the only experiment which allows verification of the neutron balance in a system of natural uranium which is effectively infinite for 14-MeV neutrons. More detailed measurements were performed in an assembly 99 cm in diameter. The accuracy of all the measurements, without taking into account the accuracy of the constants, is 3-4%. In Table I the experimental results are compared with the calculations using the BLANK code with UKNDL, ENDL and domestic-file ^{238}U data. For estimation of the effects due to the one-dimensional approximation and various temperatures of the fission spectrum, the calculations by the BLANK code are made for two geometries, a sphere and an infinite cylinder, and two temperatures of the Maxwellian distribution, 1.33 and 1.5 MeV. The calculated ^{238}U fission and capture rates, obtained with the BLANK code with the ENDL and domestic-file data, agree with the experiment within the error, while the calculation based on the UKNDL data underestimates the rate of ^{238}U fissions. The difference in temperatures of the fission spectrum gives an effect of 5-8% in the rates of the $^{238}U(n,f)$ and $^{238}U(n,\gamma)$ reactions. The (n,2n) reaction rate for the domestic-file agrees with the experiment within the error while the UKNDL and ENDL data overestimate it by 13-15%. The differences between the calculation and experiment in the (n,3n) reaction rate are 30%, 90% and 83% for UKNDL, ENDL and domestic-file ^{238}U data, respectively.

Table I. The number of reactions per source neutron in a natural uranium assembly 99 cm in diameter

Reaction	Experiment [12]	Calculation with the BLANK code					
		UKNDL, MAT 401		ENDL, MAT 7055		^{238}U domestic file	
		Cylinder	Sphere	T_f=1.33[a]	T_f=1.5	T_f=1.33	T_f=1.5
^{235}U(n,f)	0.281±0.017	0.225	0.213	0.222	0.232	0.238	0.246
^{235}U(n,γ)	-	0.05	0.047	0.048	0.05	0.046	0.052
^{238}U(n,f)	1.18±0.07	0.954	0.95	1.08	1.18	1.207	1.31
^{238}U(n,γ)	4.08±0.24	4.12	3.86	3.91	4.08	4.2	4.39
^{238}U(n,2n)	0.277±0.08	0.317	0.32	0.315	0.315	0.278	0.278
^{238}U(n,3n)	0.327±0.05	0.244	0.245	0.168	0.168	0.178	0.178
Leakage	0.41±0.020	0.314	0.593	0.665	0.72	0.729	0.789
Leakage+ ^{238}U(n,γ)	4.49±0.28	4.43	4.45	4.58	4.8	4.93	5.17

a. T_f is the temperature (in MeV) used in constructing the fission-spectrum Maxwellian

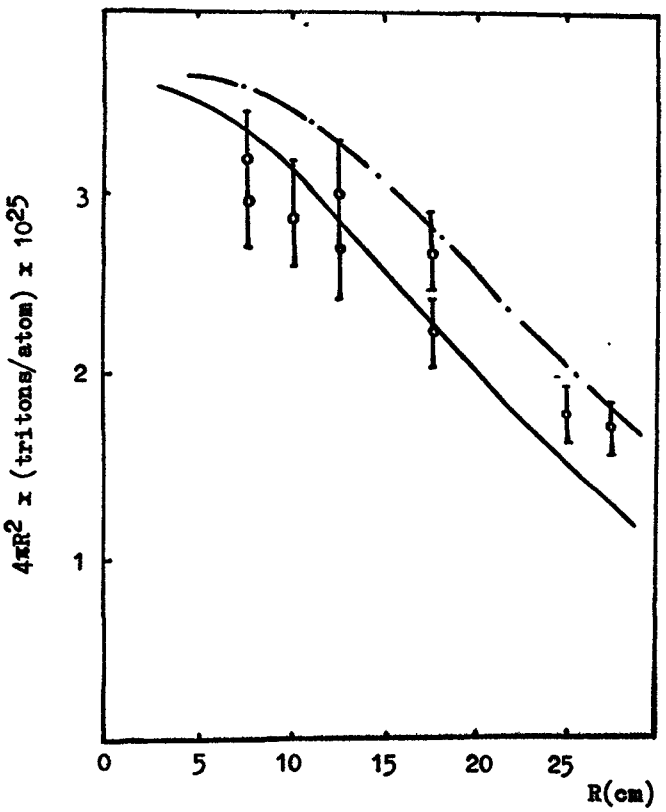

Fig. 2

The ^{7}Li(n,n'α)T reaction rate over the radius of the lithium deuteride sphere. The data points with error bars show the experimental results, while the curves show calculations using the BLANK code with UKNDL (——) and ENDL (—— . ——) data.

LITHIUM

Experiments with a neutron source located inside lithium-containing assemblies are described in Refs. 11-14. Hiroka et al. [11] measured relative distributions of the fission rates using ^{232}Th, ^{235}U and ^{238}U fission chambers in a system close to spherical, containing stainless-steel-canned lithium blocks. Comparison of these distributions with a BLANK calcula-

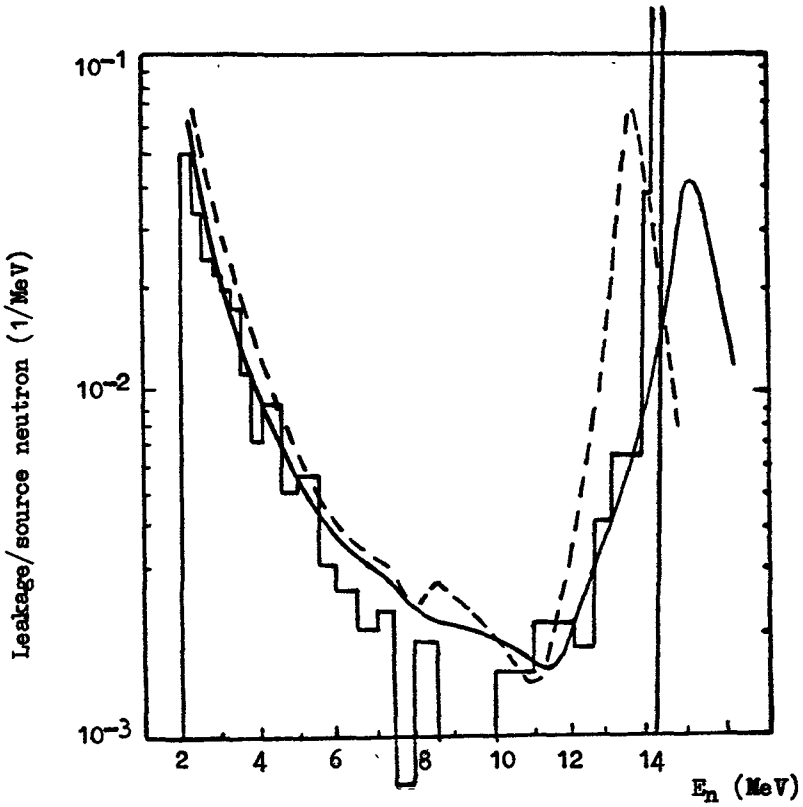

Fig. 3 The neutron leakage spectrum of the iron sphere with 22.3 cm radius at the 30° and 120° angles to the beam: —— experiment, θ=30°; --- experiment, θ=120°; ⌐⌐ calculation by the BLANK code with the ENDL data.

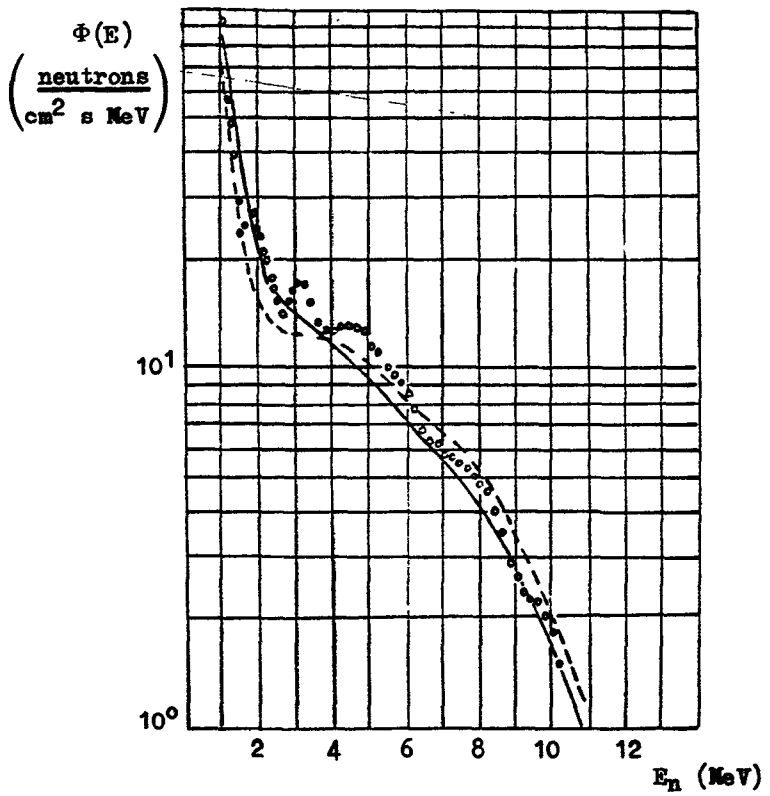

Fig. 4 The leakage spectrum for the Nb sphere 25.4 cm in diameter with Am-Be neutron source: ooo - experiment, —— calculation, ENDL; --- calculation, Smith's evaluation [17].

tion based on the UKNDL and ENDL data allows one to make a general conclusion that the calculation describes reasonably well the relative trend of the fission rates over the assembly radius.

Kappler et al. [12] measured the neutron angular flux at 0° relative to the beam in a 1 m diameter sphere of natural lithium, using the time-of-flight technique. The measurements were made at 20 cm and 32 cm from the center. The authors state a significant disagreement of the experimental spectra above 1 MeV with a discrete ordinates calculation based on the ENDF/B-III library, but they find good agreement at lower energies.

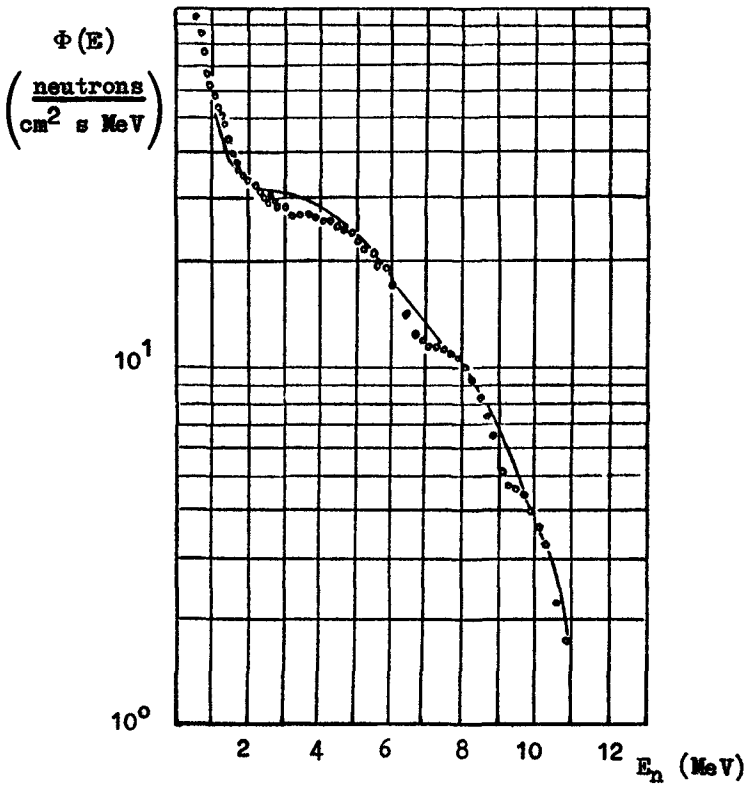

Fig. 5 The leakage spectrum for the Mo sphere 23 cm in diameter. Source Am-Be. o - experiment; —— calculation, ENDL.

In the experiments reported by Muir and Wyman [13] the 14-MeV neutron source was set in the center of a sphere, 30 cm in radius, made of lithium deuteride with the natural lithium isotopic mixture. A comparison of the $^{7}Li(n,n'\alpha)T$ reaction rates measured in the experiment with the BLANK calculation with Li data from the UKNDL (MAT 215) and ENDL (MAT 7007) is shown in Fig. 2. The curve of the $^{7}Li(n,n'\alpha)T$ reaction rate for the UKNDL data, shown in Fig. 2, has a steeper slope and goes lower than the curve corresponding to the ENDL data. It might be supposed that this is due to the significant difference (~40%) between the UKNDL and ENDL evaluations of inelastic scattering to the first level of ^{7}Li within the energy range 3-8 MeV. Besides, the $^{7}Li(n,n'\alpha)T$ reaction cross section is 10% lower in the UKNDL file than in the ENDL file, for energies from 4 to 10 MeV.

Byrjukov et al [14] measured double differential cross sections for neutron scattering by ^{7}Li nuclei at an initial energy of 9.1 ± 0.2 MeV. The inelastic scattering cross sections with excitation of the first level at 0.48 MeV, the $^{7}Li(n,n'\alpha)T$ reaction, and total cross section reported in Ref. 14 agree reasonably well with the ENDL library data.

STRUCTURAL MATERIALS

If significant amounts of structural materials are placed in a region with a hard neutron spectrum, their influence on the balance of neutrons and energy can be significant. In hybrid reactors this applies particularly

to the materials of the first wall: stainless steel (iron) for a low-temperature blanket and niobium and molybdenum for a high-temperature one.

The neutron leakage spectra from iron spheres with 4.46, 13.41 and 22.3 cm radii and a D-T source were measured by Hansen et al. [15]. The measurements were performed using the time-of-flight method at 30° and 120° relative to the beam direction. Fig. 3 shows a comparison of the experimental spectra from the 22.3-cm radius sphere with a BLANK calculation using ENDL (MAT 7029) data.
The experimental results are given as the smooth curves plotted through the points of Ref. 15. The dashed curve shows the spectrum for 120° and the solid one corresponds to 30°. The source neutron energies for these angles are 14.97 and 13.65 MeV, respectively. The calculation spectra are shown as histograms. The calculation with the ENDL data agrees reasonably well with the experiment. The discrepancy in the 8-10 MeV range seems to be due to a large statistical error in the calculation of small portions in the spectrum by the Monte-Carlo method.

Figs. 4 and 5 show a comparison of leakage spectra, calculated with the BLANK code, with experimental spectra [16] obtained with the spheres of Nb and Mo surrounding an Am-Be neutron source. The accuracy of the experiment is estimated to be about 10%. Both the measured and calculated spectra are normalized to a source strength of 1.3×10^8 neutrons/sec. For niobium (Fig. 4) the calculation was carried out using the ENDL (MAT 7034) and data evaluated by Smith et al. [17]. Both versions within the error limit give agreement with the experiment above 6 MeV and below 2 MeV. Within the 4-6 MeV range a distribution, harder and closer to the experiment, is obtained from the calculation with the constants evaluated by Smith et al [17]. The experiment with molybdenum, Fig. 5, is calculated only with the ENDL (MAT 7035) data. Above 5 MeV and below 2 MeV the results agree well; within the 2-5 MeV range the calculation somewhat overestimates the neutron flux.

CONCLUSIONS

1. It is necessary that a complete library of neutron data be created for fusion reactor calculations. The calculations based on the available data sets give results with differences which exceed the admissible uncertainty of key blanket functionals.

2. For confident application of the calculational results in the construction of the fusion installations being designed, an extensive program of neutron-physics experiments with the 14 MeV neutron source must be carried out, including the following phases:

(2.1.) Integral experiments with pure material samples. In these experiments the absolute neutron and photon leakage spectra should be measured as well as the reaction rates within the volumes of the samples with a thickness of several mean-free-paths for the source neutrons. It is reasonable to use a set of threshold detectors in the experiments. Of great interest is the estimation of the neutron balance in the sample. On the basis of the analysis of data reported in the literature, integral experiments on samples of the following materials could be recommended: fissile materials - ^{238}U, ^{235}U, ^{232}Th; lithium and lithium-containing materials - $LiAlO_2$, Li_2O, Li_2C, LiH; and structural materials - C, Al, Cu, stainless steel.

(2.2.) Differential measurements of individual properties of the materials (cross sections, secondary neutron spectra) can be carried out if it becomes necessary to improve them on the basis of an analysis of all the known integral experiments and their comparison with the calculations. In the experiments with thin samples it is also reasonable to determine the integrated characteristics of the spectra using the threshold detectors.

At present evaluations and, possibly, measurements of the characteristics of the following materials are required:

Lithium - There is a significant discrepancy in the UKNDL and ENDL library evaluations of the cross sections of the $^{7}Li(n,n'\alpha)T$ reaction and inelastic scattering with excitation of the first level within the energy range 3–10 MeV, as well as the secondary neutron spectra of the $^{7}Li(n,n'\alpha)T$ reaction.

^{238}U - Agreement between the evaluated data on the secondary neutron spectra and the experimental results is required.

(2.3.) For calibration of the calculation method together with the evaluated data and verification of the characteristics of the particular blanket schemes, simulation experiments are required, using a 14 MeV neutron source located inside assemblies simulating the composition of the design schemes.

3. A common source of basic information for the creation of working libraries of functional–calculation constants listed in the introduction is required. For this purpose it is reasonable that the files of evaluated data should include not only KERMA-factor and gamma-ray source cross sections but also cross sections for activation and radiation damage. Evaluators should continuously enrich these data files with information for a wide set of materials. To maintain energy conservation, the quantities responsible for energy yield must be evaluated simultaneously. The required cross-section accuracy for calculations of the production of tritium and fissile fuel is estimated to be 2–5%, while the required accuracy for the other constants is about 10%.

4. For estimation of the uncertainty in calculated values, files of cross section uncertainties, as well as uncertainties of angular and energy distributions of secondary neutrons, must be developed.

When representing the variation of secondary neutron spectra as a function of initial energy, interpolation rules giving a smoother dependence of the functionals on the initial neutron energy should be used.

REFERENCES

[1] GOLOVIN, I.N., et al., "The Nuclear Fuel Problem and Hybrid Reactors", IAE Report-2931, Moscow (1977).

[2] KOTOV, V.V., SHATALOV, G.E., "Gas Cooled Blanket of a Hybrid Thermonuclear Reactor with Solid Lithium-Containing Materials", Proc. US-USSR Symposium on Fusion-Fission Reactors (Livermore, California, July 13–16, 1976) CONF-760733.

[3] MARIN, S.V., et al., "The BLANK code for Space-Energy One-Dimensional Neutron Calculations", IAE Report-2832, Moscow (1977).

[4] BARYBA, V.Y., et al., "The Secondary Neutron Spectrum During the Bombardment of ^{238}U Nuclei by 14.3 MeV Neutrons", FEI Report-671, Obninsk (1976).

[5] BIRYUKOV, N.S., et al., "The Energetic and Angular Distributions of Secondary Neutrons During the Bombardment of ^{238}U by Neutrons with Energy 9.1 $\pm$ 0.2 MeV", FEI Report-687, Obninsk (1976).

[6] PARKER, K., "The Aldermaston Nuclear Data Library as at May 1963", AWRE O-70/63, AWRE Aldermaston (1963).

[7] HOWERTON, R.J., et al., "Evaluated Nuclear Cross Section Library", Lawrence Livermore Laboratory, UCRL-50400 4 (1971).

[8] ABAGYAN, A.P., et al., Proc. All-Union Conf. on Neutron Physics (Kiev, 1973), Obninsk 1 (1974) 239.

[9] WONG, C., et al., "^{238}U Pulsed Sphere Measurements and CTR Fusion-Fission Blanket Calculations", Proc. Conf. Nucl. Cross Sections and Technology (Washington, D.C., March 3–7, 1975), National Bureau of Standards special publication 425.

[10] WEALE, J.W., et al., "Measurements of the Reaction Rate Distribution Produced by a Source of 14-MeV Neutrons at the Center of a Uranium Metal Pile", React. Sci. Tech. 14 (1961) 91–99.

[11] HIRAOKA, T., et al., "Integral Neutronic Experiment on a Lithium Assembly", First Topical Meeting on the Technology of a Controlled Nuclear Fusion (San Diego, April 16–18, 1974) CONF-740402.

[12] KAPPLER, F., et al., "Determination of Neutron Spectra in a Lithium Sphere", Proc. 8th Symp. on Fusion Technology (Noordwijkerhout, The Netherlands, June 17-21, 1974), EUR-5182e. (Editors note. A related article by the same authors appears in Nucl. Sci. Eng. 67 (1978) 74-78).
[13] MUIR, D.W. and WYMAN, M.E., "A Tritium-Production Measurement with Application to Fusion Reactor Blanket Design", Trans. Am. Nucl. Soc. 22 (1972) 631.
[14] BIRYUKOV, N.S., et al., "The Scattering of Neutrons with Energy 9.1 ± 0.2 MeV by ^{7}Li Nuclei", Sov. Atomic Energy (Engl. Trans.), 43 (1978) 804-807.
[15] HANSEN, L.F., et al., "Measurements and Calculations of the Neutron Spectra from Iron Bombarded with 14 MeV Neutrons", Nucl. Sci. Eng. 51 (1973) 278-295.
[16] BOGART, D., et al., "Transport Analysis of Measured Neutron Leakage Spectra from Spheres as a Test of Evaluated High Energy Cross Sections", Nucl. Sci. Eng. 53 (1974) 285-303.
[17] SMITH, A.B., et al., "Fast Neutron Processes in Niobium", AP/CTR/TM-4 Argonne National Laboratory (1973).

INVITED PAPERS: SESSION B

STATUS OF NUCLEAR DATA REQUIRED FOR FUSION REACTOR DESIGN

CROSS-SECTION SENSITIVITY AND UNCERTAINTY ANALYSIS FOR FUSION REACTORS (A REVIEW)*

AG-159/B1
Review Paper

Donald J. Dudziak
Theoretical Division
University of California
Los Alamos Scientific Laboratory
Los Alamos, New Mexico, USA

ABSTRACT

A review is presented of neutron cross-section sensitivity and uncertainty studies as applied to fusion reactor concepts. General observations are made concerning the applicability and potential value of such studies, as well as their current limitations. While literature is cited relative to sensitivities to D-D and D-T cross sections, as well as to temperature of the D-T reaction, these topics are excluded from discussion. After a brief review of cross-section and secondary-energy-distribution sensitivity theory, most emphasis is focused upon published studies of the TFTR, experimental power reactors, and a conceptual commercial reactor (NUWMAK). Salient results of these studies, as they pertain to cross-section measurement and evaluation requirements, are summarized. Lastly, some comments are made relative to cross-section data requirements in the 14-50 MeV region.

I. INTRODUCTION

Under the topic of sensitivity and uncertainty analysis we consider primarily the work performed using classical perturbation theory and cross-section uncertainty covariance data. Specifically excluded are several studies performed using alternate evaluated data sets or credibly deviant data sets devised by the analyst. Fusion reactor nucleonics analysis being a comparatively new field of endeavor, the scope of this review is thus confined to relatively few papers, mainly those reporting cross-section sensitivity**studies of the Tokamak Fusion Test Reactor (TFTR) and experimental power reactor (EPR) design studies. In order to keep the topic more manageable, we also exclude any detailed discussion of hybrid reactor sensitivity studies. However, this does not imply a lack of recognition of the importance of hybrid reactor concepts or of the vital role cross-section data play in conceptual hybrid design exercises. Rather, it reflects a lack of published investigations in this area, with two notable exceptions.[1a,1b] Likewise, application of sensitivitity methods to design and analysis of integral experiments, although very important, is beyond our scope.

Upon the recommendation of the International Nuclear Data Committee, data up to 50 MeV are included in this review. However, no uncertainty studies per se have been performed for neutron energies above ~ 14 MeV, so review comments are necessarily mostly qualitative.

Other areas where sensitivity studies exist in the literature, but which are specifically excluded from this review, are the sensitivity of multigroup cross sections to thermal broadening of the fusion peak,[2] and of plasma burn to the D-D and D-T cross sections.[3]

The theory of cross-section sensitivity is fortuitously simpler for fusion reactors than for fission reactors, because eigenvalue problems are obviated. Most analyses involve only inhomogeneous source terms in the linear Boltzmann equation, leading to a relatively simple logarithmic derivative of a reaction rate with respect to a cross-section. In Sec. II below a brief summary of the theory is given, including recent extensions to secondary energy and angular distributions.[4,5] Section III then presents a discussion of detailed results from the literature, for the TFTR, EPR, and a conceptual commercial power reactor (NUWMAK). Also, comments are made in Sec. III regarding data in the region above 14 MeV. Conclusions from the studies in Sec. III are then summarized in Sec. IV.

At the outset it is useful to make a salient, if perhaps obvious, point regarding sensitivity studies. That is, such studies are intrinsically design dependent, as is explicitly shown in the theory (Sec. II). The immediate implication is that the question, "Are the available cross-section data for a particular nuclide 'N' satisfactory for fusion reactor design?" is unfinished, leaving wanting two key qualifiers; viz, 1) for what design model, and 2) for which response functions.

---

*Work performed under the auspices of the U. S. Department of Energy.

**In this review we will use the abbreviated phrase "sensitivity" studies to include uncertainty analyses where it is clear from the context.

Another clear observation is that sensitivity studies are analogous to cross-section assessments done previously by cruder methods for fission and fusion devices, albeit more comprehensive and providing differentials of uncertainty rather than just point values. Being design-dependent does not, however, mean that broader conclusions than those for a specific design cannot be drawn from a sensitivity analysis. On the contrary, for a generic class of designs the sensitivity results for a prototypic set of design models can span the range of sensitivities for that class. A practical case in point is the sensitivity analysis[6] performed for an EPR design, where the conclusions drawn may be largely valid for a later design study of a reactor concept called The Next Step (TNS).

Another facet of sensitivity studies which may be self-evident is that they are of direct value to both the reactor designer and the cross-section technologist. Their immediate value to the designer is to furnish him requirements for a margin-of-safety component attributable to nucleonic uncertainties, which he can then factor into design conservatisms. Secondly, the sensitivities can guide him in selection of materials and configurations which will perhaps minimize nucleonic uncertainties while still satisfying design criteria (e.g., selection of shielding materials). Concurrently, the cross-section technologist is able to determine which additional experiments and/or evaluations are most likely to, first, significantly decrease uncertainties, and, second, yield the lowest cost-benefit ratio. While the foregoing qualitative introductory discussion deals with a somewhat idealized application, many of the benefits mentioned have already been realized. One case in point is the TFTR, where the value of the sensitivity analysis manifested itself in the "negative" result that anticipated cross-section errors should not be unacceptable for calculations of radiation exposure rate during required access after reactor shutdown.

Historically, the modern development of sensitivity and uncertainty analysis can be traced from the work of Prezbindowski[7] in 1968, to a mushrooming expansion and application by Conn,[8] Bartine,[9,10] Gerstl,[11,12] and their respective colleagues in the early 1970's. Some of these early applications were already to fusion reactors.[8,9,12,13,14] The total fusion reactor sensitivity literature, however, is still somewhat limited because of the relative newness of fusion reactor nucleonics. It is still possible for a serious practitioner interested in nuclear analysis or cross-section technology to readily familiarize himself with most of these publications (e.g., Refs. 1, 4, 6, 8, 9, 12-19). More basic literature on the theoretical foundations of sensitivity theory can be found among the references given in Refs. 8 and 19.

With the notable exception of secondary energy and angular distribution sensitivity, sensitivity studies have been hindered not primarily by theoretical methods or computer code availability, but rather by lack of cross-section covariance data. Strictly sensitivity (not including uncertainty) analyses are readily performed using standard discrete-ordinates transport codes and subsequent straightforward integrations over the Boltzmann equation phase space. However, the uncertainty analysis then requires covariance data which can be equally voluminous as the cross-section data entering the purely sensitivity analysis. In practice, evaluated covariance data have only recently become available in the ENDF, and those are still preliminary and sparse. Hence, most uncertainty analyses to date have by necessity used ad-hoc covariance data, most of which contain no covariances among partial cross-sections. From the outset it is clear that the surface has just been scratched in uncertainty analysis and, to extend the metaphor, the cutting edge is now the covariance evaluation efforts.

II. SENSITIVITY AND UNCERTAINTY THEORY

Cross-section sensitivity theory has been derived by various authors from several points of view. Here the approaches of Refs. 10, 18, and 19 are eclectically synthesized for an exposition ending with a transparent parallelism to the actual computational procedure. Secondary energy and angular distribution sensitivity theory discussions follow the approach of Refs. 4 and 5.

A. Cross Sections

Given a cross-section uncertainty, $\Delta\Sigma$, the objective is to determine the uncertainty, ΔR, in a selected response, R, where R is a linear functional of the flux $\phi(\vec{\xi})$. In general, we will deal with the phase space of the Boltzmann equation,

$$\vec{\xi} = (\vec{r},\vec{\Omega},E) \tag{1}$$

in the conventional notation.

Concentrating on a set of multigroup cross-section data $\{\Sigma_i\}$, we seek an expression for the standard deviation of R, which we denote ΔR, in terms of the known covariances of the $\{\Sigma_i\}$. First, we note that R is defined by

$$R = \langle \phi, \rho \rangle \ , \tag{2}$$

where ρ is a given response function, and the inner-product notation $\langle , \rangle$ represents integration over the phase space $\vec{\xi}$. Also, the forward and adjoint Boltzmann equations can be written conveniently in operator notation as

$$L\phi = S \tag{3}$$

$$L^*\phi^* = \rho \ , \tag{4}$$

where L and L* are the respective transport operators, S is the inhomogeneous source term, and $\rho(\xi)$ is the response function of interest (i.e., the adjoint source). Then from well-known variational principles it can be shown that for $R = \langle \phi, \rho \rangle = \langle \phi, L^*\phi^* \rangle$,

$$\delta R = \langle \phi, \delta\rho \rangle - \langle \phi, \delta L^*\phi^* \rangle + O^2 \ . \tag{5}$$

Then if L_i is the portion of the operator containing Σ_i, by the linearity of L we can write[10,18]

$$\frac{\partial R/R}{\partial \Sigma_i/\Sigma_i} = \frac{\langle \phi, \rho \rangle_i}{R} - \frac{\langle \phi, L_i^*\phi^* \rangle_i}{R} \ , \tag{6}$$

where the first term on the right is a direct effect of a change in the response function, and is nonzero only if the response function depends directly on Σ_i (e.g., if ρ is a linear function of Σ_i). In practice the two terms are treated separately because only the second term involves any complexity. Note that Eq. (6) involves integration over all phase space, except the variable E when i denotes an energy group. By convention the energy variable is usually kept explicit and a differential (with respect to lethargy) *sensitivity profile* is defined as follows:

$$P'_{\Sigma_i} \triangleq - \frac{\partial(\ell n R)}{\partial(\ell n \Sigma_i) d(\ell n E)} = \frac{\partial R/R}{\frac{\partial \Sigma_i}{\Sigma_i} du} \ , \tag{7}$$

or

$$P'_{\Sigma_i} \triangleq - \frac{\langle \phi, L_i^*\phi^* \rangle_i}{R \Delta u_i} \tag{8}$$

when i denotes an energy group of lethargy width Δu_i. An important point to keep in mind, however, is that in the theory leading to Eq. (6), the subscript i can denote any partition of the transport operator (e.g., into partial cross-sections), not just an energy-group partition. Thus, P_{Σ_i} has a supressed index which in normal practice represents the partial cross-section, while i represents an energy group. Further, the domain of phase space is often subdivided so as to determine sensitivity profiles for individual material zones, for example. In fact, the definition of a sensitivity profile as in Eq. (8) can follow naturally from a differential sensitivity profile given by

$$P_{\Sigma_i}(\vec{\xi}) = - \frac{\partial(\ell n R)}{\partial(\ell n \Sigma_i) d\vec{\xi}} = \frac{\phi L_i^*\phi^*}{R} \ . \tag{9}$$

Returning now to the calculation of ΔR, which is defined as the positive square root

$$\Delta R \triangleq [E\{\delta R^2\}]^{1/2} \equiv [\mathrm{Var}(R)]^{1/2} \ , \tag{10}$$

where $E\{\ \}$ denotes an expectation value, we formally can write

$$\mathrm{Var}(R) = E\left\{ \sum_{i,j} \frac{\partial R}{\partial \Sigma_i} \delta\Sigma_i \frac{\partial R}{\partial \Sigma_j} \delta\Sigma_j \right\} \ , \tag{11}$$

where we accept the assumptions of linear perturbation theory; i.e.,

$$\delta R = \sum_i \frac{\partial R}{\partial \Sigma_i} \delta \Sigma_i \ . \tag{12}$$

Equation (11) can then be written

$$\mathrm{Var}(R) = \sum_{i,j} \frac{\partial R}{\partial \Sigma_i} \frac{\partial R}{\partial \Sigma_j} E\{\delta \Sigma_i \delta \Sigma_j\} \ , \tag{13}$$

where $E\{\delta \Sigma_i \delta \Sigma_j\}$ is commonly called the covariance or dispersion matrix for the set $\{\Sigma_i\}$. Dividing Eq. (13) by R^2 yields

$$\left(\frac{\Delta R}{R}\right)^2 = \sum_{i,j} P_{\Sigma_i} P_{\Sigma_j} \left[\frac{\mathrm{Cov}(\Sigma_i, \Sigma_j)}{\Sigma_i \Sigma_j}\right], \tag{14}$$

where $P_{\Sigma_i} = \Delta u_i P'_{\Sigma_i}$. For compactness we define a sensitivity profile vector

$$\underline{P} = [P_{\Sigma_i}] \tag{15}$$

and a relative covariance matrix

$$\underline{C} = \left[\frac{\mathrm{Cov}(\Sigma_i, \Sigma_j)}{\Sigma_i \Sigma_j}\right] \tag{16}$$

Then

$$\left(\frac{\Delta R}{R}\right)^2 = \underline{P}\ \underline{C}\ \underline{P}^t \ , \tag{17}$$

and the quantity of final interest, as computed by multigroup sensitivity and uncertainty analysis computer codes, is the relative standard deviation of the response,

$$\frac{\Delta R}{R} = (\underline{P}\ \underline{C}\ \underline{P}^t)^{1/2} \ . \tag{18}$$

The problem is clearly separated into a design-dependent vector $\underline{P}$, and a cross-section covariance matrix $\underline{C}$ which is dependent only on the data.

Of interest for preliminary scoping studies is the integral sensitivity, defined by

$$S_\Sigma = \sum_i P_{\Sigma_i} \ . \tag{19}$$

The integral sensitivity can be interpreted as the fractional change in a response from simultaneous unit fractional increases in all Σ_i; viz, a logarithmic derivative.

B. Secondary Energy and Angular Distributions

For brevity we will consider only secondary-energy-distribution (SED) sensitivity theory; the development for secondary angular distributions is directly analogous. Gerstl observed[4,5] that if one looks at the adjoint parallel to the computation of cross-section sensitivity, an SED sensitivity immediately results.

Starting with the adjoint expression for R,

$$R = \langle \phi^*, S \rangle$$

$$= \langle \phi^*, L\phi \rangle \ , \tag{20}$$

one can define a quantity

$$P^{SED}_{\Sigma^i_{E',E}} \triangleq \frac{\langle \phi^*, L_i \phi \rangle_{E',E}}{R} , \tag{21}$$

where i represents a specific transfer matrix component in the scattering-in integral of the transport operator (e.g.; i = elastic or i = n,2n) and $\langle , \rangle_{E',E}$ denotes integration over all phase space except E' and E. Writing out Eq. (21) explicitly gives

$$P^{SED}_{\Sigma^i_{E',E}} = \frac{1}{R}\int d\vec{r} \int d\vec{\Omega} \int d\vec{\Omega}' \phi^*(\vec{r},\vec{\Omega},E)\Sigma^i(\vec{r},\vec{\Omega}'\rightarrow\vec{\Omega},E'\rightarrow E)\phi(\vec{r},\vec{\Omega}',E') . \tag{22}$$

Equation (22) can be interpreted physically in complete analogy to P_{Σ_i} in Eq. (8) as the percent change in R due to a unit percent change in Σ^i. In a multigroup representation a two-dimensional array results, where the incident energy E'ϵg' is considered as a parameter. In other words, for each incident energy group, g', a sensitivity profile is computed as a function of the secondary neutron energy E. Integrating Eq. (22) over E'ϵ g', we can write

$$P^{SED}_{\Sigma^i_{g',g}} (E \epsilon g) = \frac{\partial R/R}{\partial \Sigma^i_{g'\rightarrow g} / \Sigma^i_{g'\rightarrow g}} , \tag{23}$$

as the SED sensitivity profile for incident neutrons in group g' as a function of secondary energy group g. These SED sensitivity profiles are always non-negative because they include no loss term. Gerstl[4] gives multigroup discrete-ordinates equations for $P^{SED}_{\Sigma^i_{g',g}}$ and shows representative plots of $P^{SED}_{\Sigma^i_{g'}}/\Delta u_g \Delta u_{g'}$, the doubly-differential SED sensitivity profiles, where g' is a parameter and E is the independent variable.

In order to provide a manageable framework for applying the above formalism in practice, Gerstl defines integral SED sensitivities in analogy to Eq. (19), but with an added concept to characterize the secondary energy distribution. After defining a median-energy group g_m as that group into which the median energy of the secondary energy distribution falls, the distribution itself is divided into a low-energy ("cold") and high-energy ("hot") portion. The integral sensitivity

$$S^{SED}_{g'} = \sum_{g=1}^{g_m} P^{SED}_{g',g} - \sum_{g=g_m+1}^{G} P^{SED}_{g',g} \begin{cases} > 0 \Rightarrow \text{HOT} \\ \leq 0 \Rightarrow \text{COLD} \end{cases} \tag{24}$$

reduces the SED sensitivity to one integral parameter which is "hot" or "cold" depending upon whether $S^{SED}_{g'}$ is positive or negative. That is, $S^{SED}_{g'}$ is a quantitative measure of how much more sensitive the response is to the "hot" secondary neutrons than to the "cold" ones.

Quantification of the uncertainty, $\Delta R/R$, resulting from SED uncertainties, proceeds in parallel to that for cross sections. First, one can define a fraction, f, by which the hot portion of the spectrum is increased and the cold portion correspondingly decreased; i.e.,

$$\frac{\delta\sigma_{g'\rightarrow g}}{\sigma_{g'\rightarrow g}} = \alpha_m f_{g'} \qquad \alpha_m = \begin{cases} +1 , & g \leq g_m \\ -1 , & g > g_m \end{cases} . \tag{25}$$

Formally, one can then write the variance of the response as[4]

$$\left(\frac{\Delta R}{R}\right)^2_{SED} = \sum_{i,j} S^{SED}_i S^{SED}_j \mathrm{Cov}(f_i, f_j) . \tag{26}$$

Of more immediate practical interest is the change in response associated with an estimated change in an SED,

$$\left(\frac{\delta R}{R}\right)_{SED} = \sum_{g'} S^{SED}_{g'} f_{g'} . \qquad (27)$$

III. SELECTED RESULTS FROM SENSITIVITY STUDIES

As is noted in one of the first comprehensive sensitivity and uncertainty analysis for a fusion reactor,[13,18] there are three essential steps to providing a rational basis for cross-section measurement or evaluation priorities; viz, 1) specifying the accuracy required in predicting important nuclear design parameters, 2) determining the sensitivity of these nuclear design parameters to selected cross sections, and 3) making quantitative estimates of the uncertainty of currently available cross-section data (i.e., covariance data). A final step, the performing of an uncertainty analysis, is of course implied. The first step is largely outside the domain of sensitivity analysis, but is an extremely important interface with the design project that must be initiated prior to commencement of the sensitivity analysis. Once the accuracy criteria are set, the sensitivity analysis can begin if a preliminary design model exists. Due to the large number of cross-section data needed for fusion reactor nucleonics calculations, it is clear that complete covariance data cannot be provided in a short time frame. Perhaps even more difficult a task is improving, within a short time frame, data which are found to be deficient. Thus, the initial sensitivities determined for a preliminary design can be used to semiquantitatively limit the scope of subsequent uncertainty analysis. That is, at this time in the evolution of uncertainty analysis the preliminary sensitivity studies guide the assignment of priorities for covariance data evaluations. In the future, when extensive covariance files are available in ENDF, the sensitivity and uncertainty analyses may be performed contiguously in time, but such is far from the case today.

The following review illustrates the methodology used for sensitivity studies in several cases - the TFTR, EPR, and NUWMAK designs. A detailed discussion is given for the TFTR, an experimental device now under construction. Then the sensitivity of two EPR designs are discussed and summarized. Although the EPR design studies were superseded by reactor concepts called TNS, which were subsequently superseded by present design studies of a fusion Engineering Test Facility (ETF), the resulting cross-section requirements are still mostly relevant.

A. TFTR

The first step in performing a sensitivity analysis is selection of a nuclear design model, which includes the material zones in which responses of interest are to be computed. A one-dimensional computational model used for TFTR nucleonics calculations is shown in Fig. 1. Since the main objective of the TFTR is to demonstrate the scientific feasibility of a tokamak fusion reactor, it is not required to breed tritium, and therefore does not employ a lithium blanket. The reactor is expected to operate in a pulsed mode, yielding a maximum of 1 000 pulses per year and generating a maximum neutron fluence of 1.4×10^{19} fusion neutrons per m^2 per year on the first wall.[20] Due to this low neutron fluence, radiation damage or nuclear heating problems are not of major concern. However, the activation of magnet coils, structural materials, and instruments is considered a major nucleonics problem area; in particular, the generation of long-lived radioactive isotopes. Therefore, and for biological shielding reasons, a radiation shield is provided as close to the plasma as possible. In cooperation with Princeton and Westinghouse, ten threshold activation reactions in the structural material (zones 9 and 11 in Fig. 1) and the main copper coil (zone 10 in Fig. 1) were selected as important nuclear design parameters of interest. Our objective was to estimate the uncertainties introduced in the calculation of these activation rates due to estimated errors in the neutron cross sections of the system. Of particular interest are uncertainties in the cross sections of the shield zone 7, which consists of a lead-borated polyethylene, and uncertainties in the activation cross sections themselves.

In order to calculate the sensitivity profiles P_{Σ_i} and $P_{\Sigma_i^R}$ according to Eq. (6), where Σ_i^R is the ρ_i of Eq. (6), we performed a forward transport calculation for the TFTR model of Fig. 1 and an adjoint calculation for each of the ten activation reactions considered, thus determining the angular fluxes ϕ and ϕ^*. All transport calculations were performed with the one-dimensional S_n code DTF-IV in an S_8 approximation, using 20-group P_3 neutron cross sections. This cross-section set covers neutron energies between 2.02 and 14.92 MeV, which is sufficient for the activation reactions considered. Cross sections and covariance data for the activation reactions were evaluated at LASL.[21] The angular fluxes

φ and ϕ^* from the transport calculations were then used in the LASL sensitivity code SENSIT-1D to evaluate Eqs. (6) and (19), and to plot the sensitivity profiles of interest.

Integral sensitivities of all ten activation reactions to all significant transport cross sections in the TFTR were calculated and found to be all negative, indicating that an increase in such cross sections would cause the respective activation rate to decrease. The largest integral sensitivity found is that of ^{65}Cu $(n,p)^{65}$Ni to the copper cross sections, which indicates that a 1% increase in the total cross section of copper would decrease the ^{65}Ni production in the coil by 2.05%.

Since explicit covariance matrices could be produced for only a limited number of partial cross sections (called "transport" cross sections in this analysis to distinguish them from the activation cross-section used as a response function) and for all activation cross sections, it was necessary to use upper limit estimates for many "transport" cross-section errors, $(\Delta\Sigma/\Sigma)_{max}$. Upper limit uncertainties are then computed by

$$\left(\frac{\Delta R}{R}\right)_{max} = \hat{S}_{\Sigma}\left(\frac{\Delta\Sigma}{\Sigma}\right)_{max} , \tag{28}$$

where

$$\hat{S}_{\Sigma} = \sum_i |P_{\Sigma_i}| . \tag{29}$$

Table I gives the results of applying Eqs. (14), (28), and (29) for two reactions of interest, denoted

$$R_1: \ ^{54}Fe(n,p)^{54}Mn$$

and

$$R_{10}: \ ^{65}Cu(n,p)^{65}Ni .$$

In order to obtain the predicted response uncertainties in each of the ten activation rates due to the cross-section error estimates, it was assumed that the cross-section errors are uncorrelated among the partial cross-sections and materials listed in Table I; i.e.,

$$\frac{\Delta R_i}{R_i} = \left[\sum_k \left(\frac{\Delta R_i}{R}\right)_k^2\right]^{1/2} , \tag{30}$$

where k denotes a particular partial cross section and material. Table II shows the results of this quadratic combination of errors, as well as those due to the response function (activation cross section) errors, $\Delta\Sigma_i^R$. The last two colums in Table II are the result of a further quadratic combination of the "transport" and activation cross-section errors. Note that the final uncertainty in reaction rates is due overwhelmingly to estimated "transport" cross-section errors, primarily because of the conservatism inherent in the calculation of $(\Delta R/R)_{max}$ via Eq. (28). In Table II the zone numbers are abbreviated as, for example, Z9 for zone 9. Also Al was treated as an alternative to steel in Z9 and Z11.

Having estimates of the reaction rate uncertainties, the question then is whether these are within acceptable bounds. However, a nuclear designer is not concerned with activation rates, but rather with biological dose-equivalent rates. Thus, in conjunction with the designers, a criterion was established that the maximum allowable uncertainty (standard deviation) in personnel radiation exposure rates should be 50%. The absolute reaction rates were then used to compute exposure rates, E, shielded and unshielded, along with their corresponding uncertainties. Shielding was specified to satisfy the designers' criteria:

$$E < \begin{cases} 100 \text{ mrem/h at 2 h after 1 pulse} \\ \\ 10 \text{ mrem/h at 1 d after 1 y operation} . \end{cases} \tag{31}$$

Table III shows the results of the analysis, where the ΔE_i are calculated analogously to ΔR_i in Eq. (30). However, in summing uncertainties ΔE_i over all indivicual isotopes i, care must be taken to observe possible correlations. First, all "transport" cross-section errors were assumed to be uncorrelated with all activation cross-section errors, so the ΔE_i can be computed by quadratic combination of these errors. But the "transport" cross-section errors generate an error in the flux ϕ used to calculate the reaction rates R_i. Clearly then the uncertainties in the R_i's due to "transport" cross-section errors are fully correlated and should be summed linearly over i. Further, it appears reasonable to assume that the activation cross-section (response function) errors are totally uncorrelated, because they are in general independently measured and evaluated. The total uncertainty, ΔE, from these considerations can be written

$$\Delta E = \left\{ \left[\sum_i E_i \left(\frac{\Delta R_i^{trans}}{R_i} \right) \right]^2 + \sum_i E_i^2 \left(\frac{\Delta R_i^{act}}{R_i} \right)^2 \right\}^{1/2} . \qquad (32)$$

In conclusion, the uncertainty in the TFTR dose rates is 41.4% for the most stringent exposure rate criteria (10 mrem/h at 1 d after 1 y operation) and 49.3% for the less stringent criteria, as can be seen in the bottom line of Table III. These values just barely meet the allowable criterion of 50%, but have a known conservatism in many of the $(\Delta\Sigma/\Sigma)_{max}$ estimates. However, if the allowable uncertainty criterion had been more stringent, the uncertainty analysis could have been traced backward from the largest contributors to ΔE in Table III (e.g., ^{58}Co and ^{54}Mn) to their production reactions. An examination of the sensitivity profiles for the production reactions and the corresponding covariance data would then give insight into which reaction cross sections and energy ranges are potential candidates for additional measurement or evaluation.

B. EPR, TNS, etc.

After no unacceptable cross-section uncertainties were found in the TFTR study, attention was turned to a possible first generation of power producing reactors, the EPR designs. The EPR designs extant, as well as later conceptual studies of a TNS or Ignition Test Reactor (ITR), are generically similar in many respects. For example, they have superconducting toroidal field (TF) coils in which several key response functions are of interest. Also, iron (or stainless steel), borated hydrogenous materials, or B_4C are used for shielding the TF coils.[6,16,17]

For the LASL assessment task,[16,17] we chose the EPR design described in Ref. 22 and in private communications. The design has two shield assemblies, denoted "inner" and "outer". The inner shield refers to a segment of shielding toward the toroidal axis. Figure 2 shows a one-dimensional model based upon a radial traverse from the poloidal axis (plasma centerline) through the inner shield. The thinner inner shield is of effective but costly stainless steel/B_4C, while the thicker outer shield is composed largely of less costly lead mortar. The technical basis for alternative shields is in magnetic field profile considerations. With the D-shaped toroidal field (TF) coils, there exists a relatively large space for the outer shield, whereas the inner shield must be as thin as possible.

At this point we consider the general approach used in the EPR data assessment. First, a broad-ranging sensitivity study was performed simply using the total, scattering (matrix) and absorption cross sections from the transport code cross-section sets. These included neutron interaction, gamma-ray production, and gamma-ray scattering matrices. From the large mass of these survey calculations, which are automated in the LASL system,[17] we then isolated materials, partial cross sections and energy regions of potential interest. This latter step is greatly assisted by computing integral sensitivities. After a semiquantitative review of the germane cross-section errors, we chose a manageable number of potentially important materials and partial cross sections for more detailed error evaluation. For these we processed available covariance data into multigroup form.

Cross-section covariance data were obtained by processing preliminary ENDF/B-V data into thirty energy groups (cf. Ref. 23 for group structure) with the NJOY multigroup processing code. The ENDF/B-V data are still preliminary at this date, so the multigroup covariance matrices are subject to change. Many errors (mistakes) were discovered and corrected in the processing of the ENDF/B-V covariance data. Several deficiencies still exist in ENDF/B-V ; e.g., no covariance data exist for Cu, and such data for ^{10}B extend only up to 1.02 MeV. The latter deficiency is not significant for the EPR analysis,[6] however, because the important (sensitive) energy range for ^{10}B lies mostly from approximately 10 keV to 1 MeV. In order to perform a preliminary uncertainty analysis for the EPR and TNS, the covariance data

for Cr were adapted as an approximation for the Cu data. Table IV lists those 30-group covariance matrices currently available.[24]

Because of the thinner inner shield, radiation effects in the inner TF coils are more critical[22] than in the outer TF coils. However, for access during maintenance the outer structure and TF coil activation are important, as opposed to the inner. Thus, for our analysis we chose four radiation effects in the inner TFC, and activation of the stainless steel outer dewar. Specifically, we considered:

INNER SHIELD: 1) neutron and gamma-ray heating in the TF coil superconductor, 2) neutron and gamma-ray dose to the MYLAR insulation in the TF coils, 3) displacements per atom (dpa) in the Cu matrix of the TF coils, and 4) transmutation of the Cu matrix.

OUTER SHIELD: 1) activation of the stainless steel (SS) dewar [e.g., $^{58}Ni(n,p)^{58}Co$ or $^{56}Fe(n,p)^{56}Mn$].

Details of all the response functions, as well as sensitivites, etc., are presented in Ref. 6. In this paper only selected sample results are presented.

As a sample case, let us consider the total neutron and gamma-ray heating in the inner TF coil. Table V shows theintegral sensitivities, Eq. (19), for this response, to SS total cross sections. From this table we find the region(s) in Fig. 2 which contribute most to the sensitivity. It is worth noting that these data also give insight into the sensitivity of the response to design alterations in these regions. From Table V it is clear that the blanket SS regions 6-8 are most important. Also, it can be seen that Fe is the largest contributor to the integral sensitivities, regardless of which region is considered.

Narrowing our example further we show in Table VI the component sensitivities for Fe in regions 6-8. Here the sensitivity has been divided into the gain term and loss term (cf. Ref. 18, App. B for details)

$$P_{\Sigma_i} = -P_{\Sigma^{tot}_{i,loss}} + P_{\Sigma^{scat}_{i,gain}} .$$

In this case most of the net integral sensitivity is clearly due to the neutron scattering cross section. Thus, the uncertainty analysis should concentrate especially on Fe, and in particular on the scattering cross sections.

A representative sensitivity profile is shown in Fig. 3, where again the sensitivity of the TF coil heating to the Fe scattering cross section was selected. Notice the high sensitivity in the top two groups, with a subsidary peak below 1 MeV. This general shape is characteristic of all the sensitivity profiles, for all responses and all materials pertaining to this EPR design.

Referring again to Table VI, the low sensitivity to the gamma-ray production cross section, $\Sigma_{(n\to\gamma)}$, is caused by the relatively short mean free path of the gamma-rays in SS. However, the sensitivity increases monotonically as the region approaches the TF coil.

Turning now to the B_4C component of the shield, Table VII presents integral sensitivity results comparable to those of Table V for SS. Here we see that the sensitivity is highest for the outboard regions, where the neutron spectrum is softened somewhat. However, the spatial variation is not nearly as strong as for Fe (cf. Table V). Also, the ^{10}B component of the B_4C does not overwhelmingly dominate the sensitivity as does Fe in SS. As would be expected, the net integral sensitivity is in all cases negative, because almost any interaction decreases the probability of a neutron's transmission to the TF coil.

Sensitivity profiles for the B and C cross sections show the same general shape as those for Fe (Fig. 3), with a peak in the top group and another peak in the 100 keV-1 MeV region. For ^{10}B, however, the sensitivity to the total cross section is of comparable magnitude in the two peaks, and the lower peak is much broader. This high sensitivity at the lower energy peak is due in part to the neutron spectrum, which shows this same peak at all positions in the shield regions.[10-18] One can conclude that even though these lower energy neutrons have lower transmission probabilities to the TF coil, they are so prevalent in the spectrum as to be a major contributor to the neutron and gamma-ray flux reaching the TF coil.

As a final example from our detailed sensitivity analysis[6] of the EPR, consider the sensitivity of heating in the TF coils to the cross sections in the TF coil region itself. The response here is in the inboard edge (first mesh interval) of the TF coil, while the sensitivity is to cross sections in the entire region 24. The analysis shows a very low sensitivity to all neutron cross sections except for Cu. This is to be expected because interactions in the TF coil itself do not significantly alter the probability of a neutron contributing to heating at the

inboard edge of the coil. Although it is of somewhat academic interest (because of the precision with which gamma-ray interaction cross sections are known), a relatively high negative sensitivity to Cu gamma-ray interaction cross section is as expected.

Several major conclusions were reached in the sensitivity and uncertainty analysis for an EPR. First, the wide ranging survey calculations, using transport-code cross sections, have provided a rapid and thorough coverage of all materials and regions of potential interest. This has proven to be an effective way of eliminating the need for further analyses of many partial cross-section sensitivities. From a pragmatic viewpoint, these partials are of interest only if they provide significant contributions to the total sensitivity, and have significant errors associated with them.

The complete sensitivity analysis[6] indicates that the scattering cross sections of Fe and Cu, along with the absorption cross sections of the ^{10}B in B_4C, are the most significant contributors to the integral sensitivities of the responses considered. Of somewhat lesser importance were the scattering cross sections of H, C, and Pb.

A similar study[16] for an alternative EPR design concentrated on sensitivities to C and Fe partial cross sections. The integral sensitivities of TF coil heating to Fe and SS total cross sections, as an example, are quite similar for the two different designs; viz, -7.55 from Ref. 16 vs -7.375 in Table V. Using preliminary ENDF/B data for C covariances, the authors of Ref. 16 found $\Delta R/R$ to be approximately 2% for all three responses they considered. On the other hand, they assumed $\Delta\Sigma_i$ values for several partial cross sections of Fe that, along with assumed correlation information, gave $\Delta R/R$ values of 99 to 110% (testing the limits of applicability of linear perturbation theory). Although some of the assumed covariances for Fe leave a wide latitude for revision as newer data are incorporated, the uncertainties in responses will probably remain appreciable. No definitive design criteria have been set for the various response, but uncertainties of approximately 100% are in most cases almost certainly unacceptable. Values for acceptable nuclear heating and dpa uncertainties in the TF coils are more likley to be in the 10-20% range,[25] so clearly Fe is a prime candidate for further uncertainty analysis.

C. NUWMAK

Recently a sensitivity and uncertainty analysis has been reported[19] for a conceptual commercial power reactor design, the NUWMAK. A schematic drawing of the reactor poloidal cross section is shown in Fig. 4, which is reproduced from Ref. (19). The reactor is a moderately sized tokamak power reactor[26] which has evolved from a series of comprehensive conceptual design studies at the University of Wisconsin. An eutectic $Li_{62}Pb_{38}$ compound is used in the blanket for breeding and thermal inertia purposes. Also, different inner and outer shields are used, for the same reasons as mentioned above for an EPR design.

Referring again to Fig. 4, several features of the design are germane to the sensitivity analysis. Unlike the TFTR/EPR/TNS designs, the NUWMAK employs low-activation materials (H, B, C, Li, Ti, Pb) for all regions except the inner W shield. Also, 90% of the tritium breeding was found[19] to be contributed by $^6Li(n,t)^4He$ reactions. Another very pertinent result of the design study was that the most restrictive criterion for the inner shield was the resistivity change of the TF coil Al stabilizer, caused by the Al displacement rate of 2×10^{-6} dpa/y. The inner shield is only 1.05-m thick and must attenuate the neutron intensity by a factor greater than 10^8.

The sensitivity study in Ref. (19) goes beyond the determination of response uncertainties, to address the cost/benefit analysis of integral measurements proposed to reduce the uncertainties. The theory and results presented in the latter area, although they provide a concinnity to uncertainty methods, are beyond the scope of this review.

Sensitivity analysis of NUWMAK used the same methodology as discussed in Secs. III.A and III.B, employing the ANISN one-dimensional discrete-ordinates code for S_4P_3 neutron transport calculations, and SWANLAKE for the sensitivity calculations. Wu and Maynard chose six key responses for analysis, as shown in Table VIII. They caution the reader to interpret the results carefully, because the table only includes the second, or indirect term in Eq. (6) of Sec. II.A. For example, the large negative sensitivity of R_1 to the ^6Li total cross section (-0.865) is counterbalanced by a +0.9 sensitivity from the direct effect on the $^6Li(n,t)^4He$ response function, for a net sensitivity of only +0.035.

The responses of most practical interest are R_5 and R_6 in Table VIII, which have the higher integral sensitivities and, in the case of R_6, is design limiting. It was observed that the (n,2n) cross sections of W and Pb are the dominant contributors to the sensitivity, with all of the sensitivity concentrated in the

higher energy groups and peaking in the top group. In performing an uncertainty analysis, however, data covariances for only four applicable materials - ^{6}Li, ^{10}B, ^{12}C, Pb - were available in ENDF/B-V (cf. Table IV). Therefore, the authors assumed a 10% uncorrelated uncertainty at all energies for ^{7}Li, ^{11}B, Ti and W. Their uncertainty results are presented in Table IX, where the uncertainties in R_5 and R_6 are overwhelmingly caused by W cross-section uncertainties. Clearly, for this reactor a major improvement in the shield design would result from improved accuracy of the W cross sections. Curiously enough, in discussing cross-section evaluations and measurement priorities, it was surmised[27] that W would also become a "priority 1" material if used for the inner shield of a TNS.

D. CROSS-SECTION REQUIREMENTS ABOVE 14 MeV

In a departure from sensitivity and uncertainty analysis per se, we consider here several aspects of cross-section data above ~ 14 MeV. With two exceptions,[28,29] the author is not aware of any sensitivity studies in this energy region. Reference 28 alludes to a sensitivity study of dose-equivalent through thick shields, to elastic and nonelastic cross sections, but no literature regarding the study is cited. The second study[29] was performed for D-Be source neutrons in a medical application, where sensitivity methods in LASS[17] were used to select an optimum group structure.

The overwhelming interest in cross sections above ~ 14 MeV presently seems to be associated with the Fusion Materials Irradiation Test (FMIT) Facility design project. This facility will have a deuteron beam of ~ 35 MeV incident on Li, with a resulting spectrum at 0° which peaks at ~ 14 MeV and has a high-energy tail to ~ 50 MeV. Although the spectrum is roughly bell-shaped, experiments have verified a knee in the curve at ~ 35 MeV, producing more neutrons than originally expected in the energy region where the neutrons are most penetrating. In a discussion of the bulk shielding for the FMIT facility, Carter and Morford[28] emphasize that the most severe problem in the shield design is uncertainties in the cross-section data base $\gtrsim$ 14 MeV.

As mentioned in a previous paper,[27] there has not been much technological activity requiring neutronics data at $\gtrsim$ 14 MeV. A lack of demand coupled with the lack of widely available monoenergetic neutron sources has restricted the amount of such data available. The FMIT facility has brought forth the importance of remedying this situation, with concomitant demands for careful selection of priorities. It is unlikely that the cross-section needs for shielding, activation, spectrum tailoring, radiation damage, and dosimetry can all be met by the projected operation date of the FMIT. Satisfying even the minimum needs will require a well planned program with strict priorities, concentrating on nuclear model calculations to fulfill most requirements.

Any listing of relative importance of particular nuclides and reaction types must be associated with neutronics applications of those data. For example, in studies of radiation-induced damage, the fact that important damage cross sections are only weakly energy dependent above ~ 14 MeV makes it likely that most damage will be caused by neutrons in the 14-25 MeV region, where most of the > 14 MeV source neutrons originate. Similarly, the dosimetry reactions will need to be determined with highest accuracy in this 14-25 MeV region.

In contrast to damage and dosimetry reactions, cross-section data in the 30-50 MeV region are the most important for bulk shielding calcualtions. It was determined[28] for the FMIT facility, where concrete shields 3 to 4 metres thick were analyzed, that ~ 90% and ~ 70% of the dose-equivalent are due to source neutrons with energies greater than 30 MeV and 40 MeV, respectively. A removal cross section was then defined as the sum of the nonelastic cross section and that portion of the elastic cross section scattering neutrons beyond 25°. It is because this removal cross section is a monotonically decreasing function of energy that the dose-equivalent is dominated by the higher energy neutrons. The authors state[28] that O and Fe are the most important elements in their shield design, and measurements at a few incident energies between 20 and 50 MeV are now being made for these elements.

IV. CONCLUSIONS

The usefulness of sensitivity studies to help define cross-section evaluation and measurements requirements is indisputable. However, much remains to be done before such studies can be made comprehensive and complete. While the theoretical methods and codes are generally adequate for simple one-dimensional reactor models considered heretofore, an extension to multidimensional and complex models is imminently required. In particular, Monte Carlo sensitivity methods promise great advantages in complex geometries, especially the important streaming problems already uncovered in fusion reactor nucleonics. Even more important than methods and codes is the urgent need for extensive covariance data files. Additional large data evaluation requirements are being elicited by the recently developed SED sensitivity

methods, which require some characterization of secondary energy distribution uncertainties, perhaps in the form of the f_g, factors discussed in Sec. II.B.

Results of sensitivity studies to date were summarized in Sec. III, but it is useful to re-emphasize the recurring importance of the Fe cross sections in both fusion reactor and irradiation facility shields. In the case of some inner shields for tokamak reactors, the overwhelming dominance of uncertainties in the W cross sections is clearly seen for responses in the TF coils. The large uncertainties (40-100%) in TF coil responses found for several conceptual reactor designs are understandable in terms of the large attenuations of neutron and gamma-ray fluxes involved - generally > 10^6. Although not reviewed in this paper, a hybrid reactor sensitivity study[1b] showed appreciable integral sensitivities of tritium breeding to ^{238}U and Fe total cross sections; viz, -0.97 and -0.19, respectively. In this case Fe was included only in SS as a 5-mm first wall and as an 8.6 v/o structure in fission and breeding zones. Another study[9] of tritium breeding sensitivity, in this case for a pure fusion reactor, showed fairly low values of sensitivity to ^6Li, ^7Li, and Nb cross sections. This study also presented a comparison of the response uncertainty as computed by both the methods of Sec. II and direct recalculation. As must be expected for total uncertainties in tritium breeding of < 5%, the agreement is very good. A further result of this study, interesting in light of the current questions concerning the $^7Li(n,n't)^4He$ cross section,[30] was that most of the sensitivity is attributable to just that cross section.

A growing interest in D-Li neutron sources for fusion materials irradiation experiments has intensified interest in neutron cross-section data above 14 MeV. Since the status review of these data at a Symposium in May 1977 (cf. Ref. 27), model calculations[28,29] have been used to devise cross sections for shielding analysis of the FMIT facility. For shielding applications the data in the 30-50 MeV range are most significant, analogous to fission reactors where source neutrons of ~ 6-8 MeV dominate for deep penetrations. By contrast, for dosimetry, damage functions, and neutron transport in the target area of the FMIT facility, data in the 14-25 MeV region are expected[27] to be most important.

V. ACKNOWLEDGMENT

The author is pleased to acknowledge many helpful comments by S. A. W. Gerstl and P. G. Young of LASL. Also, the comments of C. W. Maynard of the University of Wisconsin, along with his permission to reproduce figures and tables from a preprint of Wu and Maynard's forthcoming paper, are gratefully acknowledged.

REFERENCES

1a. V. V. Kotov, C. W. Maynard, D. V. Markovskii, and G. E. Shatalov, "Analysis of the Sensitivity of Hybrid Reactor Parameters to Nuclear Data," I. V. KURCHATOV INSTITUTE OF ATOMIC ENERGY report IAE-2817 (English translation LA-TR-78-65 by A. D. Cernicek, Los Alamos Scientific Laboratory.)

1b. Long-Poe Ku and W. G. Price, Jr., "Neutronic Calculations and Cross-Section Sensitivity Analysis of the Livermore Mirror Fusion/Fission Hybrid Reactor Blanket," Princeton Plasma Physics Laboratory report PPPL-1370 (1977).

2. D. W. Muir, "Sensitivity of Neutron Multigroup Cross Sections to Thermal Broadening of the Fusion Peak," Proc. First Topical Meeting on Technology of Controlled Nucl. Fusion, San Diego, CA, 16-18 Apr. 1974, CONF-740402.

3. R. T. Santoro and J. Barish, "Cross-Section Sensitivity of the D-T Fusion Probability and the D-T and T-T Reaction Rates," Oak Ridge National Laboratory report ORNL-TM-4933 (1975).

4. S. A. W. Gerstl, "Sensitivity Profiles for Secondary Energy and Angular Distributions," Proc. Fifth Intl. Conf. on Reactor Shielding, Knoxville, TN, 18-22 Apr. 1976.

5. S. A. W. Gerstl, "Uncertainty Analysis for Secondary Energy Distributions," Proc. RSIC Seminar on Theory and Application of Sensitivity and Uncertainty Analysis, Oak Ridge, TN, 23-24 Aug. 1978.

6. E. L. Simmons, S. A. W. Gerstl, and Donald J. Dudziak, "Cross-Section Sensitivity Analyses for a Tokamak Experimental Power Reactor," Los Alamos Scientific Laboratory report LA-6942-MS (1977).

7. David Leon Prezbindowski, "An Analysis of the Effects of Cross Section Uncertainties on the Multitable S_n Solution of Neutron Transport through Air," Doctoral Dissertation Purdue University (January 1968). Cf. also Trans. Am. Nucl. Soc. 11, 193 (1968).

8 R. Conn and W. M. Stacey, Jr., "Variational Methods for Controlled Thermonuclear Reactor Blanket Studies," Nucl. Fus. 13, 185 (1973).

9. D. E. Bartine, R. G. Alsmiller, Jr., E. M. Oblow, and F. R. Mynatt, "Cross-Section Sensitivity of Breeding Ratio in a Fusion-Reactor Blanket," Nucl. Sci. Eng., 53, 304 (1974).

10. D. E. Bartine, E. M. Oblow, and F. R. Mynatt, "Radiation-Transport Cross-Section Sensitivity Analysis -- A General Approach Illustrated for a Thermonuclear Source in Air," Nucl. Sci. Eng. 55, 147 (1974).

11. S. A. W. Gerstl, "Second-Order Perturbation Theory and its Application to Sensitivity Studies in Shield Design Calculations," Trans. Am. Nucl. Soc. 16, 342 (1973).

12. S. A. W. Gerstl, "Blanket Design and Cross-Section Sensitivity Calculations Based on Perturbation Methods," Proc. First Topical Meeting on Technology of Controlled Nucl. Fusion, San Diego, CA, 16-18 Apr. 1974. (CONF-740402-P2, p. 136).

13. S. A. W. Gerstl, D. J. Dudziak, and D. W. Muir, "Application of Sensitivity Analysis to a Quantitative Assessment of Neutron Cross-Section Requirements for the TFTR: An Interim Report," Los Alamos Scientific Laboratory report LA-6118-MS (1975).

14. R. G. Alsmiller, Jr., R. T. Santoro, J. Barish, and T. A. Gabriel, "Comparison of the Cross-Section Sensitivity of the Tritium Breeding Ratio in Various Fusion Reactor Blankets," Nucl. Sci. Eng. 57, (1975).

15. S. A. W. Gerstl, D. J. Dudziak, and D. W. Muir, "The Application of Sensitivity Analysis to Nuclear Data Assessment," Proc. Specialist's Mtg. on Sensitivity Studies and Shielding Benchmarks, Paris, France, 7-10 Oct. 1975.

16. R. G. Alsmiller, Jr., J. Barish, and C. R. Weisbin, "Uncertainties in Calculated Heating and Radiation Damage in the Toroidal Field Coil of a Tokamak Experimental Power Reactor due to Neutron Cross-Section Errors," Oak Ridge National Laboratory report ORNL/TM-5198 (1976).

17. Donald J. Dudziak, S. A. W. Gerstl, and D. W. Muir, "Application of the Sensitivity and Uncertainty Analysis System LASS to Fusion Reactor Nucleonics," Proc. Specialists' Meeting on Differential and Integral Nuclear Data Requirements for Shielding Calculations, Vienna, Austria, 12-16 Oct. 1976, IAEA-207.

18. S. A. W. Gerstl, Donald J. Dudziak, and D. W. Muir, "Cross-Section Sensitivity and Uncertainty Analysis with Application to a Fusion Reactor," Nucl. Sci. Eng. 62 (1), 137 (1977).

19. T. Wu and C. W. Maynard, "The Application of Uncertainty Analysis in Conceptual Fusion Reactor Design," Proc. RSIC Seminar on Theory and Application of Sensitivity and Uncertainty Analysis, Oak Ridge, TN, 23-24 Aug. 1978.

20. "TCT-Two-Component Torus," joint conceptual design study performed by Princeton Plasma Physics Laboratory and Westinghouse Electric Corp., Vol. III, Sec. 6.1 (1974).

21. D. W. Muir in "Applied Nuclear Data Research and Development Quarterly Progress Report, July 1-Sept. 30, 1974," Los Alamos Scientific Laboratory report LA-5804-PR (1974).

22. M. A. Abdou, "Nuclear Design of the Blanket/Shield System for a Tokamak Experimental Power Reactor," Nucl. Technol. 29, 7 (1976).

23. H. A. Sandmeier, G. E. Hansen, R. E. Seamon, T. J. Hirons, and A. H. Marshall, "Coupled Neutron-Gamma Multigroup-Multitable Cross Sections for 29 Materials Pertinent to Nuclear Weapons Effect Calculations Generated by LASL/TD Division," Los Alamos Scientific Laboratory report LA-5137 (1974).

24. R. J. LaBauve and D. W. Muir, Los Alamos Scientific Laboratory, private communciation (1978).

25. D. J. Dudziak (chairman), "Report of the Sub-group on Fusion Reactors," Proc. Specialists' Meeting on Differential and Integral Nuclear Data Requirements for Shielding Calculations, Vienna, Austria, 12-16 Oct. 1976, IAEA-207.

26. E. T. Cheng and C. W. Maynard, "Nucleonic Design for a Compact Tokamak Fusion Reactor Blanket and Shield," Trans. Am. Nucl. Soc. 30, 73 (1978).

27. Donald J. Dudziak and D. W. Muir, "Review of Magnetic Fusion Energy Neutron Cross-Section Needs: Neutronics Viewpoint," Proc. Symposium on Neutron Cross Sections from 10-40 MeV, Upton, NY, 3-5 May 1977.

28. L. L. Carter and R. J. Morford, "Shielding Calculations for the Fusion Materials Irradiation Test Facility," Trans. Am. Nucl. Soc. 30, 618 (1978).

29. William Bradley Wilson, "Nuclear Data Development and Shield Design for Neutrons Below 60 MeV," Los Alamos Scientific Laboratory report LA-7159-T (1978).

30. Donald J. Dudziak and Gene L. Woodruff, "Nucleonic Aspects of Synfuel Blankets," Los Alamos Scientific Laboratory report LA-7485-MS (1978). (Cf. Addendum on ^{7}Li Cross-Section Uncertainty).

TABLE I

Predicted Uncertainties of Selected Activation Rates R_1 and R_{10} Due to Estimated Errors in Transport Cross Sections Σ

"Perturbed" Transport Cross Sections	Error Estimates: COV[a] or $\left(\frac{\Delta\Sigma}{\Sigma}\right)_{max}$ (%)	Maximum Integral Sensitivity $\hat{S}$ and Predicted Activation Rate Uncertainty $\Delta R/R$ for R_1		for R_{10}	
		$\hat{S}$ (% per %)	$\frac{\Delta R}{R}$ or $\left(\frac{\Delta R}{R}\right)_{max}$ (%)	$\hat{S}$ (% per %)	$\frac{\Delta R}{R}$ or $\left(\frac{\Delta R}{R}\right)_{max}$ (%)
C	25	0.87	21.8	0.66	16.5
C($n,n'3\alpha$)	COV	---	2.4	---	2.2
Pb	25	1.52	38.0	1.12	28.0
Pb(n, $2n$)	COV	---	18.3	---	14.8
O	25	0.47	11.8	0.36	9.0
H	2	1.08	2.2	0.73	1.5
Fe	25	0.70	17.5	0.93	23.3
Fe(n, tot)	COV	---	2.2	---	3.2
Fe(n, abs)	COV	---	0.71	---	1.7
Fe(n,n'cont)	COV	---	4.4	---	7.4
Fe(n, elas)	COV	---	2.5	---	3.7
Fe(n, inel)	COV	---	3.5	---	6.7
Fe(n, $2n$)	COV	---	1.2	---	3.6
Cr	25	0.20	5.0	0.25	6.3
Ni	25	0.12	3.0	0.17	4.3
Mn	25	0.021	0.53	0.027	0.68
Al	25	0.45	11.3	0.62	15.5
Cu	25	0.039	0.98	2.05	51.3
Cu(n, elas)	COV	---	0.12	---	5.0
Cu(n, inel)	COV	---	0.13	---	6.8
Cu(n, $2n$)	COV	---	0.04	---	9.6
Cu(n, tot)	COV	---	0.12	---	5.1
Cu(n, abs)	COV	---	0.04	---	16.8

[a]COV means Complete Covariance Matrix.

TABLE II

Summary of Predicted Uncertainties of Activation Rates R_i Due to Estimated Errors in Activation Cross Sections, COV(Σ_i^R, Σ_j^R), and All Transport Cross-Section Uncertainties

Activation Reaction R_i	$\frac{\Delta R_i}{R_i}$ (%) Due to *Activation* Cross-Section Errors	Due to Transport Cross-Section Errors: Stainless-Steel Structure	Due to Transport Cross-Section Errors: Aluminum Structure	Due to All Cross-Section Errors: Stainless-Steel Structure	Due to All Cross-Section Errors: Aluminum Structure
R_1 = ^{54}Fe(n, p)^{54}Mn in Z9 and Z11	15.7	49.1	---	51.5	---
R_2 = ^{55}Mn(n, $2n$)^{54}Mn in Z9 and Z11	15.6	41.4	---	44.2	---
R_3 = ^{56}Fe(n, p)^{56}Mn in Z9 and Z11	12.8	42.8	---	44.7	---
R_4 = ^{58}Ni(n, p)^{58}Co in Z9 and Z11	20.7	42.6	---	47.4	---
R_5 = ^{27}Al(n, α)^{24}Na in Z9 and Z11	8.7	---	41.0	---	41.8
R_6 = ^{27}Al(n, p)^{27}Mg in Z9 and Z11	5.5	---	44.0	---	44.3
R_7 = ^{63}Cu(n, $2n$)^{62}Cu in Z10	24.3	62.3	59.9	66.9	64.6
R_8 = ^{63}Cu(n, α)^{60}Co in Z10	29.3	63.5	62.8	69.9	69.3
R_9 = ^{65}Cu(n, $2n$)^{64}Cu in Z10	13.4	63.1	60.7	64.5	62.2
R_{10} = ^{65}Cu(n, p)^{65}Ni in Z10	32.6	66.1	63.3	73.7	71.2

TABLE III

Predicted Absolute Uncertainties in Calculated Radiation Exposure Rates Due to All Cross-Section Uncertainties—TFTR Design with Steel Structure

Radionuclide, i	$T_{1/2}$	Production Mechanism	Production Rate, R_i (Atoms per Fusion Neutron)	Exposure Rate $E_i \pm \Delta E_i$ After			
				1 Pulse and 2 h		1 yr and 1 day	
				E_i (rem/h)	ΔE_i (rem/h)	E_i (rem/h)	ΔE_i (rem/h)
^{54}Mn	313 days	^{54}Fe(n, p)	1.35 E-3	7.05 E-4	3.63 E-4	4.38 E-1	2.26 E-1
^{54}Mn	313 days	^{55}Mn(n, $2n$)	4.80 E-4	2.49 E-4	1.10 E-4	1.72 E-1	7.60 E-2
^{56}Mn	2.6 h	^{56}Fe(n, p)	3.32 E-3	5.11 E+0	2.28 E+0	6.31 E-3	2.82 E-3
^{58}Co	71 days	^{58}Ni(n, p)	2.30 E-3	6.16 E-3	2.92 E-3	1.67 E+0	7.92 E-1
^{62}Cu	9.8 min	^{63}Cu(n, $2n$)	9.89 E-3	6.94 E-1	4.64 E-2	<E-10	<E-10
^{60}Co	5.2 yr	^{63}Cu(n, α)	1.03 E-3	2.30 E-4	1.61 E-4	2.19 E-1	1.53 E-1
^{64}Cu	12.7 h	^{65}Cu(n, $2n$)	9.55 E-3	6.66 E-1	4.29 E-1	4.26 E-1	2.75 E-1
^{65}Ni	2.6 h	^{65}Cu(n, p)	2.69 E-4	1.53 E-1	1.13 E-1	1.91 E-4	1.41 E-4
Total exposure rate (unshielded): $E = \sum_i E_i$, ΔE according to Eq. (32)				6.53 rem/h	3.22 rem/h	2.90 rem/h	1.20 rem/h
Total personnel exposure rate (shielded): $(E^P \pm \Delta E^P) = 3.45 \times 10^{-3} (E \pm \Delta E)$				22.5 mrem/h	11.1 mrem/h	10.0 mrem/h	4.14 mrem/h

TABLE IV

Preliminary ENDF/B-V Covariance Data (MF=33) Processed with NJOY Code

MAT	Nuclide	MT-Nos. Processed	Reaction Cross Sections
305	B-10	1,2,107,780,781	Total, elastic (n,α), (n,α_0), and (n,α_1)
306	C	1,2,4,51-68,91,102 104,107	Total, elastic, total inelastic, inelastic levels 1-18, inelastic continuum, (n,γ), (n,d), (n,α)
324	Cr	1,2,3,4,16,17,22,28, 102,103,104,105,106, 107	Total, elastic, nonelastic, total inelastic, (n,2n), (n,3n), (n, n'α), (n,n'p), (n,γ), (n,p), (n,t), (n,d), (n,^{3}He), (n,α)
326	Fe	1,2,3,4,16,22,28,102, 103,104,105,106,107	Total, elastic,nonelastic, total inelastic, (n,2n), (n,n'α), (n,n'p), (n,γ), (n,p), (n,d), (n,t), (n,^{3}He), (n,α)
328	Ni	1,2,4,16,22,28,51-76, 91,102,103,104,107, 111	Total, elastic, total inelastic, (n,2n), (n,n'α), (n,n'p), inelastic levels 1-26, inelastic continuum, (n,γ), (n,p), (n,d), (n,α), (n,2p)
329	Cu	1,2,3,4,16,17,22,28, 102,103,104,106,107	Total, elastic, nonelastic, total inealstic, (n,2n), (n,3n), (n,n'α), (n,n'p), (n,γ), (n,p), (n,d), (n,^{3}He), (n,α)
382	Pb	1,2,3,4,16,17,51,52, 64,102	Total, elastic, nonelastic, total inelastic, (n,2n), (n,3n), inelastic levels 1,2, and 14, (n,α)
1301	Hl	1,2	Total, elastic

TABLE V

Neutron Integral Sensitivity, S_{Σ_T}, of the Inner TF Coil Nuclear Heating Response to the Total Cross Sections of Stainless Steel Components

Component	Region					Total
	6–8	12	14	16	23	
Cr	-0.601	-0.212	-0.188	-0.150	-0.014	-1.168
Mn	-0.103	-0.034	-0.031	-0.026	-0.005	-0.202
Fe	-2.480	-0.868	-0.767	-0.602	-0.058	-4.775
Ni	-0.526	-0.182	-0.164	-0.140	-0.010	-1.032
Mo	-0.091	-0.033	-0.030	-0.024	-0.008	-0.187
TOTAL	-3.801	-1.330	-1.180	-0.944	-0.097	-7.375

TABLE VI

Partial and Net Neutron Integral Sensitivities of the Inner TF Coil Nuclear Heating Response to the Fe Component in Stainless Steel Regions 6–8

Neutron Cross Section, Σ_x	Integral Loss Term	Integral Gain Term	Integral Net, S_{Σ_x}
Σ_a	- 0.17	——	0.17
Σ_s	12.98	10.33	- 2.65
Σ_T	12.81	10.33	- 2.48
$\Sigma_{(n\to\gamma)}$	——	0.014	0.014

TABLE VII

Neutron Integral Sensitivity, S_{Σ_T}, of the Inner TF Coil Nuclear Heating Response to the Total Cross Sections of B_4C Components

Component	Region				Total
	11	13	15	17	
10_B	-0.221	-0.268	-0.375	-0.543	-1.409
C	-0.166	-0.190	-0.243	-0.196	-0.796
TOTAL	-0.387	-0.459	-0.618	-0.739	-2.206

TABLE VIII

Energy-Integrated Relative Sensitivities for NUWMAK

R_1 --- Outer Blanket Breeding Ratio
R_2 --- Outer Blanket Neutron Heating
R_3 --- First Wall Ti dpa Rate
R_4 --- First Wall Ti Gas Production Rate
R_5 --- Neutron Energy Leakage to Inner Magnet
R_6 --- dpa Rate in Al Stabilizer

Cross Section	R_1	R_2	R_3	R_4	R_5	R_6
Ti total	-0.050	-0.079	-0.016	-0.039	-0.349	-0.334
Pb total	0.137	-0.051	0.120	-0.003	-1.598	-1.238
^{12}C total	0.048	-0.024	---	---	-0.633	-0.595
^{10}B total	---	-1.795	---	---	-2.106	-2.094
^{6}Li total	-0.865	-0.652	-0.011	---	-0.025	-0.024
^{7}Li total	-0.011	-0.105	---	0.013	-0.319	-0.303
W total					-5.214	-5.282
Pb(n,2n)	0.115	0.006	0.064	---	-1.078	-0.712
inel. level	0.002	-0.025	-0.024	---	-0.146	-0.154
inel. cont.	-0.022	-0.031	-0.002	---	-0.181	-0.127
elastic	0.040	0.001	0.085	---	-0.181	-0.231
$^{6}Li(n,\alpha)T$	-0.864	-0.644	-0.011	---	-0.001	-0.001
$^{7}Li(n,n'\alpha)T$	-0.036	-0.047	---	-0.007	-0.132	-0.129
elastic	0.023	-0.042	---	0.018	-0.131	-0.119
Ti(n,2n)	0.011	---	0.004	-0.025	-0.097	-0.084
inel. cont.	-0.028	-0.037	-0.017	-0.028	-0.157	-0.152
elastic	0.007	---	0.014	0.018	-0.052	-0.054
W(n,2n)					-4.123	-4.030
inel. cont.					-0.474	-0.622
inel. level					-0.126	-0.143
elastic					-0.451	-0.449

TABLE IX

Relative Uncertainty (%) of the Responses Contributed From the Uncertainties of Total Cross Sections in NUWMAK

Material	$\Delta R/R$ (%)					
	R_i	R_2	R_3	R_4	R_5	R_6
^{6}Li	0.72	0.55	----	0.03	----	----
Pb	0.34	0.10	0.02	0.39	5.02	3.89
^{12}C	0.02	0.02	----	----	1.09	1.78
^{10}B	----	0.39	----	----	----	----
^{7}Li					2.89	2.65
W					42.35	39.86
Ti					2.46	2.14
^{11}B					1.50	1.07
TOTAL $(\sqrt{\Sigma\ \Delta R/R)^2})$	0.80	0.68	0.02	0.39	42.88	40.24

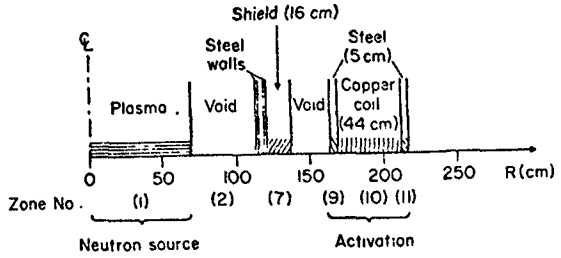

Fig. 1. One-dimensional computational model for TFTR cross-section sensitivity analysis.

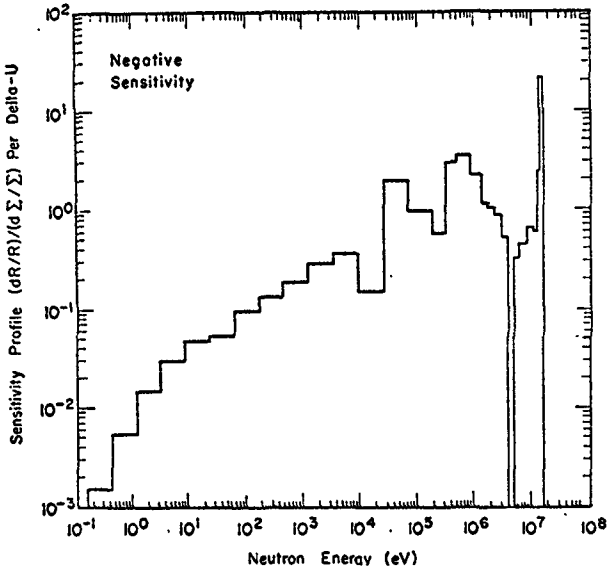

Fig. 3. Sensitivity of the maximum neutron plus gamma-ray heating in the TF coils to all scattering cross sections of Fe.

Region No.	Region Material	Radius (cm)
1	PLASMA	0.0
2	VACUUM	210.0
3	1st WALL S. S.	240.0
4	1st WALL S. S.	241.0
5	1st WALL S. S.	242.0
6	BLANKET S. S.	244.0
7	BLANKET S. S.	254.0
8	BLANKET S. S.	264.0
9	VACUUM	272.0
10	S. S.	273.0
11	B_4C	276.0
12	S. S.	281.0
13	B_4C	291.0
14	S. S.	297.0
15	B_4C	307.0
16	S. S.	315.0
17	B_4C	325.0
18	S. S.	333.0
19	TFC DEWAR S. S.	335.0
20	VACUUM, TUBING, ETC.	337.0
21	THERMAL SHIELD	339.8
22	VACUUM	340.7
23	TFC BOBBIN (S. S.)	343.2
24	TFC	345.7
25	TFC	350.7
26	TFC	355.7
27	TFC	360.7
28	SUPPORT CYLINDER	416.2
29	OHC	440.0
		465.0

Fig. 2. One-dimensional computational model for EPR inner blanket/shield.

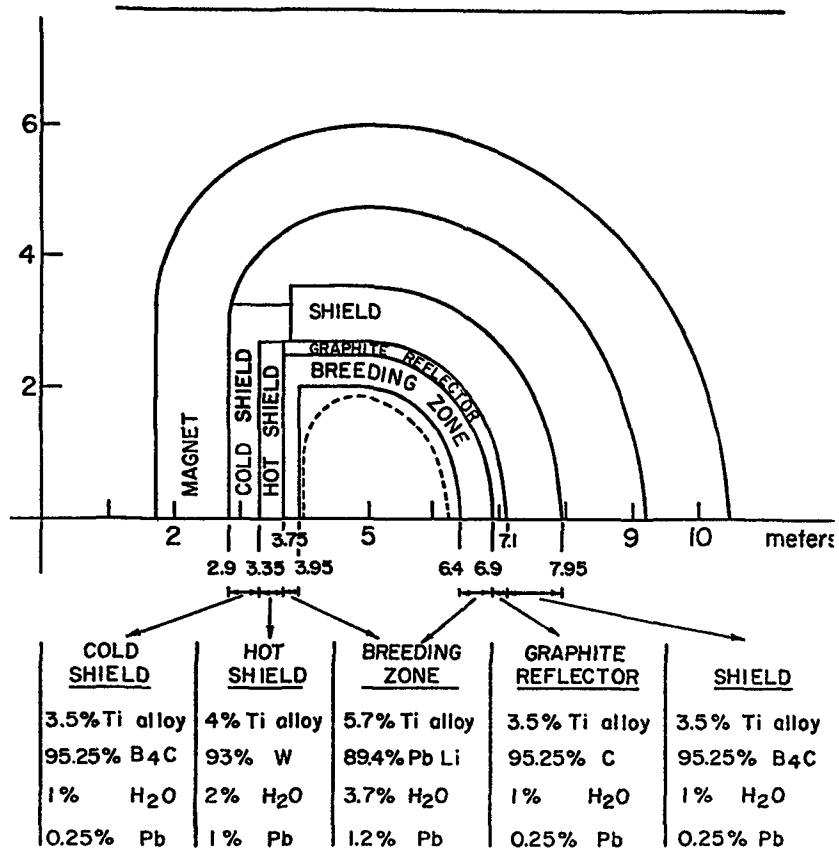

Fig. 4. SCHEMATIC OF THE BLANKET AND SHIELD FOR NUWMAK

THEORETICAL APPROACH TO NUCLEAR DATA REQUIRED FOR FUSION REACTOR CALCULATIONS

AG-159/B2
Review Paper

D. SEELIGER

Technical University, Dresden, GDR

Abstract:
By several examples the performance of some computer codes, based on pre-equilibrium and equilibrium statistical models, is demonstrated. Angular integrated cross sections for neutron induced reactions, which are of interest for the fusion reactor, are well described by the multi-step Hauser-Feshbach code STAPRE. The present situation of angular distribution calculations is discussed.

INTRODUCTION

The near-term fusion reactor is expected to operate on the $T(d,n)^4He$ reaction, which has a maximum neutron energy below 15 MeV. While the energy region of neutron induced reactions below about 6 MeV has been intensively investigated in connection with the fast breeder programmes, the specific area of interest for fusion reactor systems is mainly concentrated within the energy range from 8 to 16 MeV. However, in connection with radiation damage studies at high-intense d - Li sources for special reactions the energy region of interest for fusion research will be extended up to about 40 MeV.
And so, speaking about theoretical approaches to neutron nuclear data for fusion research programmes, we have to consider mainly neutron energies below 20 MeV and have a look also to higher energies.

In this energy region, excluding light nuclei, statistical descriptions of nuclear reaction processes are valid. At present the most succesful theories of that type are equilibrium and pre-equilibrium statistical theories, i.e. evaporation theory, Hauser-Feshbach theory and exciton models. Inrecent years with averaged direct reaction theory calculations a good description of the high energy part of continuous spectra and angular distributions of emitted particles have been obtained also.
In this paper, we describe calculations employing the optical, the pre-equilibrium and statistical models by several examples. At first, some results, obtained with the pre-equilibrium code GLUNE for neutron emission spectra at 14 MeV incident energy and some results of an evaluation for ^{93}Nb + n reactions are presented.

As a next step, results obtained mainly with the Hauser-Feshbach model code STAPRE for reactions Fe + n, in comperison with excisting evaluations, and some results of γ-emission spectra for ^{93}Nb + n and ^{56}Fe + n are briefly presented. Finally, the possibilities of angular distribution calculations of continuous neutron emission spectra are discussed.

NEUTRON EMISSION SPECTRA

A well established way of calculation of angular integrated neutron emission spectra at incident energy around 14 MeV is connected with the combination of the simple phenomenologic exciton model with the classical Weisskopf evaporation theory [1.2].

The physical picture of this type of calculations is the following: After the bombardment of the nucleus by a neutron, the compound system, starting with a small number of degrees of freedom (two particles plus one hole correspond to n= 3 excitons), is gradually transformed into a more complex configuration (for each transition Δ n = 2), until a state of statistical equilibrium is reached, i.e. the state of the compound nucleus. There is a specific probability of the emission of a nucleon from each pre-equilibrium state with n quasiparticles. Every emission will lead to a unit decrease in A and n and to a decrease in the excitation energy. The nucleus (Z, N) will therefore give rise to a nucleus (Z - 1,N) in the case of emission of a proton or (Z , N - 1) in the case of emission of a neutron and so on.

Absolute spectra for both types of nucleons from all intermediate nuclei are calculated as long as the excitation energy does not become less than the nucleon binding energy. The calculations are performed on the basis of the hybrid model [3] , according to which the probability $_nP_x(E)$ of pre-equilibrium emission of a nucleon of type x from a state with n excitons is equal to

$$ {}^nP_x(E) = {}^nP_x \frac{\rho_{n-1}(U)}{\rho_n(E)} \frac{\lambda_{em}(E)}{\lambda_{em}(E) + \lambda_+(E)} \qquad (1) $$

where

^nP_x is the number of nucleons of type x in the state n;

$\rho_{n-1}(U), \rho_n(E)$ represent the densities of states with n - 1 and n quasiparticles in the final and intermediate nucleus, respectively, as obtained by combination of equidistant, single-particle levels;

λ_{em} is the probability of emission, obtained from σ_{inv} by means of the detailed balance principle; and

λ_+ is the probability of an intranuclear transition with Δ n = 2.

The equilibrium spectrum $P_x^p(E)$ of particles of type x is calculated from the comprehensive statistical theory of nuclear reactions:

$$P_x^p(E) = \frac{(2s+1)\, mE\, \sigma_{inv}(E)\, \rho_R(U)}{\sum_\nu m_\nu g_\nu \int_0^{E_{max}} E\, \sigma_{inv,\nu}(E)\, \rho_\nu(U)\, dE_\nu} \qquad (2)$$

where $\rho_R(U)$ is the level density of the residual nucleus, given in terms of the Fermi-gas model by

$$\rho_R(U) = \frac{1}{(U_{eff}+t)^2} \exp\left[2(aU_{eff})^{1/2}\right]. \qquad (3)$$

Given the known cross section of formation of an initial system with n = 3, we thus obtain absolute spectra of the emitted nucleons and after summation with respect to energy we get the cross sections of the (n,n'), (n,p),(n,2n), (n,np), (n,pn), etc. reactions. Calculations have been carried out by the programme GLUNE.

As an example at fig. 1 for three target nuclei experimental and calculated neutron emission spectra, including pre-equilibrium as well as first and second evaporated neutron components are shown. The influence of pre-equilibrium emission on (n,2n) and (n,pn) cross sections is discussed in more detail in the paper [2].

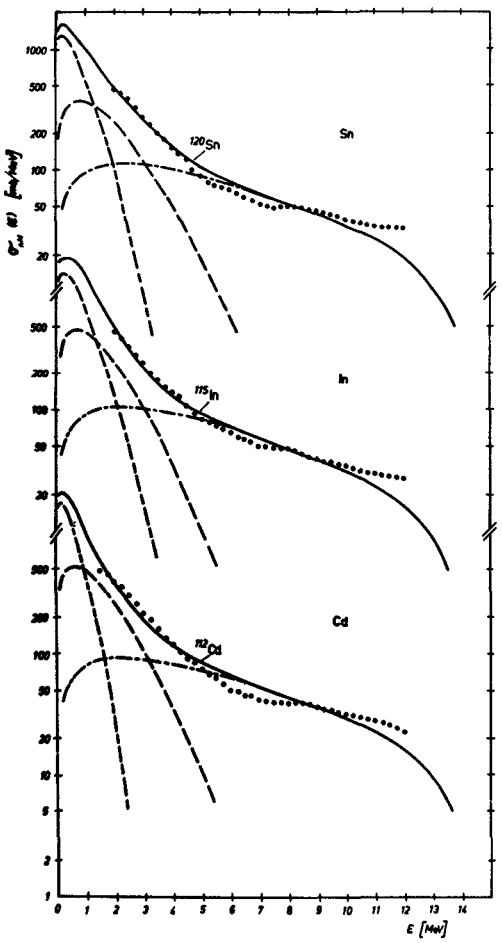

Fig. 1
Neutron emission spectra at 14 MeV incident energy 4 in comparison with calculations with the combined pre-equilibrium and equilibrium code GLUNE

NEUTRON CROSS-SECTION EVALUATION FOR ^{93}Nb

The recently published neutron cross section evaluation for all reaction channels ^{93}Nb + n in the energy range up to 20 MeV [5] may serve as an example for what one can due with optical and statistical pre-equilibrium and equilibrium models in a wide incident energy range.

One of the main features of this evaluation is the use of a unique set of parameters for different model calculations, i.e. nuclear level density parameter a, Q-values, pairing energies, optical, potential parameters, transmission coefficients (inverse cross sections), nuclear level scheme etc. The consistency of calculation results for different reaction channels strongly depends on the quality of these parameters.

In this sense the following reaction models and computer programs have been applied:
The Hauser-Feshbach program ELISA [6] for calculation of σ_{nT}, $\sigma_{n,n}$, $\sigma_{n,n'}$ as well as $\sigma_{n,\alpha}$ and $\sigma_{n,p}$ in the energy range 0.03 MeV to 5 MeV. Whole spectroscopie information up to an excitation energy of about 1.5 MeV (16 and 10 isolated levels in the neutron and proton channel, respectively) was treated exactly, whereas the continuum region was taken into account by a nuclear level density-dependent part. The calculations are based on a spherical optical potential with energy dependent parameters which have proved very successful for niobium [7] .

Optical model calculations (also by means of the program ELISA) in the energy region 10 to 20 MeV to clarify some ambiguities in σ_{nT} and $\sigma_{n,n}$. Here Holmqvist's parameter set [8] has proved convenient to get cross-sections in fair agreement with experimental one.

Calculations by means of statistical models including pre-equilibrium and equilibrium particle emission in the energy range above 9 MeV. The programs GLUNE and WPREC [9] have been applied. Especially GLUNE, proved very successful for consistent calculations of the excitation functions for $\sigma_{n,n'}$, $\sigma_{n,2n}$, $\sigma_{n,3n}$, $\sigma_{n,p}$, $\sigma_{n,np}$ and $\sigma_{n,pn}$ as well as neutron and proton emission spectra. This formalism has been extended also for description of the (n,α) reaction channel [10] .

Based on the complete statistical model (Weisskopf-Ewing formalism) there are some known computer programs for data evaluation purposes [11, 12] . Especially, Pearlstein's program THRESH [12] has been tested extensively.

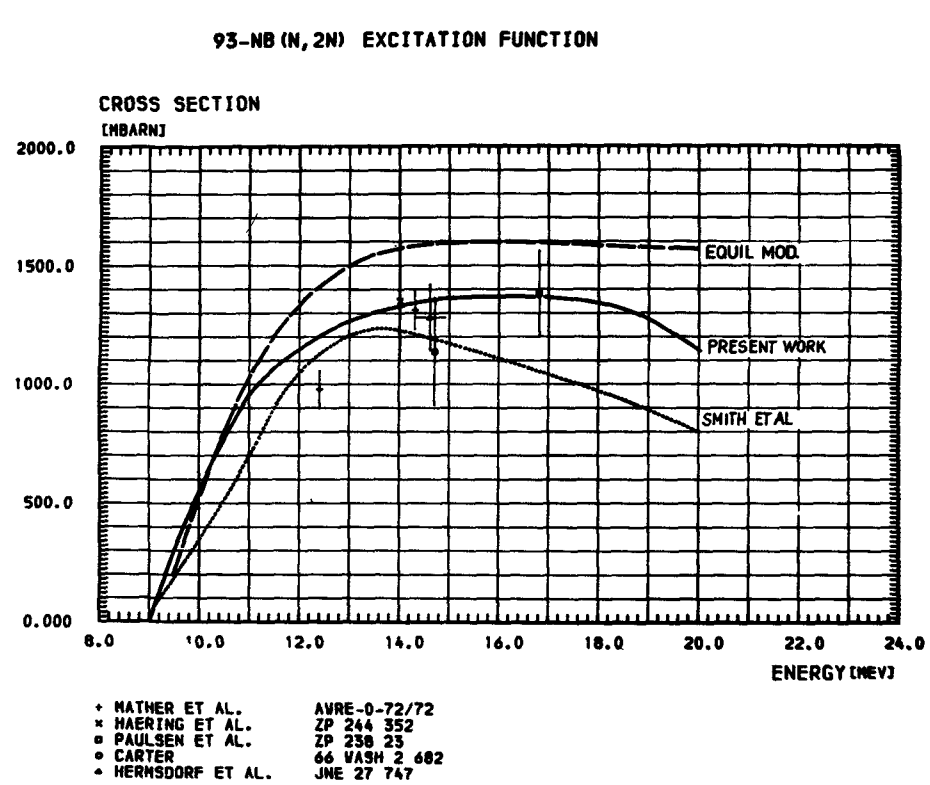

Fig. 2 Excitation function of the (n,2n) reaction; experimental data are compared with the present evaluation (full line), the evaluation by A.B. Smith et. al. [7] (pointed line) and with an equilibrium statistical model (dashed line)

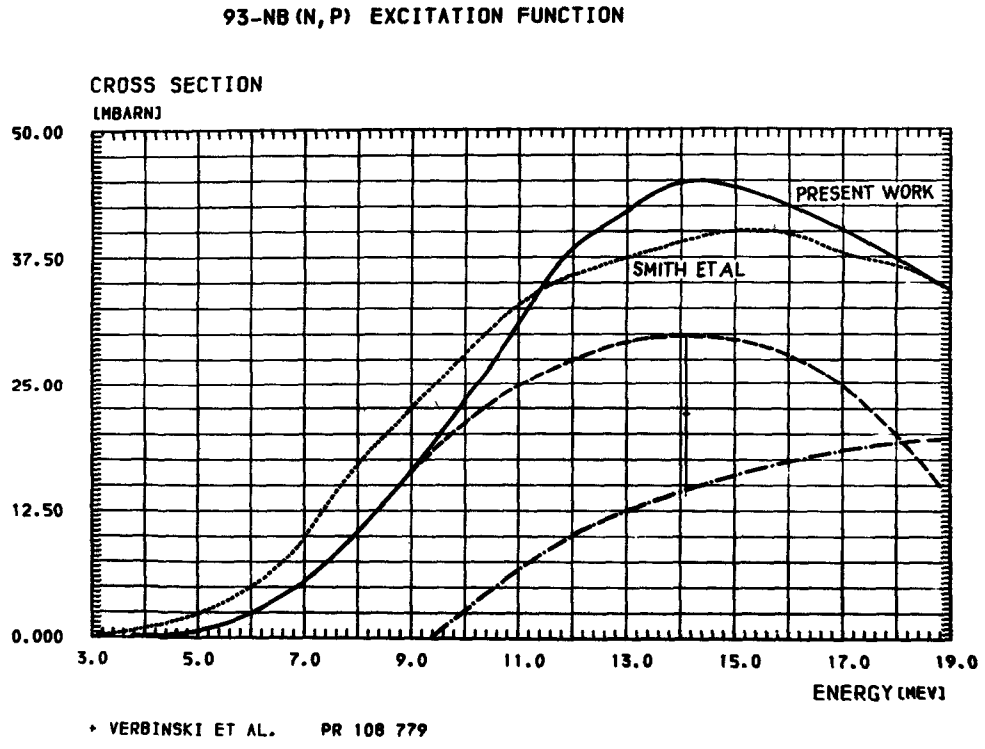

Fig. 3 Excitation function for the reaction ^{93}Nb (n,p) ^{93}Zr; the equilibrium (dashed line) and pre-equilibrium (dashed-dotted-line) of the present calculation are separately shown.

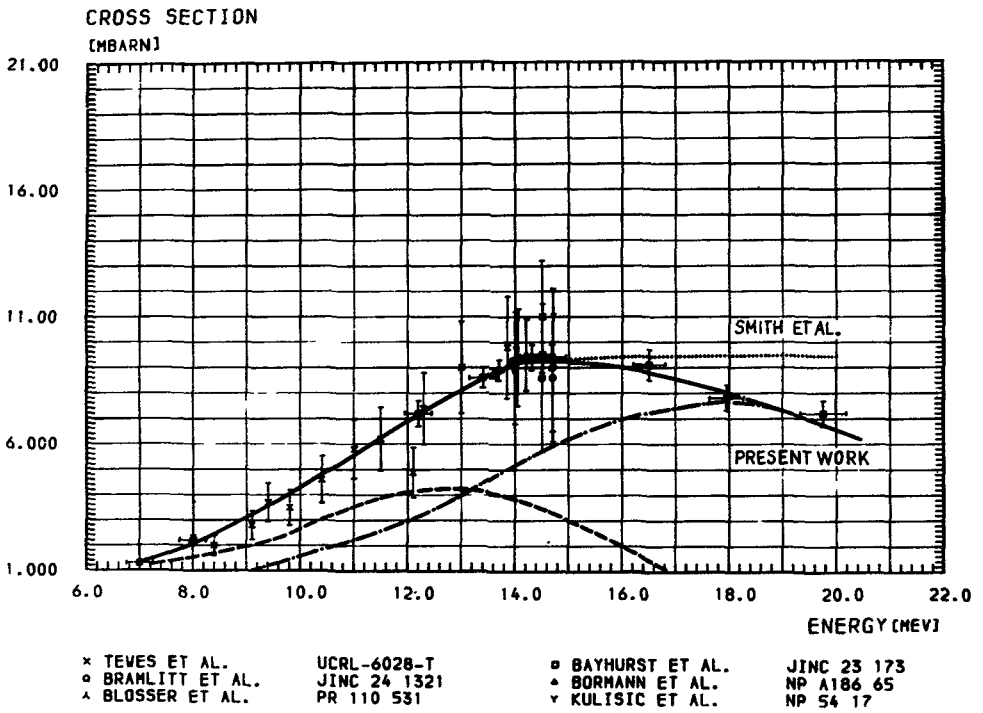

Fig. 4 Excitation function for the reaction $^{93}Nb(n,\alpha)\,^{90}Y$; the pre-equilibrium component (dashed-dotted-line) is calculated by the method, proposed in [10] .

Some selected results of this evaluation are presented at the figs. 2 - 4 for the excitation functions of the (n,2n), (n,p) and (n,α) reactions. The present evaluation curve is in good agreement with recently published new experimental (n,2n) data [13] .

APPLICATION OF MULTI-STEP HAUSER-FESHBACH THEORY

An intercomparison between the different neutron data evaluations SOKRATOR, KEDAK, ENDL-2, UKNDL, RIGA, SAND for Fe + n cross sections, including voluminous calculations for the iron isotopes ^{54}Fe, ^{56}Fe and ^{57}Fe with the programs GLUNE, THRESH and STAPRE as well as considerations of new experimental data has been carried out recently [14] . Some results of this work we choose to demonstrate the performance of the multi-step Hauser-Feshbach code STAPRE [15] , which also takes into account pre-equilibrium emission.

With STAPRE the (n,α), (n,p), (n,2n), (n,n') and (n,pn) cross sections for ^{54}Fe, ^{56}Fe and ^{57}Fe between threshold and 20 MeV incident energy have been obtained. The results of this calculations strongly depend on a careful selection of level density parameters a, backshift parameters Δ , transmission coefficient,

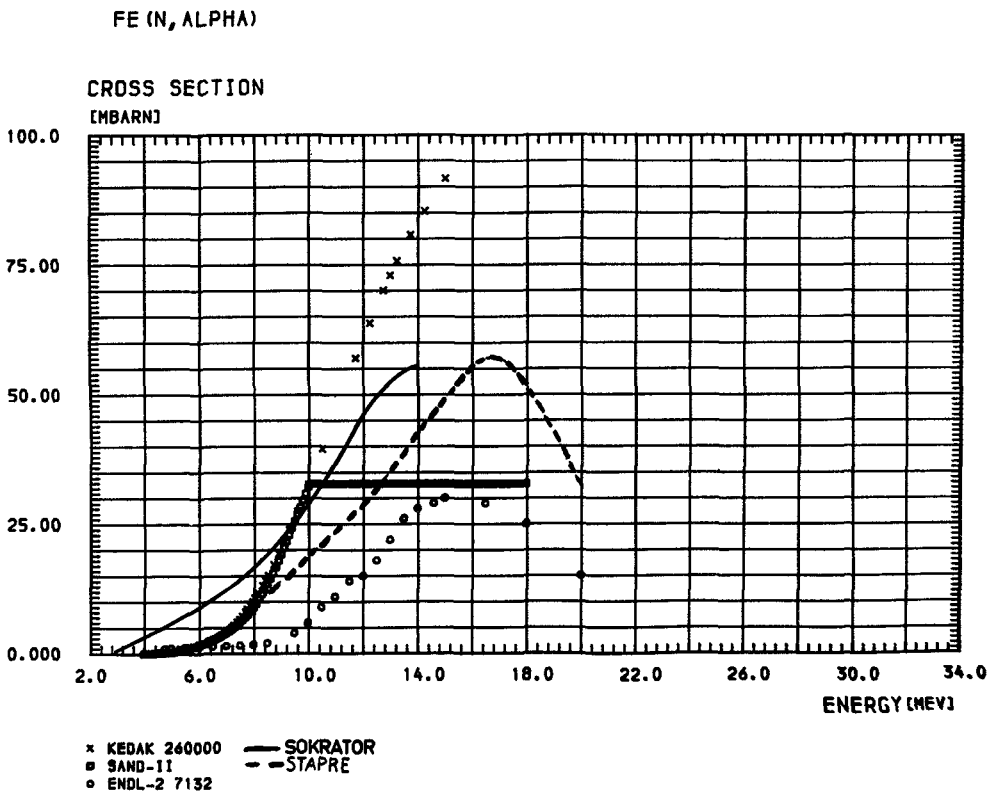

Fig. 5 Excitation function of Fe (n,α) reaction; the STAPRE calculation is considered as the new recommended excitation function

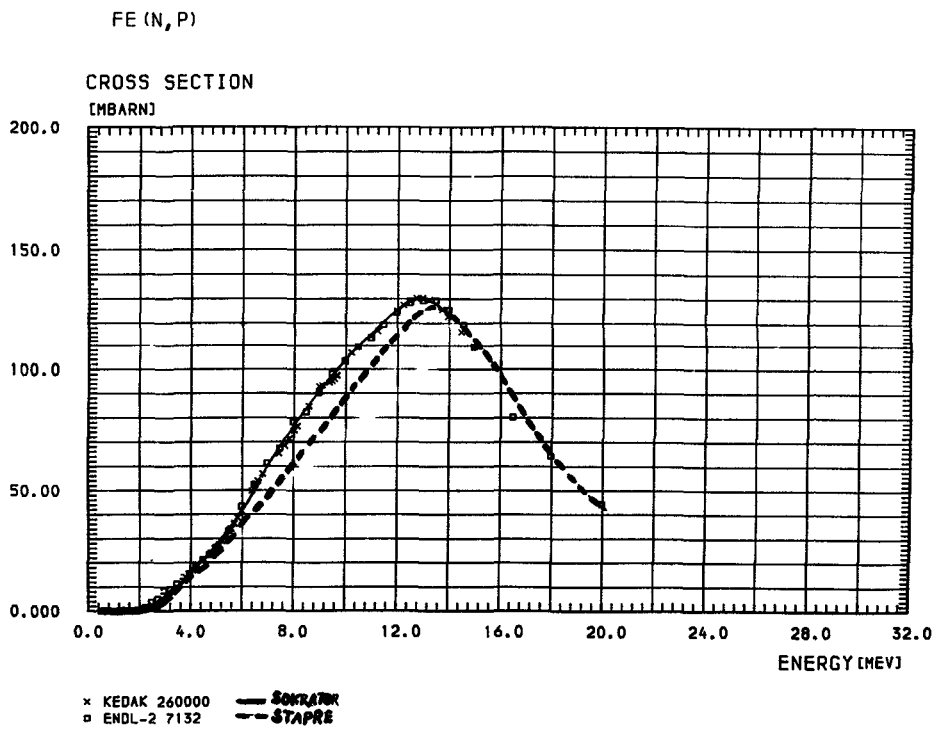

Fig. 6 Excitation function of Fe (n,p) reaction the STAPRE caculation is in agreement with existing evaluations

level schemes and other parameters for 19 isotopes between ^{49}Cr and ^{58}Fe. A careful choose of adequate parameter sets by intercomparison with experimental data is an essential feature of the application of the STAPRE code.

At the figs. 5 - 7 results for the (n,α), (n,p) and (n,2n) excitation functions for the natural isotope mixture of iron are shown. Existing evaluations for the (n,α) channel (s.fig. 5) show considerable differences between each other, due-to discrepancies between experimental data. The results, obtained with STAPRE may be considered as the new recommended excitation function for this case. The calculations of the (n,p) excitation function

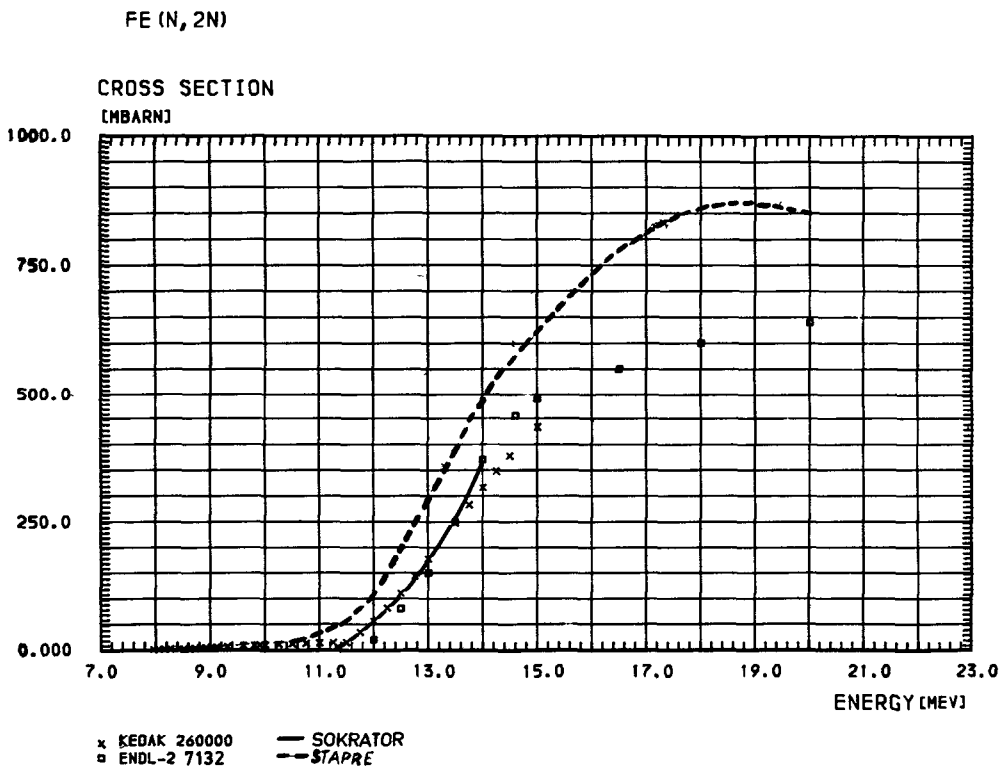

Fig. 7 Excitation function of Fe (n,2n) reaction; theoretical curve indicates some-what higher cross sections than existing data files

is in fairly good agreement with the evaluations KEDAK, ENDL-2 and SOKRATOR, as shown at fig. 6. Calculations with the chosen parameter set lead to some-what higher (n,2n) cross sections than existing evaluations. However, this higher cross sections in the energy region up to 15 MeV are in fairly good agreement with new experimental data [16] and, therefore, are considered as recommended data.

One of the further advantages of the STAPRE program is the possibility to obtain δ -spectra and γ-ray emission cross sections

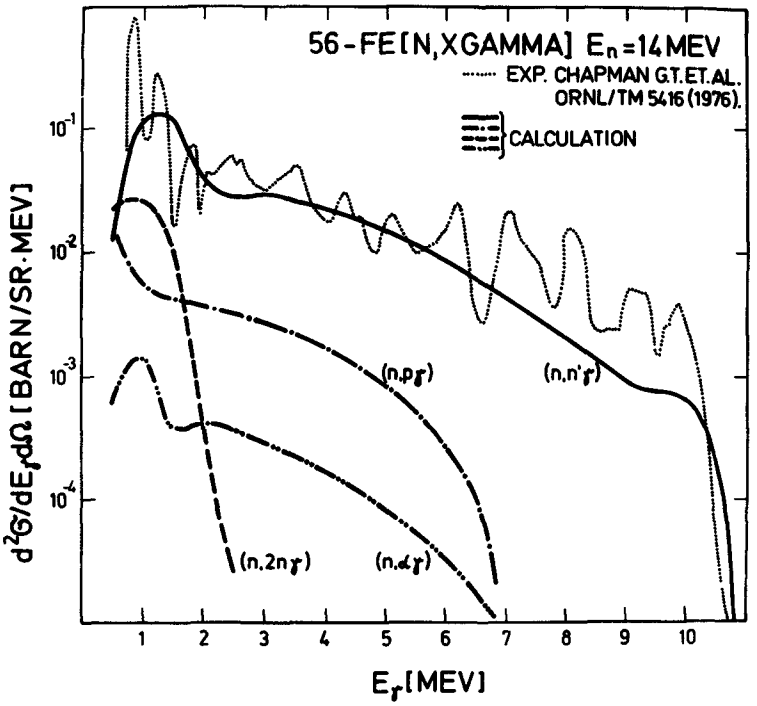

Fig. 8 Experimental and calculated γ-spectra from ^{56}Fe + n at 14 MeV incident energy

also. These quantities are extremly important for fusion reactor transport and nuclear heating calculations. Recently both spectra and production cross sections for ^{93}Nb + n and ^{56}Fe + n in an incident energy range up to 20 MeV have been calculated and compared with experimental data [17] . In this case γ-width are obtained from the Weisskopf single-particle model, using the Axel - Brink hypothesis [18] . Two examples of results from this work are shown at figs. 8 and 9. The γ-spectra from ^{56}Fe at 14 MeV (s.fig.8) incident energy is mainly due-to the (n,n'γ) process, whereas γ-rays from (n,2nγ), (n,pγ) and (n,$\alpha\gamma$) processes contribute mainly to the lower part of the total γ-spectra. The results, obtained with STAPRE are in agreement with experimental data by Chapman et al. The calculated γ-production cross section (s.fig.9) has a maximum near 12 MeV. The pre-equilibrium particle emission slightly changes the σ(n,n'γ) cross section. It is decreased below the maximum and increased above the maximum. In the energy range above 17 MeV γ-rays are mainly produced by the (n,2nγ) process. Experimental data in this case are scarce, several data points by Drake et al. are in agreement with the calculations.

ANGULAR DISTRIBUTIONS OF EMITTED PARTICLES

Concerning the theoretical description of angular distribution of emitted particles in the continuous part of spectra the situation is not so satisfactory as demonstrated above for angular integrated spectra and cross sections. In recent years several attempts have

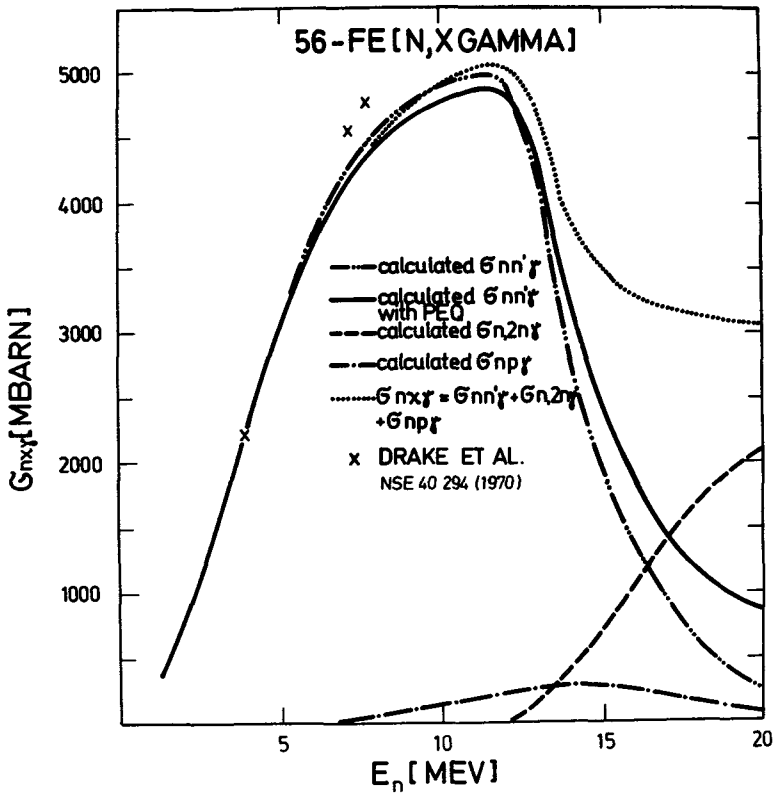

Fig. 9 Gamma production cross section for ^{56}Fe + n up to 20 MeV neutron incident energy

been done to overcome this problem. Some of them are reviewed here briefly.

Irie et al. [19] considered the pre-equilibrium emission spectrum by an analytic expression based on (1), but with emission rates $\lambda_{em}^{l_i}$ separately accounted for every orbital momentum l_i. Thus, energy distribution of emitted particles is calculated with exciton model, whereas the angular distribution is coming from the plane wave born approximation (PWBA), the simplest modification of direct reaction theory. Following this way, the double differential pre-equilibrium cross section $\sigma_{oi}^{PE}(\epsilon_o, \epsilon, \vartheta)$ is calculated with the formula

$$\sigma_{oi}^{PE}(\epsilon_o, \epsilon, \vartheta) = \sigma_o^{abs}(\epsilon_o) \sum_{l_i} \sum_{\substack{n=n_o \\ \Delta n=2}}^{\bar{n}} \sum_{\substack{J_c= \\ I \mp I_o+s}}^{I+l_o+s} \sum_{I_R=0,1/2} H \cdot \frac{\lambda_{em}^{l_i}(\epsilon)}{\lambda_{em}^{l_i}(\epsilon) + \lambda_+(n,E)\rho(p,h,E,J_c)} \cdot \frac{\rho(p-1,h,U,I_R)}{\rho(p,h,E,J_c)} \cdot \sigma_{PWBA}(\epsilon,\vartheta), \quad (4)$$

where the PWBA cross section $\sigma_{PWBA}(\epsilon,\vartheta)$ determines the shape of the angular distribution

$$\sigma_{PWBA}(\epsilon,\vartheta) \sim (2l_i+1) \sum_l (l_0 l_i 00 / l\,0)\; j_l^2(QR) . \qquad (5)$$

H is a free normalisation factor.

In several cases with this approach a good description of experimental angular distributions of emitted neutrons has been obtained. From a physical point of view this 'hybrid' of two different models is not satisfying.

Weidenmüller and Mantzouranis [20] introduced the information on scattering angle into the master equation of the exciton model. They assumed, that anisotropy of pre-equilibrium angular distribution is determined by the direction of motion of a 'leading particle'. States are characterized by n,E and the angle of leading particle $\vec{\Omega}$. Consequently, occupation probalities are also functions of three parameters $P = P(n,t,\vec{\Omega})$ and transition probabilities include information on the angle of leading particle before and after the collission $\vec{\Omega}$ and $\vec{\Omega}'$ (i.e.only those transitions are selected, in which leading particle participates). Further it is assumed, that transition rates can be factorized in two functions

$$\lambda_{\pm}(n,E,\vec{\Omega}\rightarrow\vec{\Omega}') \doteq \lambda_{\pm}(n,E)\cdot g(\vec{\Omega}\rightarrow\vec{\Omega}'), \qquad (6)$$

where function g does not depend on n.
The usual master equations without emission are changed to the following equations:

$$\frac{\partial P(n,t,\vec{\Omega})}{\partial t} = \int d\vec{\Omega}' \Big\{ \lambda_+(n-2,E,\vec{\Omega}'\rightarrow\vec{\Omega})\; P(n-2,t,\vec{\Omega}') + \lambda_-(n+2,E,\vec{\Omega}'\rightarrow\vec{\Omega})\; P(n+2,t,\vec{\Omega}') - P(n,t,\vec{\Omega}')\Big\{\lambda_+(n,E,\vec{\Omega}\rightarrow\vec{\Omega}') + \lambda_-(n,E,\vec{\Omega}\rightarrow\vec{\Omega}')\Big\} \qquad (7)$$

With $P(n,t,\vec{\Omega})$, determined from (7), the double differential cross section $\sigma_{oi}^{PE}(\epsilon_o,\epsilon,\vartheta)$ is derived through the expression

$$\sigma_{oi}^{PE}(\epsilon_o,\epsilon,\vartheta) \sim \sum_{n_o}^{\bar{n}} W_i(n,\epsilon) \int_o^{t_{eq}} P(n,t^*,\vec{\Omega})\; dt^* . \qquad (8)$$

The used concept of one leading particle among all excited Particles p is not inherent in the original exciton model, but it is similar to the 'philosophy' of the hybrid model. In several cases a satisfactory aggreement with experimental angular distributions has been achieved.

A scheme of parametrisation for angular distributions of inelastic scattered neutrons based on the direct PWBA reaction theory linked with the Maxwellian evaporation theory was elaborated by Lukyanov et al. /21/. Roughly speaking, in this approach the shape of angular distributions is determined by 6_{PWBA} (5), calculated for singleparticle transitions in the target nucleus within an averaging energy interval near $U = \epsilon_o - \epsilon$, which corresponds to the experimental energy resolution. The energy dependence of the spectra is determined by the function $(\epsilon/\epsilon_o)^{1/2} \cdot U$, which was obtained empirically by comparison with the shape of integrated (n,n')-spectra.
The absolute value of cross sections is determined by an normalization factor. On this way for many cases both double differential and angular integrated scattering cross sections have been parametrized and typical structures in the angular distributions could be connected with the quantuum numbers of a comparatively small number of transitions between shell model single-particle states. Similar results have been obtained by Jahn /22/.

A more rigorous treatment by several groups is based on DWBA, one of them was elaborated by Reif /23/. In this case direct excitation of 1p1h states through two-particle residual interactions of Gaussian type $\sum_{i=1}^{A} v_{io}$ is calculated on an absolute base, starting from the wave functions for the ground state and excited states

$$/ \mathrm{IM}\,\pi\, U\rangle = \sum_{p,h} c_{ph}^{I\pi}(U) \,/\, 1p1h\ \mathrm{IM}\pi\rangle + /c\rangle \,. \qquad (9)$$

Calculated DWBA matrix elements

$$T_{fi}^{DWBA} = \sum_{p,h} c_{ph}^{I\pi}(U) \quad (\chi_f^{(-)} / \langle (1p1h)\mathrm{IM} / \sum_{i=i}^{A} v_{io} / 0\rangle \chi_i^{(+)}) \qquad (10)$$

are averaged over a suitable energy interval ΔU. Distorted waves result from an optical model analysis of the elastic scattering. Calculated twice differential cross section for several cases investigated are in agreement with the experiment.
An application of multi-step direct reaction (MSDR) theory to the description of continous spectra recently was presented by Tamura and Udagawa /24/. In this approach the excitation of both 1p1h and 2p2h states in the target nucleus, i.e. one-step and two-step direct tow-particle excitation processes have been taken into account. It can be concluded, that the MSDR approach is in fact a rather powerful tool in describing cross sections with continuous spectra. The lower the energy of the outgoing particle and the larger the angle of observation, the larger is the relative contribution of the two-step processes. Nevertheless one may suspect that this approach can only fit the portion of spectra in which the outgoing particles still retain comparatively high energy. At less emission energy contributions from more complex and compound nucleus processes are expected.

CONCLUSIONS

There are very few data for neutron energies above 15 MeV and not enough data in the energy region between 8 and 13 MeV. Therefore, nuclear reaction model calculations must play an important role in meeting the data requirements for fusion reactor calculations and radiation damage research.

As it was shown by several examples, the combination of statistical evaporation theory and precompound models either Hauser-Feshbach theory and precompound models appears to be capable of providing much of the required data. Although, existing nuclear data evaluations are restricted to energies below 20 MeV, there are no principal limitations for application of this models to energies up to 40 MeV.

The most useful theoretical tool at present seem to be computer codes combining pre-equilibrium and multi-step Hauser-Feshbach theory, such as the code STAPRE. Several other similar codes are known from publications.

A general problem concerning nuclear model calculations are the uncertainties of the used model parameters, such as optical model parameters, level densities, gamma-ray strength functions and others. Systematic studies in this field and model parameter evaluations are needed.

Further improvement of theoretical approaches are necessary. Present treatments of pre-equilibrium decay do not include spin, parity and other nuclear structure effects, which might be important in the considered energy region. In addition, present codes do not include angular distributions of emitted particles. During the past years, several approaches have been elaborated for calculation of distribution of particles emitted from highly excited compound systems before statistical equilibrium is reached. It seems to be necessary to continue the development of different approaches as well as to include the most practicable approaches in-to computer codes for nuclear data calculations.

REFERENCES

[1] SEIDEL, K., SEELIGER, D., MEISTER, A., Proc. Consultants Mtg. Use of Nuclear Theory in Neutron Nuclear Data Evaluation, Trieste, 1975, IAEA - 190, Vienna (1976)

[2] MEISTER, A., SEELIGER, D., SEIDEL, K., Kernenergie 20 (1977) 395

[3] BLANN, M., Phys. Rev. Letters 27 (1971) 337
BLANN, M., MIGNERY, A., Nucl.Phys. A 186 (1972) 245

[4] HERMSDORF, D., MEISTER, A., SASSONOFF, S.,
SEELIGER, D., SEIDEL, K., SHANIN, F.
Report ZfK - 277 (Ü) INDC (GDR) 2/L (1975)

[5] HERMSDORF, D., KIESSIG, G., SEELIGER, D.,
Kernenergie 20 (1977) 166

[6] KIESSIG, G., Thesis, TU Dresden, 1975

[7] SMITH, A.B., WHALEN, J.F., GUENTHER
ANL - AP / CTR / TM - 4, 1973

[8] HOLMQVIST, B., WIEDLING, T., Journ Nucl. Energy 27 (1973) 543

[9] GUDIMA, K.K., TONEEV, V.D.
Preprint P4-7821, JINR DUBNA, 1974

[10] MILAZZO-COLLI, L., BRAGA-MARCAZZAN, H.G.
Nucl.Phys. A 210 (1973) 297

[11] AZZIZ, N., CONNELLY, J.W., WCAP - 7280, 1970

[12] PEARLSTEIN, S., Journ. Nucl. Energy 27 (1973) 81

[13] FREHAUT, J., MOSINSKI, G. et al. CEA - N - 1998 (1977)

[14] BYCHKOV, V., HERMSDORF, D., RÖSNER, P., SEELIGER, D.,
to be publ.

[15] UHL, M., IKR 76 / 01, Vienna, 1976

[16] FREHAUT, J. EXFOR - entry 20416

[17] BASSARAGTSHA, B., HERMSDORF, D., SEELIGER, D.,
Proc. VIIIth Sympos. on Interactions of fast Neutrons
with Nuclei, Gaussig, Nov. 1978 to be publ.

[18] AXEL, P., Phys. Rev. 126 (1962) 671

[19] IRIE, Y. et al. Phys. Lett. Vol. 26 b (1976) 9

[20] MANTZOURANIS, G., et al. Z. Phys. A 276 (1976) 145

[21] LUKYANOV, A. A., et al. Journ. of Nucl. Phys. (Sov.)
21 (1975) 67

[22] JAHN, H., Proc. Consultants Mtg. Use of Nuclear Theory in
Neutron Nuclear Data Evaluation, Trieste, 1975, IAEA - 190,
Vienna (1976), p. 315

[23] REIF, R., Kernenergie 20 (1977) 177

[24] TAMURA, T., UDAGAWA, T. Proc. Symp. on Neutron Cross
Sections 10 to 40 MeV, Brookhaven, 1977, ed. by BHAT, M.R.,
PEARLSTEIN, S., BNL - NCS - 50681, p. 533

EVALUATED FILES OF NUCLEAR CROSS-SECTIONS FOR FUSION REACTOR CALCULATIONS*

AG-159/B3
Review Paper

M.R. Bhat
National Nuclear Data Center
Brookhaven National Laboratory
Upton, New York 11973

ABSTRACT

The status of available evaluated nuclear cross-section data for fusion reactor calculations is reviewed. The data files consist mostly of neutron and gamma ray production cross-sections up to 60 MeV and a few charged particle evaluations. In addition, evaluated nuclear structure and decay data needed for the various fusion related applications are listed, their present uncertainties discussed, along with future needs and suggestions for improvements.

1. INTRODUCTION

The need of neutron cross-section data for fission reactor calculations was the impetus behind the creation of many experimental and evaluated data libraries. The international activity in this field has recently been reviewed by Schmidt [1]. The evaluated neutron data libraries are listed in Table I. In general, they extend from about 1.0E-05 eV to 15 or 20 MeV and consist of neutron and gamma-ray production data. The evaluations are based mostly on available experimental data supplemented by nuclear model calculations where such data do not exist. In this review, the discussion will be mostly confined to one data library - the ENDF/B system.

The growth of the ENDF/B library from its inception in 1967 is shown in Table II. In this Table, the numbers pertaining to Version V are to be considered tentative until the formal release of the library. From this Table, one notices that the types of data available in the library have increased to keep pace with an increase in the number of applications. Over the years, there has also been an increase in the quality and amount of experimental data and the sophistication of the physics content of the evaluations. The various checking codes had to be expanded to verify the consistency and reasonableness of the evaluations, thus improving their quality. Also, greater use is made of nuclear structure and decay information in addition to the neutron cross-section data.

The fusion community used these evaluations in their initial calculations and also told the evaluators what additional information they would like to see suited for their applications. As a result, starting from about 1970, after the release of Version II library, greater emphasis was

* Research carried out under the auspices of the U.S. Department of Energy.

placed on the energy region around 14 MeV in the ENDF/B evaluations. This was followed by format modifications to include new data for fusion applications and a conscious, planned attempt to satisfy their needs in the subsequent versions of the library. This accounts for the inclusion of gas production, activation and decay data information in ENDF/B-V expected to be released in early 1979.*

Materials damage studies for the alloy development program for the fabrication of the first wall of a fusion reactor need high fluences [2] of about 10^{22} n/cm^2 as well as experimental volume in the range of ten liters [3]. Hence, there are plans to construct a d-Li facility - the Fusion Material Irradiation Testing (FMIT) facility. In this facility, it is expected that there will be an appreciable neutron flux up to 50-60 MeV. This, in turn, has shown the need to extend the upper energy limit of evaluated data files to these energies. However, experimental data above 14 MeV are sparse and nuclear model code calculations at these higher energies have to be checked against data before they could be used with confidence. Some of these problems were discussed at a Symposium [4] held at Brookhaven National Laboratory (BNL) last year and a number of recommendations of this Symposium, as well as what has been accomplished since, will be discussed in this review. Since there are some special problems involved in extending the evaluations from 20 to 60 MeV, this paper is divided into two parts: Section 2 will be devoted to a discussion of evaluated data up to 20 MeV, and Section 3 to evaluated data from 20 to 60 MeV. In each of these Sections, neutron as well as charged particle evaluations and the relevance of nuclear structure and decay data will be discussed. In addition, mention will also be made of nuclear model codes which the evaluator needs to fill in the lacunae in differential experimental data and the influence of integral benchmark experiments on the evaluations.

2. EVALUATED NUCLEAR DATA UP TO 20 MeV

There are many evaluated cross-section data files extending up to 20 MeV. They consist mostly of neutron cross-section data and, in some cases, gamma-ray production cross-sections are also given. This energy region is characterized by the fact that there are many experimental data available, though the quality gets poorer above 14 MeV and the data get sparser. This is also the energy region where a number of experiments have been conducted with a view towards understanding the basic physics of nuclear reactions because the interpretation of data is relatively easier, as many reaction channels do not open up at these energies. Nuclear model codes have also been checked against experimental data and

---

* Evaluated data files on neutron cross-section standards, dosimetry and fission products will be available for international distribution.

their input parameters adjusted, so that they could be used with some confidence. This section will be divided into various subsections, each dealing with a particular fusion related application [5]. They are:

2.1 Fuel Cycle
2.2 Plasma Diagnostics
2.3 Tritium Breeding
2.4 Nuclear Heating
2.5 Neutron Dosimetry
2.6 Radiation Damage Effects
2.7 Induced Activity
2.8 Radiation Shielding
2.9 Hybrid Concepts

This will be followed by a brief discussion of the nuclear model codes used in evaluations.

The first two applications need charged particle data which will be discussed in detail in another paper [6] at this meeting and they will be discussed only very briefly for completeness. In each of these subsections, the status, adequacy and accuracy of experimental data and evaluated files will be discussed. This will be followed by results of any sensitivity studies. The need for better or more extensive data or evaluations will also be indicated with mention of relevant nuclear model calculations and any integral experiments that materially affect the evaluations. These applications cover a wide range of materials and types of data; hence, a detailed discussion of the experimental data and their accuracies is not possible within the scope of this paper. Such discussion, therefore, will be confined to a few illustrative examples. Similarly, error estimates on evaluated files are meant to convey a general idea of how good the evaluations are and for details one should consult the data covariance files or the evaluation report of a particular evaluation.

2.1 Fuel Cycle

It is expected that the first generation fusion reactors will be based on the D+T reaction:

$$D + T \rightarrow {}^{4}He(\sim 3.5\ MeV) + n(\sim 14.1\ MeV)$$

The discussion in the rest of the paper will be based on this assumption with its attendant problems of tritium breeding and the interaction of the 14.1 MeV neutrons in the surrounding blanket. This reaction cross-section plotted as a function of the deuteron energy shows a broad resonance at E_d = 109 keV and a peak cross-section of about 5 b [7]. Because of this large cross-section it appears possible to obtain high enough reaction rates at lower temperatures in a D,T plasma to achieve a self-sustaining fusion reaction.

The data on this reaction have been recently reviewed by Stewart and Hale [7] and their evaluation of the reaction cross-section described. This evaluation is based on an R-matrix fit to all the available data corresponding to the different reaction channels for the five nucleon systems - ^{5}He and ^{5}Li. Thus, the final parameters extracted from the analysis have to satisfy the constraints imposed by the experimental data for the different reaction channels and are clearly better than those obtained from a parametrization of D-T reaction alone. Further, they observe that the R-matrix fit agrees much better with experimental data than a Gamow penetrability fit below 20 keV. The R-matrix calculation deviates at most by 9% from measured values while the Gamow fit deviates by 30% at several points. Thus, an R-matrix fit appears to be a more reliable tool for extrapolating evaluated curves to lower energies below a few keV where no experimental data exist. These low energy cross-sections are needed for plasma diagnostics, as will be discussed in Section 2.2.

This charged particle cross-section evaluation is not part of the ENDF/B library as yet; the evaluated cross-section is given in reference [7] from 5 keV to 1 MeV. It is estimated [8] that the uncertainty in the evaluation is 5-10% below 10 keV and better than 5% everywhere above 10 keV. The status of T(t,2n)^{4}He cross-section was also reviewed in reference [7] and the data have been further analyzed by Hale and Young [9] up to E_t = 2 MeV using a multi-channel multi-level R-matrix analysis. It is estimated [9] that the uncertainty in this cross-section is about 15% below 10 keV and 5-10% above it.

The cross-section sensitivity of the D-T fusion probability has been studied by Santoro and Barish [10] for incident deuteron energies of E_d = 200 and 500 keV and plasms electron temperatures T_e = 5 and 10 keV to find the influence of the D-T cross-section. For these deuteron energies and plasma electron temperatures, they conclude that the fusion probability is most sensitive to the D-T cross-section for $E_d \gtrsim 50$ keV. Based on the reported errors in the cross-section in this energy range [7] they conclude that the errors in the calculated fusion probability should be $\leq$ 10%. For E_d below $\sim$ 50 keV, they found that the sensitivity of the fusion probability to the D-T cross-section becomes increasingly small, so that errors in the calculated fusion probability will be small, even though the data uncertainties are large. The cross-section sensitivities of the D-T reaction rates in a D-T plasma and the T-T reaction rate in a tritium plasma were also calculated for deuteron and triton temperatures of 0.300 keV, 1 keV and 5 keV. These reaction rates are of interest in plasma diagnostics (see Section 2.2) to determine plasma ion temperatures. For ion temperatures of 0.3 and 1 keV all the contribution to the sensitivity of reaction rates is from data below 100 keV and for the 5 keV ion temperature most of it is from the same energy region and the errors in the calculated reaction rates are determined by the errors in the D-T cross-section in this energy range. For the T-T reaction rate, all of the

contribution to the sensitivity is from energies below 60 keV where there are no experimental data and the errors in the calculated reaction rates are large, reflecting large errors in the T-T cross-section.

From the above discussion it appears necessary to have better low energy data on D-T and T-T cross-sections. In the forthcoming updated version of the Compilation of Requests for Nuclear Data [11] there are requests to improve the accuracy of D-T cross-section below 10 keV and the T-T cross section. The desired accuracies are 10% relative and 30% absolute. It is expected that the National Bureau of Standards program to measure the helium σ_{total} [12] and the Los Alamos Laboratory project [13] to measure low energy cross-sections for $T(t,2n)\alpha$, $D(t,n)\alpha$ and $D(d,n)^3He$ cross-sections in the 5-120 keV energy range will satisfy these data needs. The other data needed for fuel cycle studies are elastic cross-section data up to a few MeV to determine the interaction between the alphas and D-T fuel. The desired accuracies are: relative $\pm$ 10%, absolute $\pm$ 30%.

In addition to the D-T reaction, the attractive possibilities of using other exotic fuels of higher Z materials such as lithium, beryllium and boron have also been suggested [14,15]. These could provide fuel cycles which are essentially free of neutrons and tritium. However, these fuel cycles need higher temperatures and could suffer from radiation losses [16]. There is need to have experimental data for a number of reactions [11] associated with these fuels from several hundred keV to a few MeV. They are $^{11}B(p,n)^{11}C$, $^{11}B(\alpha,p)^{14}C$, $^{11}B(\alpha,n)^{14}N$, $^{6}Li(^{3}He,p)2\alpha$ or ^{8}Be and $^{6}Li(^{6}Li,x)Y$. The desired accuracies are: relative $\pm$ 10%, absolute $\pm$ 30%. Also, data with the same accuracy are desired for the elastic scattering of the product ions from these reactions with the rest of the plasma. Compilation of the experimental data for these reactions as well as for D-T and T-T reactions in this energy range are needed to obtain σ vs. E as well as the reaction rate $\langle\sigma v\rangle$ as a function of temperature. Evaluation of the $p + {}^{11}B$ reaction by Hale and Dei at Los Alamos is in progress [17].

2.2 Plasma Diagnostics

A variety of physical methods may be employed for probing plasmas and determining their important characteristic parameters. These methods as applied to Tokomak plasma diagnostics have been recently reviewed [18] where there is an extensive bibliography. In discussing nuclear cross-section data, it is appropriate to discuss here those diagnostic methods which involve nuclear data and are based on detecting neutrons or α particles produced in D-T plasmas in the thermonuclear reaction.

The neutron yield from thermonuclear reactions is a function of the ion temperature and may be used to determine it. A comparison of the

ion temperature determined in a deuterium plasma using the $D(d,n)^3He$ reaction with values obtained by charge-exchange measurement shows good agreement [18]. A successful use of this method depends on (i) a knowledge of the relevant reaction cross-section with sufficient accuracy at the low energies involved in the reaction, and (ii) the ability to identify unambiguously neutrons due to thermonuclear processes from those due to other spurious sources. The ion temperatures obtained from neutron detection assuming Maxwellian ion distribution may be compared with temperatures obtained by other methods, e.g. charge exchange, to verify how well this assumption is justified. In addition to ion temperature measurement in an ohmically heated plasma, neutron detection can be used to study high energy neutral beam injection experiments. In this case, the energy and angular distribution of the neutrons from thermonuclear reactions may be used to study the initial state of motion of the reacting particles viz. the beam ions and the target plasma ions. Hendel [19] has proposed to make energy, time and angle resolved fast-neutron spectroscopy measurements to determine TFTR power multiplication factor, beam-ion energy distribution, target-plasma ion temperature, and beam-ion loss rate, together with their time and spatial dependences. These methods depend on the development of suitable detectors and refinement of experimental techniques, as well as knowing the relevant charged-particle reaction cross-sections accurately at low energies involved in these experiments.

2.3 Tritium Breeding

A fusion reactor based on the D-T fuel cycle will require a tritium breeding blanket containing lithium. Tritium is produced in lithium by $^6Li(n,\alpha)t$ and $^7Li(n,n')\alpha t$ reactions. The first is an exothermic reaction and varies approximately as 1/v below 100 keV with a thermal value of 936b. The second reaction has a threshold of about 2.82 MeV and produces tritium without neutron absorption. Some blanket designs also include a neutron multiplier like beryllium which increases the number of neutrons via the (n,2n) reaction with a Q-value of only -1.665 MeV. Tritium production for different blanket designs is given in terms of the tritium breeding ratio which is defined as the number of tritons produced per fusion neutron or equivalently per D-T fusion reaction. The calculated breeding ratio depends on the details of blanket design and, if present, the amount of neutron multiplier, such as Be, and is estimated to vary [20] from 1.04 to 1.52.

It is estimated [8] that $^6Li(n,\alpha)t$ cross-section is known to 0.5% at 1.0E-05 eV, 1.0% at 10 keV, 2.0% at 30 keV, 3.0% at 230 keV, 4.0% at 450 keV, and 5.0% at 750 keV and above. The $^7Li(n,n')\alpha t$ cross-section in ENDF/B-V is taken over unchanged from Version IV and its error estimates are given in reference [21], page 19. They are 15% from threshold to 3.0 to 14.0 MeV and about 25% at 20 MeV. The Be(n,2n) cross-section based on the latest experimental data is uncertain by about 15% from threshold to

15 MeV and by 40% at 20 MeV. The breeding ratio calculations depend on the secondary neutron energy distribution of the $^{7}Li(n,n')\alpha t$ reaction [22] and the $^{9}Be(n,2n)$ reaction. There are data on the neutron energy distribution for ^{7}Li and are being reevaluated. For Be(n,2n) they are not adequately represented in the ENDF/B-V [23] and one might have to use the ENDL library [24].

There have been a number of studies of various blanket designs [22,25,26] as well as sensitivity studies [20,22,27] to determine the effect of cross-section uncertainties on the breeding ratio. For the particular design they considered, Bartine, et al [27] concluded that the breeding ratio is most sensitive to changes in the $^{7}Li(n,n')\alpha t$ cross-section, though the sensitivity to changes in this cross-section is not large. Steiner and Tobias [22] using the ENDF/B-III data library found that the status of $^{6}Li(n,\alpha)t$ cross-section data was adequate to determine tritium breeding ratio to 1% for the class of blanket designs studied by them. They assumed a 20% error in the $^{7}Li(n,n')\alpha t$ cross-section from 3 to 15 MeV and determined that the cross-section error and that of the secondary neutron energy distribution could introduce uncertainties in excess of 5% in the breeding ratio. The secondary neutron energy distribution was described by an evaporation model and an energy dependent temperature $\Theta(E)$ where E is the energy of the incident neutron. The temperature was changed by ± 50% over the energy range of interest and the total breeding ratio decreased by $\sim$ 2.5% for the soft spectrum and increased by $\sim$ 1% for the harder spectrum. In general, the conclusions are [5] that $^{6}Li(n,\alpha)t$ cross-section data are adequate for tritium breeding calculations of the order of 1% and the cross-section and secondary neutron energy distribution uncertainties in ^{7}Li introduce errors of the order to 2-7% in the tritium breeding ratio. Uncertainties in the Be(n,2n) data and the secondary neutron energy distribution could introduce errors of the order of several percent in the tritium breeding ratio and additional measurements are needed to improve the evaluations. It was recommended by a group at the BNL Blanket and Shield Workshop [28] that the angular distribution of the secondary neutron spectra of ^{7}Li be measured between 11 and 14 MeV with a 10% accuracy, and in the forthcoming request list [11] there will be a similar request for neutron emission spectra from 9-14 MeV with 10% accuracy.

There have been several integral experiments to check the calculations of breeding ratios. The earliest was by Wyman in 1954 which was later analyzed by Muir and Wyman [29] in 1974 using improved calculational procedures. This experiment showed for the first time the importance of $^{7}Li(n,n')\alpha t$ reaction for tritium breeding [30]. The authors observe [29] that their reference calculations using ENDF/B-III and the LASL evaluation for deuterium are in general good agreement with experimental data though there were discrepancies of the order of 20%. They also noted that a 15% reduction of the 14 MeV ^{7}Li cross-section would improve

the agreement significantly. Herzing, et al [31] also carried out an integral experiment and determined the tritium production by three different counting methods. ENDF/B-III data were used for their calculations and they found good agreement between their experimental data and calculations within an estimated error (1σ) of $\leq$ 3%. This reference also lists some of the earlier integral experiments. Recently, Bachmann, et al [32] performed a measurement using a 1 m diameter sphere of lithium metal with natural isotopic composition and a 14 MeV D-T neutron source in the center. They measured directional neutron spectra with time-of-flight methods and the scalar neutron spectra with a small spherical proton recoil proportional counter with $\pm$ 5% error. They estimate the error in the experimental data for tritium production to be $\pm$ 5% comprising of tritium counting, source strength determination and uncertainty of the true radial distance to the source center. Calculations were performed using ENDF/B-III for lithium and the KEDAK3 for iron and they found that the calculated tritium production rate is 35% higher than the measured value. This is also consistent with conclusions drawn from the measured and calculated spectra. They conclude that about half the discrepancy is caused by excess neutron flux in the energy range from 3 to 11 MeV and a great deal of the rest is attributable to $^{7}Li(n,n')\alpha t$ cross-section which seems to be too high. They recommend that it be lowered by 15-20% with respect to ENDF/B-III which is identical to ENDF/B-V. New differential data on this cross-section are therefore needed to solve this problem.

2.4 Nuclear Heating

In fusion reactor design studies, it is important to calculate nuclear heating in the blanket and other parts of the reactor. For calculating heating due to the interaction of nuclear radiation with matter, one usually proceeds by calculating the kerma (kinetic energy released in matter) factors from basic nuclear data. As is well known, [33] the microscopic kerma factor $k_i(E)$ is defined as:

$$k_i(E) = \sigma_i(E)\ E_i(E) \quad \text{(barns. ev/atom)}$$

where $\sigma_i(E)$ is the microscopic cross-section for a particular isotope for reaction i at neutron energy E and $E_i(E)$ is the energy deposited locally due to reaction i. If these are known and the neutron flux determined from other calculations, the heating rates can be determined. It is usual to define a neutron kerma factor and a gamma-ray kerma factor - the first takes into account heat generated by neutron reactions, and the second that resulting from the absorption of secondary gamma radiation originating from the neutron reactions. To these must be added the contribution of the radioactive decay of the final state - which will be in general, time dependent. The work of Abdou and Maynard [33] describes the details of calculations of kerma factors for a variety of reactions. Their results are compared with previous work and the results and improvements in

technique summarized. They conclude that the limitation on these calculations is solely that determined by the availability and accuracy of nuclear data. The calculation of neutron kerma factors require: (i) reaction cross-sections, (ii) energy, and (iii) angular distribution of secondary neutrons, (iv) energy angular distribution and yields of secondary photons, (v) energy deposition for reaction from radioactive decay, and (vi) reaction Q-values. If all these data for an isotope are available, then the calculation of the neutron kerma factors is straightforward. However, all these data may not be usually available in an evaluated data file. First, gamma-ray production data are less well-known and the evaluated data may not even be consistent with neutron data. Second, the evaluated data may be available for the element and not for the individual isotopes. The solution to the problem is to have stringent tests built into the physics checking codes to check the consistency of neutron, and gamma ray production data. Also, the neutron and gamma ray data should be analyzed at the same time and the validity of the kerma factors checked by energy balance. However, this may not be possible in all cases. Because, usually experimental data are not available for gamma production from individual reactions: rather, one has measured data for (n,xγ) reactions. In this case, nuclear model codes which generate gamma ray production data for each reaction in an isotope could be used and their results adjusted to agree with measured (n,xγ) data. This could partly be an answer to the second problem, viz. the elemental evaluations. In practice, however, it is not easy. It is usual to find that most of the measured differential data including gamma ray production cross-sections is for an element rather than for the individual isotopes. The isotope data tend to be sparse and spotty. It is possible, in principle, to calculate the non-existent data for the isotope using nuclear model codes and obtain isotope evaluations consistent with their and elemental data. In practice, this could be a major task, further complicated by systematic errors in different data sets. Heat deposition calculations for a mixture of isotopes show that energy independent parameters like reaction Q values, decay energies, etc., are energy dependent for an element ("effective Q values", "effective decay-energy", etc.) as a consistent definition of these quantities must be weighted by the isotopic abundances and energy-dependent cross-sections [33]. Thus, kerma factor calculations can not be carried out accurately if only elemental data are available. Heating due to the decay of the residual nucleus can be significant depending on the composition of the system under consideration and the neutron spectrum. These calculations should also take into account the time dependence of the radioactive decay and its possible transmutations. Earlier calculations indicated a need to have this decay data information for all isotopes of importance. Suitable changes in formats have been made and in ENDF/B-V, data such as the half-life, for each branch, branching ratios, $\langle E_\beta \rangle$ and $\langle E_\alpha \rangle$ and other quantities are given. For details, one should consult the Data Formats and Procedures Manual for ENDF [34].

There have been a number of sensitivity studies of heating [35, 36] and comparative studies of various blanket designs and nuclear heating in them [37,26]. In the following, the conclusions arrived at by Abdou and Maynard [33] in their sensitivity studies of neutron energy deposition to changes in basic nuclear data will be discussed. In understanding these sensitivity studies, one should recall from the above equation defining the kerma factor that the energy deposition is the product of the reaction cross-section and the energy released per reaction which depends on the energy and angular distribution of the secondary particles, the energy and angular distribution of the secondary gamma rays and the reaction Q-values. In addition, data changes could bring about changes in the neutron and gamma-ray fluxes. Abdou and Maynard found that (n,charged particle) reactions in general contribute about 30-50% to the neutron heating in typical fusion reactor spectra in the energy range 10-15 MeV. In materials such as stainless steel this contribution could be > 70%. The importance of the (n,2n) reaction increases at high energy with a decrease in inelastic scattering. It also depends on the Q-value as a higher Q-value means a smaller cross-section in the 10-15 MeV range and also smaller energy will be available to the recoil nucleus. The (n,n' charged particle) reactions contribute a smaller amount to heating when compared with (n, charged particle) reactions because their thresholds are higher and part of the available energy is carried away by the secondary neutrons. It is estimated that their contribution is about 20-30% of that of the (n, charged particle) reactions. Also, approximating the (n,n' charged particle) reactions by that from the (n,n') part only amounts to neglecting 80-90% of the heating due to these reactions. Most of the neutron heating in a typical CTR blanket is from ^{6}Li and ^{7}Li; the ^{7}Li (n,n')αt reaction being the most important. Neutron heating depends strongly on the secondary neutron energy distribution from this reaction. It is found that the relative change in neutron heating in ^{7}Li is about one-third of the relative change in the average energy of the secondary neutrons. The effect of angular distribution of secondary neutrons is also important - thus ignoring anisotropy of elastic scattering can result in overestimated kerma factors. The local energy deposition by radioactive decay is $\sim$ 2% or less in most materials in typical spectra for fusion reactors. These studies are very important and indicate the (n, charged particle) and other high energy data should be carefully evaluated with due consideration being given to the angular and energy distributions of secondary particles and gamma rays.

2.5 Neutron Dosimetry

Neutron dosimetry attempts to define as accurately as possible the neutron field pertaining to a number of applications, e.g. materials radiation damage studies, shielding and biomedical work. The experimental techniques and analytical procedures were originally developed for fission reactors and have a long history of improvement of experimental techniques, comparison with integral benchmarks and further refinement of differential

measurements. The experimental methods may be broadly divided into differential measurements which include time-of-flight spectrometry, the proton-recoil counters, and other techniques which give the neutron spectrum as a function of energy. In addition, there are integral techniques, e.g. multiple foil activation measurements and helium production data which give results integrated over the neutron spectrum and the detector response function. The multiple foil activation techniques are especially attractive as they could be used in normally inaccessible places. It is also noted that some of these differential techniques could be used in plasma diagnostics discussed in Section 2.2.

Dosimetry cross-sections were first part of the ENDF/B library for Version III and later updated for ENDF/B-IV. These files for Version IV consisted of some 36 reactions in 26 isotopes and are described and discussed in detail by Magurno [38]. The reactions in Versions IV and V are the same, though the evaluations in V are new. If some of these reactions are in the General Purpose File (a file containing all neutron and possibly γ producing reactions of interest and extending from 1.0^{-5} eV to 20 MeV) they will be taken from them and all of them will have data covariance files. In addition, they will be consistent with the ENDF/B-V cross-section standards. These evaluations will be tested against integral benchmarks (Phase II testing) at a later date. It is interesting to review here briefly the results of such testing on Version IV dosimetry cross sections [39]. For integral testing, three benchmark spectra were specified: a fission neutron spectrum, and the fast spectra of ΣΣ [106] and CFRMF [107] facilities. Reaction rates were measured in these spectra. The result of these tests were that for most of the cross-sections the disagreement between calculated and measured reaction rates is a few percent or more and is outside the range of uncertainty reported for the measurements. From the wide range of disagreement between calculations and measurements, indications are that not only are some of the cross-sections in the dosimetry file in error, but also the benchmark spectra are not known well enough. It was felt that the benchmark testing procedure should be investigated and improved.

Greenwood et al [40] have carried out integral tests on some 27 dosimetry reaction cross-sections in 13 materials. The neutron fields used for this test were obtained by stopping 14 and 16 MeV deuterons in a thick beryllium target and extended from about 800 keV to about 18 MeV in the first case, and about 22 MeV in the second. The neutron spectra of these sources were measured by time-of-flight spectrometry. 13 foils were irradiated in a well-defined geometry in these fields and their activities measured. The differential neutron cross-sections were taken either from ENDF/B-IV, Bayhurst et al [41], Smith and Meadows [42], or BNL-325 [43]. The ratios of measured to calculated activities were determined with an estimated error of $\pm$ 10% except for thermally sensitive reactions, in which case the error could be $\pm$ 15% due to uncertainties in the neutron spectrum

below 800 keV. The two E_d = 16 MeV runs showed an overall standard deviation for the ratios of 10.2% and 11.8%. The one E_d = 14 MeV run showed a standard deviation of 18.2%. This run appeared to show a small bias with the low energy activity ratios being consistently low and the high energy activity ratios being high, though the differences are within experimental errors. Several reactions, e.g. $^{60}Ni(n,p)$, $^{45}Sc(n,\alpha)$, $^{197}Au(n,2n)$ and $^{45}Sc(n,2n)$ showed large discrepancies indicating the need for further work. The unfolded spectra using SAND-II Code and the results of E_d = 16 MeV time-of-flight data agree very well; the E_d = 14 MeV unfolded spectrum was slightly harder as would be expected from the bias in this run.

The status of neutron cross-sections for reactor dosimetry has been recently reviewed by Vlasov, et al [44] and dosimetry methods for fuels, cladding and structural materials discussed [45]. In this reference there are descriptions of attempts to extend dosimetry files to cover the energy range above 20 MeV and extend it to 50 or 60 MeV. These will be discussed in Section 3 of this paper.

2.6 Radiation Damage Effects

Radiation damage effects on solids from neutron irradiation may be due to (i) displacements of the materials' atoms from their initial positions, (ii) gas production, especially of helium and hydrogen, and (iii) non-gaseous transmutation reaction products as a result of nuclear reactions.

2.6.1 Displacement Damage

The displacement damage due to neutron irradiations is described as a two-stage process. A neutron of energy E incident on a target atom scatters from it, transferring to it kinetic energy T. This primary knock-on atom (PKA) in moving through the lattice causes further secondary displacements initiating a cascade of atomic displacements. The details of this cascade, such as the number of displaced atoms $\nu(T)$ and its dependence on T and other parameters, are calculated using models which involve solid-state physics concepts. The first stage of the process is described in terms of the PKA spectrum $\psi_i(E,T)$ (barns/eV) which is defined as the product of $\sigma_i(E)$ and $K_i(E,T)$ where $\sigma_i(E)$ is the energy dependent reaction cross-section for reaction type i and $K_i(E,T)$ is the probability that a interacting neutron of energy E will produce a recoil of energy T through the reaction i. $K_i(E,T)$ depends on the kinematics of the particular reaction and may be calculated from the data on secondary particle angle and energy distributions given in evaluated nuclear data files. The details of the PKA spectrum calculations have been given by a number of authors [46,47,48,49]. Subsequent calculations involve various integrals of different solid-state model dependent parameters over the PKA spectrum and do not concern us in this review.

Since the calculation of the PKA spectrum is the first step in radiation damage analysis and further calculations depend on it, it is interesting to study its sensitivity to the input nuclear data. Such a study has been carried out recently by Gabriel and Bishop [50]. They investigated the sensitivity of PKA spectra and displacement per atom (DPA, see references 44 and 46 for its definition) in iron by changing the energy and angular distribution of secondary neutrons inelastically scattered into the continuum and those that result from (n,2n) reactions. They tried three different angular distributions for the same energy distribution: (1), isotropic in the c- of m system, (2), 75% forward and 25% backward, and (3), that given by $1 + \cos\theta$. They found that the sensitivity of the PKA spectrum and the DPA cross-section to be reasonably large and of the order of $\sim$ 15%. For different secondary neutron spectra (A: ENDF/B-IV (histogram) and B: $\alpha E \exp(-E/T)$ the change in the DPA cross-section is smaller and of the order of $\sim$ 5%. This study is very interesting because, usually, the angular distribution of the secondary neutrons scattered into the continuum is assumed to be isotropic. Though this may be true for the equilibrium part of the secondary neutrons, it is not so for the pre-equilibrium part, as may be seen from the Hermsdorf, et al [51] data and its analysis into its equilibrium and pre-equilibrium parts as a function of angle [52]. Most of the nuclear model codes do not calculate the angular distribution of the pre-equilibrium part correctly except for a recent attempt [53]. It thus appears necessary to treat the angular distribution of the secondary neutrons scattering into the continuum correctly in the evaluated data files and put in forward peaked angular distributions supported by experimental data.

At the BNL Symposium [4] it was recommended that detailed sensitivity analysis of radiation damage parameters to variations in the input nuclear data be carried out. The study by Gabriel and Bishop is a beginning and perhaps a more systematic and detailed investigation should be done. Further, it was recommended that a damage cross-section file and an accepted PKA spectra file endorsed by an official group such as the Damage Analysis and Fundamental Studies Task Group of the Division of Magnetic Fusion Energy of the Department of Energy be established and made available. As yet, there is no standard PKA spectra file. There are two sets of recommended displacement cross-sections for iron, nickel and chromium published by EURATOM [54], and in the U.S.A. [55]; these were recommended at the IAEA Specialists Meeting at Harwell [56]. The EURATOM displacement cross-sections for iron extends only to 10 MeV so it is not applicable to fusion reactors using D-T fuel cycles. The U.S.A. cross-sections based on ENDF/B-IV extend up to 20 MeV and contain in addition, data on Al, V, Cu, Zr, Nb, Mo, Ta, W, Pb and stainless steel.

2.6.2 Gas Production

Data on gas production cross-sections will be part of ENDF/B-V and will be given for 22 materials. These will be based on (n,p),

(n,n'p), (n,d), (n,α), etc., reactions evaluated for the General and Special Purpose Files, and will be consistent with them. Traditionally radiochemical methods were used to measure (n,p), (n,n'p), (n,d) and other cross-sections. Some of the shortcomings of these methods are (i) the final state has to be radioactive, and (ii) one tends to measure a sum of different channels like (n,n'p) and (n,pn') and (n,d) rather than the proton and deuteron producing reactions separately, and (iii) no information on the energy and angular distribution of the outgoing particles is available. Recently a spectrometer for the measurement of (n,xp), (n,xd) and (n,xα) cross-sections, angular and energy distributions of outgoing charged particles for 15 MeV incident neutrons has been developed [57]. With this technique one could also study a mixture of isotopes as in a sample of an element or different types of stainless steels. Results obtained by using this technique are given in references [58] and [59] and compared with evaluations and the results of other measurements. Another new technique uses mass spectrometric methods to determine the helium produced in samples by neutron bombardment [60,61]. This method has not as yet been used to determine hydrogen production. The results of these two methods agree within experimental errors though the mass spectroscopic measurements are slightly higher. In Table III are shown the experimental data of Grimes, et al [59] and of Farrar et al [61] compared with ENDF/B-V evaluations for nickel and chromium isotopes and the elements by Divadeenam [62] and Prince [63] respectively. In general, one can say that where the differential data for the (n,particle) reactions are good the agreement between the data and evaluations is good. If there are no good data and also the nuclear model parameters are not that well-known the evaluations are not reliable and the agreement with measured data is poorer.

He and H production data are needed [11] with 10-50% accuracy for a few neutron energies 9-14 MeV for ^{7}Li, C, Ni, Si, Cu, ^{11}B, Fe, Cr and Pb. Further studies are expected to better define the data accuracies needed.

2.6.3 Non-gaseous Transmutations

These transmutations, over a period of years, can cause a change in the chemical composition of the structural components subjected to intense neutron bombardments with consequent changes in the mechanical properties. Transmutations have been calculated by Vogelsang, et al [64], Kulcinski [65] and others. The data needed for these calculations are in general available in the ENDF/B isotopic evaluations.

2.7 Induced Activity

An estimation of the amount and characteristics of radioactivity induced in the various parts of a fusion reactor is essential to assess the practical problems associated with plant maintenance, radioactive

waste disposal and reactor safety. This also enables one to calculate nuclear afterheat and biological effects associated with the activation products.

There have been a number of calculations of induced activity by Steiner [25], Vogelsang, et al [64], Kulcinski [65] and others. They have also calculated the afterheat and biological hazards after shutdown and made comparative studies of different structural materials. At that time activation and decay data were not part of ENDF/B evaluations. In Version V as part of special applications files, activation and decay data information will be available on relevant reactions. The total number of activation cross-sections which will appear in Version V is about 84. The decay data which will be part of these files will be evaluated or reviewed by C.W. Reich using all available information on the particular decay.

2.8 Radiation Shielding

The neutron data needed for radiation shielding calculations are elastic, inelastic, (n,2n), (n,3n), (n,γ) cross-sections, as well as photon production cross-sections and the angular and energy distribution of the secondary neutrons and gamma-rays. Because of their use in fission reactors, the calculational methods and procedures are well developed and there are a number of benchmarks for shielding. In the following, a brief discussion of this type of benchmark testing will be given to convey some idea of the state of the data and the evaluations.

The results of shielding benchmark testing with ENDF/B-IV data are given in reference [39]. These benchmarks test total cross-sections for a number of shielding materials in the 1-10 MeV range, gamma production cross-sections by thermal neutron capture or that averaged over a fast neutron spectrum from 1-15 MeV. Some of them also check the neutron cross-sections between 2 and 14 MeV by measuring time-of-flight spectra through several mean free paths of a large number of materials. These are all described in the bibliography given in reference [39]. The pulsed sphere experiments [66] have played a significant part in improving the quality of neutron data evaluations because they pointed out for the first time the need to include pre-equilibrium component in the spectrum of secondary neutrons scattered into the continuum. Since they are done with a 14 MeV neutron source in the center of the sphere, they are crucial for testing high energy evaluations needed for fusion reactor design. These experiments are also important for checking the codes and calculational procedures. A program to carry out a series of integral experiments to test the performance of blanket and shield assemblies and extending over a period of five years has been started at ORNL [67]. These experiments will use a 14 MeV neutron source and study deep neutron penetration in bulk media by measuring neutron and gamma-ray spectral data as a check on the experimental and evaluated data as well as the transport calculational methods.

Over a period of several years, the quality and availability of gamma-ray production data for a number of elements has improved. Some of the experimental work done at ORNL has been summarized by Dickens et al [68]. These cross-sections have been measured for $0.3 < E_\gamma < 10.5$ MeV and $0.1 < E_n < 20.0$ MeV for some 22 elements. To extend the data to lower gamma ray energies may be important for heat deposition calculatins involving thin absorber which preferentially absorb the softer gamma rays. Measurements at lower neutron energies would also be helpful as in many cases, one is forced to "extrapolate" from thermal or low energy resonance data into the epithermal region by maintaining energy balance. In many cases where there are no data one has to have recourse to various calculational procedures, two of which will be described below.

The first method is that of Perkins, et al [69] and is based on the observed systematics of gamma-ray production data and establishing an empirical calculational procedure. This is the R-parameter formalism of Howerton and Plechaty [70] for the calculation of (n,xγ) cross-sections and spectra above 4 MeV incident neutron energy. They noticed that for continuum gammas with $E_\gamma > 1$ MeV the experimental spectra follow the shape:

$$N(E_\gamma) \overset{\sim}{\propto} E_\gamma \exp(-R.E_\gamma)$$

where the R-parameter can be determined from experimental data as a function of incident neutron energy. This formalism has been refined and extended to calculate (n,xγ) cross-sections and spectra for each reaction which could then be summed to give the total spectrum. Experimental data could be used to determine R-parameter as a function of excitation energy and in addition to gamma ray spectra one could also calculate electron and x-ray production arising from internal conversion. The results of this procedure are applied to both fissile and non-fissile nuclei [65]. They did find that the technique appears to yeild satisfactory results with data for non-fissioning reactions. It is also found that the fission reaction is not described as well by the R-parameter formalism: rather it is better to use experimental data on prompt gamma rays from thermal fission. The one advantage of this formalism is that it could be used in those cases where the input data needed to run more elaborate nuclear model codes are not readily available. The other procedure is to use various types of Hauser-Feshbach type calculations to determine the gamma production cross-sections and spectra. Examples of these are the work of Gardner [71], Arthur et al [72], Fu [73] and Strohmaier et al [74]. The agreement between the calculations of these codes and the experimental data is quite impressive and these codes represent "state-of-the-art" as it stands now. These codes will be discussed briefly in Section 2.10.

Data for shielding, activation and neutron transport calculations need angular and energy distribution of secondary neutrons for a few selected energies from 9 to 14 MeV for C, Ni, Si, Cu, ^{11}B, Fe, Cr and Pb [11]. The accuracy needed is ± 10%.

2.9 Hybrid Concept

These concepts involve the use of excess neutrons from a D-T fusion reactor to interact with fissile or fertile nuclei in the blanket to produce energy from nuclear fission. The excess neutrons may also be used to burn or transmute troublesome fission product or actinide waste into less harmful or more manageable end products. These concepts have been reviewed by Leonard [75] and Lidsky [30] who have traced the growth of these ideas from the early 1950's into the later detailed design studies and discussed their merits. An up-to-date bibliography of these publications has been assembled by Leonard [76].

These devices may be divided into three categories [30], (i) the hybrid systems in which both fusion and fission events occur in the same device, (ii) the symbiotic - those systems in which fuel is bred for consumption in physically separate fission reactors and in which fission reaction in the fusion blanket are suppressed, and (iii) augean systems in which the fission reactor products are transmuted to less toxic forms.

The neutron data needed for the first two types of systems have been discussed by Wolkenhauer and Leonard [77] in their design studies of the hybrid reactors. Data are needed on neutron producing reactions and fuel breeding reactions. These are the (n,2n), (n,3n) fission and capture reactions. The tritium breeding reactions have been discussed in Section 2.3. Data for these reactions are needed from thermal energies to about 14 MeV. The number of nuclei for which data are needed depends on the complexity of the transmutation chain in a hybrid blanket and may involve, e.g. 15-20 uranium, neptunium and plutonium isotopes in a uranium blanket. The data for all these isotopes are not known equally well. In addition, information on the fission spectrum and its variation with energy and the angular and energy distribution of secondary neutrons are needed. A few illustrative examples of the data accuracies in the current evaluations of U-238 for ENDF/B-V are given to convey some idea of data errors. The less well studied actinides naturally will have larger errors. For U-238 it is estimated [78] that the fission cross-section has an error of about 9% at 0.3 MeV, 12% at 0.6 MeV, decreasing to 3% at 2.5 MeV, 2.4% at 4 MeV and about 4% at 14 MeV. The uncertainty in the capture cross-section is about 9% at 20 keV, 5% at 100 keV and 1 MeV. For the (n,2n) cross-section, the uncertainties are estimated to be less than 10% near the maximum where the cross-section is large; at about 14 MeV the observed data spread lie outside this error band. The (n,3n) data have large error bars and the uncertainty may be $\pm$ 20% or more. The fission spectra and their variation with energy are not well known. The same may also be said about the energy spectrum of secondary neutrons inelastically scattered into the continuum and those due (n,2n) and (n,3n) processes, and the evaluation was guided by macroscopic benchmark tests [78].

Pulsed sphere measurements may be used to check [79] the data evaluations for use in fusion-fission blanket calculations. In these experiments ^{238}U spheres with 3.63 cm and 10.91 cm radius (0.8 m.f.p. and 2.8 m.f.p.) were used with a 14 MeV D-T source in the center. Using the time-of-flight method, neutron spectra from the sphere were recorded and compared with results of calculations using ENDF/B-IV and ENDL evaluations. While neither library yielded good agreement over the whole of the energy range of measrued spectra, ENDF/B-IV agreed well with data for neutrons below 1 MeV and ENDL gave the best agreement with the 2.8 m.f.p. sphere high energy spectra. Similar calculations were carried out with the ENDF/B-V evaluation and the magnitude of the pre-compound component in the inelastic scattering into the continuum adjusted to give acceptable agreement with the pulsed sphere experiments [78]. The Weale experiment [80] can also serve as an integral test of the evaluated files used in fusion-fission calculations. A 14 MeV neutron source was surrounded by a natural uranium metal pile and the 14 MeV flux, the total neutron leakage and the reaction rate distributions for $^{235}U(n,f)$, $^{238}U(n,f)$, $^{238}U(n,\gamma)$ and $^{239}Pu(n,f)$ were measured. This experiment has been analyzed by Haight et al [81] using ENDF/B-III and IV and two different versions of ENDL library. The newer versions of the libraries were found to give total reaction rates differing less than those of the older versions, though there were significant deviations, especially in $^{238}U(n,f)$ rate and in neutron leakage. They ascribe these differences to differences in the neutron emission spectrum from 14 MeV neutrons.

In the augean systems, the fusion device acts as a radioactive waste burner. The radioactive wastes are of two types: (i), the fission products like ^{85}Kr, ^{90}Sr and ^{137}Cs, and (ii) the actinide group made up of transplutonium wastes such as the isotopes of americium and curium derived from successive neutron capture and decay in uranium and plutonium. Typically, the fission products in the first group have short half-lives ($\sim$ 30 years) and low thermal capture cross-sections. The actinides have very long half-lives. The transmutation of fission products in a fusion device could be achieved by means of (n,α), $(n,2n)$ and $(n,3n)$ reactions which transmute them into stable isotopes. The actinides could be changed mainly by the fission process from long-lived highly dangerous heavy elements into fission products of much shorter half-lives.

A detailed analysis of the transmutation in such a system was carried out by Wolkenhauer, et al [82]. They conclude that such burning of waste is possible. The neutron data needed to calculate the fission product transmutations are the $(n,2n)$, $(n,3n)$ and (n,γ) reactions. These data are available with varying accuracies for the nuclei in a transmutation chain. If no data are available, one could try calculating them using either cross-section systematics or nuclear model codes. The first method is used, for example, in the THRESH2 code of Pearlstein [83] and one could calculate, say $(n,2n)$ cross-sections with errors of the order of 20-30%.

However, as one goes away from the line of stability and the measured data which are used in the code are less well known, the calculated cross-section uncertainties would be larger. As regards neutron capture, if the neutron strength function and the average capture widths are known, the average epithermal capture may be calculated with 20-25% uncertainty. It is not possible to calculate thermal capture from a nuclear model. For the actinides fission cross-section, data are needed in addition to (n,2n), (n,3n) and capture cross-sections. These will have to be measured or estimated from the data from an operating system.

2.10 Nuclear Model Codes

Nuclear model codes play an extremely important part in neutron and charged particle evaluations and a few remarks about them appear to be in order. They are essential for filling in the gaps in experimental data or provide guidance where there are no data at all. However, the adequacy of nuclear model codes can be checked and their validation confirmed only by a careful comparison with experimental data. This could also lead to an adjustment of some of the input parameters which are not well known. If the experimental data to check the model and input data are not available, any nuclear model calculations will be less reliable and should be used with caution.

Amongst the nuclear codes available to the data evaluator, some are based on observed data systematics. Examples of these are the code THRESH2 [83] for (n,particle) reactions and the R-parameter formalism [69] of Perkins et al for calculating gamma production cross-sections and spectra. These codes do not need much input information and are of use in calculating, for example, properties of fission product nuclei where very little information on the target nuclei is available. Properties of such nuclei are needed, for example, in calculating fission product burn-up in fusion-fission hybrids.

The pulsed sphere experiments [66] carried out at Lawrence Livermore with 14 MeV neutrons and their analysis gave definite evidence for the presence of a high energy component in the spectrum of secondary neutrons scattered into the continuum. Thus, the temperature model of Weisskopf had to be supplemented by a pre-equilibrium part as given, for example, by the exciton model of Griffin [84]. Later refinements of nuclear models for calculating the pre-equilibrium fraction have recently been reviewed by Blann [85] and most of the nuclear model codes in use currently take into consideration pre-equilibrium emission at least for the first neutron emitted in the reaction. This should be adequate for neutron reactions below 20 MeV. Use of these codes have markedly improved the secondary neutron energy distributions given in evaluated data files. These distributions show better agreement with both differential and integral data. Examples of these may be found in references [72] and [86]. Hansen et al [87] have compared experimental data on secondary neutron

emission spectra from 14 MeV incident neutrons with nuclear model calculations for a number of materials. They found that they had to include contributions from statistical, pre-equilibrium and direct reaction parts to achieve a good fit to the data. Experimental data [51] indicate that the pre-equilibrium part of the secondary neutron distribution is forward peaked as one would expect of a process that lies between the extremes of direct reaction and compound nucleus emission. However, none of the above codes can calculate such forward peaked angular distribution. Recently, claims have been made [88] that a new formalism does predict forward peaked angular distribution for the pre-equilibrium part. A better justification of the physical assumptions of this theory and a systematic comparison of calculations against experimental data should be made to validate this claim.

Recently, there have been a number of multistep Hauser-Feshbach codes [71,72,73,74,89] which can calculate (n,p), (n,n'), (n,α) and (n,d), etc. reaction cross-sections, spectra (and angular distributions for (n,n) and (n,n')) at each step and follow the sequence of reactions for a number of steps. They can also calculate branching ratios to isomeric states, gamma ray production cross-sections and spectra. Use of these codes has resulted in a great improvement in the representation of secondary particle spectra and angular distributions for which there are no data. Following a suggestion of Gruppelaar [90] there have been a number of code comparisons where the same input data are used and the output of different codes checked with a general improvement of this important tool available to the evaluator. These codes need as input experimental data on the energy levels, their spins and parities for the target nucleus, as well as different nuclei which form the intermediate stages of the multi-step cascade. This nuclear structure information may be extracted from ENSDF data files [91] which also have the decay data. Charged particle reaction data can be used to extract optical model parameters for use in neutron cross-section calculations as well as the deformation parameters needed for coupled channel calculations [92] needed to calculate direct reaction contributions.

3. EVALUATED NUCLEAR DATA 20 TO 60 MeV

Materials damage studies for the fusion energy program need an intense 14 MeV neutron source with fluxes $\gtrsim 10^{14} m/cm^2$ sec over large volumes of a few liters. These intense sources of fast neutrons have been reviewed by Lone [93] and by Barschall [94]. There have been several proposals [95] to achieve both the high intensity and the large irradiation volume needed and a Fusion Materials Irradiation Testing (FMIT) facility using a D-Li source is under construction at Hanford Engineering Development Laboratory (HEDL). This facility will have a neutron flux with a peak at about 14 MeV and extending up to about 50-60 MeV neutron energy. Thus, it is essential to have neutron cross-section data and evaluations up to about 50-60 MeV

to be able to interpret the data from this device. Some of these data problems were discussed at a Brookhaven Symposium [4] last year. There were sessions devoted to (i) intense high energy neutron sources and their characteristics, (ii) differential data and experimental techniques, (iii) materials damage studies, (iv) integral experiments and data testing, and (v) data evaluation and nuclear model codes. The subject of each session was discussed in detail in a workshop, its present status reviewed and recommendations for a future course of action made. These workshop reports, along with the review and contributed papers have been published. These reports emphasized the need to determine the neutron energy and angular distribution of these sources using a variety of techniques. This would mean an extension of the dosimetry methods to higher energies and measurement of new cross-section data 20-50 MeV. Since a large number of reaction channels open up at these energies, a measurement of all possible reactions for a large number of materials would be a formidable task. It was, therefore, recommended that a few important reaction cross-sections be measured at a selected number of energies to validate nuclear model codes which could then be used to calculate the cross-sections. A number of nuclear model codes which could be used for this purpose were also discussed. In the following, these problems will be reviewed along with a survey of some current work being done in this energy region.

3.1 Neutron Dosimetry

The dosimetry needs of the materials testing program were discussed by Doran et al [96] and have also been reviewed by Heinrich et al [97]. The main task here appears to be to extend the dosimetry and spectrum unfolding techniques to the energy region 15-50 MeV where the individual dosimetry reactions are not that reliable. Hence, a list of these reactions was drawn up [98] as desirable candidtaes for new measurements. Some of these cross-sections have been measured [41,99] up to 28.0 MeV and the experimental data compared with results of nuclear model calculations showing good agreement.

In order to get a set of nuclear reactions for dosimetry up to E_n = 44 MeV, Greenwood et al [100] extrapolated available evaluations to higher energies, guided by experimental data where available or a variety of calculational aids where there were no data. Integral tests on 30 of these reactions were carried out by activating these foils in the neutron field of a D-Be source formed by E_d = 40 MeV deuterons stopped in a thick beryllium target. The spectrum of this source was measured using time-of-flight methods and the experimentally measured activities were compared with the spectrum integrated values and were found to agree within $\pm$ 10%. The neutron spectra unfolded with the SAND-II code also showed excellent agreement with time-of-flight measurements. Similar unfolding of the spectrum of a D-Be source with E_d = 30 MeV has also been done by Nethaway et al [101] using multiple foil activation, and these measurements are continuing

at other angles [108]. Other experimental techniques that could be used to measure the neutron spectra are the proton recoil counters and time-of-flight techniques. Time-of-flight can measure data from about E_n = 1 MeV and up and the spectrum below 1 MeV could be measured using the $^6Li(n,t)\alpha$ reaction. Another technique that could be used is to measure the total helium produced in an irradiated sample by mass spectrometry. This is being pursued by Farrar and co-workers [102]. A number of wire rings are irradiated in a D-Be source neutron field with E_d = 30 MeV and the spectrum integrated helium production cross-section is measured to evaluate their use as neutron fluence dosimeters. The helium produced is measured with a mass spectrometer and one also obtains helium production cross-sections for this neutron field. Data requests [11] related to dosimetry are for neutron reaction data for selected neutron energies from 1 to 40 MeV for Au, Co, Ni and Fe with 10-20% accuracy from 2-25 MeV and less accurate measurements below 2 MeV and above 25 MeV.

3.2 Radiation Shielding

In constructing FMIT, it is necessary to estimate its shielding requirements. There are two data libraries suited for this purpose - the Los Alamos Library by Wilson [103] and the Oak Ridge Library by Alsmiller [104].

The Los Alamos Library was created for designing shield for neutrons produced by 50 MeV deuterons on beryllium for cancer therapy. It has data for H, B, C, N, O, Si, Fe and W. It is a sixty-group library for transport calculations and includes P_5 cross-sections in standard LASL format. The library combines processed ENDF/B-IV data below 20 MeV joined to higher energy cross-sections calculated with a Los Alamos version of the intranuclear cascade and evaporation model [103]. The nuclear model calculations were adjusted to agree with experimental data where available. The library contains total, elastic (for H only), non-elastic and scattering cross-section data and extends to 60 MeV.

The Oak Ridge Library also extends to 60 MeV and has multigroup cross-sections (47 n-groups, 21 γ-groups) in ANISN format for H, ^{10}B, ^{11}B, C, O, Si, Ca, Cr, Fe and Ni. At P_5-Legendre expansion is used at energies $\geq$ 14.9 MeV and a P_3-Legendre expansion is used below it. Below 14.9 MeV the cross-section are from ENDF/B-IV. Above this energy, differential elastic scattering cross-sections are from optical model calculations and differential non-elastic scattering cross-sections are from the intranuclear cascade and evaporation models [105] are used. The library contains total, elastic, non-elastic cross-sections and gamma-ray production cross-sections only up to 15 MeV.

Data needed [11] for FMIT shielding design are for total, non-elastic cross-sections and angular dependence of elastic scattering cross-

section for a few selected energies between 20-50 MeV with a 10-15% accuracy. The data needs for Fe and O are most urgent; those for Si, Ca and C are less critical.

The Oak Ridge Library is also being used for some materials damage calculations at Brookhaven [109]. Fu and Perey [110] calculated a number of reactions needed for radiation damage studies for Cu, Nb, Al and Au up to 32 MeV with emphasis on the spectra of light particles from binary reactions. Radiation damage calculations using these have also been published [111]

The high energy materials damage calculations need [11] transmutation rates, differential angular distributions for elastic and inelastic scattering cross-sections and the spectra of emitted particles for a few selected neutron energies up to 30 MeV for Fe, Ni, V, Ti, Nb, Cu and Sn with an accuracy of 10-50%. These accuracy requirements will be reassessed from sensitivity studies to be performed.

The following data measurements in the energy region 20-60 MeV are in progress and the data are being analyzed or they will be carried out in the near future. Total cross-sections for Fe and Ca have been measured [112] for E_n = 35, 40 and 50 MeV with an accuracy of 2%. Removal cross-sections have been measured for Fe, H_2O, Ca, C and Si for E_n = 40 and 50 MeV with better than 15% accuracy using the technique of Voss and Wilson [113]. From these data, non-elastic cross-sections for these energies may be extracted [112]. The spectra of secondary neutrons have been measured for ten angles between 0°-150° and for E_d = 35 MeV deuterons stopped by a thick lithium target using time-of-flight method between E_n = 2-50 MeV. It is also planned to cover the lower energy region up to 2 MeV by this method. These measurements were made at the Crocker Nuclear Laboratory (UCD) as a joint project with HEDL to provide data for FMIT. There are plans [112] to measure differential elastic scattering on oxygen for a number of energies in the same energy range. Activation cross-sections of a number of materials will be measured under d and n bombardment to estimate activation of FMIT components and determine the best course of action for servicing it. For E_n = 27.4, 39.7 and 60.7 MeV and targets of ^{12}C, ^{14}N and ^{16}O, the spectra of emergent charged particles, e.g. p, d, t, ^3He, and α have been measured as a function of angle between 15°-150° at the Crocker Nuclear Laboratories [114]. Total cross-sections for ^6Li, ^7Li, and C have been measured from 20-50 MeV with a 2% accuracy at the National Bureau of Standards [115]. ^4He total cross-section has also been measured from 21 to 23 MeV in connection with the D-T reaction studies. Experiments are being set up at Ohio University [116] to measure (n,xp), (n,xα) and other charged particle cross-sections using a spectrometer similar in design to the one at Lawrence Livermore Laboratory [57]. Data will be measured on Ni, Cr, Fe and other structural materials up to E_n = 26 MeV. Charged particle cross-sections of ^{12}C, ^{14}N and ^{16}O will also be measured for medical applications [116]. J.A. Harvey et al [117] have measured the total cross-section of ^7Li from about 100 eV to 40 MeV.

4. SUMMARY

In this review, a number of fusion reactor related applications of mostly neutron cross-section data have been discussed. It is noted that charged particle cross-sections, nuclear structure and decay data are also needed for these applications. A sound data base of experimental measurements is necessary to support a credible data evaluation which could also be checked against well planned integral experiments. Some of these comparisons do indicate disagreements which have to be clarified by further work. Some immediate data needs for different applications are also given. Nuclear model codes have played an important part in providing complete evaluations below 20 MeV and are expected to play an even greater role in the energy region from 20-60 MeV. However, they have to be checked against experimental data at least at a few energy points; therefore new data measurements are needed. Refinements in nuclear model codes may also be necessary to allow for those effects which are not important below 20 MeV. A more realistic estimate of effort along these lines can be carried out only by using results of sensitivity studies on radiation damage effects. This has yet to be done. Format changes in data files may also be necessary to accommodate greater details of data representation and more refined physics. This is being considered for the ENDF data files and significant work has been done on a generalized format [118]. A new cycle of evaluations is also being planned and the fusion community is invited to offer any suggestions for improvement or requests for categories of data not yet included in the data files.

5. ACKNOWLEDGEMENTS

It is my pleasure to thank the following colleagues for sending me reprints and preprints of their unpublished data or clarifying some points of their work:
D.G. Gardner, S.M. Grimes, M.W. Guinan, R.C. Haight, R.J. Howerton, S.T. Perkins (LLL); E.D. Arthur, G.M. Hale, L. Stewart, P.G. Young (LASL); R.G. Alsmiller, C.Y. Fu, T.A. Gabriel, M.T. Robinson (ORNL); D.G. Doran, D.L. Johnson, F.M. Mann, R.E. Schenter (HEDL); T.S. Subramanian (UCD); R.A. Schrack (NBS); H. Farrar (AI); B.R. Leonard (BNW); M.A. Abdou (Georgia Tech); L.R. Greenwood (ANL); M.A. Lone (CRNL); T. Burrows, M. Divadeenam, C.L. Dunford, A.N. Goland, B.A. Magurno, S. Pearlstein, A. Prince (BNL).
I would also like to thank Bonnie McNair for her efficient and excellent job of typing.

REFERENCES

[1] SCHMIDT, J.J., Nuclear Data, Their Importance and Evaluation. Lectures presented at the Course on Nuclear Theory for Applications held at the International Center for Theoretical Physics, Trieste, Italy, 1978.

[2] COHEN, M.M. and ZWILSKY, K.M., Proc. of the International Conf. on Radiation Test Facilities for the CTR Surface and Materials Program, ANL/CTR-75-4 (1975). Argonne National Laboratory

[3] STIEGLER, J.O. and REUTHER, T.C., BNL-NCS-50681, p. 51, 1978.

[4] BHAT, M.R. and PEARLSTEIN, S. (Eds.), Symposium on Neutron Cross-Sections from 10 to 40 MeV, BNL-NCS-50681 (1977).

[5] STEINER, D., Proc. of a Conf. on Nuclear Cross-Sections and Technology, NBS Special Pub. 425, Vol. II, p. 646, 1975.

[6] MUENZEL, H., Charged Particle Nuclear Data for Fusion and Other Reactions, Proc. of this meeting.

[7] STEWART, L. and HALE, G.M., The T(dn)^{4}He and T(t,2n)^{4}He Cross-Section at Low Energies, USNDC-CTR-2 (1975).

[8] HALE, G.M., Private Communication (1978).

[9] HALE, G.M. and YOUNG, P.G., Private Communication (1978).

[10] SANTORO, R.T. and BARISH, J., Nuc. Sci. & Eng. 59, 189 (1976).

[11] Compilation of Requests for Nuclear Data, compiled and edited by the National Nuclear Data Center, BNL, to be published (1979).

[12] LAMAZE, G.P., et al, BNL-NCS-24273, DOE/NDC-12/U, p. 176 (1978).

[13] JARMIE, N., et al, BNL-NCS-24273, DOE/NDC-12/U, p. 114 (1978).

[14] McNALLY, Jr., J.R., ORNL-TM-4575 (1974).

[15] WEAVER, T., et al., UCRL-74191 (1972).

[16] MOREAU, D.C., Nuc. Fusion 17, 13 (1977).

[17] HALE, G.M., et al, BNL-NCS-24273, DOE/NDC-12/U, p. 129 (1978).

[18] Equipe TFR, Nucl. Fusion 18, 647 (1978).

[19] HENDEL, H.W., TFTR Neutron Diagnostics by Time and Energy Resolved Fast-Neutron Spectroscopy, TFTR-2, Plasma Physics Laboratory (1976).

[20] ALSMILLER, R.G., et al, Nuc. Sci. & Eng. 57, 122 (1975).

[21] STEINER, D. (Ed.) The Status of Neutron-Induced Nuclear Data For Controlled Thermonuclear Research Applications. Critical Reviews of Current Evaluations. USNDC-CTR-1 (1974).

[22] STEINER, D., and TOBIAS, M., Nuc. Fusion 14, 153 (1974).

[23] HOWERTON, R.J. and PERKINS, S.T., Nuc. Sci. & Eng. 65, 201 (1978).

[24] HOWERTON, R.J. and MacGREGOR, M.H., UCRL-50400, Vol. 15, Part D, Rev. 1, May, 1978.

[25] STEINER, D., Nuc. Fusion 14, 33 (1974).

[26] ABDOU, M.A. and CONN, R.W., Nuc. Sci. & Eng., 55, 256 (1974).

[27] BARTINE, D.E., et al., Nuc. Sci. & Eng. 53, 304 (1974).

[28] POWELL, J.R., FILLO, J.A., TWINING, B.G. and DORNING, J.R. (Eds.) Proc. of the Magnetic Fusion Energy Blanket and Shield Workshop ERDA-76/117/1 Conf-76 0343, Vol. I, p. 40 (1976).

[29] MUIR, D.W., WYMAN, W.E., in Technology of Controlled Thermonuclear Fusion Experiments and the Engineering Aspects of Fusion Reactors, USAEC Conf-72111 p. 910 (1974).

[30] LIDSKY, L.M., Nuc. Fusion 15, 151 (1975).

[31] HERZING, R., et al, Nuc. Sci. & Eng. 60, 169 (1976).

[32] BACHMANN, H., et al, Nuc. Sci. & Eng. 67, 74 (1978).

[33] ABDOU, M.A. and MAYNARD, C.W., Nuc. Sci. & Eng., 56, 360, 381 (1975).

[34] GARBER et al, Data Formats and Procedures for the Evaluated Nuclear Data File, ENDF. ENDF-102 (1975).

[35] ALSMILLER, R.G., et al, Nuc. Technology 34, 376 (1977).

[36] ARCIPIANI, B., et al, Nuc. Sci. & Eng. 65, 540 (1978).

[37] STEINER, D., Nuc. Fusion 14 33 (1974).

[38] MAGURNO, B.A., (Ed.), ENDF/B-IV Dosimetry File, BNL-NCS-50446 (1975).

[39] BOHN, E.M., et al (Eds.), Benchmark Testing of ENDF/B-IV, BNL-NCS-21118, Vol. I and II, (ENDF-230) (1976).

[40] GREENWOOD, L.R. et al, Nuc. Technology 41, 109 (1978).

[41] BAYHURST, B.P. et al, Phys. Rev. 12C, 451 (1975).

[42] SMITH, D.L. and MEADOWS, J.W., Nucl. Sci. and Eng. 58, 314 (1975), Nucl. Sci. and Eng. 60, 187 (1976), ANL/NDM-13 (1975) and ANL/NDM-26 (1976).

[43] GARBER, D.I. and KINSEY, R.R., BNL-325 (Third Edition) Vol. II (1976).

[44] VLASOV, M.F., et al, Proc. of the International Conf. on the Interaction of Neutrons with Nuclei. Lowell, (1976) CONF-760715-P2, p. 1186.

[45] MORGAN, W.C. (Chairman), Proc. of the Second ASTM-EUTATOM Symposium on Reactor Dosimetry, NUREG/CP-0004, Vol. I, II & III (1977).

[46] JENKINS, J.D., Nuc. Sci. & Eng. 41, 155 (1970).

[47] DORAN, D.G., Nuc. Sci. & Eng. 49, 130 (1972).

[48] GABRIEL, T.A., et al, Nuc. Sci. & Eng. 61, 21 (1976).

[49] ODETTE, G.R. and DOIRON, D.R., Nuc. Technology 29, 346 (1976).

[50] GABRIEL, T.A. and BISHOP, B.L., Nuc. Sci. & Eng. 68, 94 (1978).

[51] HERMSDORF, D., et al, ZFK-277, Zentralinstitut für Kernforschung (1974).

[52] PEARLSTEIN, S., Private Communication (1978).

[53] MANTZOURANIS, M. AGASSI, D. and WEIDENMULLER, H.A., Phys. Letters 57B, 220 (1975).

[54] GENTHON, J.P., et al, Comission of the Euratom Communities Report, EUR 5274, (1975).

[55] DORAN, D.G. and GRAVES, N.J., ASTM-STP611, pp. 463-482 (1976).

[56] Proc. of the IAEA Specialists Meeting on Radiation Damage Units, Harwell, England, November 1976.

[57] ALVAR, K.R., et al, Nucl. Inst. and Methods 148, 303 (1978)

[58] HAIGHT, R.C. et al, Nuc. Sci. & Eng. 63, 200 (1977).

[59] GRIMES, S.M., et al, UCRL Preprint-81802 (1978).

[60] FARRAR IV, H., et al, BNL-NCS-50681, p. 175 (1977).

[61] FARRAR IV, H., et al, Trans. Am. Nucl. Soc. 28, 197 (1978).

[62] DIVADEENAM, M., Private Communication (1978).

[63] PRINCE, A., Private Communication (1978).

[64] VOGELSANG, W.F., et al, Nuc. Technology 22, 379 (1974).

[65] KULCINSKI, G.L., Plasma Physics and Controlled Nuclear Fusion Research, 1974. Fifth Conf. Proc. Tokyo 1974, Vol. II, p. 251, (1974).

[66] HANSEN, L.F., et al, BNL-NCS-50681, p. 403 (1977).

[67] ALSMILLER, R.G., Private Communication (1978).

[68] DICKENS, J.K., et al, Nuc. Sci. & Eng. 62, 515 (1977).

[69] PERKINS, et al, Nuc. Sci. & Eng. 57, 1 (1975).

[70] HOWERTON, R.J. and PLECHATY, E.F., Nuc. Sci. & Eng. 32, 178 (1968).

[71] GARDNER, D.G., NBS Special Publication 425, Vol. II, p. 651 (1975).

[72] ARTHUR, E. and YOUNG, P.G., BNL-NCS-50681, p. 467 (1977).

[73] FU, C.Y., Atomic Data and Nucl. Data Tables 17, 127 (1976).

[74] STROHMAIER, et al, Nucl. Sci. & Eng. 65, 368 (1978).

[75] LEONARD, Jr., B.R., A Review of Fusion-Fission (Hybrid) Concepts BNWL-SA-4706. See also Nucl. Technology 20, 161 (1973).

[76] LEONARD, Jr., B.R., Bibliography of Fusion-Fission Hybrid Publications, PNL-SA-6492 (1978).

[77] WOLKENHAUER, W.C. and LEONARD, Jr., B.R. Nuclear Data in Science and Technology, Proc. of a Symposium, Paris (1973), Vol. I, p. 39 (1973).

[78] POENITZ, W. et al, ANL/NDM-32 (1977).

[79] WONG, C. et al, NBS Special Publication 425, Vol. II, p. 704 (1975).

[80] WEALE, J.W. et al, Jour. Nucl. Energy A/B 14, 91 (1961).

[81] HAIGHT, R.C. et al, Nucl. Sci. & Eng. 61, 53 (1976).

[82] WOLKENHAUER, W.C., LEONARD, Jr., B.R. and GORE, B.F., BNWL-1772, (1973).

[83] PEARLSTEIN, S., J. Nucl. Energy 27, 81 (1973). Code available from Argonne Code Center.

[84] GRIFFIN, J.J., Phys. Rev. Lett. 17, 478 (1976).

[85] BLANN, M. Preequilibrium Decay, Ann. Rev. of Nucl. Sc. 25, 123 (1975).

[86] FU, C.Y., BNL-NCS-50681, p. 453 (1977).

[87] HANSEN, L.F., et al, Nuc. Sci. & Eng. 61, 201 (1976).

[88] MANTZOURANIS, G., WEIDNEMULLER, H.A. and AGASSI, D.Z., Physik A276, 145 (1976).

[89] MANN, F.M. and SCHENTER, R.E., BNL-NCS-50681, p. 485, (1977).

[90] PRINCE, A., Nuclear Theory in Neutron Nuclear Data Evaluation, Vol. I, p. 31 (1976) IAEA-190.

[91] EWBANK, W.B. and SCHMORAK, M.R., ORNL-5054/R1 (1978).

[92] TAMURA, T., Rev. Mod. Phys. 37, 679 (1965).

[93] LONE, M.A., BNL-NCS-50681, p. 79 (1977).

[94] BARSCHALL, H.H., Intense Sources of Fast Neutrons, Preprint of Paper prepared for Ann. Rev. of Nucl. Sci., Vol. 28 (1978)

[95] PERSIANI, P.J. (Chairman), Proc. of the International Conf. on Radiation Test Facilities for the CTR Surface and Materials Program, ANL/CTR-75-4, Argonne National Laboratory (1975).

[96] DORAN, D.G., et al, BNL-NCS-50681, p. 321 (1977).

[97] HEINRICH, R.R., et al, Proc. of the Second ASTM-EURATOM Symposium on Reactor Dosimetry NUREG/CP-0004, Vol. III, p. 1017 (1977).

[98] GOLAND, A.N., BNL-NCS-50681, p. 29 (1977).

[99] VEESER, L.R. et al, Phys. Rev. 16C, 1792 (1977).

[100] GREENWOOD, L.R., HEINRICH, R.R., SALTMARSH, M.J. and FULMER, C.D., "Integral Tests of Neutron Activation Cross-Sections in a $^{9}Be(d,n)$ Field at E_d = 40 MeV" to be published.

[101] Nethaway, D.R. et al, BNL-NCS-50681, p. 135 (1977).

[102] FARRAR IV, H. et al, Private Communication (1978).

[103] WILSON, W.B., LA-7159-T (1978).

[104] ALSMILLER, Jr., R.G. and BARISH, J., ORNL-TM-6486 (1978).

[105] BERTINI, H.W., Phys. Rev. 6C, 631 (1972).

[106] FABRY, A. et al, Nucl. Technology, 25, 349 (1975).

[107] HARKER, Y.D. et al, Fission Product and Reactor Dosimetry Studies at Coupled Fast Reactivity Measurements Facility, TREE-1259 (1978) E.G.&.G., Idaho, Inc.

[108] GUINAN, M., Private Communication (1978).

[109] GOLAND, A.N., Private Communication (1978).

[110] FU, C.Y. and PEREY, F.G. Jour. Nucl. Materials 61, 153 (1976).

[111] ROBERTO, J.B., ROBINSON, M.T. and FU, C.Y., Jour. Nucl. Materials 63, 460 (1976).

[112] JOHNSON, D.L. (HEDL), Private Communication (1978).

[113] VOSS, R.G.P. and WILSON, R., Proc. Roy. Soc. A236, 41 (1956).

[114] SUBRAMANIAN, T.S., Private Communication (1978) and Bull. Am. Phys. Soc. 23, p. 943 (1978).

[115] SCHRACK, R., Private Communication (1978).

[116] GRIMES, S., Private Communication (1978).

[117] HARVEY, J.A., et al, BNL-NCS-24273, p. 229 (1978).

[118] DUNFORD, C.L., Private Communication (1978).

TABLE I

EVALUATED NEUTRON DATA LIBRARIES

LIBRARY	COUNTRY	DESCRIPTION
A.A.E.C.	Australia	Cross-section data for fission product nuclides
C.E.N. Compilation	France	Compilation of properties of fission products
ENDF/B	U.S.A.	General cross-section data set
ENDL	U.S.A.	Fast reaction cross-section data set
JENDL	Japan	General cross-section data set
KEDAK	Fed. Rep. of Germany	Fast reaction cross-section data set.
SOKRATOR	U.S.S.R.	General cross-section data set
UKNDL	U. Kingdom	General cross-section data set
Los Alamos Library	U.S.A.	Neutron multigroup data $E_n \leq 60$ MeV
Oak Ridge Library	U.S.A.	Neutron-photon multigroup data $E_n \leq 60$ MeV

TABLE II

CONTENTS OF ENDF/B LIBRARY

DATA TYPE	ENDF/B-I 1967	ENDF/B-II 1970	ENDF/B-III 1972	ENDF/B-IV 1974	ENDF/B-V 1979
General Purpose	48	52	69	90	117
Lumped Fission Products	9	9	9	9[a]	9[a]
Thermal Scattering Data	7	7	7	7[a]	7[a]
Fission Products		55	55	825	825
Photon Production			11	42	53
Photon Interaction			yes	yes	yes
Standards			7	7	7
Dosimetry				36	36
Decay Data				825	932
Data Covariance				3	65+
Actinides					40
Gas Production					22
Activation					84

a. Available in ENDF/B-III format only.

TABLE III

PROTON, DEUTERON AND ALPHA-PARTICLE EMISSION

CROSS SECTIONS FOR E_n = 15 MeV

TARGET	P		D		^{4}He		^{4}He
	Expt[a] mb	Evaln mb	Expt[a] mb	Evaln mb	Expt[a] mb	Evaln mb	Farrar[b] mb
^{50}Cr	830±100	811	12±4	5	94±15	105	
^{52}Cr	108±25	165	8±3	∿ 0	36±6	85	
Cr	180±25	179	10±3	0.3	38±6	80	
^{58}Ni	1000±120	1008	14±6	29	106±17	194	
^{60}Ni	325±40	190	11±4	2	76±12	53	
Ni	790±100	752	13±5	21	97±16	150	98±6

a. S.M. Grimes et al, UCRL-Preprint-81802 (1978).

b. H.Farrar and D.W. Kneff, Trans. Am. Nuc. Soc. 28, 197 (1978).

NEUTRON REACTION DATA IN THE MeV RANGE

AG-159/B4
Review Paper

H. LISKIEN

CBNM Geel, Belgium, JRC of the CEC

Abstract

The energy range and reaction types of relevance for neutron reaction data for fusion reactors are shortly discussed followed by a summary of the presently available methods to determine such data. Principal deficiencies are underlined and examples, typical for the data status are given.

SCOPE

Concerning neutron energies one would think that energies up to 14.1 MeV are relevant here. However, the usual assumption of emission of a 14.1 MeV neutron from a D-T plasma is unprecise. A Monte Carlo calculation [1] shows (see Fig. 1) that for inclusion of neutrons with at least 5 % of the maximum intensity, energies up to 15 MeV have to be included. There is however an essential field which perhaps demands data for even much higher energies namely microscopic neutron cross sections for the interpretation of material damage under intense neutron irradiation. If the necessary intense neutron source for radiation damage studies is not built based on the T(d,n)-reaction [2] but based on the Li(d,n)-reaction [3] then the produced neutron spectrum will extend to ≈ 40 MeV and the relevant microscopic data for the interpretation of the results will also be needed up to that energy.

Concerning reaction types a breakdown according to application subfields is given in Table 1. The rare reactions (n, 2p), (n, d), (n, ^{3}He) and (n, t) will not be regarded; of course with the exception of the breakup reaction ^{6}Li(n, t)^{4}He and ^{7}Li(n, n't)^{4}He due to their special importance for tritium breeding. (n, np)-and (n, nα)-reaction can reach the same size as those for (n, p) and (n, α).
Only a few relevant isotopes have (n, 3n) thresholds below 15 MeV. However it has been suggested [4] to use Au(n,xn) with x = 2, 3, 4, 5 simultaneously as dosimetry reactions in case of an INS based on Li(d,n). Gold is a monoisotopic element and the mentioned reactions all lead to radioisotopes of convenient half life and radiation.

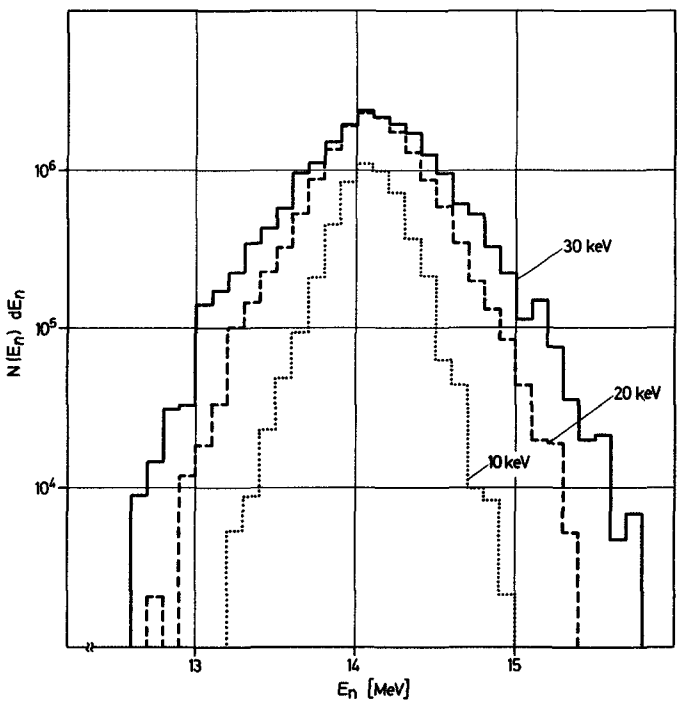

Fig. 1. The neutron spectrum to be expected from a d-t plasma at 10, 20 and 30 keV temperature. The integral over each spectrum is proportional to the average fusion cross section at the given temperature.

Concerning the materials of interest (fuel, coolant, structural materials, magnet system, moderator, reflector, multiplier etc.) the relevant part of WRENDA [5] still contains a broad spectrum of materials covering a large part of the periodic table. Instead of reviewing the status of data for all these materials I decided to review the presently available ex-

Table 1 : Relevant reaction types and their application subfield.

	(n,p)	(n,np)	(n,2n)	(n,3n)	(n,t)	(n,α)	(n,nα)
tritium breeding					x		
neutron multiplication			x	x			
neutron shielding	x	x	x	x		x	x
heating/cooling	x	x	x	x		x	x
activation/transmutation	x	x	x	x		x	x
gas production	x	x			x	x	x
radiation damage	x	x	x	x		x	x

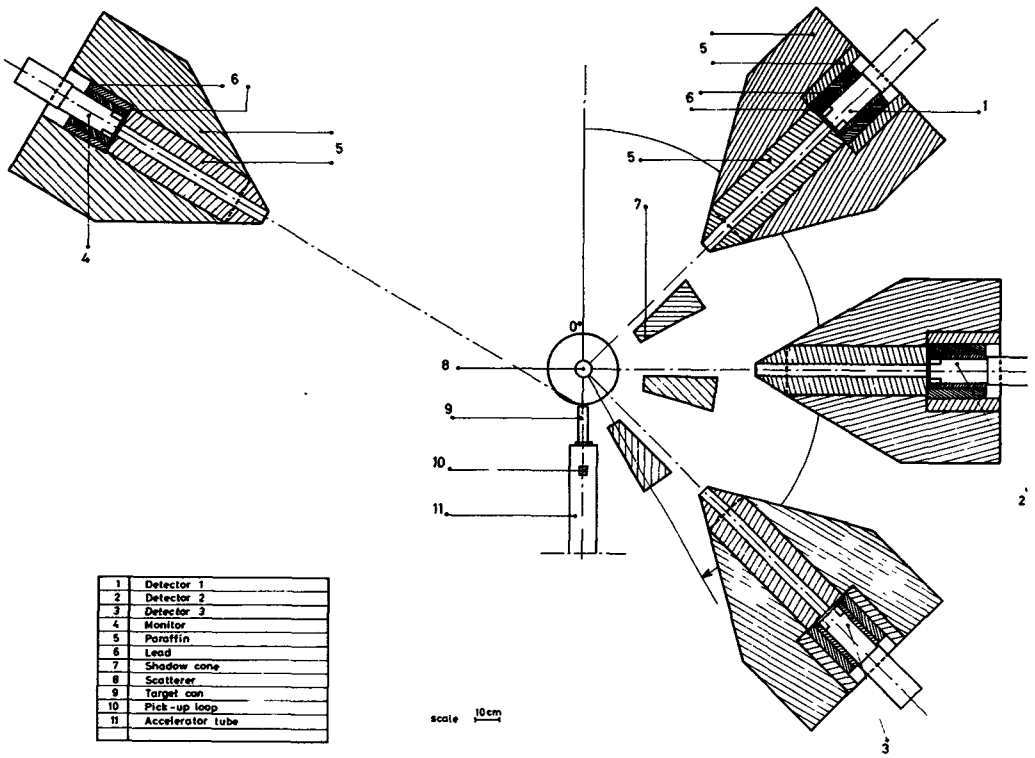

Fig. 2. A typical set-up [6] to determine double differential neutron emission cross sections using TOF spectrometers.

perimental set-ups to determine such data. This approach underlines the principal deficiencies, does not anticipate the findings of the earlier papers of this meeting, and allows a concept-independent view. Typical examples on the corresponding data status are given at the end of the paper.

NEUTRON TOF - SPECTROMETER

Looking with a neutron TOF spectrometer at a sample which itself is bombarded with pulsed monoenergetic neutrons allows to determine double differential (with respect to emission angle and secondary neutron energy) neutron emission cross sections.

A typical set-up [6] is given in Fig. 2. Normally this method is applied below the (n,2n) threshold delivering the double differential scattering cross section and therefore will be discussed in the following paper [7]. The fact that the method does not allow the separation between (n,n'), (n,2n) and (n,3n) events in certain regions of secondary neutron energy should not prevent the application of this method also above the (n,2n) threshold. Many neutronics calculations do not request as input data separated (n,n'), (n,2n) and (n,3n) cross sections but may be run with neutron emission cross sections.

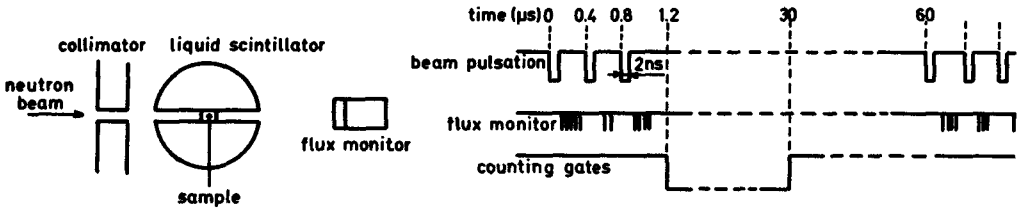

Fig. 3. A typical set-up [13] to determine partial neutron emission cross sections using a big scintillator tank.

Applied above the (n,2n)-threshold and with two detector systems in coincidence the method allows to study energy and angular correlations of the emitted neutrons. However, with neutron sources nowadays available, this application suffers from low count rates and has therefore mainly applied to ^{9}Be(n,2n) and at 14 MeV [8].

NEUTRON MODERATION METHOD

This method delivers the partial neutron emission cross sections for the emission of x = 2, 3, 4 etc. neutrons. It does not distinguish between neutrons from a (n,xn)-process and x neutrons from the fission process. No information on the energy spectrum and the angular distributions are obtained.

The method has been developed at Livermore [9] and Aldermaston [10] and is now routinely applied at Los Alamos [11] and Bruyères-le-Châtel [12]. A typical set-up [13] is given in Fig. 3. A monoenergetic pulsed and collimated neutron beam from a Van de Graaff accelerator is passing a through-tube of a big scintillator tank in the center of which the material of investigation is placed. After having irradiated the sample material for 1.2 μs the counting gates of the photomultipliers viewing the gadolinium loaded scintillator are opened for 30 μs. Neutrons emitted from the sample are moderated in the scintillator and eventually captured by the gadolinium, producing a 9 MeV γ-cascade transformed to scintillation light. Data have to be corrected for natural and accelerator dependent background, for dead time losses and the detector efficiency, which typically is determined using ^{252}Cf-neutrons. Background conditions are such that (n,n') events cannot be evaluated, (n,2n) events have to be corrected for two (n,n') events occuring in the same gate period. If fissionable materials (e.g. for hybrids) are studied, then the method per se does not distinguish between a (n,2n)-process and a fission process with $\nu = 2$; of course similar for (n,3n) and $\nu = 3$. For many neutronic calculations this distinction may be unimportant. If not, the fission part may be found out by replacing the ordinary sample material with a fission chamber containing the same material and demanding coincidences. The so obtained ν-distribution may be normalized for higher multiplicities, for which (n,xn) processes are energetically excluded, and used to substract fission events with lower multiplicity.

GAS EXTRACTION

The method delivers gas production cross sections. Evidently no distinction of (n,α) and (n,nα), for example, is possible and no information on the energy spectrum is obtained. The gas may stem from the produced charged particle (p,d,^{3}He,t,^{4}He) or may be produced as residual nuclei.

For non-radioactive gases the method employs post-irradiation high-sensitive mass spectrometry. Helium production, when boron is irradiated in a fast breeder reactor (EBR II), has been investigated [14], also the ^{3}He/^{4}He-ratio, when materials are irradiated in the broad neutron spectrum (11.5-43.5 MeV) of a thick target Be(d,n) source on a cyclotron [15]. Helium production in aluminium, iron and copper has been used for fluence mapping at RTNS-I, the most intense 14 MeV source nowadays available, for fluence mapping and results compared to those of foil activation [16]. In general one may say that the sensitivity of the method is not sufficient to obtain neutron energy dependent He-production cross sections with the available neutron sources.

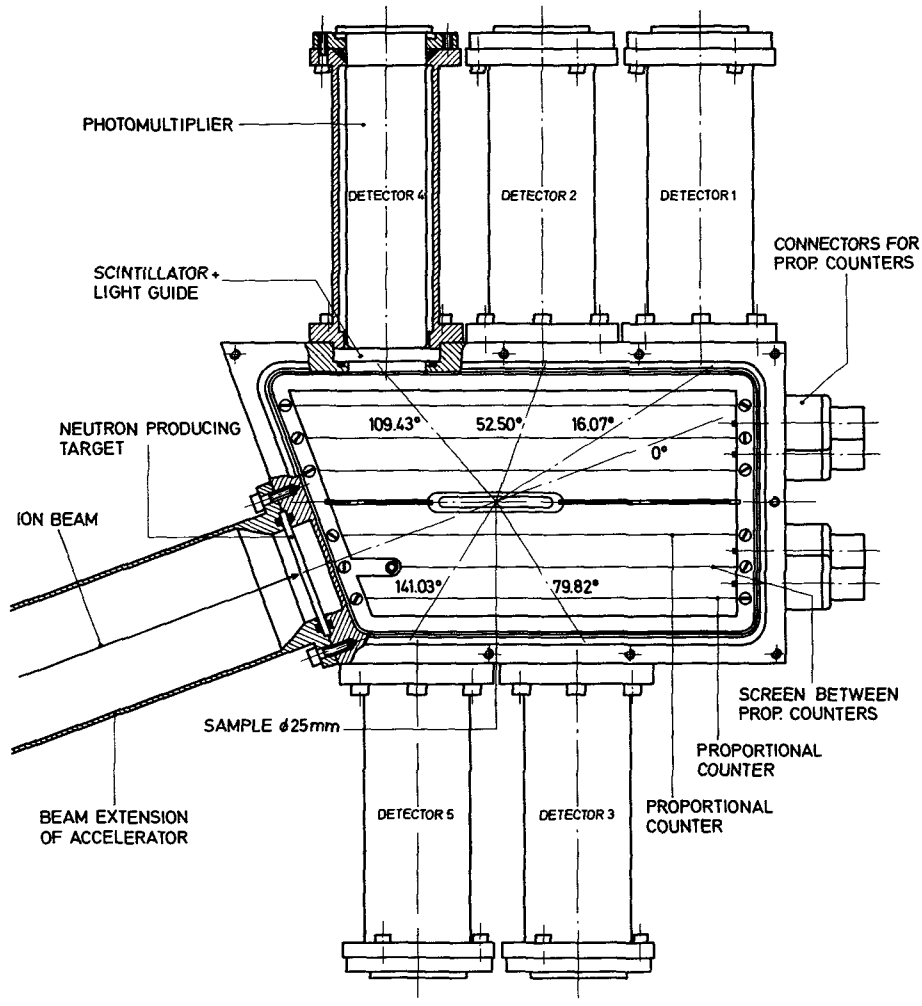

Fig. 4. A multi-angle telescope counter arrangement to determine charged particle emission cross sections [23].

Much higher sensitivities can be obtained if the extracted gas is radioactive with suitable half-life and the mass spectrometric measurement is replaced by radioactivity determination. This technique has been applied for tritium production cross sections at 14 MeV [17-19]. Although neutron sources away from 14 MeV are weaker, the same method can and should be applied for lower energies, especially to determine the tritium production cross section of ^{6}Li and ^{7}Li. To this end Uttley et al. [20] are using Li_2CO_3 enriched to 99.97 % in ^{7}Li. The tritium produced according to the reaction $^{7}Li(n,n't)^{4}He$ is converted to HTO and measured by β-counting after mixing with a suitable liquid scintillator.

The gas extraction method combined with radioactivity determination may also be applied if the residual nucleus of a nuclear reaction is a radioactive gas. Using radio gas chromatography and internal gas proportional counting this method has been applied in case of the reaction $^{40}Ca(n,\alpha)^{37}Ar$ [21] at 14.6 MeV. Again, the same method should be applicable also for lower energies and for a few other reactions leading to radio active gases.

DIRECT OBSERVATION OF CHARGED PARTICLES

Direct observation of charged particles emitted from material under neutron bombardment allows in general to determine double differential (with respect to emission angle and charged particle energy) cross sections.

However, in principle this demands that the sample material has to be thin compared to the range of the charged particles and that possibilities exist to discriminate against other charged particles (and gammas)

which may be produced by neutrons in the sample, the structural material of the sample/detector housing or in the detector itself. Technically it is difficult to realize a 4π geometry. Both points, thin sample and the geometry, are only partly compensated by the efficiency of 1 for the charged particle detector. Therefore, the difficulties in performing such experiments are (1) the low count rates and (2) the background discrimination. Consequently most of the existing measurements have been performed around 14 MeV, where with the 110 keV T(d,n) resonance an intense neutron source is available. These experiments will be described in a later paper [22].

If, however, the charged particle detector can serve at the same time also as sample, then the intensity problem can easily be overcome and background events from the detector housing are of minor importance. Integration over all emissionangles is performed by the method itself and the results are differential (with respect to the particle energy) cross sections [23]. In this way ^{3}He, ^{10}B, ^{14}N (counting gas) ^{6}Li, ^{39}K, ^{40}Ca, ^{127}Cs (scintillators) ^{28}Si, ^{73}Ge (solid state detectors) and ^{7}Li, ^{14}N, ^{16}O (emulsions) have been studied.

Triggered by the importance of neutron induced helium production in structural material of fast fission reactors the CBNM Geel of Euratom has implemented a programme to determine (n,α)-cross sections below 14 MeV [24]. As neutron source the D(d,n) reaction at 0° is used by bombarding a deuterium gas target with accelerated deuterons from a 7 MeV single stage Van de Graaff machine. Fig. 4 shows the constructed multi-angle telescope. Two 25 mm diameter metal foils (for example Cr, Fe, Ni etc.) of about 3 mg/cm^2 thickness are mounted on both sides of a backing on a movable slide in the centre of the chamber. Charged particles emitted from these foils are observed in five energy counters positioned under 16, 52, 80, 109 and 141° extending solid angles between 40 and 160 msr. Two pairs of proportional counters on each side of the foils working with 50 Torr CO_2 are serving as energy loss counters. Typical coincidence resolution is between 300 and 500 ns. The five E-signals and the two combined dE/dx-signals from each side are fed into a modern 8-parameter data acquisition system (ND 6660) for further analysis. At first the chamber was used with the neutron source as near as possible to the chamber (source-foil distance 6.5 cm) and scintillators as E-counters. Although this geometry results in maximum count rates the random coincidence rate was unacceptable high. At present the system is running with a brass collimator between source and chamber (source-foil distance 30 cm) which allowed also to replace the scintillators by silicon surface barrier detectors. Data taking has started for nickel.

NEUTRON ACTIVATION METHOD

The method is applicable for all reactions relevant for this paper, if a radioactive residual nucleus with suited half-life and radiation is produced. The reaction rate are determined not by the number of emitted particles but by the number of produced residual nuclei and this via their characteristic decay. The result is a cross section integrated over all emission angles and energies. If sample material in its natural isotopic composition is used the induced activity may be allocated to different reactions, for ecample $^{46}Ti(n,p)^{46}Sc$ and $^{47}Ti(n,d)^{46}Sc$. The method is unable to distinguish between (n,d), (n,np) and (n,pn)-processes.

A, the activity at the end of a neutron irradiation, is related to the integrated reaction rate R by

$$R = A \frac{T}{1 - \exp(-\lambda T)}$$

$$R = A/\lambda \quad \text{if} \quad \lambda T \ll 1$$

$$R = AT \quad \text{if} \quad \lambda T \gg 1 \quad \text{(saturation)}$$

T is the irradiation time and λ the decay constant of the residual nucleus. This relation assumes a time constant neutron flux : a correction factor can be easily calculated, if this is not the case.

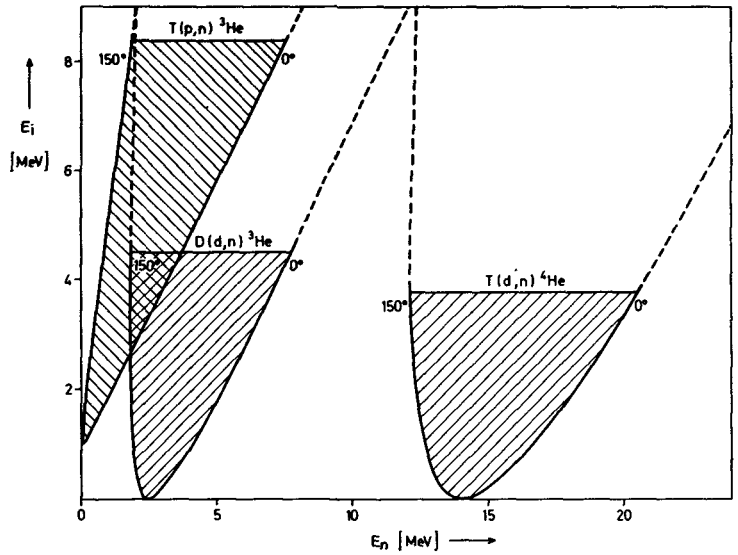

Fig. 5. Obtainable neutron energy as function of ion energy and neutron emission angle for the reactions $T(p,n)^3He$, $D(d,n)^3He$ and $T(d,n)^4He$. Strictly monoenergetic neutrons are obtained only in the hatched areas.

With decreasing cross section and increasing half-life the method becomes more and more difficult to apply. Using chemical separation S.M. Quaim [25] succeeded in the determination of $(n, {}^3He)$ cross section as small as 3 μb while the excitation function for the reaction $^{63}Cu(n,\alpha)$ leading to the 5.2 y ^{60}Co have been determined at Geel [26-27]. Induced activities in this case were in the order of pCi/g and demanded low-level counting using γ-γ coincidence techniques. When extreme short half-lives are involved, attention must be paid to rapid transport between the place of irradiation and the counting position. When determining the $^6Li(n,p)^6He(0.8\,s)$ cross section, R. Prasad and D. C. Sakar used a sample-transferring rabbit [28] device. Another possibility is not to move the sample but to pulse the source, a method which has been successfully applied by R. H. August and H. O. Menlove when determining delayed neutron [29] production cross sections for the $^9Be(n,p)^9Li(170ms)$ reaction. In general whenever it is feasible γ-counting is prefered compared to β-counting, especially since the availability of Ge(Li) detectors. In many cases the application of radiochemical separation methods increases the sensitivity of the activation method considerably [30].

NEUTRON SOURCES

Only in special cases of the direct observation of charged particles a "white" pulsed neutron source can be employed together with energy determination of the primary neutron by time-of-flight. In all other cases the methods of relevance here demand the availability of monoenergetic neutron sources which are typically produced employing the hydrogen reactions $T(p,n)^3He$, $D(d,n)^3He$ and $T(d,n)^4He$. Fig. 5 shows the obtainable neutron energy as function of ion energy and neutron emission angle. If care is taken that no neutrons are produced in the target backing or beam stop then these neutrons are strictly monoenergetic in the hatched areas. For higher ion energies break-up neutrons from the reactions T(p,np)D, D(d,np)D, T(d,np)T and $T(d,2n)^3He$ are complicating the measurements. The absence of experimental data in the 6 to 12 MeV neutron energy region is most often due to the small number of accelerators suited for neutron work and covering the needed ion energy range of 5 to 8 MeV. Break-up neutrons and neutrons from parasitic (d,n)-processes add to the difficulties.

DATA STATUS

The following remarks strictly disregard the 14 MeV range as this is a different paper to be presented at this meeting [22]. It refers to neutron energy dependent data sets which may however include the 14 MeV range. The bulk of 14 MeV results may help to clear up discrepancies between such sets or allow renormalization.

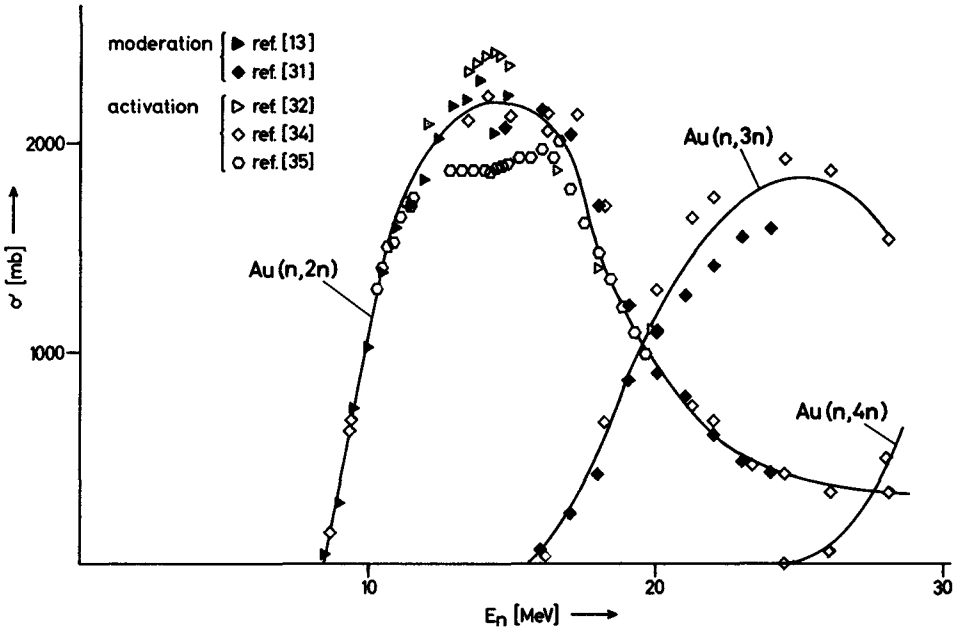

Fig. 6. Available cross sections for the reaction $^{197}Au(n,xn)$ x = 2,3,4 obtained by moderating and capturing the neutrons in a big scintillator tank [13, 31] or by activation [32,34,35].

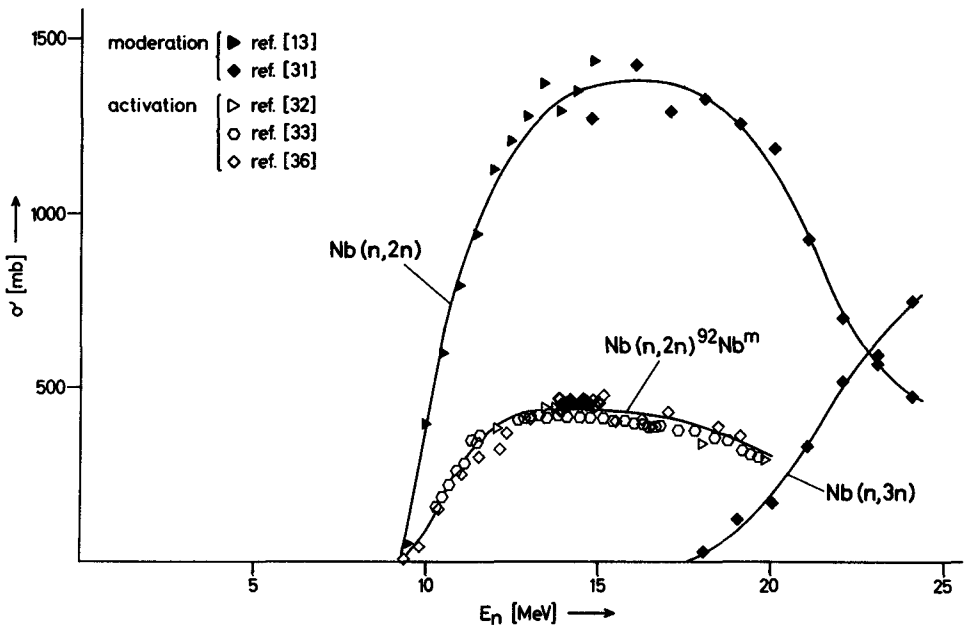

Fig. 7. Available cross sections for the reaction $^{93}Nb(n,xn)$ x = 2,3 obtained by moderating and capturing the neutrons in a big scintillator tank [13,31]. Data obtained by activation [32,33,36] are the partial (n,2n) cross section leading to the 10.5 days isomeric state of ^{92}Nb.

(n,xn)-RESULTS

Cross sections integrated over the secondary neutron spectrum and over the emission angles are obtained via the moderation method or via activation. As example Figs. 6 and 7 show results for the monoisotopes gold and niobium. Full signs refer to moderation [13,31], open signs refer to activation [32 - 36]. Typical uncertainty for the results of both methods is $\approx \pm 7$ %. The curves represent eye-guides through the data to distinguish (n,2n), (n,3n) and (n,4n) results; for no means they should be taken

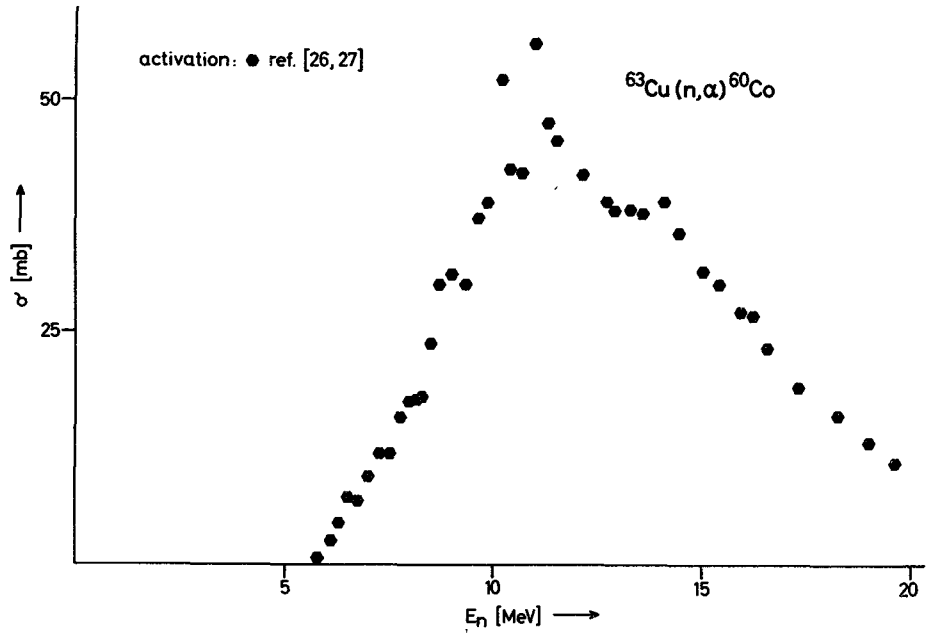

Fig. 8. Available cross sections for the reaction $^{63}Cu(n,\alpha)^{60}Co$ [26,27]. In cases where only one data set is available, a second measurements should be encouraged.

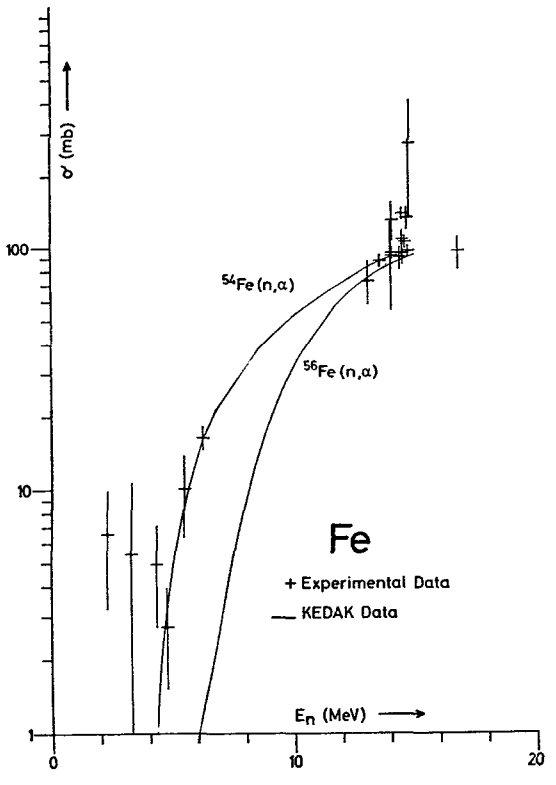

Fig. 9. (n,α)-cross sections available for the main isotopes of iron as compiled in ref. [40].

as an evaluation. For Au(n,2n) the scatter of results around 14 MeV exceeds the ± 10 % level. For Nb(n,2n) the activation method is delivering only the partial cross section for the population of the 10.5 d isomeric state in ^{92}Nb. Experimental information on angular-and energy-distributions and correlations are completely missing. Even if one disregards the distinction between (n,n'), (n,2n) and (n,3n) and looks for double differential emission cross sections similar to those which Hermsdorf et al. [37] determined at 14.6 MeV, one has to realize that above the (n,2n)-threshold such experimental information is not existing. The recent work of Drake et al. [38] on beryllium at 5.9, 10.1 and 14.2 MeV specifically carried out for controlled fusion reactor applications, is more an exception proving the rule.

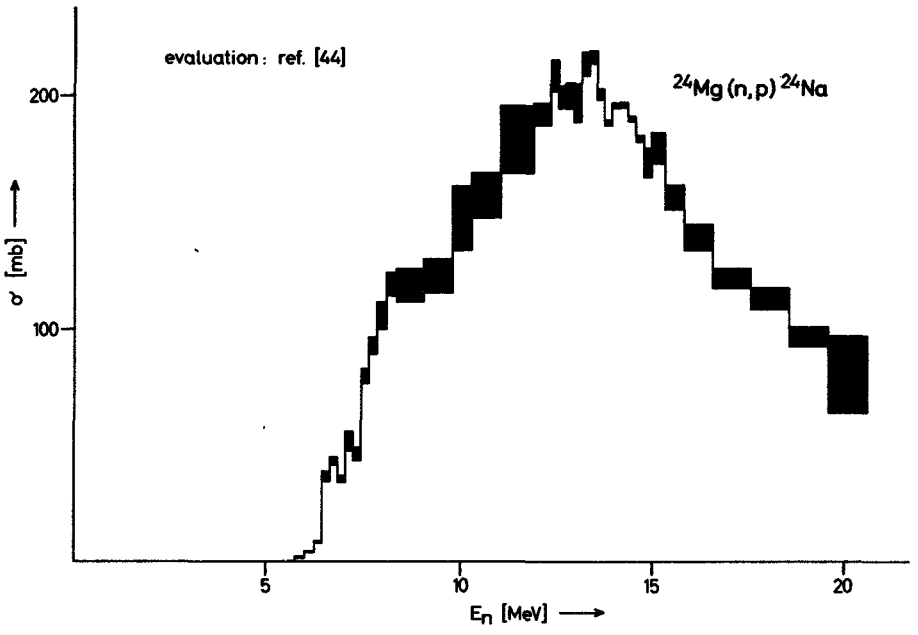

Fig. 10. Results of a recent evaluation [44] for the reaction ^{24}Mg(n,p)^{24}Na.

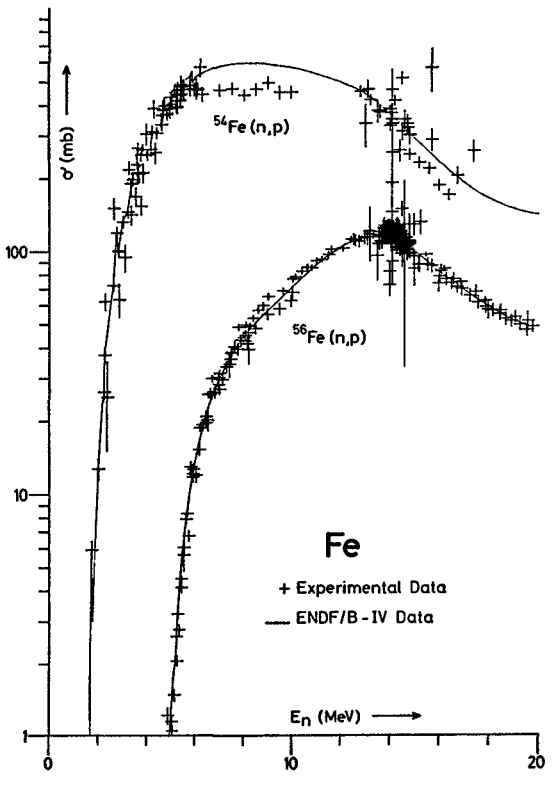

Fig. 11. (n,p)-cross sections available for the main isotopes of iron as compiled in ref. [40].

(n,α) + (n,nα)-RESULTS

As has been shown above, the method of gas extraction is too insensitive, and direct observation of the emitted α-particles is difficult with respect to intensity and background. At present our knowledge is entirely based on results from the activation method. Existing excitation functions have been recently compiled [39]. The best known of these excitation functions is that for Al(n,α) which may reach an accurary of ± 4 % and is used even as standard for relative measurements. Very often only one set of data is available as for example for ^{63}Cu(n,α) [26,27] shown in Fig. 8. This reaction is of importance not only for gas production in copper, but also for production of long living activity (^{60}Co). In all such cases at least one further measurement should confirm the presently available results.

Fig. 9 has been taken from a contribution [40] to a recent specialists meeting in which neutron data of structural materials for fast fission reactor were discussed. $^{54}Fe(n,\alpha)$ can be studied by the activation method and at present data are taken at Geel. Information for nickel and chromium are not existing. (n,nα)-reactions have been studied only by activation for ^{51}V, ^{65}Cu, ^{71}Ga, Cs, I [41, 42] and by charged particle detection in scintillators (sample = detector) for Na [43] and ^{39}K [41].

(n,p) + (n,np)-RESULTS

All the general remarks made above for the (n,α) + (n,nα)-results are also valid here. Fig. 10 shows results of a recent evaluation on $^{24}Mg(n,p)$ [44]. Although we are dealing here with a well-studied reaction, one finds back the 'data gap' between 8 and 12 MeV, here manifested by increased uncertainties. (n,p) data for the main isotopes of iron and nickel are shown in Figs. 11 and 12. They stem again from ref. [40]. No data are available for the chromium isotopes. Two discrepant data sets for $^{58}Ni(n,np)$ [45,46] exist and (n,np) results for all titanium isotopes [47] obtained by activating enriched material.

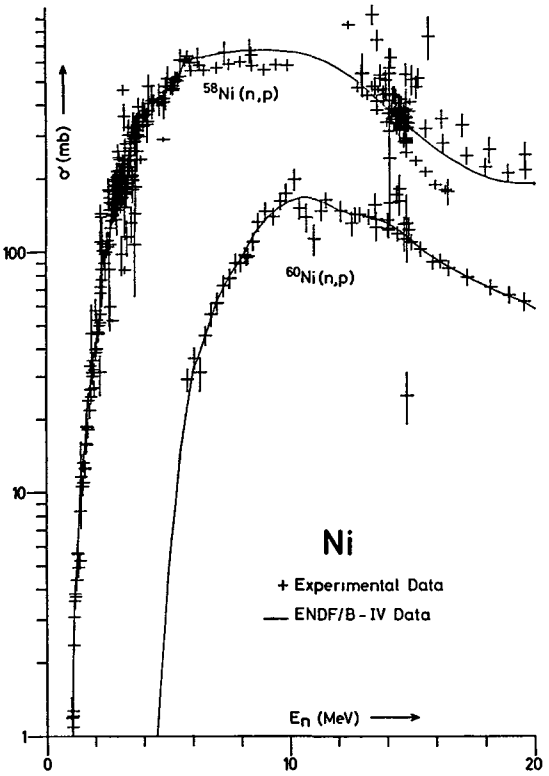

Fig. 12. (n,p)-cross sections available for the main isotopes of nickel as compiled in ref. [40].

Li(n,t)-RESULTS

The reaction $^{6}Li(n,t)^{4}He$ below the 240 keV resonance is one of the few accepted neutron cross section standards [48]. Therefore the reaction has been studied very intensively below 500 keV. Data above this energy are plotted in Fig. 13. The confusion in the 1 to 4 MeV range, which existed when the low values of Clements and Rickard [49] and the high values of Friesenhahn et al. [50] were published, has been cleared up in the mean time by new data published by several groups [51-54, 59-60]. Compared to the importance for the breeding ratio the data status for $^{7}Li(n,t)$ must be regarded as poor.

New results may be expected from Harwell [20] where the tritium extraction method is used. At Ohio university work is going on to determine the angle integrated elastic and inelastic (478 keV) cross section [63] which - together with the total cross section - allows to deduce the (n,t) contribution.

CONCLUSIONS

The 14.1 MeV neutron 'line' is in fact broadened by ± 1 MeV. To cover the full range of neutron energies in the original spectrum, data taking should not stop at 14.1 MeV but should extend to 15.0 MeV

Concerning neutron data relevant for material damage, the neutron energy range is governed by the intense neutron source applied. In case of a Li(d,n) source neutrons with energies up to ≈ 40 MeV are produced. Data above 20 MeV are very sparse.

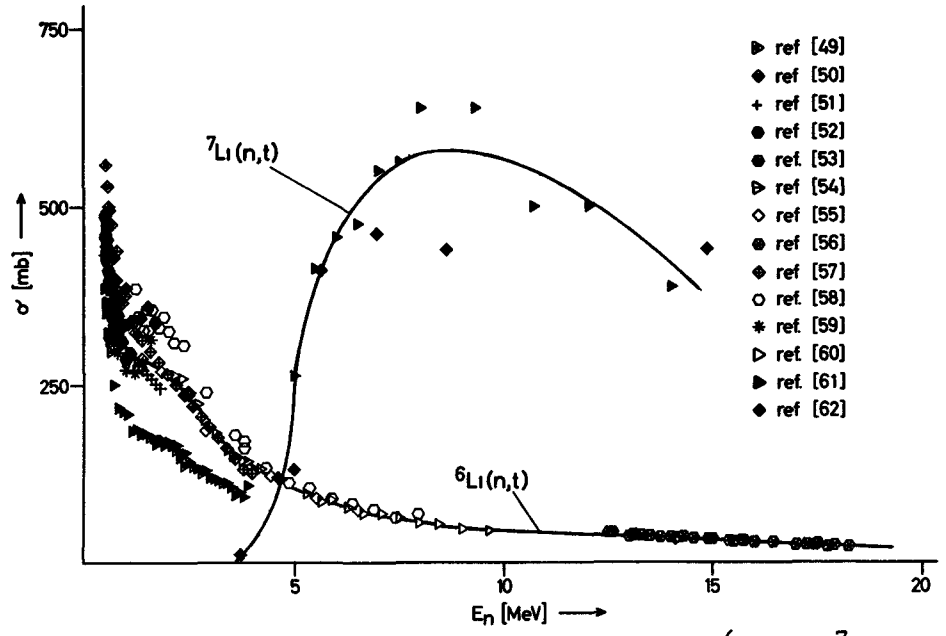

Fig. 13. Available tritium production cross section for ^{6}Li and ^{7}Li above 500 keV [49 - 62]. Work goes on to improve the situation for $^{7}Li(n,n't)$ [20,63].

Nearly all available methods to determine (n,2n), (n,3n), (n,α), (n,p) etc. cross sections demand the use of "monoenergetic" neutron sources. However, there are no pure monoenergetic sources available for neutron production in the 7.7-12.2 MeV range. This and the reduced interest in energies above ≈ 8 MeV for the field of fast fission breeder reactors is responsable for the typical data gap (8-12 MeV). Our knowledge on break-up neutrons from T(p,n) and D(d,n) should be improved.

Nearly no experimental information on angular and energy distribution of neutrons from (n,2n) and (n,3n) processes exist. For many applications such distributions for the total neutron emission are sufficient. This information can be obtained employing neutron TOF-spectrometers. Work also above the (n,2n)-threshold should be encouraged.

With the exception of a few 14 MeV results (n,p), (n,np) and (n,α) and (n,nα) cross sections are experimentally known only if the activation method is applicable. This lack of knowledge on such gas production data seem to be most serious.

The tritium production cross sections of ^{7}Li is unsufficiently known.

REFERENCES

[1] LISKIEN, H., to be published.

[2] BATTAT, M., DIERCKX, R., EMIGH, C.R., Neutron Cross-Sections from 10 to 40 MeV (Proc. Symposium Brookhaven 1977) NNDC Brookhaven (1977) 185.

[3] SALTMARSH, M.J., WORSHAM, R.E. Report ORNL-TM 5233 (1976).

[4] SMITH, A.B., private commucication (1978).

[5] LESSLER, R.M., editor, WRENDA 76/77 World Request List for Nuclear Data, INDC(SEC)-55/URSF.

[6] KNITTER, H.-H., COPPOLA, M., ISLAM, M.M., AHMED, N., JAY, B., Prompt Fission Neutron Spectra (Proc. Cons. Meeting 1971) IAEA Vienna (1972)41.

[7] PEREY, F.G., this Advisory Group Meeting

[8] BOUCHEZ, R., GONDRAND, J.C., PERRIN, P., PERRIN, G., GIORNI, A., DARVES-BLANC, R., QUIVY, P., Nuclear Data for Reactors (Proc. Conf. Paris 1966) 1, IAEA, Vienna (1967) 211.

[9] ASHBY, V.J., CATRON, H.C., NEWKIRK, L.L., TAYLOR, C.J., Phys. Rev. 111 (1958) 616.
[10] MATHER, D.S., PAIN, L.F., Report AWRE 047/69(1969).
[11] VEESER, L.R., ARTHUR, E.D., Neutron Physics and Nuclear Data for Reactor and other Applied Purposes (Proc. Conf. Harwell 1978) to be published.
[12] FREHAUT, J., MOSINSKI, G., Report CEA-R-4627(1974).
[13] FREHAUT, J., MOSINSKI, G., Nuclear Cross Sections and Technology (Proc. Conf. Washington 1975) 2, NBS Washington (1975) 855.
[14] FARRAR, H. IV, McELROY, W.N., LIPPINCOTT, E.P., Nucl. Techn.25 (1975)305.
[15] QAIM, S.M., WÖLFLE, R., to be published.
[16] FARRAR, H. IV, KNEFF, D.W., BRITTEN, R.A., HEINRICH, R.R., Neutron Cross-Sections from 10 to 40 MeV (Proc. Symposium Brookhaven 1977) NNDC, Brookhaven (1977) 175.
[17] QAIM, S.M., WÖLFLE, R., Nucl. Phys. A 295 (1978) 150.
[18] BIRO, T., SUDAR, S., MILIGY, Z., DEZSO, Z., CSIKAI, J., J. Inorg. Nucl. Chem. 37 (1975) 1583.
[19] SUDAR, S., BIRO, T., CSERPAK, F., CSIKAI, J., Nuclear Data for Reactor and other Applied Purposes (Proc. Conf. Harwell 1978) to be published.
[20] UTTLEY, C.A., COOKSON, J.A., SWINHOE, M., Report INDC(UK)-30/U (1978).
[21] QAIM, S.M., RUSHEED, A., STÖCKLIN, G., WÖLFLE, R., Int. J. appl. Radiat. Isotopes, 28(1977)585.
[22] CSIKAI, J., this Advisory Group Meeting.
[23] LISKIEN, H., Nuclear Cross Sections and Technology (Proc. Conf. Washington 1975) 1, NBS Washington (1975) 156.
[24] PAULSEN, A., Report INDC(EUR)-11/G bis (1978).
[25] QAIM, S.M., J. Inorg. Nucl. Chem. 36 (1974) 239.
[26] LISKIEN, H., PAULSEN, A., Nukleonik 8 (1966) 315.
[27] PAULSEN, A., Nukleonik 10 (1967) 91.
[28] PRASAD, R., SARKAR, D.C., Nuovo Cim. 3A (1971) 467.
[29] AUGUSTSON, R.H., MENLOVE, H.O., Nucl. Sci. Eng. 54 (1974)190.
[30] QAIM, S.M., Neutron Physics and Nuclear Data for Reactor and other Applied Purposes (Proc. Conf. Harwell 1978) to be published.
[31] VEESER, L.R., ARTHUR, E.D., YOUNG, P.G., Phys. Rev. C 16 (1977) 1792.
[32] PRESTWOOD, R.J., BAYHURST, B.P., Phys. Rev. 121 (1961) 1438.
[33] PAULSEN, A., WIDERA, R., Z. Physik 238 (1970) 23.
[34] BAYHURST, B.P., GILMORE, J.S., PRESTWOOD, R.J., WILHELMY, J.B., JARMIE, N., ERKKILA, B.H., HARDEKOPF, R.A., Phys. Rev. C 12 (1975) 451.
[35] PAULSEN, A., LISKIEN, H., WIDERA, R., ATKE 26 (1975)34.
[36] NETHAWAY, D.R., J. Inorg. Nucl. Chem. 40 (1978) 1285.
[37] HERMSDORF, D., MEISTER, A., SASSANOFF, S., SEELIGER, D., SEIDEL, K., SHAHIN, F., Report ZfK-277 (Ü), INDC(GDR)-2/L(1975).
[38] DRAKE, D.M., AUCHAMPAUGH, G.F., ARTHUR, E.D., RAGAN, C.E., YOUNG, P.G., Nucl. Sci. Eng. 63 (1977)401.
[39] BORMANN, M., NEUERT, H., SCOBEL, W., "Handbook on Nuclear Activation Cross Sections" p. 139 IAEA (1974).
[40] PAULSEN, A., Neutron Data of Structural Materials for Fast Reactors (Proc. Specialists Meeting 1978). Pergamon Press (1979)261.
[41] BORMANN, M., CIERJACKS, S., LANGKAU, R., NEUERT, H., Z. Physik 166 (1962)477.
[42] SANTRY, D.C., BUTLER, J.P., Can. J. Phys. 44 (1966)1183.
[43] WÖLFER, G., BORMANN, M., Z. Physik 194 (1966) 75.
[44] TAGESEN, S., VONACH, H., STROHMAIER, B., to be published.
[45] JERONYMO, J.M.F., MANI, G.S., OLKOWSKY, J., SADEGHI, A., WILLIAMSON, C.F., Nucl. Phys. 47 (1963) 157.
[46] TEMPERLEY, J.K., Nucl. Sci. Eng. 32 (1968) 195.
[47] PAI, H.L., Can. J. Phys. 44 (1966) 2337.
[48] DERRIEN, H., EDVARSON, L., Neutron Standards and Applications (Proc. Symposium Gaithersburg 1977) NBS Special Publication 493 (1977) 14.
[49] CLEMENTS, P.J., RICKARD, I.C., Report AERE R-7075 (1972).

[50] FRIESENHAHN, S. F., ORPHAN, V. J., CARLSON, A. D., FRICKE, M. P., LOPEZ, W. M., Report INTEL-RT-70011-001(1974).
[51] OVERLEY, J. C., SEALOCK, R. M., EHLERS, D. H., Nucl. Phys. A221 (1974)573.
[52] POENITZ, W. P., Z. Physik 268 (1974) 359.
[53] GAYTHER, D. B., Ann. Nucl. Energy 4 (1977) 515.
[54] LAMAZE, G. P., SCHRACK, R. A., WASSON, O. A., Nucl. Sci. Eng. 68 (1978)183.
[55] RIBE, F. L., Phys. Rev. 103 (1956)741.
[56] KERN, B. D., KREGER, W. E., Phys. Rev. 112 (1958) 926.
[57] GABBARD, F., DAVIS, R. H., BONNER, T. W., Phys. Rev. 144 (1959)201.
[58] MURRAY, R. B., SCHMITT, H. W., Phys. Rev. 155(1959) 1707.
[59] FORT, E., MARQUETTE, J. P., Report EANDC(E) 148 "U" (1972).
[60] BARTLE, G. M., Nuclear Cross Section and Technology (Proc. Conf. Washington 1975) 2, NBS Washington (1975) 688.
[61] ROSEN, L., STEWART, L., Phys. Rev. 126 (1962) 1150.
[62] BROWN, F., JAMES, R. H., PERKIN, J. L., BARRY, J., Reactor Sci. Techn. (J. Nucl. Energy A/B) 17 (1963) 137.
[63] KNOX, H., WHITE, R., LANE, R., Report INDC(USA)-79/U (1978).

STATUS OF 14 MeV NEUTRON CROSS SECTION DATA

AG-159/B6
Review Paper

J. CSIKAI
Institute of Experimental Physics, Kossuth University,
Debrecen, Hungary

ABSTRACT. The review outlines the present status of total, elastic, nonelastic and partial nonelastic [(n,xn), (n,charged), (n,f), (n,γ)] cross sections for 14 MeV neutrons. Systematics in the data as well as the theoretical and semi-empirical approximations are also discussed.

INTRODUCTION

Recent studies on fusion reactors show that the D+T→^{4}He+n reaction will probably be used to release the thermonuclear energy in the D-T-Li fuel cycle. A lithium blanket around the plasma is required for the tritium regeneration via the ^{7}Li(n,n't)^{4}He and ^{6}Li(n,t)^{4}He reactions. In the D+T fusion about 80 % of the total energy is carried off by the 14 MeV neutrons; therefore, the investigations on the interaction of fast neutrons with structural materials are of primary importance for the design of the reactor. Because intense 14 MeV neutron sources are not available at present for the engineering testing of the working conditions of fusion reactors, neutron data are needed for the calculations of the tritium breeding, radiation damage effects, radiation shielding, neutron multiplication, isotope production, energy deposition in the first wall and superconducting magnet, fission reaction and fissile fuel breeding in the fusion-fission hybrid systems, etc. [1,2,3].

The expected structural materials that will be used in fusion reactors, along with their functions are summarized in Table I [4]. This compilation shows that about one third of the elements are considered in one form or another as structural materials, so it is worthwile to survey the status of 14 MeV neutron cross section data.

The majority of the recent fast neutron cross section data has been determined for D+T neutrons in the interval of 13.5-15 MeV and similarly to the earlier measurements, in most cases the activation method was used. Haight [26] has given a review on the neutron data for incident energies between 10 and 40 MeV. A plot of the number of cross section vs. atomic number of the target shows that for differential elastic scattering and neutron emission the data are very scanty in the interval of $55 \leq Z \leq 70$.

For threshold reactions the cross section curves change significantly around 14 MeV which may be a reason of the large

spread in the data published by different authors. The neutron energy depends on the emission angle especially in the case of D+T reaction. If $E_d \simeq 200$ keV, the angular variation of energy is $\Delta E_n \gtrsim 1.5$ MeV, therefore the apparent cross section depends

Table I.

Materials that will be damaged during operation in thermonuclear reactors

Material function	Typical examples
Structural components of first wall and blanket	Austenitic stainless steels (Fe,Cr,Ni,Mn,Mo,Ti,C)
	Nickel-based alloys: PE 16, Inconel, Incoloy (Ni,Cr, Mo,Nb,Fe,Si,Al,Mn,C,S,P,etc.)
	Refractory metals (V,Nb,Mo or alloys of those metals with Ti,Zr or Cr)
	Sintered aluminium product, silicon carbide, graphite
Reflection, moderation	Graphite, D_2O
Neutron multiplication	Be, BeO
Breeding	Li, Li_2O, $Li_2Al_2O_4$, Li-Al, LiF, BeF_2
Radiation shielding	B, B_4C, Pb austenitic steel
Electric insulation (especially for pulsed reactors)	Al_2O_3, MgO, Y_2O_3
Optics for laser systems	Windows: Ge, alkali halides, chalcogenides (GaAs, CdSe)
	Mirrors: Al, Al-7178, Al-Ni, Be-Ni, Be-Cu
Thermal insulation (for superconducting magnets)	Mylar or other hydrocarbons
Superconduction stabilizing materials	Cu, Al
Superconduction magnet filaments	NbTi, Nb_3Sn, V_3Ga
Magnet-support structure (below 10 K)	Austenitic steel
Redox couple	CeF_3/CeF_4, UF_3/UF_4
Cryogenic refrigerant	He

on the position and dimension of the samples. In order to obtain comparable results for the observation of any trend in the data, well defined energies are needed for the measurements. For normalization, the angular interval from 93°-103° seems to be acceptable in which the energy spread of neutrons does not exceed a few ten keV, resulting in negligible errors in the cross sections [5]. These data would serve as standard points

for the cross section curve. The choice of standard reference data has a great importance; at 14 MeV the n-p elastic scattering, the $^{27}Al(n,\alpha)$ and $^{93}Nb(n,2n)$ cross sections are widely used. The advantage of $^{93}Nb(n,2n)$ reaction is that its excitation function is flat around 14 MeV. The cross section curve for $^{27}Al(n,\alpha)$ reaction has been determined by Vonach et al.[30] with an uncertainty of less than 1 %. The $^{235}U(n,f)$ and $^{238}U(n,f)$ processes are used as fission standard cross sections.

In this review the total, elastic, non-elastic, inelastic, reaction, fission and capture cross section data for the $13 \leq E_n \leq 15$ MeV interval are discussed, without making an effort for the completeness. This interval covers the range of the primary neutron spectrum to be expected from a D+T plasma of temperature T=30 keV. Liskien [25] has pointed out that the 14.1 MeV line is strongly broadened and has a width of about 2 MeV if neutrons with at least 5 % of the maximum intensity are included (see Fig. 1).

TOTAL NEUTRON CROSS SECTIONS

Among fast neutron data the total cross sections are the most complete and accurate, so they give reliable information on the average properties of nuclei. The σ_T values measured by different authors are approximately consistent with the given errors. Although there are some exceptions, on average the inconsistency does not exceed 1 %. There are no data at 14 MeV for the following elements: Ru, Rh, Po, At, Rn, Fr, Ra, Ac, Pa and for most of the stable isotopes. The white neutron sources based on cyclotrons, electron linacs and tandem generators have been used in the last decade for the measurements of $\sigma_T(A,E)$ (see Refs. in [26]). Some work on the determination of σ_T for the isotopes of Ti, Ni, Cr, Cu, Zn, Ag, Cd, In, Sn, Sb, Te, Nd, Sm and Gd elements has been done at 14.2 MeV by Dukarevich et al. [7,8,9]. They found, in agreement with the prediction of the "black nucleus" formula $\sigma_T = 2\pi(R+\lambda\!\!\!^{-})^2$ that for a given element the cross section increase smoothly with increasing atomic weight of its isotopes.

The $\sigma_T(A)$ data at Z = const. can be approximated by straight lines with an average slope of $\Delta\sigma \approx 2.3 \cdot 10^{-2}\ \Delta A$ barn.

In our earlier investigation [6] it was found that the ratio of $\sigma_T^{exp}/2\pi(R+\lambda\!\!\!^{-})^2$ shows a sinusoidal form as a function of $A^{1/3}$ and can be well described by the following empirical expression (dashed curve in Fig. 2):

$$\frac{\sigma_T^{exp}}{2\pi(R+\lambda\!\!\!^{-})^2} = 1.021 - 0.104 \cos(2.18\ A^{1/3} - 1.25) \qquad (1)$$

where $R = r_o A^{1/3}$, $r_o = 1.4$ fm and $\lambda\!\!\!^{-} = 1.22\ (A+1)/A$.

The good fit of this empirical analitical formula to the experimental data for A>27, independent of the fact that the elements are monoisotopic of not, suggests that if any systematic trend in σ_T exists, its magnitude does not exceed a few per cent and so eq.(1) can be used for the calculation of unknown data. This conclusion is supported by the measurements for the isotopic dependence of total cross sections [7], where the relative change of σ_T for $\Delta A = 1$, varies from Ni to Te in the interval of 0.8 to 0.4 %. Expression (1) could be interpreted quantitatively by a semiclassical optical picture [10,11] with reasonable values of the nuclear radius parameter r_o, potential depth and surface thickness.

ELASTIC SCATTERING CROSS SECTIONS

Most of the elastic scattering cross sections σ_{EL} have been determined by measuring the energy of scattered neutrons. Because of experimental difficulties (poor energy resolution, background, incomplete knowledge of the energy dependence of the neutron detection efficiency), integrated σ_{EL} data were determined from direct measurements only for 26 elements at 14 MeV. Recently using neutron T.O.F system [35] in Bruyeres-le-Chatel the angle-integrated elastic and inelastic cross sections, as well as the angular distribution for elastic and inelastic scattering from carbon were measured [36]. The angle-integrated cross sections in the energy range from 8 to 14.5 MeV show significant disagreements with the ENDF/B-III. and -IV. evaluations based on the very scarce data. The new differential elastic cross sections for Be at 14.2 MeV measured in LASL [37] are in good agreement with the ENDF/B-IV. evaluation. A number of σ_{EL} were derived by subtracting the measured nonelastic σ_{NE} from the total cross sections $\sigma^*_{EL} = \sigma_T - \sigma_{NE}$. In Fig. 3 the 14 MeV σ_{EL} data divided by their "black-nucleus" values are plotted as a function of $A^{1/3}$. The dashed curve shows the result of calculations using the semiclassical model with the same parameter values as determined from the total cross sections. Unknown σ_{EL} values for $A \geq 15$ may be calculated with the simple analytical expression

$$\sigma_{EL} = \pi(r_o A^{1/3} + \lambda)^2 \, [1.03 - 0.208 \cos(2.18 \, A^{1/3} - 1.25)] \quad (2)$$

Eq. (2) is very useful in normalizing angular distributions. The integrated σ_{EL} and differential $\sigma_{EL}(\vartheta)$ elastic scattering cross sections can be reproduced within a few per cent by the nuclear optical models [13]: however, these models need a number of adjustable parameters depending on energy and/or mass number and the calculations require at least medium-sized computers.

As there are no measurements for the differential elastic scattering cross sections of about 30 % of the elements, while for the remaining nuclei significant deviations are present in the shapes and absolute values of the $\sigma_{EL}(\vartheta)$ function, any conclusion concerning the potential form and the values of the parameters rather uncertain. It was shown that the semiclassical model can be used to describe not only total and integrated elastic but also differential elastic and nonelastic neutron cross sections in a wide range of mass numbers, using the same parameter sets for each nucleus.

The mass number dependence of $\sigma_{EL}(\vartheta)$ at 14 MeV is:

$$\sigma_{EL}(\vartheta) = \left(\frac{\lambda}{2}\right)^2 [1.03-0.208 \cos(2.18\, A^{1/3} - 1.25)] \cdot \cdot [\sum_{l=o}^{l_{max}} (2l+1) P_l \cos\vartheta]^2 \qquad (3)$$

where $l_{max} = \frac{r_o(A)\, A^{1/3}}{\lambda}$. Figure show experimental and calculated elastic scattering cross sections for ^{56}Fe and ^{209}Bi. Normalizing constants were not used. The dashed line shows the sum of the shape elastic scattering and a constant background of 10 mb/sr. Using Eq. (3) the forward peaks are fairly well reproduced in a wide range of mass numbers both in form and in absolute values, while there are deviations at some of the remaining peaks especially for the heavy nuclei. It should be noted however, that no free parameters were used in the calculations.

Pearlstein [14] has also given a simple method for the calculation of differential elastic scattering cross sections of 14 MeV neutrons, using a Bessel function expansion as suggested by the diffraction model. The $\sigma_{EL}(\vartheta)$ values can be estimated for $12 \leq A \leq 238$ mass numbers.

NONELASTIC CROSS SECTIONS

The neutron nonelastic cross section σ_{NE} is equal to that of the $\sigma_T - \sigma_{EL}$. The components of σ_{NE} are inelastic scattering, capture, reactions and fission. At 14 MeV the main processes are: (n,n'γ), (n,2n), (n,p), (n,d), (n,α) and (n,f). The cross sections for (n,t), (n,^{3}He), (n,γ) and for charged particle emission following inelastic neutron scattering are very low except for light nuclei. The determination of the nonelastic cross section can be performed directly using the sphere transmission method or indirectly either by summing the reaction cross sections or by measuring σ_T and σ_{EL}. Using a more complete data set for σ_T, σ_{EL} and σ_{NE} at 14 MeV the reduced σ_{NE} values are plotted in Fig. 5 as a function of mass number. It can be seen that there are no data for about half the elements; the existing data, however, show a decrease with increasing mass number A

which means that r_o is A-dependent. Since 1970 no new data have been published for σ_{NE}. The nonelastic cross sections can be calculated by the expression[10,11]

$$\sigma_{NE} = \pi[r_o(A)\cdot A^{1/3} + \lambda]^2(1-\rho^2) \qquad (4)$$

where at 14 MeV $r_o(A) = 1.21 + \frac{4.0}{A^{2/3}} - \frac{15}{A^{4/3}}$ fm, and $\rho = 0.104$ from eq.(1).

The energy dependence of σ_{NE} around 14 MeV is smooth and no additional tendency, e.g. isotopic effect can be observed in the data within their relatively high limits of errors.

The semiclassical optical model is capable to describe the σ_T, σ_{EL}, $\sigma_{EL}(\vartheta)$ and σ_{NE} data above 10 MeV for $14 \leq A \leq 238$ interval. The cross sections are given as closed analytical expressions of the optical parameters; this renders possible both the quick estimates of unmeasured cross sections and the analytical operations.

Considering the fact that the total, elastic and nonelastic cross sections at 14 MeV can be well described both by exact or simplified optical models and by empirical expressions with an accuracy of 1-2 %, further accurate measurements are needed first of all for the $\sigma_{EL}(\vartheta)$ function at which the agreements rather poor.

PARTIAL NONELASTIC CROSS SECTIONS

The techniques used for the determination of reaction cross sections can be divided into three groups, namely activation, accumulation and spectrum methods. The latter is rather difficult because it needs the measurement of the spectrum and angular distribution of emitted particles in a high background. Recently a charged-particle magnetic-quadrupole spectrometer has been constructed for H and He to increase the solid angle at large source-to-detector separation and to suppress the background caused by other charged particles [23]. The improvement in the spectrum methods for the emitted charged particles and neutrons has been surveyed by Qaim [15,24]. The accumulation method is simple because only the emitted particles should be collected. In the case of fission, the fragments are storaged by a track detector, while for (n,α) and (n,p) reactions the accumulated He and H gases can be measured by gas mass spectrometer [18]. The relative emission of ^{3}He and ^{4}He is being investigated by Qaim et al. [19] at Jülich using quadrupole mass spectrometer. In the case of (n,t) reactions, the accumulated tritium can be separated by vacuum extraction or oxidization techniques and measured through its beta decay [20,21]. This method is applicable for other radioactive gaseous products,

e.g. the ^{37}A content produced in $^{40}Ca(n,\alpha)$ and $^{39}K(n,t)$ [22] reactions was measured by its soft radiation.

Recently the activation technique has been improved [15] by application of separated isotopes as targets, quick radiochemical separations and high-resolution counting systems (Ge(Li), HPGe, Si(Li), etc.). 14 MeV neutrons can give rise to about 1800 reactions on the 290 stable or long half-life isotopes leading to radioactive residual nuclei. In this number the reactions (n,p), (n,α), (n,2n), (n,3n), (n,γ), (n,np), (n,d), (n,nα), (n,^{3}He), (n,t), (n,nt) and (n,n'γ) were taken into account. These reactions give rise to about 600 different radioactive isotopes, i.e. a given isotope on the average can arise from three different interfering reactions. The number of known fission products in $^{238}U(n_{14},f)$ is about 450, from which 363 has a cumulative yield higher than 0.1 %, with half-lives ranging from 10^{-1} to 10^{9} s. There are a few compilations and surveys of the available 14 MeV neutron reaction and fission cross sections based on recent publications [15,42,43,44,45,46, 47,48,49,50] which were used in this review.

In spite of the simplicity of measuring activation cross sections, there are considerable disagreements between published data; therefore, more accurate trends can be revealed from the data measured by the same author because of the higher relative accuracy. The activation cross sections for (n,2n), (n,p) and (n,α) reactions vs. target proton number Z at 14 MeV are plotted in Figs. 6 a-e, 7 a-e, 8 a-d, respectively. The deadline date for the literature survey for points was 1969, while the crosses represent the modern data. In these Figures the target mass numbers and the half-lives (<1y) of the residual nuclei (in parenthesis) are indicated above the experimental points. The numbers shown above the question marks denote the mass numbers of those nuclides for which data are not available. As in most cases the differences between the data relating to the same nuclide considerable exceed the errors given in the references, the error limits are not indicated. As it can be seen the spread is significant in the modern data, too. The main sources of errors are as follows: interfering reactions caused by impurities in the samples; half-life data; abundance of the radiation detected; converting counting into disintegration rate; efficiency of the separation technique; absolute neutron flux and its variation in time; energy and energy spread of neutrons; cross section of monitor reaction; escape of residual nuclei by nuclear recoil or diffusion. A few among these sources can be eliminated by using the arrangement given in Fig. 9 for irradiation. The fission on depleted ^{238}U layer can serve as flux monitor and standard cross section. The accuracy of the

measurement of differential cross sections for threshold reactions has been discussed in detail by Smith [17].

(n,n') and (n,2n) cross sections

The ratios of $\sigma_{n,2n}$ and σ_{NE} values plotted against the target neutron number at 14 MeV show that the (n,2n) cross sections give about 80 % of σ_{NE} above N=60; therefore, by the study of the (n,2n) reaction one can get information on those properties of nuclei which are dominant in nuclear reactions.

According to a recent survey by Bödy [27] (n,2n) cross sections have been measured at 14 MeV for about 30 % of the stable nuclei. The observed N-Z dependence in the (n,2n) cross sections [28] provides a possibility to estimate unknown values for isotopes and elements. On the basis of measured and estimated data, recommended values of (n,2n) cross sections at 14.7 MeV were given for 114 nuclides from experimental data, for 137 nuclides from N-Z systematics and for 71 elements from the averaging of $\sigma_{n,2n}$ over isotopic abundances [29].

In addition to the activation technique a new method based on pulsed sources and a large liquid scintillator to detect neutrons [31] is used for the measurement of $\sigma_{n,2n}$ [32]. Frehaut et al. [32] obtained higher $\sigma_{n,2n}$ values for heavy nuclei than those measured by activation method. Using this scintillator-tank method the $\sigma_{n,2n}$ values obtained by Veeser et al. [34] at 14 MeV for a number of nuclides are in good agreement with our recommended values, except for ^{103}Rh. The (n,2n) cross sections for elements have been measured for FRT-structural materials in LASL by spectrometric method [41]. Results at 14.7 MeV are in good agreement with the recommended values [29] except for Ti at which the deviation is about 50 %. There is however considerable spread among existing old and new (n,2n) data in the 13 to 15 MeV region determined by the activation method. The discrepancies are attributed to the accepted decay schemes and insufficient energy resolution of the detectors in the past [33].

The plot of (n,2n) cross sections (Figs. 6a-e) enables the following rough trends to be established: a) In the mass number region 19<A<40 the cross section decreases from 50 mb to 4-5 mb, b) at A~48 it rises rapidly to ~1000 mb and shows a trend of increasing slowly up to a maximum value of ~2200 mb for the heaviest nuclei, c) in the region 48<A<100 strong local fluctuations exist. The trends in (n,2n) reaction cross sections have been investigated by several authors [39] and both isotopic and isotonic as well as odd-even effects have been observed.

Taking into account the differences of σ_{NE} and $\sigma_{n,2n}$ as well as the values of partial cross sections at 14 MeV, for

$\sigma_{n,n'}$, in average a few hundred mb can be expected. So, in first approximation for A≥100, $\sigma_{NE} \simeq \sigma_{n,2n} + \sigma_{n,n'}$, around 14 MeV, i.e. the difference $\sigma_{NE} - \sigma_{n,2n}$ is due to the inelastic scattering and the same trends in opposite direction should appear in $\sigma_{n,n'}$, as in $\sigma_{n,2n}$. Very few data are available for the total inelastic scattering cross sections because the direct measurements by the angle-integrated neutron spectra are difficult. Using the simple activation method a lower limit for $\sigma_{n,n'\gamma}$ process can be given for nuclei that have low-lying isomeric states. According to the few data available, the σ_n^m, values lie in the interval of 100 to 600 mb. As $\sigma_{n'} = \sigma_{n'}^g + \sigma_{n'}^m$, from the calculation of isomeric cross section ratio in the knowledge of σ_n^m, the value of σ_n^g, can be estimated. Another way is to measure the neutron emission cross section σ_{nM}:

$$\sigma_{nM} = \sigma_{n,n'} + \sigma_{n,2n} + \sigma_{n,n \text{ charged}}.$$

At 14 Mev $\sigma_{n,n \text{ charged}}$ can in most cases be neglected or in some sases can be measured by activation method. Systematic measurements were carried out in Dresden for σ_{nM} [38]. It is assumed that in the case of vibrational even-even nuclei following inelastic scattering, the excited states decay through the 2_1^+ state, and so by measuring the number of gammas from the $2_1^+ \rightarrow 0^+$ transitions the total inelastic saccering cross section can be determined. Koopman [55] has given the results for $\sigma_{n,n'}(2_1^+ \rightarrow 0^+)$ in comparison with that obtained from $\sigma_{NE} - \Sigma \sigma_{i \neq n,n'}$. The agreements between the data are satisfactory except for ^{110}Cd and ^{116}Cd.

Several semi-empirical and empirical formulae are available for the estimation of $\sigma_{n,2n}$ at 14 MeV [39], among these, the expression given by Pearlstein [40] shows the best approximation [29]. Kumabe [66] calculated (n,2n) cross sections at 14.7 MeV in the region of rare-earths taking into account both statistical and precompound effects. His results show good agreement with Qaim's experimental values [67]. The excitation function of (n,2n) reactions can be well described by the Hauser-Fesbach model [51] : above the (n,3n) threshold, however, the preequilibrium contribution is also present [34]. For the analysis of neutron emission spectra from 14 MeV neutron reactions, Pearlstein [52] has used the nuclear model code ALICE, developed by Blann [53] and a global set of input nuclear constants. Over 70 % of the cases the calculated spectra can be fit to within 30 % of experimental values in the range Na to Bi.

(n,p) and (n,α) cross sections

The plot of (n,p) cross sections vs. proton number of the target nucleus (Figs. 7a-e) shows an increasing trend up to Z~16, from $\sigma_{n,p} \leq 10$ mb to ~300 mb. In the region $16 \leq Z \leq 24$ a broad maximum can be observed, then $\sigma_{n,p}$ gradually decreases to 2-3 mb for the heaviest elements. The $\sigma_{n,\alpha}$ values (Figs. 8a-d) generally decreases from ~100 mb to ~1 mb from the lightest nuclei to the heaviest elements. Two definite maximum can be seen, one in the region from Na to Cl($\sigma_{n,\alpha} \geq 100$ mb), the other in the rare earth region ($\sigma_{n,\alpha}$~100 mb). At N=50 the $\sigma_{n,\alpha}$ data are considerably higher than for the neighbouring nuclides. Gardner and Yu-Wen [69] have given a relationship for the isotopic dependence of $\sigma_{n,\alpha}$.

The (n,p),(n,α) as well as the hydrogen and helium producing cross sections for FRT-related structural materials were measured for a number of nuclei during the last years [56-63]. Molla and Qaim [56] have determined the $\sigma_{n,p}$ data at 14.7 MeV for 48 nuclides of 19 elements using the activation method. In the cross sections from the systematic measurements and from the evaluation of literature data they found a strong dependence on (N-Z)/A in the case of medium and heavy nuclei supporting the prediction of an earlier formula given by Levkovskii [65] for the interval $12 \leq A \leq 150$:

$$\sigma_{n,p} = 45.2(A^{1/3} + 1)^2 \, e^{-33(N-Z)/A} \text{ mb.} \qquad (5)$$

The (N-Z)/A dependence of $\sigma_{n,p}$ and $\sigma_{n,\alpha}$ is confirmed by recent data indicated in Fig. 10 [49].

Haight et al. [58,60,62] have used a Magnetic Quadrupole Spectrometer (MQS) [64] for the measurement of the spectra of proton and alpha particles from 14 MeV neutron induced reactions. The agreement between the results obtained at Livermore by MQS and Jülich by activation for ^{48}Ti, ^{58}Ni and ^{65}Cu is satisfactory. Fig. 11 shows a typical angle-averaged proton spectrum from ^{48}Ti.

It was shown by Qaim and Stöcklin [72] that the contribution of (n,np) and (n,nα) reactions to the production of hydrogen and helium at 14 MeV are not negligible. The limited number of data shows, as a gross trend, the (N-Z)/A dependence [15]; however, further measurements are needed to observe any fine structure and to understand the reaction mechanisms.

Reaction mechanisms in fast neutron induced reactions have been discussed in detail by Cindro [68]. The compound nucleus emission is able to account for the $\sigma_{n,\alpha}$ in the region $20 \leq A \leq 80$, while for the explanation of the alpha emission from heavy nuclei both preequilibrium and direct effects should be

taken into account. The fine structure in the angle integrated alpha spectra was described by dispersion theory [70]. The excitation functions of (n,p) and (n,α) reactions can be satisfatorily described [51] by the Hauser-Feshbach model (see e.g. Figs. 12 and 13). Pearlstein [71] has given an empirical model based on statistical theory to calculate reaction cross section curves for medium ass nuclei. He obtained fair agreement between calculated and measured (n,2n), (n,α) and (n,p) cross sections at 14 MeV.

(n,t) and (n,^{3}He) cross sections

The study of (n,t) and (n,^{3}He) reactions may add to our understanding of the emission of the three-nucleon structures ^{3}H, ^{3}He and to obtain important data for the tritium and helium concentration build up in fission reactors and thermonuclear devices.

The cross sections for (n,t) and (n,^{3}He) reactions at 14 MeV have been recently investigated by the activation and tritium beta counting techniques mainly at Jülich [73], Debrecen [21,51] and Zagreb [74].

Values of (n,^{3}He) reaction cross sections measured in Zagreb [74] are much higher than those (~1-100 μb) obtained in Jülich and Debrecen. Qaim [15] has given the following empirical formula to predict the unknown data for medium and heavy nuclei:

$$\sigma_{n,^3He} = 0.54\ (A^{1/3} + 1)^2 \exp[-10(N-Z)/A]\ (\mu b) \qquad (6)$$

The same formula is valid for $\sigma_{n,t}$, but the constant factor is 4.52 instead of 0.54 [15].

The (n,t) cross sections for very light nuclei are relatively large (~100 mb), while for medium and heavy nuclei they lie in the ~10-100 μb region. Extensive investigations were carried out for the determination of tritium production rates in the model Li blanket [3], and also for Li isotopes [42].

Qaim and Stöcklin [73] found that a maximum appears in the $\sigma_{n,t}$ values at Z=26, and an (N-Z)/A dependence exits for Z>22. According to our earlier results, a strong decreasing tendency with increasing atomic number can be found in $\sigma_{n,t}$ data, on which deviations arising from individual properties of nuclei are superimposed [21]. The Hauser-Feshbach model calculation can reproduce both the shape and the magnitude of (n,t) excitation functions [51]. As can be seen in Fig. 14 the cross section curves change significantly around 14 MeV especially for even nuclei; this may be a reason of the large spread in the literature data. Similarly to Qaim's observation we also found the

(N-Z)/A dependence for odd target nuclei, but the $\sigma_{n,t}$ data are higher than for even nuclei by one order of magnitude. For even nuclei the triton energy is less with about 2 MeV than that for odd ones, which may be a reason of the separation of the cross sections in Fig. 15. This means that the formula given by Qaim [15] for the calculation of $\sigma_{n,t}$ values should be completed with an additional term containing the odd-even effects. Further measurements are needed to clear up the systematics in the data.

(n,γ) cross sections

For the determination of (n,γ) cross sections at 14 MeV two methods are used: the activation technique σ_{act} and measurements of prompt gamma ray spectra σ_{int}. The σ_{act} values from earlier measurements were higher by a factor of ten than σ_{int}, because of the presence of scattered neutrons. The measurements for σ_{act} have been repeated with improved methods, eliminating the effects of secondary neutrons, and good agreement was found between σ_{act} and σ_{int}. Results indicated in Fig. 16 [75] show that $\sigma_{n,\gamma}$ is ~1 mb in a wide range of mass number, and that data are scanty especially for light nuclei. The A dependence of the cross section is in qualitative agreement with the expectation of the direct-semidirect model [75]. The magnitude of the γ-ray cascade through unbound levels could be determined from the difference of $\sigma_{act} - \sigma_{int}$, which requires further precise activation (n,γ) measurements.

(n,xγ) cross sections

During the last years there have been measurements at 14 MeV for neutron induced gamma-ray production cross sections and spectra. In such experiments pulsed beam and T.O.F method are used and the time spectrum of gammas is detected by plastic or NaI(Tl) scintillators. Gamma-ray production cross sections were measured at 14.2 MeV by Drake et al. [76] for 20 samples ranging from Be to Pu, including elements that are of interest for CTR program. Cox et al. [77,78] have measured the gamma rays associated with scattering of 14 MeV neutrons in extended samples of possible fusion reactor materials. Fig. 17 shows a typical example for the shape of a spectrum measured for ^{27}Al [26]. The discrepancies in the results indicate the difficulties of such measurements. It would be important to obtain data for standard $\sigma_{n,x\gamma}$ values and spectrum at 14 MeV neutron energy.

Fission by 14 neutrons

Fast neutron fission cross sections for ^{233}U, ^{235}U, ^{238}U and ^{239}Pu have been reviewed in detail by Poenitz and Guenther [79], and Lapenas [48]. The deviations in $\sigma_{n,f}$ values measured

by different authors around 14 MeV are related to the energy dependence of the fission cross section near the (n,2nf) threshold as the bombarding energy is not always well defined. At 14 MeV the change in $\sigma_{n,f}$ is especially marked for ^{235}U, while for ^{239}Pu it is negligible.

Most recently, Cance and Grenier [80] measured the absolute neutron fission cross sections of ^{235}U and ^{239}Pu around 14 MeV. In disagreement with earlier observations no significant energy dependence was found for ^{235}U in the interval 13.9 to 14.6 MeV and the results for ^{239}Pu are 12 % lower than the old data. Further measurements are needed around 14 MeV with good energy resolution to solve the questions.

As for the fission yields at 14 MeV, data for $^{234,236}U$ and ^{240}Pu are incomplete and it is necessary to extend the measurements over the ^{231}Pa, $^{236,237}Np$ and $^{242,244}Pu$ isotopes. More accurate data are needed for the wings and valleys of the mass distributions.

In order to study the fine structures, the present 5-10 % errors in the determination of yields in the peaks should be reduced as low as 2-3 %. In the case of independent yields the data are not sufficient even for ^{232}Th, $^{233,235,238}U$ and ^{239}Pu, which makes the conclusion on the charge distribution, polarization and dispersion, as well as on odd-even effects rather uncertain at 14 MeV [81]. The present status of fission yield data have been surveyed by Cuninghame [82].

ACKNOWLEDGEMENTS

The author is indebted to Dr.Z.T.Bődy and Mr.I.Szalóky for their willing assistance in a part of the compilation of data.

REFERENCES

[1] STEINER, D., Nucl.Sci.Eng. 58 (1975) 107.
[2] STEINER, D., TOBIAS, M., Nuclear Fusion 14 (1974) 153.
[3] QAIM, S.M., WÖLFLE, R., STÖCKLIN, G., J. of Radioanal. Chem. 30 (1976) 35.
[4] VOOK, F.L., Physics Today 28 No 9 (1975) 34.
[5] CSIKAI, J., BUCZKÓ, M., BŐDY, Z., DEMÉNY, A., Atomic Energy Rev. 7 (1969) 93.
[6] ANGELI, I., CSIKAI, J., NAGY, J.L., SCHARBERT, T., SZTARICSKAI, T., Acta Phys.Hung. 30 (1971) 115.
[7] DURAKEVICH, Yu.V., DYUMIN, A.N., KAMINKER, D.M., Nucl. Phys. A92 (1967) 433.

[8] DYUMIN, A.N., KAMINKER, D.M., POPOVA, G.N., SMOLIN, V.A., Izv.Akad.Nauk SSSR., Ser.Fiz., 36 (1972) 852.
[9] DYUMIN, A.N., EGOROV, A.I., POPOVA, G.N., SMOLIN, V.A., Acad. of Sci. USSR, Leningrad Nuclear Physics Institute, N14 (1973).
[10] ANGELI, I., CSIKAI, J., Nucl.Phys. A158 (1970) 389.
[11] ANGELI, I., CSIKAI, J., Nucl.Phys. A170 (1971) 577.
[12] ANGELI, I., CSIKAI, J., NAGY, P., Nucl.Sci.Eng. 55 (1974) 418.
[13] HODGSON, P.E., Ann.Rev.Nucl.Sci. 17 (1967) 1.
[14] PEARLSTEIN, S., Nucl.Sci.Eng. 49 (1972) 162.
[15] QAIM, S.M., in Proc. Int. Conf. on Neutron Physics and Nuclear Data for Reactors and other Applied Purposes, Harwell, U.K., 25 to 29 Sept. 1978.
[16] LAMPHERE, R.W., "Fission Detectors", in Fast Neutron Phys. I, eds. MARION, J.B., FOWLER, J.L., Interscience, New York, p. 721 (1960).
[17] SMITH, D.L., ANL/NDM-23 (1976).
[18] FARRAR, IV.H., KNEFF, D.W., BRITTEN, R.A., HEINRICH, R.R., BNL-NCS-50681, p. 175 (1977).
[19] QAIM, S.M., WU, C.H., WÖLFLE, R., to be published.
[20] QAIM, S.M., WÖLFLE, R., STÖCKLIN, G., J.Inorg.Nucl.Chem. 36 (1974) 3639.
[21] BIRÓ, T., SUDÁR, S., MILIGY, Z., DEZSŐ, Z., CSIKAI, J., J.Inorg.Nucl.Chem. 37 (1975) 1583.
[22] QAIM, S.M., RUSHEED, A., STÖCKLIN, G., WÖLFLE, R., Int. J. appl. Radiat. Isotopes 28 (1977) 585.
[23] GRIMES, S.M., HAIGHT, R.C., ANDERSON, J.D., Nucl. Sci. Eng. 62 (1977) 187.
[24] QAIM, S.M., Nucl. Cross Section and Technology, Vol. II. NBS-SP 425, p. 664 (1975).
[25] LISKIEN, H., private communication.
[26] HAIGHT, R.C., Review of Neutron Data: 10 to 40 MeV, Preprint UCRL-79453, LLL (1977).
[27] BŐDY, Z.T., private communication.
[28] CSIKAI, J., PETŐ, G., Phys. Lett. 20 (1966) 52.
[29] BŐDY, Z.T., CSIKAI, J., Atom.Energy Rev. 11 (1973) 153.
[30] VONACH, H., HILLE, M., STENGL, G., BREUNLICH, W., WERNER, E., Z.f. Phys. 237 (1970) 155.
[31] FREHAUT, J., Nucl. Instr. Methods 135 (1976) 511.
[32] FREHAUT, J., HOLUB, E., CATES, M., MOSINSKI, G., CEA-N-1998 (1977).
[33] PAULSEN, A., LISKIEN, H., WIDERA, R., Atomkernenergie 26 (1975) 34.
[34] VEESER, L.R., ARTHUR, E.D., YOUNG, P.G., Phys. Rev. 16 (1977) 1792.

[35] LACHKAR, J.C., McELLISTREM, M.T., HAOUAT, G., PATIN, Y., SIGAUD, J., COCU, F., Phys. Rev. C14 (1976) 933.
[36] HAOUAT, G., LACHKAR, J., SIGAUD, J., PATIN, Y., COCU, F., Nucl.Sci.Eng. 65 (1978) 331.
[37] DRAKE, D.M., AUCHAMPAUGH, G.F., ARTHUR, E.D., RAGAN, C.E., YOUNG, P.G., Nucl.Sci.Eng. 63 (1977) 401.
[38] HERMSDORF, D., MEISTER, A., SASSONOFF, S., SEELIGER, D., SEIDEL, K., SHAHIN, F., ZfK-277(Ü), Rossendorf (1975).
[39] CSIKAI, J., Atomic Energy Rev. 11 (1973) 415.
[40] PEARLSTEIN, S., Nucl.Sci.Eng. 23 (1965) 238.
[41] AUCHAMPAUGH, G.F., DRAKE, D.M., VEESER, L.R., BNL-NCS-50681 (1977).
[42] EXFOR MASTER-FILE INDEX, IAEA.
[43] TSUKADA, K., JAERI 1252 (1977).
[44] QAIM, S.M., Handbook of Spectroscopy, Vol III. CRC (to be published).
[45] Fission Product Nuclear Data (FPND) - 1977, Vol I. IAEA-213 (1978).
[46] NESTEROV, B.V., Yadernye Konstanty 27 (1977) 45.
[47] IGARASI, S., KANDA, Y., MATSUNOBU, H., MURATA, T., OHSAWA, T., KIKUCHI, Y., JAERI-memo 6315 (1975).
[48] LAPENAS, A.A., Izmerenye spektrov neytronov aktivationnym metodom, IzdatelstvoZinatne, Riga (1975).
[49] QAIM, S.M., STÖCKLIN, G., Proc. Neutron Data of Structural Materials for Fast Reactors, Geel, Belgium 5-8 Dec. (1977).
[50] Progress in Fission Product Nuclear Data, Ed. by G.Lammer, INDC (NDS)-95/G+P, (1978); INDC (NDS)-86/G+P (1977).
[51] SUDÁR, S., CSIKAI, J., Proc. Int. Conf. on Neutron Physics and Nuclear Data for Reactor and other Applied Purposes, Harwell 25 to 29 Sept. p. 128. (1978).
[52] PEARLSTEIN, S., BNL-NCS-24066 (1978).
[53] BLANN, M., Annual Rev. of Nucl.Sci. 25 (1975) 123.
[54] FU, C.Y., Atomic Data and Nuclear Data Tables 17 (1976) 127.
[55] KOOPMAN, R.P., thesis, University of California at Davis (1977).
[56] MOLLA, N.I., QAIM, S.M., Nucl. Phys. A283 (1977) 269.
[57] HAIGHT, R.C., GRIMES, S.M., ANDERSON, J.D., Nucl.Sci.Eng. 63 (1977) 200.
[58] GRIMES, S.M., HAIGHT, R.C., ANDERSON, J.D., Phys.Rev. C17 (1978) 408.
[59] GRIMES, S.M.,private communication.
[60] HAIGHT, R.C., GRIMES, S.M., Preprint UCRL-80235 (1977).
[61] PAULSEN, A., WIDERA, R., LISKIEN, H., Atomkernenergie 22 (1974) 291.
[62] GRIMES, S.M., HAIGHT, R.C., ANDERSON, J.D., ALVAR, K.R., BORCHERS, R.R., Preprint UCRL-79454 (1977).

[63] SAILER, K., DARÓCZY, S., RAICS, P., NAGY, S., Neytronnaya Fizika I. 246. Kiev (1977).
[64] ALVAR, K.R., BARSHALL, H.H., BORCHERS, R.R., GRIMES, S.M., HAIGHT, R.C., Nucl.Instr.Methods 148 (1978) 303.
[65] LEVKOVSKI, V.N., JETP. 45 (1963) 305.
[66] KUMABE, I., J.Nucl.Sci.Techn. 14 (1977) 460.
[67] QAIM, S.M., Nucl. Phys. A224 (1974) 319.
[68] CINDRO, N., Acta Phys. Slovaca 25 (1975) 158.
[69] GARDNER, D., YU-WEN, Yu., Nucl.Phys. 60 (1974) 49.
[70] GLOWACKA, L., JASKOLA, M., TURKIEWICZ, J., ZEMO, L., KOZLOWSKI, M., OSAKIEWICZ, W., Nucl.Phys. A244 (1975) 117; ibid A262 (1976) 205.
[71] PEARLSTEIN, S., J. of Nucl. Energy 27 (1973) 81.
[72] QAIM, S.M. STÖCKLIN, G., Proc. 8th Symp. Fusion Technology, Noordwijkerhout, June 1974, EUR 5182e, p. 939 (1974).
[73] QAIM, S.M., STÖCKLIN, G., Nucl. Phys. A257 (1976) 233.
[74] DIKSIC, M., STROHAL, P., SLAUS, I., J. inorg. nucl. Chem. 36 (1974) 477.
[75] BERGQVIST, I., POTOKAR, M., LUNDFD6/(NFFR-3023)/1-19 (1978).
[76] DRAKE, D.M., ARTHUR, E.D., SILBERT, M.G., Nucl.Sci.Eng. 65 (1978) 49.
[77] COX, A.J., POURMANSOORI, M., Int. J. of Appl. Rad. and Isotopes 28 (1977) 235.
[78] CONNEL, K.A., COX, A.J., Int. J. of Appl. Rad. and Isotopes, 20 (1975) 71.
[79] POENITZ, W.P., GUENTHER, P.T., Proc. NEANDC/NEARCRP Specialist Meeting on Fast Fission Cross Sections, ANL-76-90, (1976).
[80] CANCE, M., GRENIER, G., To be published in Nucl.Sci.Eng. (1978).
[81] DARÓCZY, S., private communication.
[82] CUNINGHAME, J.G., FPND in 1977, AERE-R 8753.

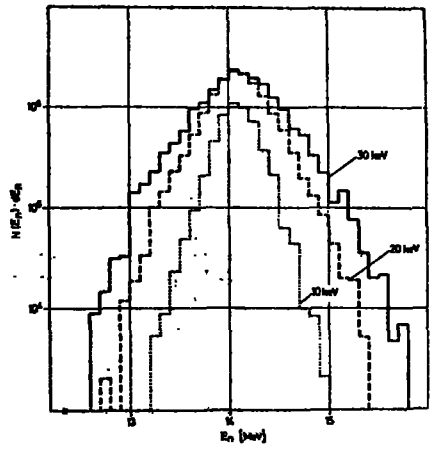

FIG. 1. Energy spectra of neutrons from a D+T plasma of temperature T=10, 20 and 30 keV

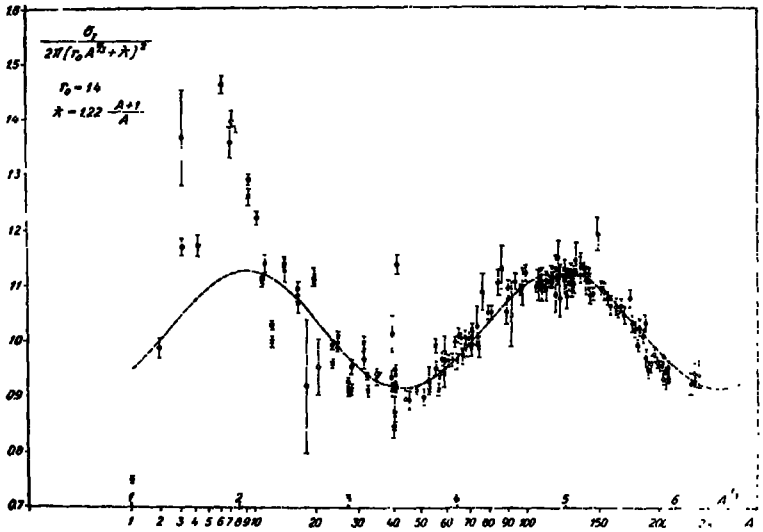

FIG. 2. 14 MeV neutron total cross sections divided by $2\pi(R+\lambda\bar{})^2$ as a function of $A^{1/3}$

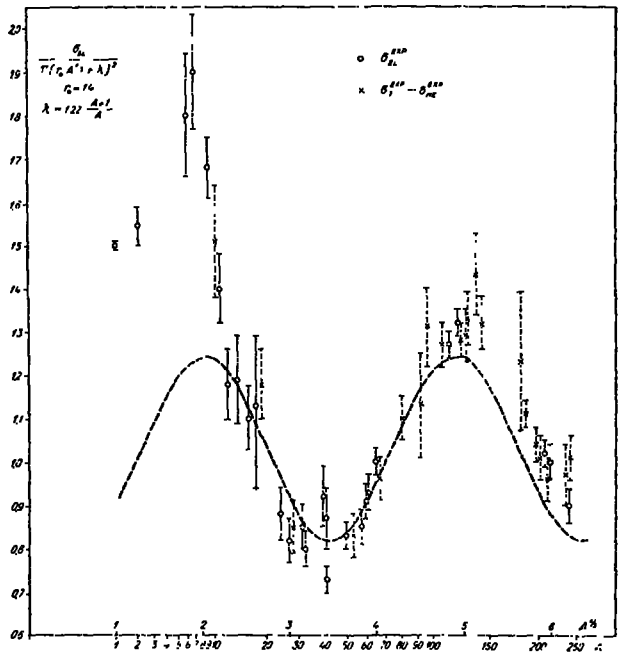

FIG. 3. 14 MeV integrated elastic scattering cross sections

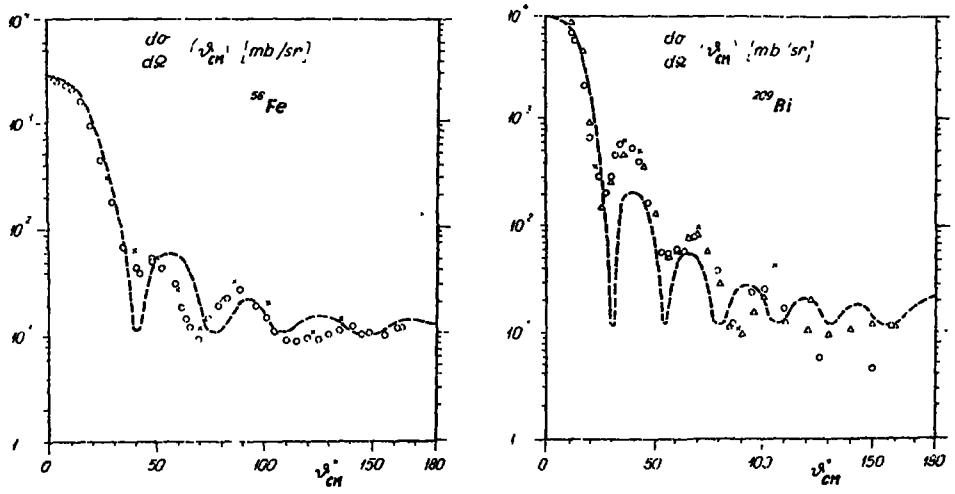

FIG. 4. Experimental and calculated (dashed curve) differential elastic scattering cross sections

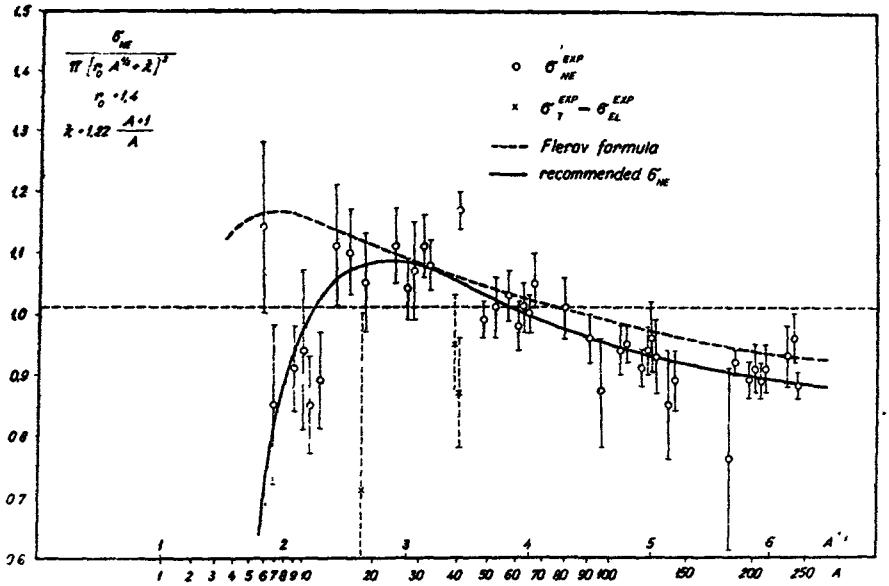

FIG. 5. 14 MeV nonelastic cross sections

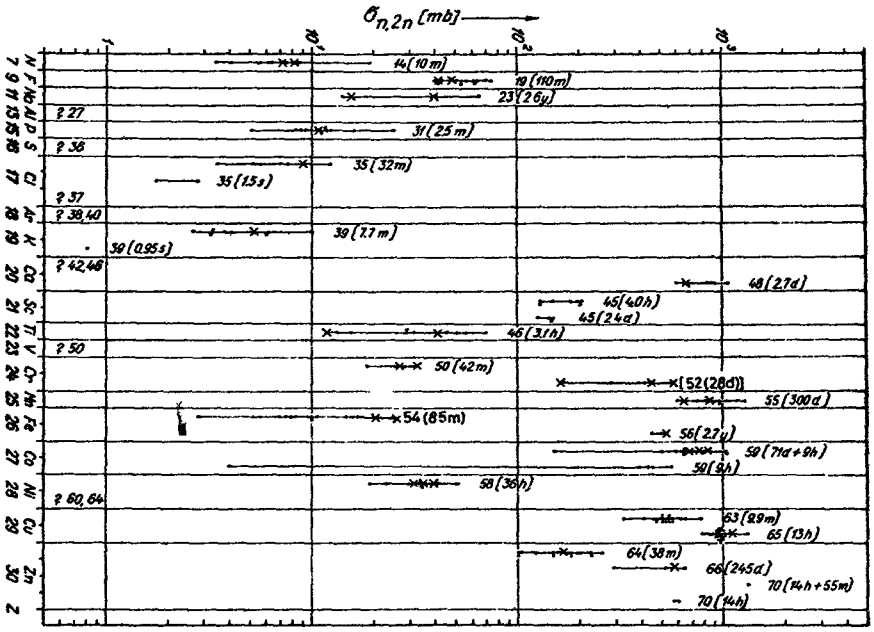

FIG. 6a-e. Activation cross section for (n,2n) reactions at 14 MeV

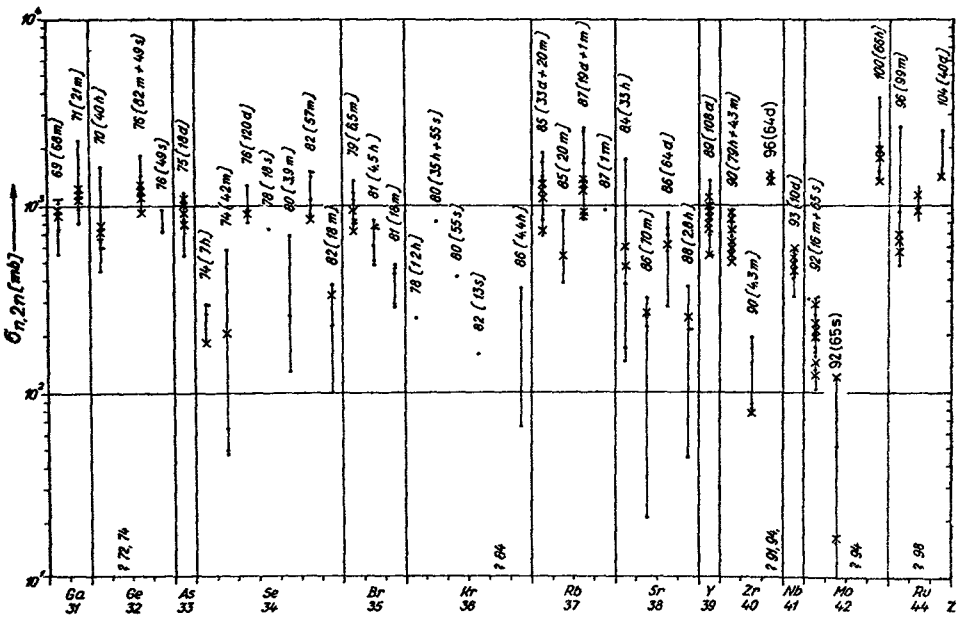

FIG. 6b.

FIG. 6c.

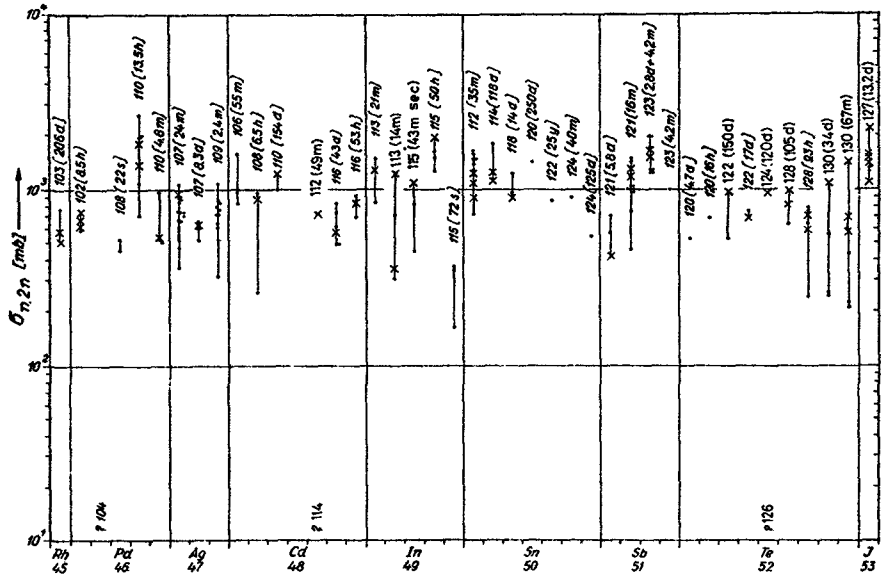

FIG. 6d.

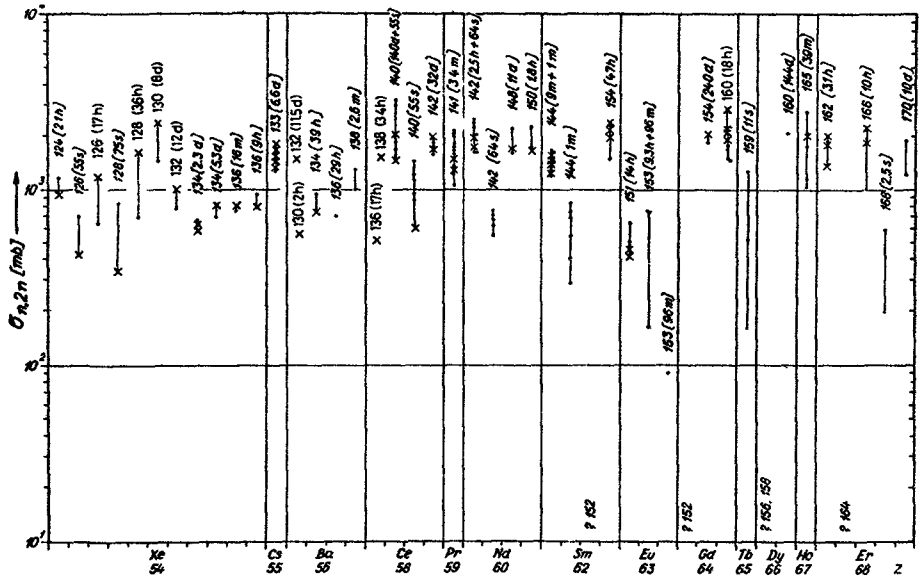

FIG. 6e.

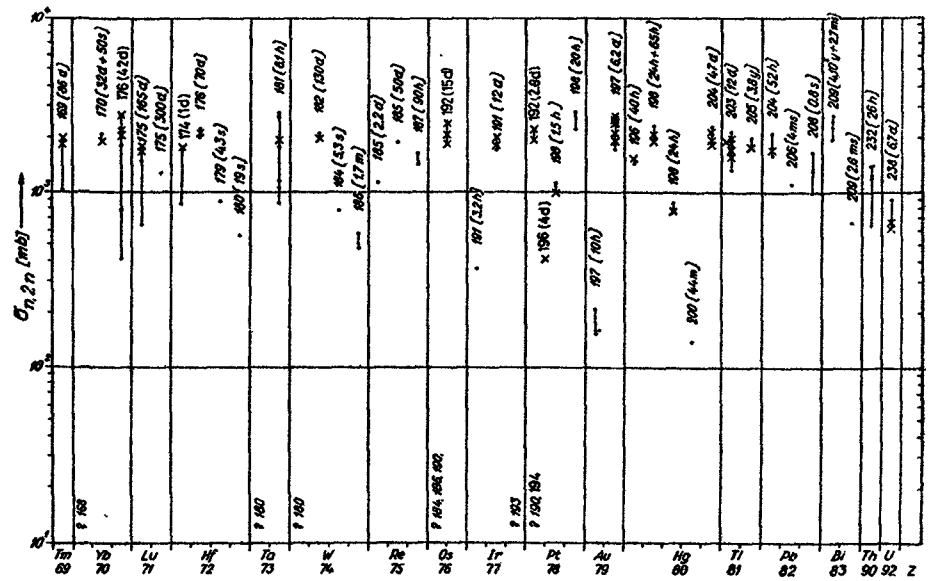

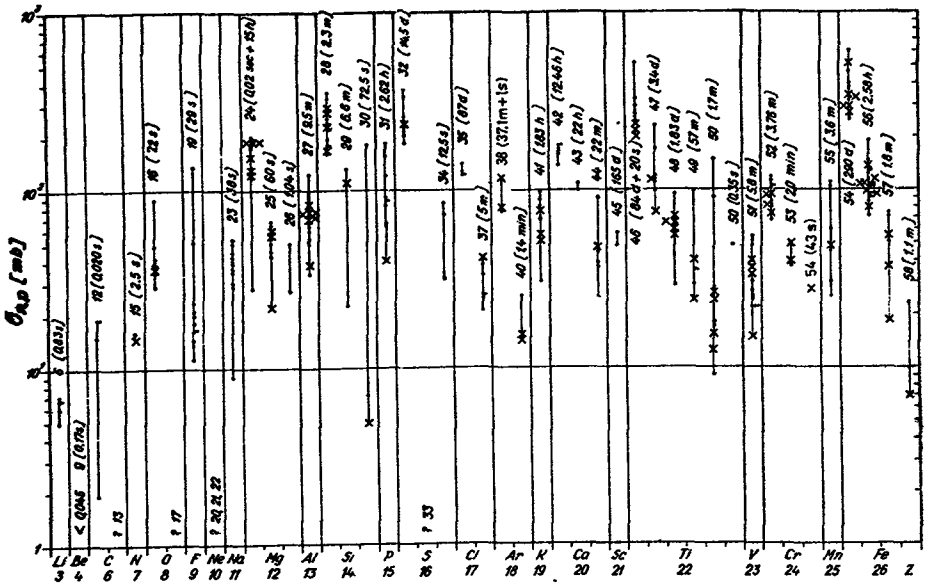

FIG.7a-e.
Activation cross section for (n,p) reactions at 14 MeV

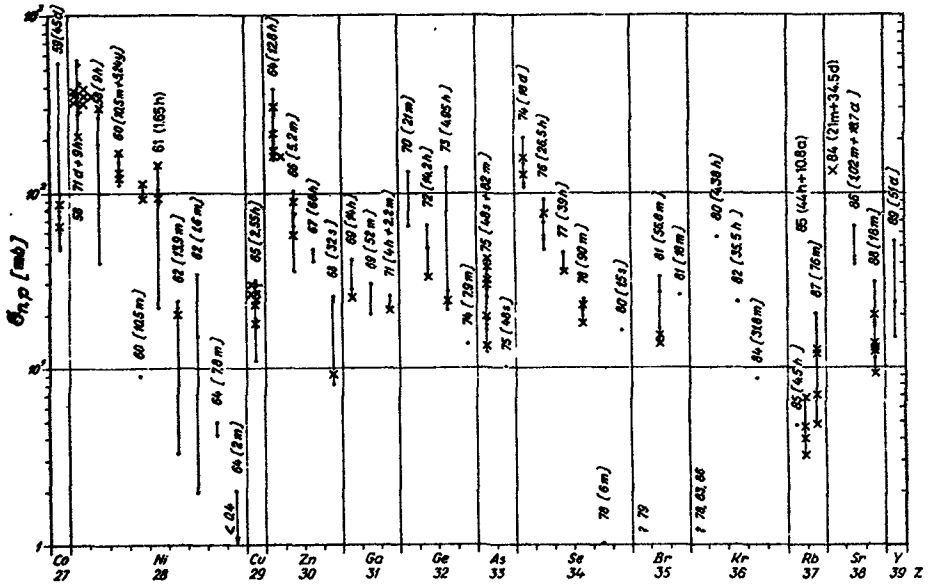

FIG. 7b.

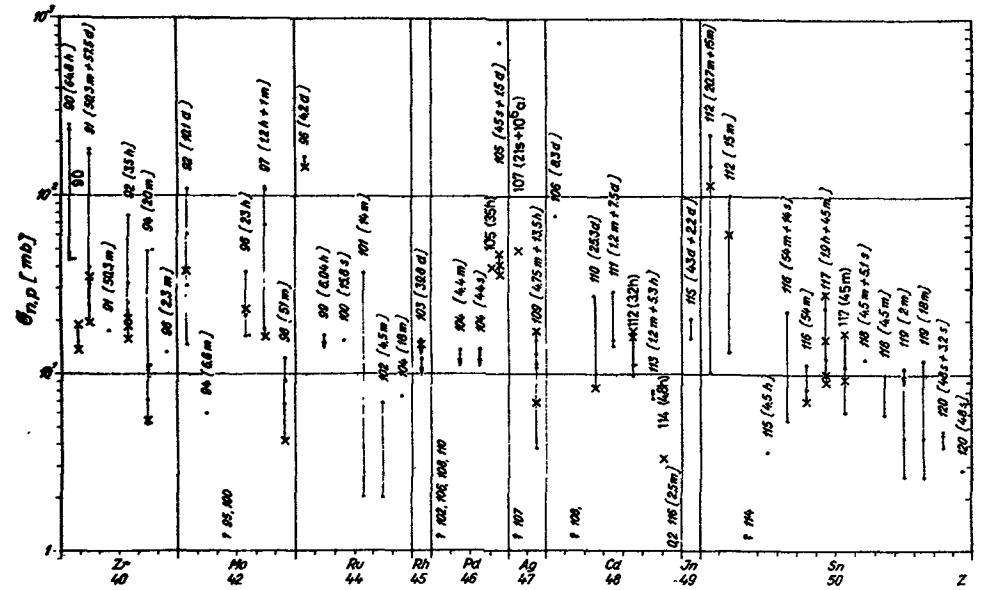

FIG. 7c.

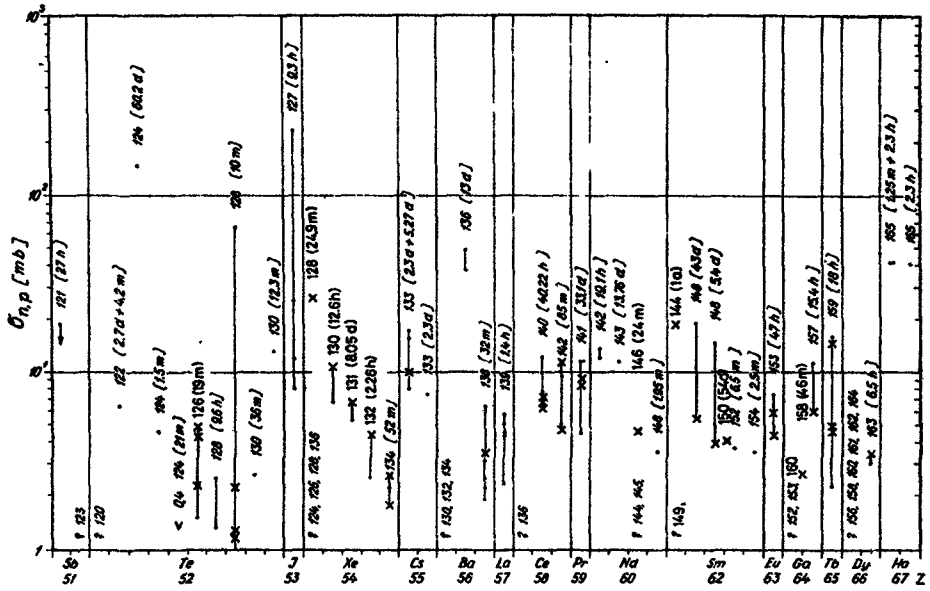

FIG. 7d.

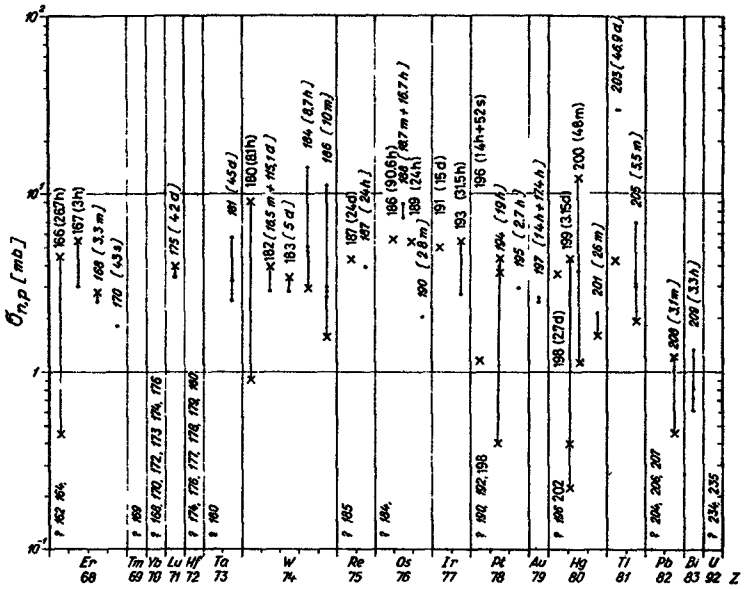

FIG. 7e.

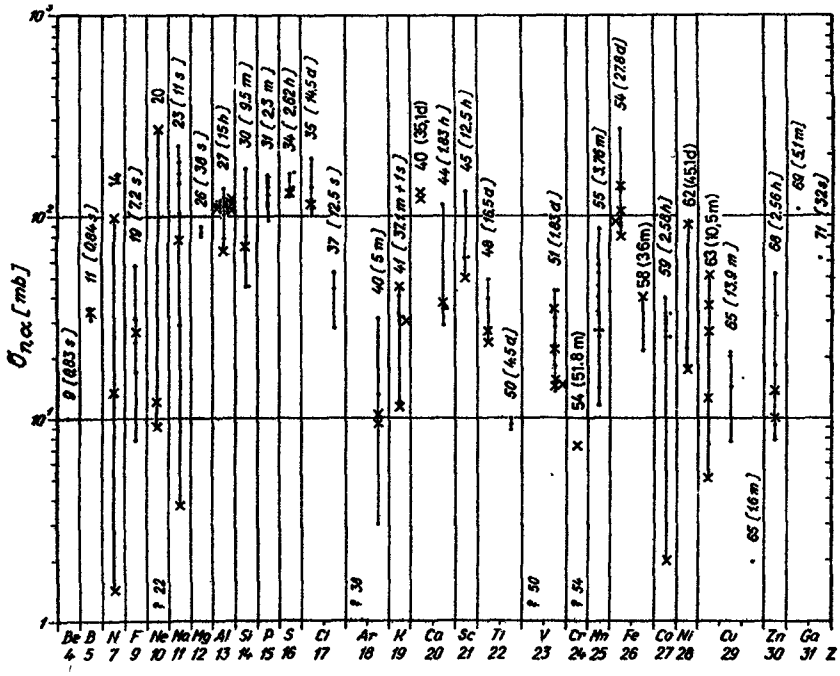

FIG. 8a-d.
Activation cross sections for (n,α) reactions at 14 MeV

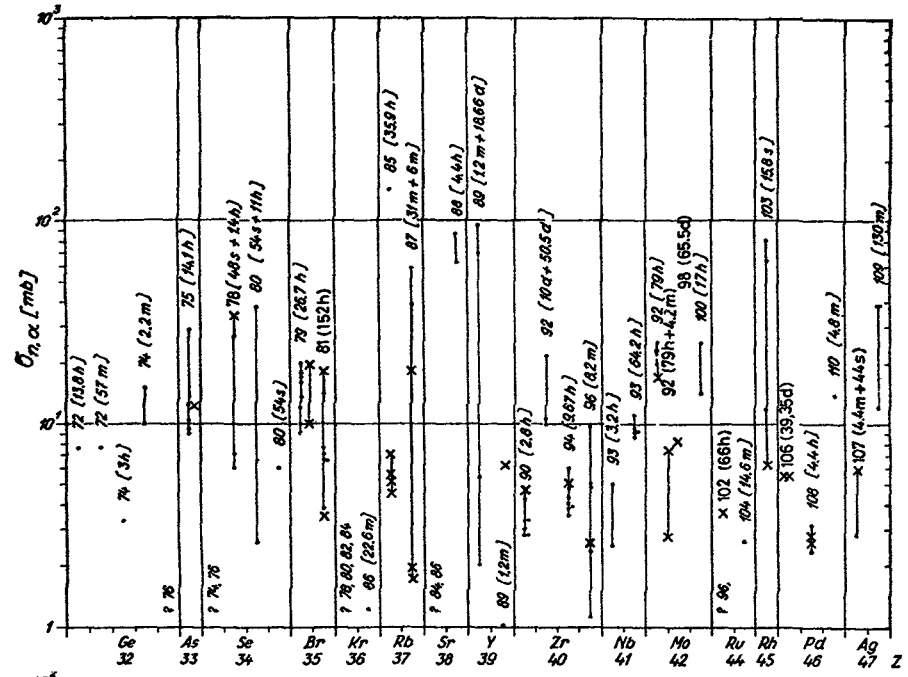

FIG. 8b.

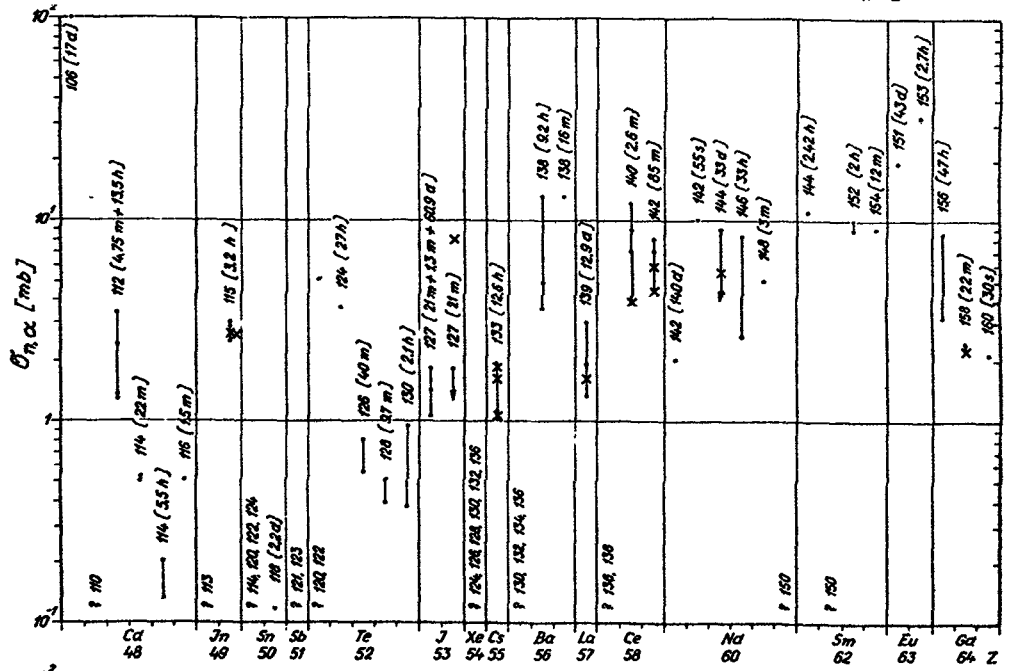

FIG. 8c.

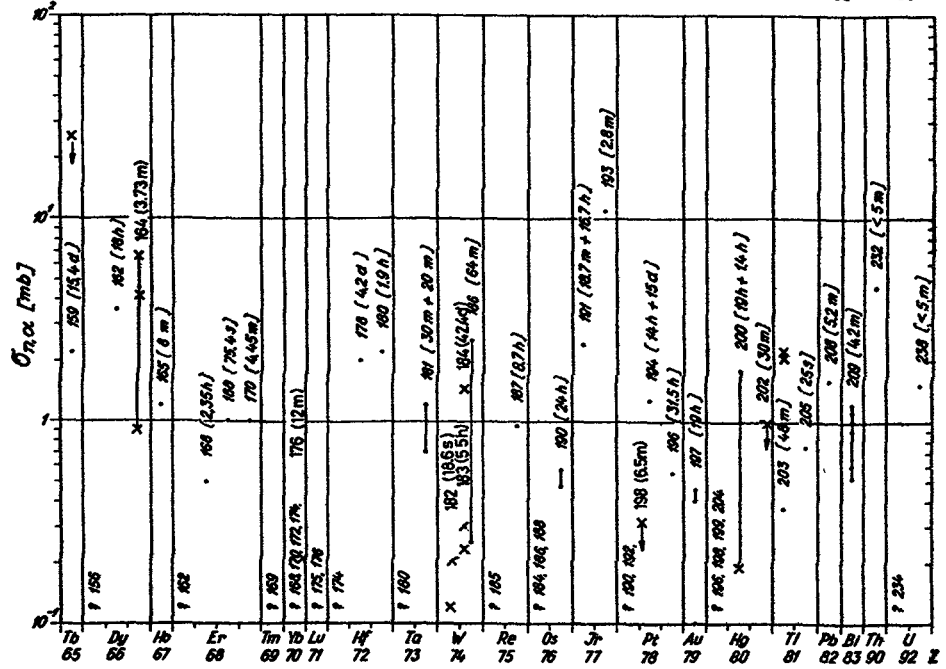

FIG. 8d.

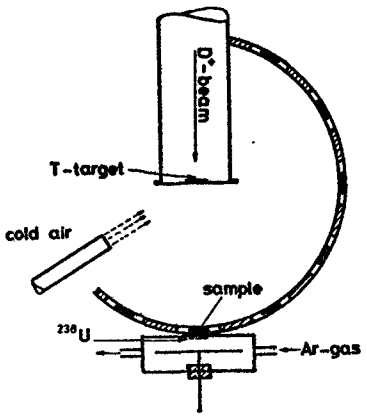

FIG. 9. Arrangement for irradiation around 14 MeV

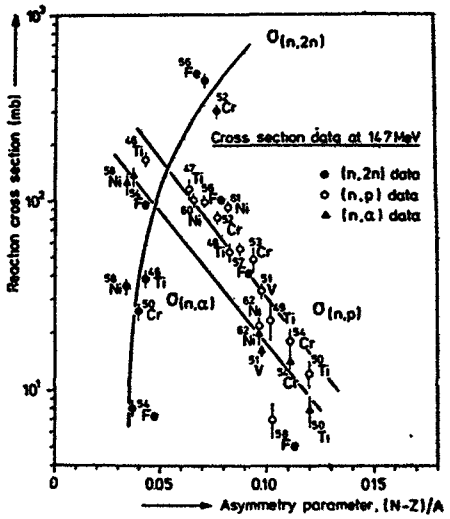

FIG. 10. Dependence of (n,2n), (n,p) and (n,α) cross sections on asymmetry parameter [49].

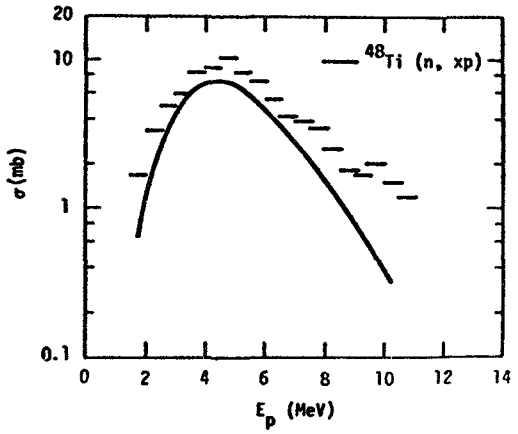

FIG. 11. Angle-averaged proton spectrum from ^{48}Ti measured with a MQS [60] at 15 MeV.

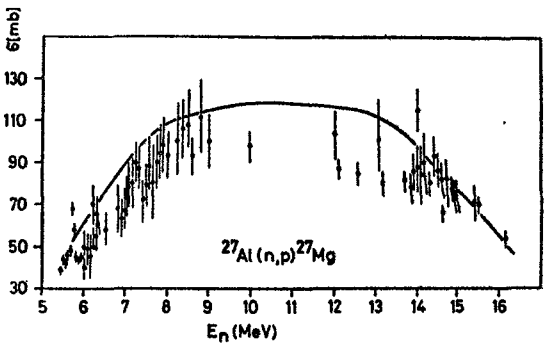

FIG. 12. Measured and calculated excitation functions for $^{27}Al(n,p)$ reaction.

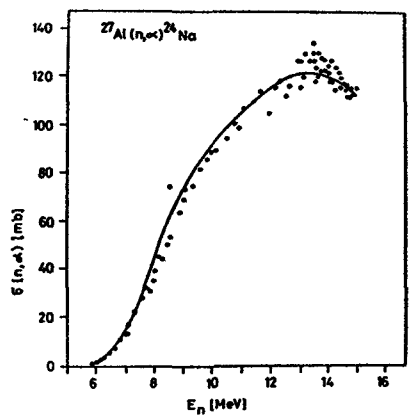

FIG. 13. Hauser-Feshbach model calculation for $^{27}Al(n,\alpha)$ reaction (points are from experiment).

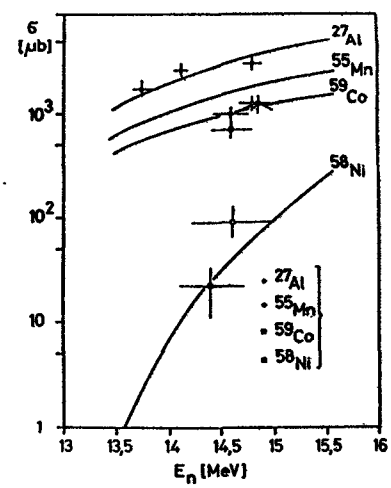

FIG. 14. Measured and calculated excitation functions for (n,t)reactions.

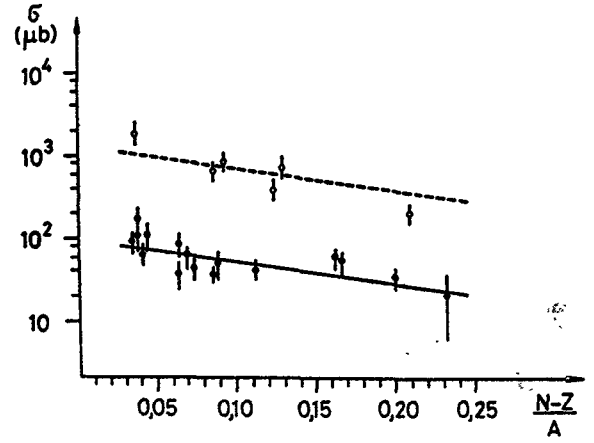

FIG.15. Dependence of $\sigma_{n,t}$ on (N-Z)/A (full points for even nuclei, open circles for odd target nuclei).

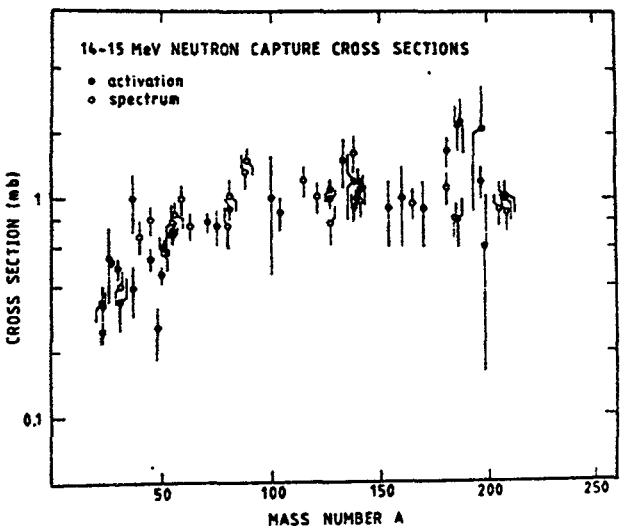

FIG.16. 14 MeV corrected σ_{act} and σ_{int} (n,γ) cross sections [75].

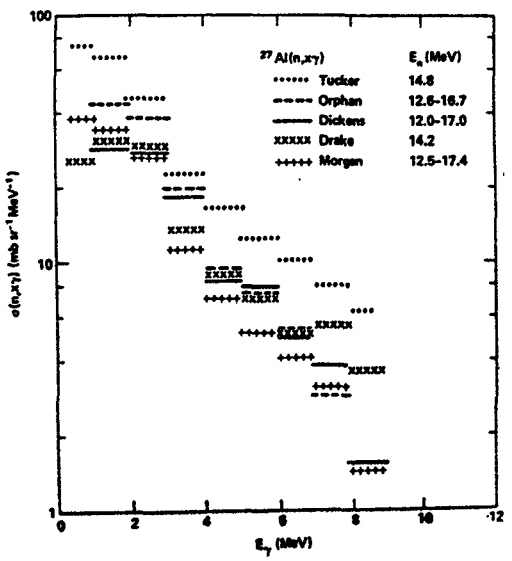

FIG.17. $\sigma_{n,x\gamma}$ values as a function of E_γ for ^{27}Al near 14 MeV [26].

Data for charged particle reactions with heavier nuclides

AG-159/B7
Review Paper

H. Münzel
Technical University Darmstadt and
Nuclear Research Center Karlsruhe
Federal Republic of Germany

Abstract: For charged particle induced nuclear reactions about 1000 papers are published each year dealing with all kinds of target nuclides, projectiles, reaction types and quantities measured. This review gives a short summary about the availability of

- bibliographies, with which one can find out if and where the data of interest are published,
- compilations and evaluations of data, and
- systematics of quantities, like excitation functions for nuclear reactions.

1. Introduction

All concept of fusion reactors depend ultimately on our knowledge about the interaction of the Hydrogen isotopes with each other as well as with the isotopes of Lithium. Accordingly, in the past the attention was focused on the data concerning these nuclear reactions. Therefore it was decided that this topic should not be included in this summary and to concentrate instead on the data for charged particle induced nuclear reactions with target nuclides heavier than Lithium.

The hot plasma in the fusion reactor will not only react with the very light isotopes but with all nuclides present as impurities or as part of the structural materials. For these reactions, like scattering or fusion, data are needed for projectile energies up to about 100 keV. In addition secondary reactions induced by emitted or recoiling protons or α-particles may occur. The energy of these charged projectiles is in general in the region of several MeV. Of interest are data for all kinds of reactions, e.g. elastic and inelastic scattering, formation cross sections for the end products, etc.

There is now a very large number of investigations dealing with charged particle induced nuclear reactions available. They cover the interactions of all kinds of projectiles with many different target nuclides, including the light as well as the very heaviest ones, deal with all types of reactions and provide data for many different quantities measured. In the last decade more than 1000 new publications containing Charged Particle Nuclear reactions Data (CPND) appear each year. Even for

a given reaction type the number of reactions for projectile energies up to 20 MeV investigated annually is quite large as can be seen from the following list:

reaction type	approx. number of annual publ.	reaction type	approx. number of annual publ.
(p,γ)	70	(α,n)	50
(p,n)	90	(α,p)	45
(p,p)	100	(α,α')+(α,α)	70
(p,p')	110		
(p,α)	40		

In the last years many experimentalists got interested in heavy ion reactions due the availability of new accelerators. However, the majority of investigations is still concerned with the level structure of the residual nuclides. For this purpose the angular distributions of the emitted particles and/or γ-rays were measured. Only few percent of the publications deal with total formation cross reactions or thick target yields for the end product. Of course, such Integral Charged Particle Nuclear reactions Data (ICPND) could in some cases be obtained from the published differential data, like angular or particle energy distributions, by integrations. However, this is a very tedious and time consuming task.

The above mentioned numbers of publications appearing each year lead in general to the misinterpretation that now all CPND of interest are available. It should be emphasized that this is *not the case. This is simply due to the large number of possible* projectile-target-end product combinations, the wide range of projectile energies available and the many aspects of the reactions which may be investigated. In many cases one has therefore still to rely on calculated or estimated values.

The first problem one encounters when dealing with charged particle reactions is to find out, if and where experimental values for the data of interest are published. In the second chapter of this review the available bibliographies will be discussed. In the next chapter the compilations of experimental results are described. Chapter 4 contains a short summary about critical evaluations and recommended values. A brief discussion about calculated or estimated CPND follows in Chapter 5. In view of the large number of new publications getting available each year it is not possible to give in a short review a comprehensive survey about the situation of all kinds of investigated quantities. However, as an example a summary about what is available and what one should expect for ICPND-

excitation functions of some low energy reactions is given in Chapter 6.

2. Bibliography

There are several bibliographic services available providing references for publications dealing with charged particle induced nuclear reactions (CPND). The most extensive compilation of CPND-references was prepared by McGowan and collaborators (1). They scanned many journals, thirty of them are explicitly stated. In this 'McGowan bibliography' (MGB) an entry is made for every reaction for which experimental data are given in a publication. In the last years references to theoretical investigations were also included. Each entry states besides the reaction, the projectile energy range and the reference also some additional information about the kind of data available in the publication. In some cases the measured values for cross sections or thick target yields are included directly. The entries are ordered according to target nucleus, projectile and product nucleus.

The McGowan bibliography provides references to all kinds of nuclear reaction data, e.g. excitation functions, angular distributions, total reaction cross sections, Coulomb excitation etc. The bibliography is therefore quite large, it consists now of a comprehensive volume and 4 annual addenda covering the literature up to the end of 1976. It was decided at that time to discontinue this bibliography in order to avoid duplication of work because the literature is also scanned by the Nuclear Data Project.

The bibliography provided by the Nuclear Data Project (NDP/B) is published three times a year as 'Recent References' (2) together with references to nuclear structure and decay data. The entries give information about the reaction and the type of data available. They are ordered in the first part according to product nucleus and in the second part according to reaction type. Again all types of CPND are included in this bibliography. In addition to journals many reports and conference abstracts are also scanned providing also in this way a wider coverage as the MGB. Therefore, the NDP-Bibliography is much larger, but due to the clear arrangement of the entries an unambiguous search for a given reaction is possible. For the convenience of the users cumulative volumes for the 'Recent References' are published, the first one covering the time from 1969 - 1974 (3) and the second one from 1975 - 1977 (4).

References to CPND can also be obtained from other bibliographic services. Up to 1977 the Nuclear Science Abstracts (5) covered the literature including Reports. Since 1977 this activity was incorporated in the International Nuclear Information System (INIS) existing since about 1970, which stores the bibliography and the abstracts of the publications on magnetic tape. Therefore, retrievals with respect to a set of keywords describing the data of interest are now possible. In addition a printed version of this file is also available (6). However, because the scope of these bibliographies is very wide and the Thesaurus can contain only a limited number of keywords such retrievals yield in general many more references as relevant for the problem. If on the other side one tries to decrease the number of excess references then the probability for missing information will increase very rapidly.

The just mentioned problem applies also for the MGB as well as for the NBP/B, but due to the narrow scope of these bibliographies in a much less stringent way. However, this disadvantage could still be reduced if for certain user groups subsets of the bibliography would be provided, because then the keywords might be better adjusted to their needs. One such group can be identified with those scientists who would like to know, for instance, how much activity is formed in the target under given irradiation conditions. For this purpose the excitation functions, i.e. the dependence of the cross section or the thick target yields on the projectile energy, have to be known. Therefore, the National Nuclear Data Center (7) publishes now every year a comprehensive reference list for such integral data (ICPND). This bibliography includes also references to the Karlsruhe Charged particle Reaction Data Compilation (see below), if the respective data are available there.

3. Compilation

The bibliographies provide mainly references to publications which might be relevant for the data of interest. In general one therefore has to look up the original literature to obtain the information and the values needed. This search can be done in a reasonable time if the literature is readily available and if the publication contain the data of interest in an easy accessible form. Unfortunately, especially the second requirement is not very often fulfilled. Even more difficulties will araise in such cases were no experimentally determined values are available for the data wanted. Then one has to look up many more reactions to enable an estimate of the data by inter- or

extrapolation. Therefore, comprehensive compilations of CPND would be very helpful.

Jarmie and Seagrave (8) prepared the first large compilation of excitation functions for charged particle induced reactions, covering target nuclides with proton numbers Z up to 19 (= Fluor). Smith (9) compiled excitation functions for target nuclides ranging from Z = 20 (Ne) up to Z = 24 (Cr). McGowan and collaborators continued these activities and published from 1964 till 1967 compilations for reactions with Mn, Fe, Co(10), Ni, Cu(11), Li, Be, B (12), C (13) and O, N (14). In these compilations the data are given in a table as well as in a diagram. In addition some information about the reaction and the experimental conditions are mentioned. All kind of reaction data are included, like angular distributions. Therefore the compilations are quite large, for instance the carbon colume contains 241 pages. Since 1967 no extension of this very valuable work was published although McGowan et al. (15) did continue for some years to collect data on magnetic tape.

Kunz and Schintlmeister (16) prepared also a compilation of CPND for target elements from H (Z =1) to Sulfur (Z = 16) covering the time up to 1967.

Since 1967 no comprehensive compilation for scattering data was published any more even not for a restricted set of target nuclei. This is mainly due to the increasing number of publications for which a very large group of scientists would be needed to compile all the data. In addition it is quite difficult to obtain for all reactions the data determined because, for instance, for angular distributions normally only representative curves in small pictures are published. To obtain the full data set a lengthy correspondence with the authors is necessary. Especially if the publication is already several years old many authors are not very cooperative. In such cases one can try to reconstruct the angular distribution with the optical model parameters given in the publication. There is an extensive compilation for these parameter sets available (17).

For some subsets of CPND the situation is better. For example, the neutron production probabilities for the d+d-, ^{3}H+p- and ^{3}H+d-reaction are summarized by Liskien et al. (18) and total reaction cross sections are given by Nemets (19). For ICPND there are now several compilations available. Lorenzen did collect excitation functions mainly for light target nuclides with low energy projectiles (20), which are of interest for activation analysis. Tobailem and Lassus St-Genies did also

publish compilations covering many monitor reactions (21) as well as reactions of p,d and α with F, Ne, Na, Mg (22) and Fe (23). These volumes give not only the excitation functions but also additional information about the data used for evaluating the measured values. For high energy reactions cross section compilations were prepared by Bruninx (24) and Silberberg et al.(25).

Münzel and collaborators became interested in the systematics of the excitation functions for radionuclides formed in charged particle induced reactions. They collected therefore cross sections for the formation of ground and metastable states of the end product. These integral charged particle nuclear data (ICPND) were published preliminary in a Report (26) and later in an extended version containing about 1800 excitation functions (27). The excitation functions are given as smooth curves and no individual cross sections are shown. In general, the curves were obtained by reading off values from the curve drawn by the authors of the publications. The ordinate gives the cross sections and the abscissa the difference between projectile energy and threshold energy.

To obtain projectile energies from values read off one therefore has to add the threshold energies given elsewhere in the compilation or which can be obtained from extensive Q-value tables (28, 29). Nevertheless this scale was chosen because it offers two important advantages:

1) Large deviations between the excitation functions indicate the possibility that one of them may be in error. This assumption is based on the similarity of excitation functions for the same reaction type within a limited range of the nucleon number A and proton number Z of the target nuclides. If there are no special reasons, like a relative large neutron excess or deficit of the target nucleus, then one should check carefully, if for instance wrong decay data were used for evaluating the cross sections. For such comparisons the systematics (see below) may also prove to be very helpful.

2) Quite often no experimental values for the excitation function of interest will be available in the literature. Then with the curves given for other reactions an estimate can be made by inter- or extrapolation. Again one makes use of the above mentioned similarity.

In Chapter 6 an example for the practical application of these advantages will be discussed.

Although this compilation contains, as already mentioned, more than 1800 excitation functions not all available data are included. So, for lighter projectiles only an energy range up to 150 MeV was taken into account. Individual cross sections are also not included because the authors were mainly interested in the systematics of the excitation functions. Other drawbacks of the above mentioned ICPND compilation are that no numerical values and no additional informations are given about the reaction, the experimental conditions, the data used in the evaluation of the measured values and the uncertainties of the cross sections. These drawbacks are now avoided in the Karlsruhe Charged Particle Reaction Data Compilation (30). The information about ICPND is stored on magnetic tape in the generalized EXFOR-Format (31). Therefore retrievals with respect to most of the information on the tape are possible. Copies of the master file are sent regularly to 5 Data Centers (32) which are prepared to provide retrievals on request. A printed version of this compilation is now in preparation and should be available in spring 1979. It will consist of a collection of loose pages. Up to now preferentally proton reactions with medium heavy nuclides were compiled. However, in the future new publication will be considered with highest priority.

4. Critical evaluation

There is no doubt that the evaluation of recommended data is a very important task. However, the difficulties start already with the collection of the data because not only the cross sections σ have to be known but also the values used in calculating σ from the measured quantities, like γ-spectra. Unfortunately, quite often one or more of these additional values are missing or are at least not precisely stated in the publication. The subsequent comparison with the now available "best" values for monitor cross sections, decay data, and so on, again is time consuming because quite often one first has to evaluate these "best" values itself. In addition excitation functions for a given reaction were determined experimentally only in few cases two or more times. As a consequence, there are in general not enough experimental data for any kind of averaging procedure to obtain recommended values. Therefore, in these cases the only possibility to check the experimental data is to compare them with the excitation functions obtained from the systematics.

Due to the difficulties mentioned no comprehensive evaluation of recommended CPND is available. Even for ICPND such evalu-

ated excitation functions are published only for few reactions used mainly for flux determinations (21, 22, 23, 33). The Karlsruhe Charged Particle Reaction Data Compilation contains now all the necessary data for such evaluations, if they are given in the publication. Therefore it should be easier in the future to obtain recommended values for important ICPND.

5. Systematics

Despite the large number of published experimental results one has - as already mentioned - quite often to rely on calculated or estimated values for the data of interest. Therefore it is very important to develop such estimation procedures and test the reliability of the results.

In many publications experimental results are compared with calculated values. The agreement found is quite often remarkably good. Therefore such calculations should provide a means for obtaining the data of interest. However the reliability of the calculated values is rather uncertain. An analysis based on a large body of data is available only for ICPND (34). For the calculations one of the following models can be applied and within a given model many different assumptions and approximations may be used:

compound nucleus model
compound and precompound nucleus model
cascade reaction model

Surprisingly enough the analysis of about 30 publications did show that the uncertainty of the calculated values did not depend very much on the sophistication of the model applied. Using the relative differences of experimental and calculated values at several characteristic points, like height and position of the maximum cross section, an overall deviation of 20 up to 50% was obtained. In many of the publications included in this analysis some of the input data needed for the calculations were used as more or less freely adjustable parameters. Therefore one should in general expect that the deviations between calculated and experimental excitation functions are larger than given above because the "best" values for these adjustable parameters are not accurately known.

For p-, d-, ^{3}He- and α-reactions a semiempirical procedure was developed (26, 35, 36) with which excitation functions for many reaction types can be estimated without the aid of

a computer. The uncertainty of these estimated ICPND is only slightly larger than those calculated with simple models. This systematic is based on the dependence of some characteristic values, like the maximum cross section, on a parameter which itself is a function of the binding energies of the last neutron and proton and the Coulomb barrier. With the aid of the excitation functions given in (36) expectation values for thick target yields were calculated and also published in (36).

One important point in the application of such a systematics is the uncertainty of the estimated values. We therefore tested the accuracy in two ways. First, the deviations of the maximum cross sections from the predicted values were calculated for (p,xn)- and (α,xn)-reactions, with x ranging from 1 to 4. The mean values of the deviations obtained were less than 30% (35). Another test was performed to check the whole excitation function (37) which will be descussed below.

6. Excitation functions for low energy reactions

The general form of excitation functions for low energy reactions can be seen in Fig. 1: The curve reaches after a steep rise a maximum and falls off at higher energies to approach after about 30 MeV the approximately constant tail cross section which is up to a factor of 100 smaller than the maximum cross section σ_M. The region of the maximum is in general the most accuratly known part of the excitation function. For most of the cross sections in this region an uncertainty of considerably less than 20% is claimed. However, the reliable evaluation of these uncertainties is very difficult leading quite often to an underestimation of the (systematic) errors. This was checked by comparing with each other all those excitation functions for (p,xn)- and (α,xn)-reactions which were determined at least twice (37). To include the whole maximum region in this comparison thick target yields were calculated using the 106 different sets of cross sections. The average standard deviation for the differences between the two or more thick target yields available for each reaction amounts to 31%. This is a factor of about 1.5 larger than expected from the uncertainties claimed by the authors. The agreement between the different sets of data could presumably be improved if for the calculation of the cross sections from the measured activities the now available "best" values for γ-ray abundances and monitor reaction cross sections would be used.

The average values of the above mentioned thick target yields for a given reaction were used by Jäger et al. (37) to check the reliability of the predictions of the systematics discussed in section 5. They found a standard deviation of 45%

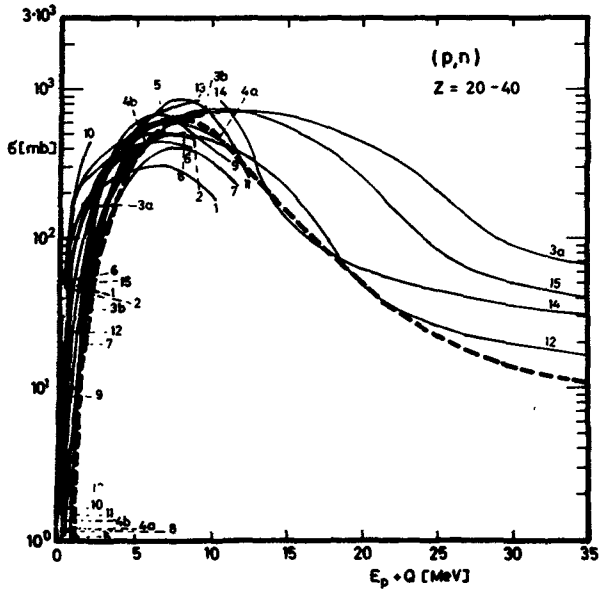

Fig. 1: Excitation functions for (p,n)-reactions as given in (26). On the energy scale the sum of the projectile energy and the Q-value of the reaction is given. The charge number Z of the target nuclides varies between 20 and 40. The dashed curve represents the excitation function expected according to the compound nucleus model.

for the differences between the thick target yields obtained from the systematics and those calculated with the aid of experimental excitation functions for (p,xn)- and (α,xn)-reactions with a wide variety of target nuclides. This is not very much larger than the experimental uncertainties discussed above. A similar check for calculated excitation functions is not available yet.

The comparison of published excitation functions for a given reaction type and a limited region of target nuclides is only very rarely possible due to the lack of data. However, if the reactions proceed mainly via the compound nucleus formation and if the influence of the Coulomb barrier can be neglected then such a comparison can be based on the expected similarity of the excitation functions. As an example 17 excitation functions for (p,n)-reactions with medium target nuclides ($20 \leq Z \leq 40$) are shown in Fig. 1 as full curves. In addition the excitation function expected according to the compound

nucleus model are also given (dashed curve). Due to the energy scale chosen all curves are clustered very near together. Only at higher energies larger deviations seem to occur. However, we know now that the values for the reactions with V (curve 3a) and Y (curve 15) are wrong and that the redetermined values agree much better with the dashed curve. From this observation one can draw two important observations:

1) Some of the experimentally determined excitation functions may have a large systematic error for which no hint or explanation can be found in the publication.

2) Published values should be used with great caution if the excitation function deviates considerably from the expected trend.

At higher projectile energies deviations from the curves derived with the aid of the compound nucleus model are expected due to the influence of precompound emission and surface reactions. If these reaction mechanism are taken into account the agreement between experimental and calculated data can be improved considerably.

The average maximum cross section $\langle\sigma_M\rangle$ of the curves shown in Fig. 1 amounts to 567±163 mb and the position of the maximum $\langle E_M\rangle$ to 7,3±0,7 MeV (excluding the curves 3a and 15). One can expect that the uncertainties of the predicted values (calculated or from systematics) for σ_M and E_M for a (p,n)-reaction in this limited region of target nuclides should not be much larger than the standard deviation given above.

For other low energy reactions with only few emitted nucleous it also can be assumed that the cross sections in the region of the maximum of the excitation functions are known or may be predicted with reasonable accuracy. This is however, not the case for projectile energies E_P just above the threshold energy of the reaction. In this region the values published for the cross sections as well as for the corresponding projectile energies are much less certain especially if the stacked foil technique was used for the determination of the data. An analysis of the effective Coulomb barrier in low energy reactions (38) revealed uncertainties in the projectile energies of about 1 MeV. The systematic errors which are due to the distribution of the projectile energies around the mean value can also be quite large in the region of steep rise of the excitation function. Therefore it is in general not possible to calculate with reasonable certainty the acti-

vity formed just above the threshold energy. This is especially true for the activation by a hot plasma if the reaction of interest was not investigated explicitly in this very low energy region.

References

1) McGowan, F.K., Milner, W.T., et al., Nuclear Data Reprints, Vol. 2, Academic Press, New York 1973 (covering the literature from 1948 to 1971); Atomic Data and Nuclear Data Tables A11 (1972) 1, 12 (1973) 499, 15 (1975) 189 and 18 (1976) 1

2) Recent References in each Volume of 'Nuclear Data Sheets', Academic Press, New York

3) Ewbank, W.B., Haese, R.L., Hurley, F.W., McGinnis, M.R., Nuclear Data Sheets 16 (1975) Supplement "Nuclear Structure References, 1969 - 1974"

4) Ewbank, W.B., Haese, R.L., Hurley, F.W., McGinnis, M.R., Nuclear Data Sheets 24 (1978) 445

5) Nuclear Science Abstracts, USAEC, Technical Information Service

6) INIS Atomindex, IAEA, Vienna

7) Burrows, T.W., Burt, J.S., BNL-NCS-50640, Second Edition, 1978

8) Jarmie, N, Seagrave, J.D., LA-2014 (1957)

9) Smith, D.B., LA-2424 (1961)

10) McGowan, F.K., Milner, W.T., Kim, J.J., ORNL-CPX-1(1964)

11) McGowan, F.K., Milner, W.T., Kim, H.J., ORNL-CPX-2(1964)

12) Kim, H.J., Milner, W.T., McGowan, F.K., Nuclear Data Tables A1 (1966) 203

13) Kim, H.J., Milner, W.T., McGowan, F.K., Nuclear Data Tables A2 (1966) 1

14) Kim, H.J., Milner W.T., McGowan, F.K., Nuclear Data Tables A3 (1967) 123

15) McGowan, F.K., Private Communication; for details of the file contact the National Nuclear Data Center, Brookhaven

16) Kunz, W., Schintlmeister, J., "Nuclear Tables, Part II: Nuclear Reactions", Vol. 1 and 2, Pergamon Press, Oxford (1965, 1967)

17) Perey, C.M., Perey, F.G., Atomic Data and Nuclear Data Tables 17 (1976) 1

18) Liskien, H., Paulsen, A., Nucl. Data Tables 11 (1973) 569

19) Nemets, O.F., Slyusarenko, L.I., Tokarevskij, V.V., Fiz Ehlem. Chastits At. Yadra 6 (1975) 827

20) Lorenzen, J. Brune, D., "Excitation functions for charged particle induced nuclear reactions in light elements at low projectile energies", Handbook on nuclear activation cross-sections, p. 325-473, Int. At. Energy Agency Tech. Rep. Series, Vol. 156 (1974)

21) Tobailem, J., Lassus St-Genies, C.H.de, l.Leveque, L., CEA-N-1466 (1) (1971)

22) Lassus St-Genies, C.H.de, Tobailem, J., CEA-N-1466(2) (1972)

23) Tobailem, J., Lassus St-Genies, C.H.de, CEA-N-1466(3) (1975)

24) Bruninx, ., CERN 61-1 (1961), CERN 62-9 (1962) CERN 64-17 (1964)

25) Silberberg, R., Tsao, C.H., NRL 7593 (1973)

26) Lange, J., Münzel, H., KFK 767 (1968)

27) Lange, J., Münzel, H., Keller, K.A., Pfennig, G., "Excitation functions for charged particle induced reactions", Landolt-Börnstein: Zahlenwerte und Funktionen aus Naturwissenschaften und Technik, Neue Serie Gruppe I, Vol. 5b, Springer, Berlin 1973

28) Wapstra, A.H., Bos, K., Atomic Data and Nuclear Data Tables 19 (1977) 215

29) Keller, K.A., Münzel, H., Lange, J., "Q-values", Landolt-Börnstein: Zahlenwerte und Funktionen aus Naturwissenschaften und Technik, Neue Serie Gruppe 1, Vol. 5a, Springer, Berlin 1973

30) Contact for details the Charged Particle Group, Institute for Radiochemistry, Nuclear Research Center, Karlsruhe, FRG

31) Contact for details about EXFOR (data EXchange FORmat) the Nuclear Data Section, Int. At. Energy Agency, Vienna

32) Nuclear Data Section, Int. At. Energy Agency, Vienna; National Nuclear Data Center, Brookhaven; CaJaD, Kurchatov Institute, Moscow; Fachinformationszentrum Energie.Physik.Mathematik, Kernforschungszentrum Karlsruhe; OECD, Nuclear Energy Agency, Datenbank Gif-sur-Yvette

33) Cumming, J.B., Ann. Rev. Nucl. Sci 13 (1963) 261

34) Röhm, H.F., Keller, K.A., Münzel, H., KFK 1730 (1973)

35) Röhm, H.F., Münzel, H., Lange, J., Nucl. Instr. Meth. 113 (1973) 101; Röhm, H.F., KFK 1447 (1971)

36) Münzel, H., Keller, K.A., Lange, J., "Systematics of excitation functions for nuclear reactions induced by p,d,^{3}He and α", Landolt-Börnstein: Zahlenwerte und Funktionen aus Naturwissenschaften und Technik, Neue Serie, Gruppe 1, Vol 5c; Springer, Berlin 1974

37) Jäger, U. Münzel, H., Proc. of the Symp. on Application of Nuclear Data in Science and Technology, Paris, 12. - 16. 3. 1973, Vol. 2, p. 475, IAEA, Vienna, 1973

38) Münzel, H., KFK 1955 (1978)